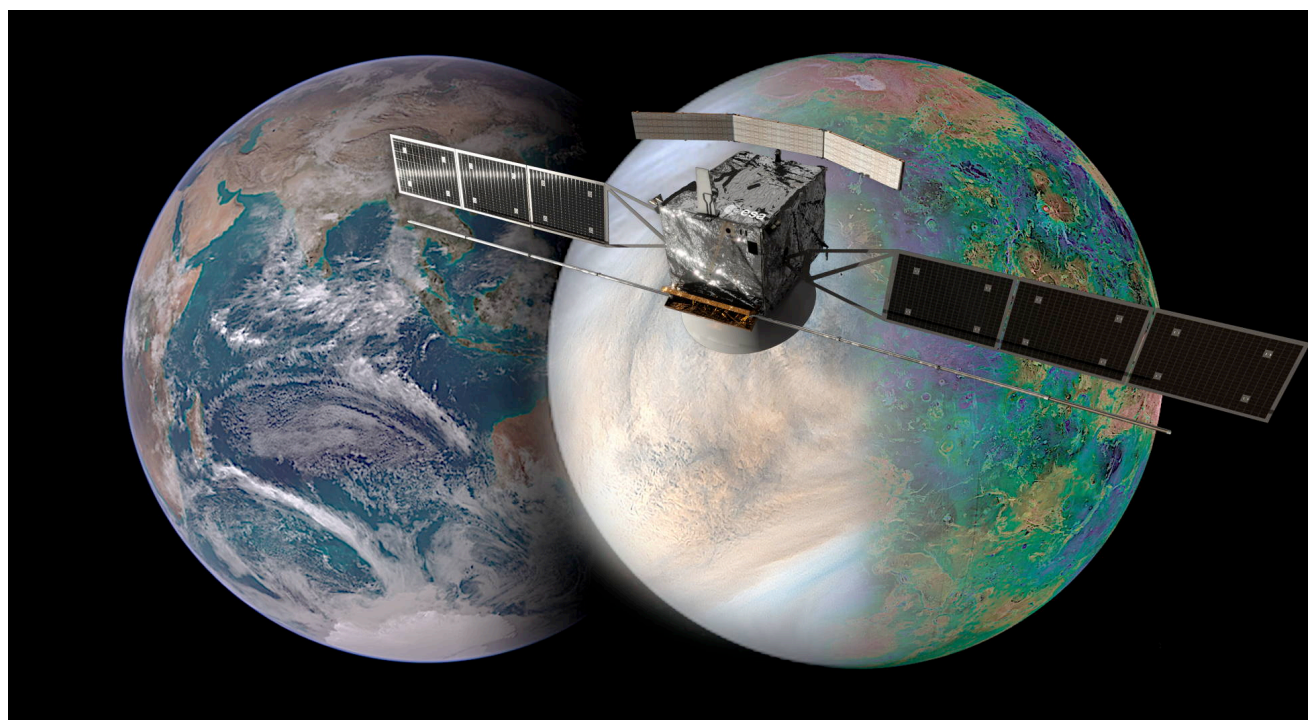


EnVision

Understanding why Earth's closest neighbour is so different



Assessment Study Report

The front page shows an artist's impression of the evolution of Venus through an Earth-like phase to what we see today. Venus is the most Earth-like telluric planet, in size, composition and distance to its star, yet at some point in planetary history there was a bifurcation between the two: Earth has been continually habitable since the end of its formation, whereas Venus became uninhabitable, providing a natural laboratory to study the evolution of habitability. *Credits: JAXA / ISAS / DARTS / Damia Bouic / VR2Planets.*

| EnVision Mission Summary | |
|--|--|
| Science Questions (Section 2.1) | <p>EnVision will address the following overall science questions, in no priority order:</p> <ul style="list-style-type: none"> • History - How have the surface and interior of Venus evolved? • Activity - How geologically active is Venus? • Climate - How are Venus' atmosphere & climate shaped by geological processes? |
| Science Objectives (Section 2.2) | <p>EnVision's science objectives, in no priority order, are:</p> <ul style="list-style-type: none"> • to determine the styles of volcanic processes which have occurred on Venus, studying the sources, emplacement styles, magma properties and relative ages of different volcanic flows; • to determine the styles of tectonic deformation that have operated on Venus by studying their surface expression and gravity signatures, and determining their role in planetary heat loss; • to characterise surface modification processes such as impact crater modification, low emissivity/radar bright highlands, to improve our understanding of Venus geochronology; • to constrain Venus' internal structure, through measurements of gravity field and tidal response, to constrain the properties and thicknesses of Venus' crust, mantle and core; • to constrain the nature and occurrence of recent volcanism on Venus, how processes compare with Earth and other terrestrial planets, characterising its morphological, thermal and volatile signatures; • to study landscape evolution on Venus, such as gravity-driven mass-movements erosion and deposition, and active chemical weathering on time scales of months to years; • to explore the role of geological activity, through volcanism and surface-atmosphere chemical reactions, in sustaining the volatile and cloud content of the atmosphere, and climate evolution; • to study transport of geophysically meaningful volatile species through the atmosphere and clouds of Venus, through measurements below, within, and above the cloud layer. |
| Payload (Chapter 4) | <ul style="list-style-type: none"> • VenSAR, a reflectarray, dual polarization S-band Synthetic Aperture Radar, will map the surface using a range of modes including imaging at spatial resolutions of 10 m to 30 m, altimetry, polarimetry (HV for the 1st time) and radiometry; • A Subsurface Sounding Radar (SRS) will penetrate into the top kilometre of the subsurface, and search for underground layering and buried boundaries; • Three spectrometers VenSpec-U, VenSpec-H and VenSpec-M, operating in the UV and Infrared, will map trace gases, including search for volcanic gas plumes, above and below the clouds, and map surface composition; • A gravity & radio science investigation will use radio tracking to map the planet's gravity field, constraining internal structure, and will measure atmospheric properties through radio occultation.  |
| Spacecraft (Chapter 5) | <ul style="list-style-type: none"> • EnVision will be a three-axis stabilised orbiter, ~2m x 2m x 3m in stowed configuration. • Launch dry mass 1.35 t, max power incl. system margins 2.8 kW; • EnVision will be in a low Venus quasi-polar orbit, inclination between 87 and 89 deg with altitudes varying from 220 to 540 km and orbital period of about 92 min; • EnVision will downlink 210 Tbits of science data, using a Ka-/X-band comms system with a 2.5m diameter fixed high-gain antenna. |
| Launch and Operations (Chapters 5.1 & 6) | <ul style="list-style-type: none"> • A62 launch from Kourou in May 2032 (back-up launch window Dec. 2032), arriving at Venus after a 15-month cruise. Following orbit insertion, orbit circularisation achieved by aerobraking over a period of about 16 months, followed by a nominal science phase of 6 Venus sidereal days (4 Earth years); • Mission Operations Centre (MOC) at ESOC (Darmstadt), Science Operations Centre (SOC) at ESAC (Madrid), and Instrument Operations and operational interfaces distributed across Instrument Teams. |
| Data Policy (Chapter 7.5) | <ul style="list-style-type: none"> • EnVision will produce a large dataset (210 Terabits) covering atmosphere, surface, subsurface and interior with a quality allowing comparison to Earth and Mars across a wide range of disciplines; • EnVision science teams will adopt an open data policy, with datasets publicly released immediately after validation & verification. |

Foreword

Venus has been an object of fascination for centuries, and throughout the space age. It was the site of the first planetary flyby in 1962 (Mariner-2), first entry probe in 1967 (Venera-4), first soft landing in Dec. 1970 (Venera-7), first image from the surface of another planet in 1975 (Venera-9), first orbiter and radar in 1978 (Pioneer). The Soviet series of Venera & VeGa missions were phenomenally successful, not only in their technologically advanced landers which returned colour pictures from Venus and analysed drill samples despite 450 deg C heat, but also successfully deployed balloons in the atmosphere in 1985. Global studies of the surface have been achieved using cloud-penetrating radars, firstly from Earth using large radio antenna like those at Goldstone, California, and then from spacecraft orbiting the planet, beginning with Pioneer Venus' operations in 1980. Far more detail was revealed by the synthetic aperture radars (SARs) on Venera-15 and 16 in 1983, followed by Magellan in 1989.

From 2006 to 2014, ESA's Venus Express, a landmark in Venus exploration, answered many questions about our nearest planetary neighbour and established European leadership in Venus research. Focussed on atmospheric research, some of the enigmatic results from Venus Express nonetheless concerned its surface: hints of current volcanic activity including a tenfold change in mesospheric sulphur dioxide, anomalously dark lava surrounding volcanoes, and surface temperature changes, all pointed towards a geologically active planet. Many significant questions remain on the current state of Venus, suggesting major gaps in our understanding of how and when did Venus's evolutionary pathway diverge from Earth's. Furthermore, recent climate modelling has found that Venus might have been cool enough to maintain liquid water for up to billions of years.

To pursue these intriguing observations and other lines of investigation, the EnVision orbiter was developed, with the concept of bringing Venus geology up to date with a 21st century radar geophysics investigation, heavily informed by Earth observation heritage, in combination with atmospheric (with 3 spectrometers and radio occultations), subsurface (with a sounding radar) and interior (with radio science experiment) investigations built on heritage from across ESA's suite of planetary missions. The EnVision mission benefits from the collaboration with NASA, that provides a SAR, building on NASA-JPL's years of experience with planetary radar dating back to the original Magellan Venus radar, as well as scientific expertise from its data analysis. EnVision therefore benefits from decades of scientific and technical heritage from both Venus Express and Magellan missions, as well as from many other missions including Mars Express, Cassini, Sentinel-1 radar. The present document represents the culmination of two and a half years of work by the ESA-NASA science study team.

The study included a review of the mission requirements, the technical design and analysis of the complete payload module and development of an end-to-end performance simulator of each instrument. The industrial studies included a review of the mission requirements, the technical design and a programmatic analysis of the mission. Dedicated iterations were done in conjunction with both industrial and instrument studies to harmonise the interfaces between the S/C and the payload, and to consolidate the payload accommodation.



Figure 1.0 – EnVision will be the first mission to investigate Venus from its inner core to its upper atmosphere at an unprecedented scale of resolution, characterising the interaction between its different envelopes: its atmosphere, surface/subsurface and interior.

Authorship, acknowledgements

This Assessment Study Report has been prepared by a Science Study Team of 9 European and 2 American scientists, working closely with the Instrument teams, and by an ESA Study Team working closely with two industrial contractors.

| ESA Science Study Team (SST) | | |
|-------------------------------------|---|----------------------|
| <i>Name</i> | <i>Affiliation</i> | <i>City, Country</i> |
| Richard Ghail | Dpt. Earth Sciences, Royal Holloway, University of London | London, UK |
| Veronique Ansan | LPG, Université de Nantes | Nantes, France |
| Francesca Bovolo | DigiS, Fondazione Bruno Kessler | Trento, Italy |
| Doris Breuer | DLR Institute of Planetary Research | Berlin, Germany |
| Bruce Campbell | Center for Earth and Planetary Studies, National Air & Space | Washington, DC USA |
| Walter Kiefer | Lunar and Planetary Institute | Houston, TX USA |
| Goro Komatsu | IRSPS, Università d'Annunzio | Pescara, Italy |
| Alice Le Gall | LATMOS, IPSL, Université Versailles Saint-Quentin | Guyancourt, France |
| Philippa Mason | Dpt. Earth Science & Engineering, Imperial College | London, UK |
| Thomas Widemann | LESIA, Observatoire de Paris | Meudon, France |
| Colin Wilson | Dpt. Physics, University of Oxford | Oxford, UK |
| Instrument Leads | | |
| <i>Name</i> | <i>Affiliation</i> | <i>City, Country</i> |
| Scott Hensley | Jet Propulsion Laboratory, California Institute of Technology | Pasadena, CA USA |
| Lorenzo Bruzzone | Università di Trento | Trento, Italy |
| Jörn Helbert | DLR Institute of Planetary Research | Berlin, Germany |
| Ann Carine Vandaele | Royal Belgian Institute for Space Aeronomy (BIRA-IASB) | Brussels, Belgium |
| Emmanuel Marcq | LATMOS, IPSL, Université Versailles Saint-Quentin | Guyancourt, France |
| Caroline Dumoulin | LPG, Université de Nantes | Nantes, France |
| Pascal Rosenblatt | LPG, Université de Nantes | Nantes, France |

The ESA and NASA Team supporting the activities is composed by:

| ESA Study Team | | |
|---|------|--------------------------------|
| Thomas Voirin (Study Manager) | ESA | Noordwijk, The Netherlands |
| Dmitri Titov (Study Scientist) | ESA | Noordwijk, The Netherlands |
| Ana Rugina (System Manager) | ESA | Noordwijk, The Netherlands |
| Jens Romstedt (Payload Manager) | ESA | Noordwijk, The Netherlands |
| Jayne Lefort (Science Op.s Study Manager) | ESA | Villanueva de la Cañada, Spain |
| Arno Wielders (Deputy Payload Manager) | ESA | Noordwijk, The Netherlands |
| Christopher Buck (Microwave Payload Engineer) | ESA | Noordwijk, The Netherlands |
| ESA and NASA Coordinators | | |
| Luigi Colangeli | ESA | Noordwijk, The Netherlands |
| Adriana Ocampo | NASA | Washington, DC USA |

Table of contents

| | | |
|------------|--|-----------|
| 1 | EXECUTIVE SUMMARY | 7 |
| 2 | SCIENTIFIC OBJECTIVES | 10 |
| 2.1 | EnVision mission in context | 10 |
| 2.1.1 | EnVision scientific context..... | 10 |
| 2.1.2 | Overview of EnVision's top-level science questions..... | 11 |
| 2.2 | Scientific Objectives | 15 |
| 2.2.1 | Understanding Venus' magmatic history..... | 17 |
| 2.2.2 | Understanding Venus' tectonic history..... | 18 |
| 2.2.3 | Assessing Venus' surface modification processes..... | 18 |
| 2.2.4 | Understanding how Venus' interior and surface have evolved..... | 19 |
| 2.2.5 | Understanding Venus' volcanic activity in the present era..... | 21 |
| 2.2.6 | Assessing Venus' aeolian activity and mass wasting..... | 22 |
| 2.2.7 | Understanding the role of geological activity in Venus' climate evolution..... | 24 |
| 2.2.8 | Assessing temporal variations of the Venus atmosphere | 26 |
| 2.3 | Science Investigations | 27 |
| 2.3.1 | Establish the magmatic history of Venus: changes in style and volume with time, range of magma compositions | 27 |
| 2.3.2 | Establish the tectonic history of Venus: magnitude of deformation, implications for lithospheric thickness and heat flow..... | 29 |
| 2.3.3 | Characterise surface modification processes: impact crater modification, low emissivity/radar bright highlands | 30 |
| 2.3.4 | Constrain the size of the major internal layers (crust/lithosphere, mantle, core), and the physical state of the core..... | 31 |
| 2.3.5 | Constrain styles and occurrence of recent volcanism on Venus..... | 33 |
| 2.3.6 | Characterise geomorphological changes by mass-wasting and aeolian processes..... | 34 |
| 2.3.7 | Assess tropospheric trace gases spatial and temporal variability | 35 |
| 2.3.8 | Measure variability of sulphuric acid in the clouds, in both vapour and liquid form, and map variability of related species at the cloud-tops..... | 36 |
| 2.4 | Complementarity of other Venus missions under study to EnVision | 38 |
| 3 | SCIENTIFIC REQUIREMENTS | 40 |
| 3.1 | Science Traceability Matrix | 40 |
| 3.2 | EnVision Observation Strategy | 42 |
| 3.3 | EnVision will investigate how the surface and interior of Venus have evolved to their current state | 43 |
| 3.3.1 | Regional / Targeted Surface Mapping..... | 43 |
| 3.3.2 | Surface Topography..... | 45 |
| 3.3.3 | Surface properties: passive off-nadir radiometry, surface polarimetry, microwave emissivity and Near-IR emissivity | 46 |
| 3.3.4 | Subsurface material boundaries..... | 47 |
| 3.3.5 | Gravity Field..... | 48 |
| 3.4 | EnVision will investigate how geologically active Venus is in the present era | 49 |
| 3.4.1 | Search for surface temperature anomalies..... | 49 |
| 3.4.2 | Search for changes in surface radar imagery..... | 50 |
| 3.4.3 | Search for atmospheric changes | 50 |
| 3.5 | EnVision will investigate how Venus' atmosphere and climate are shaped by geological processes..... | 50 |
| 3.5.1 | Near-IR nightside spectroscopy to measure tropospheric trace gases and lower cloud properties | 51 |
| 3.5.2 | Radio occultation to measure Sulphuric acid liquid and vapour | 51 |
| 3.5.3 | Dayside UV and Near-IR spectroscopy to measure mesospheric trace gases and cloud-top properties | 52 |
| 3.6 | Key Questions and Answers about EnVision Science..... | 53 |
| 4 | PAYLOAD..... | 55 |
| 4.1 | Payload Overview | 55 |

| | | |
|------------|--|-----------|
| 4.2 | Synthetic Aperture Radar VenSAR | 56 |
| 4.2.1 | Instrument objectives and description | 56 |
| 4.2.2 | Interface and Resource Requirements | 58 |
| 4.2.3 | Operation Requirements | 58 |
| 4.2.4 | Heritage..... | 59 |
| 4.2.5 | Instrument Performance..... | 59 |
| 4.3 | Subsurface Radar Sounder SRS | 60 |
| 4.3.1 | Instrument objectives and description | 60 |
| 4.3.2 | Interfaces and resources requirements | 61 |
| 4.3.3 | Operation requirements | 61 |
| 4.3.4 | Heritage..... | 61 |
| 4.3.5 | Instrument performance..... | 61 |
| 4.4 | Near-IR mapping spectrometer VenSpec-M | 62 |
| 4.4.1 | Instrument objectives and description | 62 |
| 4.4.2 | Interfaces and resources requirements | 63 |
| 4.4.3 | Operation requirements | 63 |
| 4.4.4 | Heritage..... | 63 |
| 4.4.5 | Instrument Performance..... | 63 |
| 4.5 | High-resolution infrared spectrometer VenSpec-H | 64 |
| 4.5.1 | Instrument objectives and description | 64 |
| 4.5.2 | Interfaces and resources requirements | 64 |
| 4.5.3 | Operation requirements | 65 |
| 4.5.4 | Heritage..... | 65 |
| 4.5.5 | Instrument performance..... | 65 |
| 4.6 | UV spectral imager VenSpec-U | 66 |
| 4.6.1 | Instrument objectives and description | 66 |
| 4.6.2 | Interfaces and resources requirements..... | 66 |
| 4.6.3 | Operation Requirements | 66 |
| 4.6.4 | Heritage..... | 67 |
| 4.6.5 | Instrument Performance..... | 67 |
| 4.7 | Radio Science Experiment RSE | 67 |
| 4.7.1 | Experiment objectives and description..... | 67 |
| 4.7.2 | USO interfaces and resources requirements | 68 |
| 4.7.3 | Operation requirements | 68 |
| 4.7.4 | Heritage..... | 68 |
| 4.7.5 | Experiment performance | 68 |
| 5 | MISSION DESIGN | 69 |
| 5.1 | Mission requirements and design drivers | 69 |
| 5.2 | Driving mission requirements | 69 |
| 5.3 | Design drivers | 70 |
| 5.3.1 | Design-to-cost..... | 70 |
| 5.3.2 | Environment | 70 |
| 5.3.3 | Payload accommodation and observation modes | 71 |
| 5.4 | Design of the science mission profile | 71 |
| 5.4.1 | Operational point for data return | 71 |
| 5.4.2 | Conceptual design..... | 72 |
| 5.4.3 | Science observations planning strategy | 73 |
| 5.4.4 | Payload Reference Operations scenario | 75 |
| 5.5 | Strategy robustness assessment | 79 |
| 5.5.1 | Sensitivity to starting date | 79 |
| 5.5.2 | Resilience in degraded communication scenarios | 80 |
| 5.6 | Mission timeline | 81 |
| 5.6.1 | Launch | 81 |
| 5.6.2 | Interplanetary transfer phase..... | 82 |
| 5.6.3 | Aerobraking | 82 |
| 5.6.4 | Transition to science orbit and nominal science phase..... | 83 |
| 5.6.5 | Spacecraft disposal | 84 |

| | | |
|------------|---|------------|
| 5.7 | Spacecraft Design | 85 |
| 5.7.1 | Main modes of S/C operations | 85 |
| 5.7.2 | Spacecraft subsystems overview | 86 |
| 5.8 | System Budgets | 89 |
| 5.9 | Conclusions | 89 |
| 6 | MISSION OPERATIONS AND GROUND SEGMENT | 90 |
| 6.1 | Overview | 90 |
| 6.2 | Operations Ground Segment (OGS) | 90 |
| 6.2.1 | Ground Stations | 90 |
| 6.2.2 | Mission Operations Centre (MOC) | 92 |
| 6.3 | Science Ground Segment | 92 |
| 6.3.1 | Overview..... | 92 |
| 6.3.2 | Science Operations Centre Responsibilities | 93 |
| 6.3.3 | Science Operations Planning | 93 |
| 6.3.4 | Data Handling and Archiving..... | 94 |
| 7 | MANAGEMENT | 95 |
| 7.1 | Project Management | 95 |
| 7.2 | Operations Management | 95 |
| 7.3 | Share of responsibilities | 95 |
| 7.4 | Development plan | 97 |
| 7.4.1 | S/C model philosophy..... | 97 |
| 7.4.2 | Schedule..... | 97 |
| 7.4.3 | Critical elements and risks mitigation | 98 |
| 7.5 | Science Management | 98 |
| 8 | COMMUNICATIONS AND OUTREACH | 100 |
| 8.1 | EnVision public outreach and education themes | 100 |
| 8.2 | EnVision communication and public outreach resources | 100 |
| 8.2.1 | Website | 100 |
| 8.2.2 | Image and video library | 100 |
| 8.2.3 | Public access to datasets | 101 |
| 8.2.4 | Teacher resources for formal education | 101 |
| 8.3 | Implementation | 101 |
| 9 | REFERENCES | 102 |
| 10 | LIST OF ACRONYMS | 107 |
| 11 | GLOSSARY | 108 |

1 Executive summary

Venus exploration offers unique opportunities to **answer fundamental questions about the evolution of terrestrial planets and the habitability within our own solar system.** Many significant questions remain on the current state of Venus, suggesting major gaps in our understanding of **how Venus's evolutionary pathway diverged from Earth's.** Comparing the interior, surface and atmosphere evolution of Earth and Venus is essential to understanding what processes have shaped our planet, and is particularly relevant in an era where we expect thousands of terrestrial exoplanets to be discovered.

EnVision is a Venus orbiter mission that will determine the nature and current state of Venus' geological evolution and its relationship with the atmosphere, to understand how and why Venus and Earth evolved so differently. Perched at the inner edge of the habitable zone, Venus may once have had abundant liquid water and been able to sustain life, before developing the runaway greenhouse warming which rendered it uninhabitable today; thus providing a natural laboratory for understanding planetary conditions for life. Venus is Earth's closest sibling geologically: similar in size to the Earth, it has remained active into the present era, unlike the much smaller Mars and Mercury. Venus today does not have a mechanism to sequester atmospheric CO₂ in carbonate rocks and does not exhibit Earth-like plate tectonics, although both processes may have occurred in the past. With few sinks for volcanically emitted volatiles, Venus is left with its present massive atmosphere; but again, its past is very poorly constrained. Thus, Venus is essential for understanding the links between planetary geophysical evolution and habitability of terrestrial planets from our own Earth to terrestrial planets and exoplanets everywhere, including those which will be the subject of study by other missions in ESA's Space Science programme. EnVision therefore appeals to – and benefits from – a wide community ranging from geologists, geophysicists and atmospheric scientists suffused in Earth Observation, to astronomers seeking to understand terrestrial exoplanets.

Scientific Strategy. – EnVision will deliver new insights into geological history through complementary imagery, polarimetry, radiometry and spectroscopy of the surface coupled with subsurface sounding and gravity mapping; it will search for thermal, morphological, and gaseous signs of volcanic and other geological activity; and it will trace the fate of key volatile species from their sources and sinks at the surface through the clouds up to the mesosphere. Following the same approach through which our understanding of Earth and Mars has been developed, EnVision will combine global observations at low or moderate spatial resolution (e.g. surface emissivity & atmosphere composition) with regionally targeted observations of higher spatial resolutions from a modern synthetic aperture radar (SAR) and subsurface sounding radar profiles.

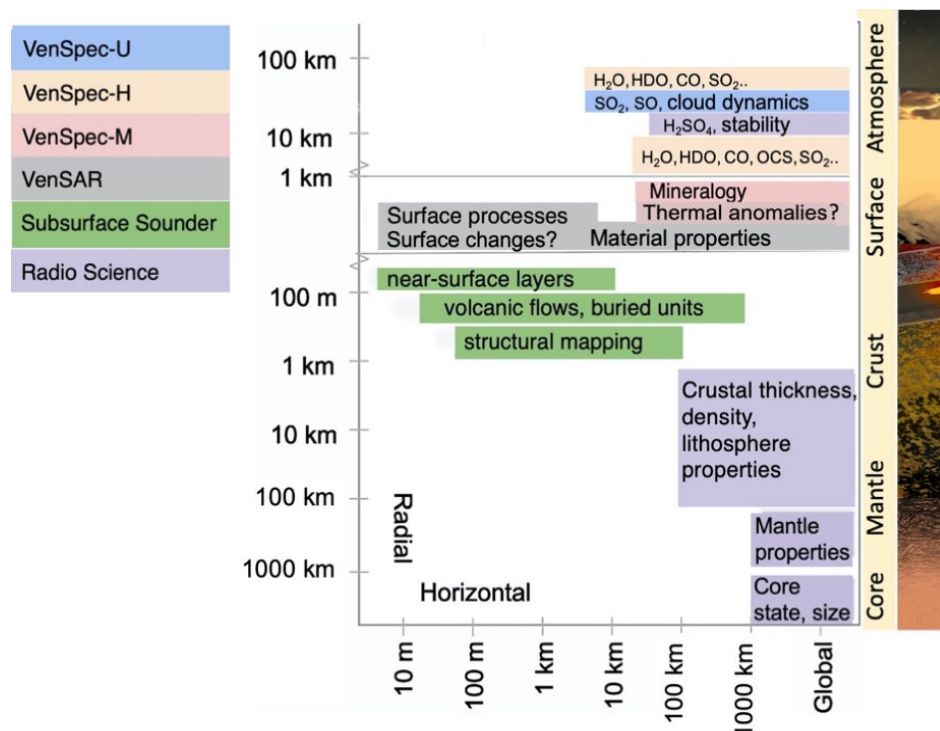


Figure 1.1 – EnVision's multi-messenger strategy combines observations at wavelengths from UV to radio- frequency waves to study geological and atmospheric processes at a range of scales, from the core to the upper atmosphere.

Payload. - EnVision's science payload consists of VenSAR, a dual polarization S-band radar also operating as microwave radiometer, three spectrometers VenSpec-M, VenSpec-U and VenSpec-H designed to observe the surface and atmosphere of Venus, and the Subsurface Radar Sounder (SRS), a High Frequency (HF) sounding radar to probe the subsurface. These are complemented by a radio science investigation which achieves gravity mapping and radio occultation of the atmosphere, for a comprehensive investigation of the Venusian surface, interior and atmosphere and their interactions. Far more than a simple radar mission, this suite of investigations works together to comprehensively assess surface and subsurface geological processes, interior geophysics and geodynamics, and atmospheric pathways of key volcanogenic gases, which together illuminate how and why Venus turned out so differently to Earth. The synergistic and holistic way in which the payload instruments collaborate to investigate processes at different altitudes, depths and spatial scales is graphically illustrated in [Figure 4.1.1](#).

A **Synthetic Aperture Radar, VenSAR**, will image pre-selected regions of interest at a resolution of 30 m/pixel, and subregions at 10 m/pixel. An order of magnitude better than Magellan and with a better sensitivity, these images are the key to understanding geological processes from the local to global scale, discriminating relationships between units of different age, and identifying the changes caused by geological activity. Topographic information at 300 m spatial and 20 m vertical resolution across these regions, derived from stereo imaging at two different incidence angles, is complemented by a global network of altimetry mode tracks with a vertical resolution of 2.5 m, providing a far better than any previous dataset, essential for resolving the geometry of faults, folds and other features, and enabling the quantitative analysis of geological processes. Surface properties such as roughness will be derived from active imaging in both HH and HV polarizations – a first for a Venus orbiter - and passive radiometry at a range of angles, which also permits the detection of surface temperature anomalies. Repeated observations and comparisons with Magellan imagery allow for the detection of volcanic, tectonic and geomorphic changes over periods of months, years and decades.

A **Subsurface Sounder, SRS**, will characterise the vertical structure and stratigraphy of geological units including volcanic flows. EnVision is the first mission to Venus with a sounding instrument that will perform the direct measurement of subsurface features. Geological inferences from Magellan data point to a range of subsurface structures and geometries that are as yet unquantified. The SRS provides a unique opportunity to sound the great variety in geologic and geomorphic units. It will also provide unprecedented information on the surface in terms of roughness, composition and permittivity (dielectric) properties at wavelengths completely different from those of VenSAR, thus allowing a better understanding of the surface properties. SRS observation will also result in altimetry measurements by providing low-resolution profiles of the topography that can be integrated with the altimetric data of VenSAR.

A **Spectrometer suite, VenSpec**, will obtain global maps of surface emissivity in six wavelength bands using five near-infrared spectral transparency windows in the nightside atmosphere, to constrain surface mineralogy and inform evolutionary scenarios; and measure variations of SO₂, SO and linked gases in the mesosphere, to link these variations to tropospheric variations and volcanism. **VenSpec-M** is a pushbroom multispectral imager optimised to map thermal emission from Venus' surface using six narrow bands ranging from 0.86 to 1.18 μm, and three bands to study cloud microphysics and dynamics. This allows mapping of surface composition, constrained by its emissivity spectrum, as well as searching for thermal anomalies associated with volcanic activity. **VenSpec-H** is dedicated to extremely high-resolution atmospheric measurements. The main objective is to quantify SO₂, H₂O and HDO in the atmosphere, below and above the clouds, characterising gas exchanges from the surface and within the atmosphere, searching for sources such as volcanic plumes. **VenSpec-U**, an ultraviolet spectrometer, will monitor minor sulphur species (mainly SO and SO₂) and investigate the complex and highly variable upper atmosphere and its relationship with the lower atmosphere. In combination, VenSpec will provide unprecedented insights into the current state of Venus and its past evolution. VenSpec will perform a comprehensive search for volcanic activity by targeting atmospheric signatures, thermal signatures and compositional signatures, as well as a global map of surface composition.

A **Radio Science Experiment** uses the spacecraft-Earth radio link for gravity mapping and atmospheric profiling. Magellan gravity data are consistent with an organised pattern of mantle convection broadly similar to Earth but lack the resolution necessary to understand its connection with geological-scale features, such as individual coronae or mountain belts. Higher spatial resolution is needed to better constrain the crustal and lithospheric structure variations; EnVision will obtain higher resolution globally,

allowing better constraints on the geodynamic evolution of the planet. EnVision's gravity measurements also will allow calculation of the tidal Love number k_2 with an accuracy of 0.01; this increased precision will constrain the distribution of internal mass, and the size and state of the core. is needed to perform Furthermore, the refraction of EnVision's radio signal in the neutral atmosphere and ionosphere of Venus will be used in combination with a reference clock (ultra-stable oscillator, USO) to obtain high-resolution vertical profiles of temperature, pressure, and sulphuric acid vapour and liquid profiles in the neutral atmosphere, and total electron content in the ionosphere.

Mission and Spacecraft Design. - EnVision will be launched on an Ariane 62 in June 2032 (with a backup date in Dec 2032). An interplanetary cruise of 15 months is followed by orbit insertion and then circularisation by aerobraking over a period of about 16 months to achieve the nominal science orbit, a low quasi-polar Venus orbit with inclination between 87 and 89 deg, altitudes varying from 220 to 540 km and orbital period of about 92 min. The nominal science phase of the mission will last six Venus sidereal days (four Earth years). The choice of science orbit around Venus is mostly driven by a need for global VenSpec, SRS, and VenSAR altimeter and radiometer coverage, stereo topography, polarimetric and repeated VenSAR imaging, and for high-resolution gravity mapping. The spacecraft is approximately rectangular, 3 m in height x 2 m in depth and width in stowed configuration, with chemical propulsion and powered by two deployable solar arrays. EnVision will downlink 210 Tbits of science data, using a Ka-/X-band comms system with a 2.5 m diameter fixed high-gain antenna.

Project, Operations and Science Management - EnVision is an ESA mission in collaboration with NASA, and contributions from individual ESA member states for the provision of payload elements. NASA is contributing the VenSAR instrument and supplies DSN support. The other payload instruments are contributed by ESA member states, with ASI, DLR, BelSPO, and CNES leading the procurement of SRS, VenSpec-M, VenSpec-H, the USO and VenSpec-U instruments respectively. The management structure for EnVision follows that familiar for ESA planetary missions. ESA has responsibility for overall management, and for launch segment, spacecraft procurement, and mission and science operations centres. The EnVision mission thus combines the European experience in Venus atmospheric science from the Venus Express mission and of Earth radar mapping from the ERS and Sentinel-1 missions, with the long heritage of NASA's Jet Propulsion Laboratory in planetary radar, and ASI in sounding radar (MARSIS, SHARAD, RIME).

EnVision will study the Venus system from core to clouds, revealing how the most Earth-like planet in the solar system has turned out so differently:

- a mission for **many communities**, from Earth to planetary to exoplanetary science;
- a mission for **many disciplines**, from interior and surface geology to atmospheric dynamics and chemistry, from planetary evolution to astrobiology;
- a mission investigating epochs **from early evolution to the present day**;
- a synergistic approach to studying **geological history**, with techniques including nested radar imagery at different resolutions, polarimetry, multispectral emissivity mapping, subsurface sounding and gravity mapping;
- a 'multi-messenger' approach to **geological activity detection**, searching for morphological, thermal, and atmospheric signatures;
- the most comprehensive look yet at **volcanogenic gases in the atmosphere**, mapping key trace gases below, within, and above the cloud layers;
- a **comprehensive scientific payload** of high-heritage instruments spanning ultraviolet, infrared, microwave and high-frequency wavelengths, for synergistic observations of unprecedented spatial, temporal and spectral resolution;
- a **robust mission and science operations plan** showing that the mission can return all of the above diverse observations over all major geological terrain and feature types;
- a mission **combining excellence in European and American expertise** in Venus science & instrumentation, with direct heritage from Cassini, Venus Express, Mars Express, Mars Reconnaissance Orbiter, BepiColombo, JUICE & Magellan.

2 Scientific Objectives

2.1 EnVision mission in context

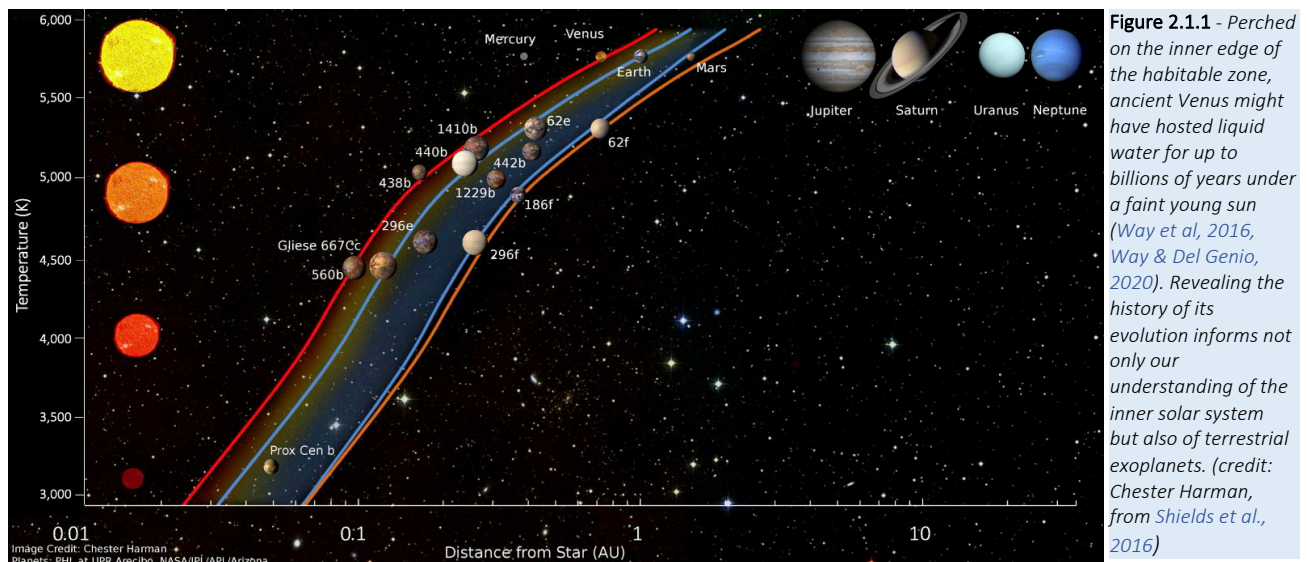
2.1.1 EnVision scientific context

ESA's Cosmic Vision

Why are the terrestrial planets so different? Venus is in many ways the most Earth-like of all our planetary neighbours: its size, bulk composition and distance from the Sun are very similar to those of Earth. Its original atmosphere was probably similar to that of early Earth, with abundant water that might have been liquid at the surface under the young Sun's fainter output (Hamano et al., 2013; Way et al., 2016; Salvador et al., 2017; Way & Del Genio, 2020). Even today, with its global cloud cover, the surface of Venus receives less solar energy than does Earth, so why did a moderate climate ensue here but a catastrophic runaway greenhouse on Venus? How and why did it all go so differently for Venus? What lessons can be learned about the life story of terrestrial planets in general, in this era of discovery of Earth-like exoplanets? Were the radically different evolutionary paths of Earth and Venus driven solely by distance from the Sun, or do internal dynamics, geological activity, volcanic outgassing and weathering also played an important part?

This question is tied to our general understanding of the universe and lies at the heart of ESA's Cosmic Vision program (ESA BR-247, 2005) What are the conditions for planet formation and the emergence of life? How does the Solar System work? Surprisingly little is known about our nearest planetary neighbour, not even the basic sequence and timing of events that formed its dominant surface features. The Magellan mission revealed an enigma: a relatively young surface, rich in apparent geological activity, but with a crater distribution indistinguishable from random (Strom et al., 1994). How can a geologically active surface be reconciled with the global stasis inferred from the apparently random impact crater distribution?

The EnVision mission's investigations of Venus and the evolution of its geology and climate are highly complementary to other Space Science missions. This is particularly true for PLATO, which focusses on terrestrial planets in the habitable zone around sunlike stars, and ARIEL, which will conduct spectroscopy of exoplanetary atmospheres. In fact, most terrestrial planets discovered within the coming decades are likely to be more Venus-like than Earth-like, given the detection bias towards short orbital periods of transit and radial velocity techniques, so EnVision's focus on understanding the inner edge of the habitable zone is particularly relevant.



Diverging evolutionary paths of Earth-like planets

The discoveries of many exoplanets, including terrestrial exoplanets, due to increasingly sensitive methods of discovery and characterisation, make exchange between exoplanetary and planetary scientific communities increasingly necessary. The search for exoplanets is largely motivated by the answers to the questions: Is our solar system common and is there life outside our solar system? Answering these questions requires also understanding the habitability of a planet, i.e. the potential of a planet to develop and maintain a living environment. Venus and Earth formed under very similar conditions and were probably supplied with water in the same way. At some point in their history, the evolution of their surfaces and atmospheres diverged

dramatically. Earth has been continuously habitable since the end of Hadean period (-4.6 to -4 Ga), while Venus' surface became uninhabitable at some point in its history (Lammer et al., 2018). Although at the inner edge of the habitable zone (Figure 2.1.1), Venus could be the type of planet that has changed from a habitable and Earth-like state to an uninhabitable one (Way & Del Genio, 2020), thus providing a natural laboratory for studying the evolution of habitability (Kane et al., 2019).

To this end, many fundamental questions need to be answered. Did Venus have condensed liquid water on its surface, how has its atmosphere evolved over time, and when and why did the runaway greenhouse begin (Figure 2.1.2)? How does Venus lose its heat, how volcanically and tectonically active has Venus been over the last billion years? Has Venus always had a “stagnant-lid”, or was a plate tectonics regime ever present earlier in her history (O'Neill et al., 2007)? What is the composition of the highland tessera terrain, are these regions the oldest rocks exposed on the Venus surface, how oxidised are those rocks and do these surfaces retain evidence of an earlier time when water was more prevalent (Khawja et al., 2020)?

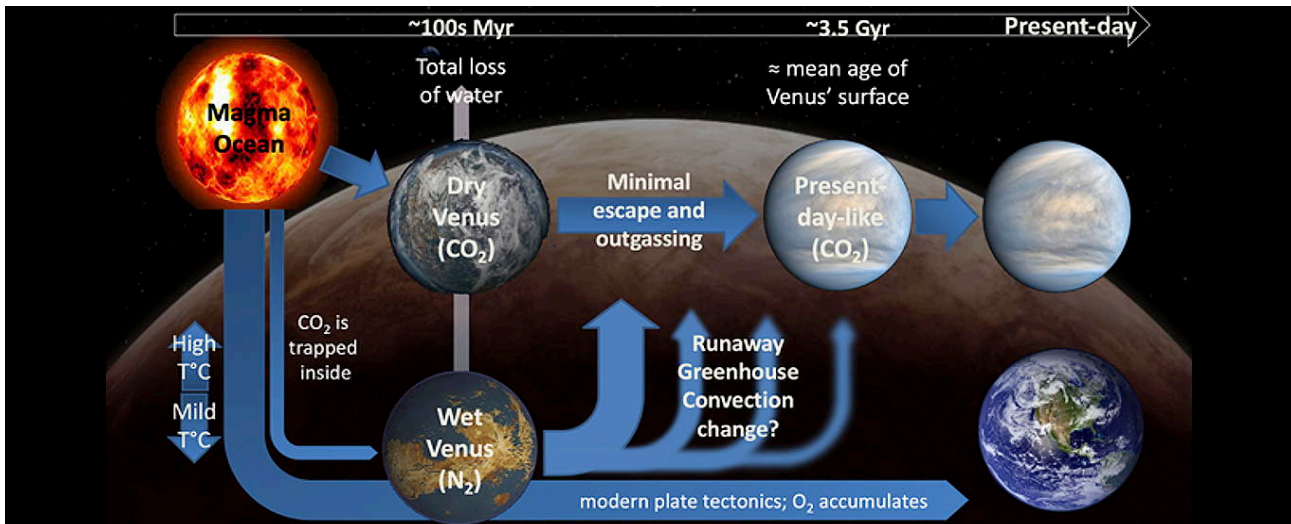


Figure 2.1.2 – Venus shares some striking similarities with Earth; at the same time, it exhibits characteristics that are widely different from that of our own planet. Indeed, it is an example of an active planet that may have followed a radically different evolutionary pathway despite the similar mechanisms at work and probably comparable initial conditions. Understanding Venus’ evolution might be a key to our comprehension of how a planet can become or cease to be habitable. The evolution of Venus is still poorly constrained, partly due to a lack of relevant measurements. Even existing data can prove inconclusive due to their dependence on many interconnected mechanisms. (Kasting 1988; Way et al., 2016; Way & Del Genio, 2020). As a result, there is currently no consensus on the history of Earth’s sister’s surface conditions, with some scenarios involving dry evolutionary pathways, while others suggest a wet past (Gillmann et al., 2009; Massol et al., 2016; Salvador et al., 2017).

2.1.2 Overview of EnVision's top-level science questions

EnVision's overarching science questions are to explore the full range of geoscientific processes operating on Venus. EnVision will investigate Venus from its inner core to its atmosphere at an unprecedented scale of resolution, characterising in particular core and mantle structure, signs of past geologic processes, and looking for evidence of past liquid water. Recent modeling studies strongly suggest that the evolution of the atmosphere and interior of Venus are coupled (Way and Del Genio, 2020; Weller and Kiefer, 2020), emphasizing the need to study the atmosphere, surface, and interior of Venus as a system. EnVision’s three top-level science questions, all of equal priority, are described in the following sections.

History - How have the surface and interior of Venus evolved?

EnVision will **characterise** the sequence of events that generated the regional and global surface features of Venus, determine crustal support mechanisms, mantle and core properties, and characterise the geodynamics framework that controls the release of internal heat over Venus history. It will: (1) determine the styles of volcanic processes which have occurred on Venus, studying the sources, emplacement styles, magma properties and relative ages of different volcanic flows; (2) determine the styles of tectonic deformation that have operated on Venus by studying their surface expression and gravity signatures, and determining their role in planetary heat loss; (3) characterise surface modification processes (impact crater modification, low emissivity/radar bright highlands) to improve our understanding of Venus geochronology; (4) constrain Venus’ internal structure, through measurements of gravity field and tidal response, to constrain the properties and thicknesses of Venus’ crust, mantle and core.

To reconstruct the history of Venus, we must examine its geological record. The cratering record shows that most of Venus’ surface is less than 1 billion years old, but some regions (in particular the tessera highlands) may be considerably older (Byrne et al., 2021). Observations from Magellan data imply a variety of age relationships and long-term activity, with at least some activity in the recent past. There is a non-random

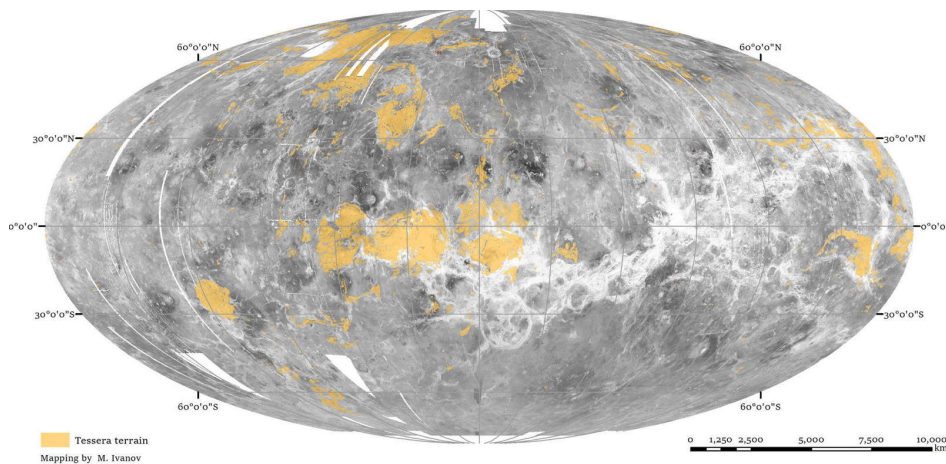


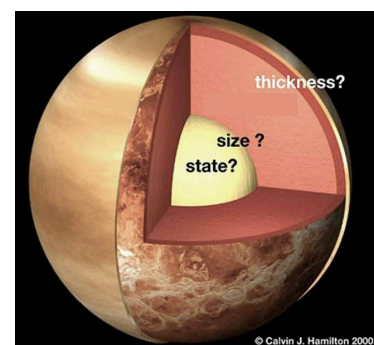
Figure 2.1.3 – In contrast to the basaltic plains, tessera terrain (in yellow) is heavily modified by tectonic deformation. The primary morphologic characteristics of its precursor materials are not readily seen. Tesserae often occur in large high-standing regions that appear older (embayed) than surrounding plains. In these characteristics, tesserae to some degree resemble terrestrial continents (old, high-standing, tectonised massifs), the bulk of which are made of non-basaltic materials. If a non-basaltic component of the crust indeed exists on Venus, tesserae appear to be one of the best candidates.

distribution of topography (the highs particularly are semi-linear features) and an association between geological features and elevation (Stoddard & Jurdy, 2012), such that the uplands are consistently more deformed than the lowlands. The distribution of impact craters is not strictly random either, with recent observations about the degree of crater alteration permitting a wider range of possible recent geological activity (e.g. O'Rourke et al., 2014). How are impact craters modified? Do dark floors form from airfall deposits or magmatism from below?

Constraining the history is critical to understanding when and how Venus was resurfaced, but it is also important to know the nature of that activity. Has there been a systematic change in volcanic style, for example, are canals confined to a past regime or still active today? Were the plains formed from a few massive outpourings in a short period of time or from many thousands of small flows over their entire history? Or were they formed, or modified, in an entirely different way? Venus exhibits perhaps more tectonic deformation even than Earth: what is the role of tectonism in resurfacing the planet? Has the history of tectonic deformation changed over time? How did tesserae, in particular (Figure 2.1.3), accumulate their extraordinary degree of deformation?

Although chemically similar to basalts, the layering observed in the Venera landers images is more akin to sedimentary or pyroclastic bedding, formed by cycles of air fall or ground flow. Based on load carrying capacities derived from the penetrometer and dynamic loads during lander impact, the strength of the surface at the Venera 13 site is similar to that of a dense sand or weak rock. At the Venera 14 and Vega 2 sites the recorded strengths are higher but similar to that of a sedimentary sandstone and less than half that of an average basalt (Marov & Grinspoon, 1998). A major problem is that almost the entire area imaged by each Venera lander sits within a single Magellan image pixel, and their landing position is known to only ~150 km, so that it is impossible to correlate features observed in the lander images with those in Magellan images. Do they represent a surface weathering veneer on otherwise intact lava flows, or thick accumulations of aeolian or pyroclastic deposits? This demonstrates the importance for reconstructing the Venus history not just understanding the emplacement of rock units, but their subsequent transport, modification and weathering processes.

Figure 2.1.4 – Sketch of the interior of Venus, showing the main open questions on its structure. To a first approximation, Venus' interior is generally held to be Earth-like, based on its similar bulk composition and radius. Higher spatial resolution gravity field measurements are needed to better constrain the crustal and lithospheric structure variations, which is essential to understand the geodynamic evolution of the planet. Higher accuracy of the tidal Love number is needed to better constrain the size and state of the core.



To a first approximation, Venus' interior is generally held to be "Earth-like", based on its similar bulk composition and radius; any differences in their evolutionary histories are likely to be reflected in differences in their internal structure. Venus is less dense than expected if it had Earth's bulk composition and its moment of inertia, the most powerful way to constrain the first order radial structure of a planet, is unknown. Indeed, the shape of the planet appears to be unconnected to its rotational rate, which is too small to explain the observed flattening. The rotation rate itself is expected to be variable, responding both to solar tides and to changes in the motion of Venus' massive atmosphere (Cottreau et al., 2011), but the detailed response function, which would constrain internal distribution of mass, has not yet been measured (Figure 2.1.4). The tidal Love number, estimated from Doppler tracking of Magellan and Pioneer Venus Orbiter spacecraft data, is not known with sufficient accuracy to constrain the size or state of the core (Dumoulin et al., 2017). The

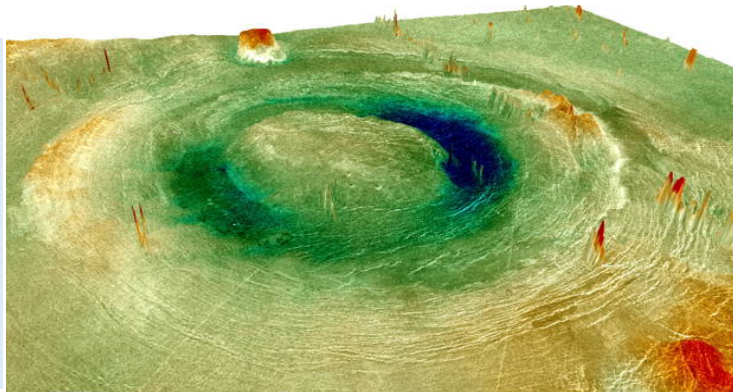
Venera landers returned a number of K, U and Th measurements that imply bulk ratios, and hence internal radiogenic heating rates, comparable with Earth (Namiki & Solomon, 1998). Magellan gravity data are consistent with an organised pattern of mantle convection broadly similar to Earth (see e.g. Smrekar et al., 2018a) but lack the resolution necessary to understand its connection with geological-scale features, such as individual coronae (Figure 2.1.5) or mountain belts. Higher spatial resolution is needed to better constrain the crustal and lithospheric structure variations, which is essential to understand the geodynamic evolution of the planet.

Activity - How geologically active is Venus?

EnVision will **search** for ongoing geological processes and determine whether the planet is active in the present era. It will: (1) constrain the style and distribution of ongoing volcanism on Venus, characterising its morphological, thermal and volatile signatures; (2) assess present era landscape evolution on Venus, on time scales of months to decades, by searching for changes in repeated radar imagery; and so (3) seek to understand the sources and sinks of the key atmospheric volatiles, SO₂ and H₂O.

Venus should be geologically active today. Because Venus is similar in size and composition to Earth, its internal heat is expected to drive mantle convection, and associated volcanic and tectonic activity, to the present day. Venus' geologically young surface, between 700 and 800 Ma old (McKinnon et al. 1997), requires extensive volcanic resurfacing, but it is not clear whether this happens in occasional episodic global-scale resurfacing events (e.g. Strom et al. 1994; Phillips et al. 1992) or whether a more continuous resurfacing occurs. (e.g. Bjornes et al., 2012; O'Rourke et al., 2014). The nature of volcanic and tectonic activity can be used to help distinguish between these different mechanisms of global heat loss: large-scale lunar mare-style flood lava units would be indicative of episodic global or regional resurfacing events that are concentrated in time, with little activity between, whereas widespread, interdigitate, small-scale flow units would be indicative of a more equilibrium resurfacing style (Mueller et al., 2017). Near-IR emissivity mapping from Venus Express found anomalously high emissivities near suspected active volcanoes (Smrekar et al., 2010), interpreted as relatively fresh, as-yet unweathered lava flows. Recent lab-based experiments suggest that the timescale of weathering is days to years, implying that the Venus volcanoes have been active within the last few years, however, the detailed nature of the mineralogy and the weathering processes are still unknown. Further hints of active volcanism were provided by the Venus Monitoring Camera on Venus Express, which observed apparent temporal changes in thermal emission from the surface, consistent with what would be expected from an ongoing volcanic eruption (Shalygin et al., 2005), but this was observed only in one location and, as a monospectral observation, it was not possible to fully discount the possibility of atmospheric influence on the signal.

Figure 2.1.5 – In the absence of global plate tectonics, mantle convection and plume–lithosphere interaction are the main drivers of surface deformation on Venus. Among documented tectonic structures, circular volcano-tectonic features known as coronae may be the clearest surface manifestations of mantle plumes and hold clues to the global Venusian tectonic regime. Yet, the exact processes underlying coronae formation and the reasons for their diverse morphologies remain controversial. This oblique view shows a typical example, located at 082°E, 25°S, is 400 km in diameter across the circumferential fractures, outside a 200 km diameter topographic trough 1100 m below the central high. Magellan SAR image on colourised topography, from -1500 m in blue to +500 m in red.



As well as understanding the nature of geological activity, it is important to understand the tectonic regime associated with this activity. Steep slopes and landslides are common on Venus, implying active uplift, but existing data provide no constraint on current rates of tectonic activity. The surface of Venus is not organised into large plates as on Earth's oceanic plates but appears to be partitioned into areas of low strain bounded by narrow margins of high strain, analogous to continental basins and microplates (Ghail et al., 2019). Are these regions actively created and destroyed, like Earth's oceanic plates, or simply mobilised locally? What is the significance of the global network of elevated rift systems, similar in extent to mid-ocean ridges but very different in appearance? Unique to Venus are coronae, quasi-circular tectonic features, typically 100–500 km across, with a range of associated volcanic feature (Figure 2.1.5). Are coronae the surface expression of active plumes or magmatic intrusions, as found in recent research (Gülcher et al., 2020), or even subduction zones (Davaille et al., 2017)? There is now growing evidence from new models and experiments, of high heat flow, mantle plume evolution and recent volcanic activity, that suggests Venus is currently geodynamically active (D'Incecco et al, 2020, O'Rourke & Smrekar, 2018, Gülcher et al, 2020, Filiberto et al, 2020). Complimentary,

repeated, multi-type and multi-scale observations, are needed to help detect the characteristics of such activity. After the formation of the surface by volcanic and tectonic processes, it is modified by weathering under Venus' extreme atmospheric conditions (high pressure, temperature), meteorite impacts and gravity-driven slope movements (landslides), all of which favour the fragmentation of surface materials. Along with clastic debris from volcanic activity (e.g. pyroclastic materials, Airey, et al, 2015, Campbell et al, 2017, Ghail & Wilson, 2018) these unconsolidated materials would form a layer of regolith subject to further remodeling, transport and deposition by winds. The formation of volcano-sedimentary rocks cannot be excluded locally if these sediments are also subject to compaction by burial, sintering and hypervelocity impacts which favour clast consolidation and accretion (Greeley et al, 1987, Kreslavsky & Bondarenko, 2018). Apparent landslides were observed (Malin, 1992, Greeley et al, 1992) and some evidence for dune fields were found in Magellan data, but these were barely resolved at the 100 m to 200 m spatial resolution of Magellan's imagery. Resolving these features and processes in more detail is critical for understanding Venus' current surface interactions between atmosphere, surface and subsurface and any near-surface activity. Comparative studies on other planetary bodies, combined with analogue and numerical models indicate that a variety of active aeolian bedforms and geomorphological features should be expected on the Venus surface (Claudin, 2006; Lorenz, 2016; Diniega et al, 2017; Neakrase et al., 2017; Bondarenko & Kreslavsky, 2018). Therefore, higher resolution data and more detailed characterisation of the physical properties and mineralogy of the materials are needed to better characterise and understand these processes.

The Magellan radar orbiter revealed snapshots of all of the above processes everywhere on Venus but, without high resolution or repeated same-geometry observations over time, it was impossible to estimate a rate at which these processes might be occurring. As discussed above, Venus Express, despite the atmospheric focus of most of its science goals, provided tantalising hints of active volcanism, including temporal variations of surface temperatures (Shalygin et al., 2015), temporal variations of potentially volcanic sulphur dioxide gas (Marcq et al., 2013), and emissivity anomalies on the flanks of volcanoes (Smrekar et al., 2010). Repeated observations of the surface with the same viewing geometry, and repeated observations of the atmosphere, are thus crucial for addressing this science question, as will be explained in §2.2 and §2.3. Changes can be detected using a range of techniques, of which repeated imagery is one. Repeated and new observations also provide opportunity for searching for changes since previous missions (Magellan, Venus Express) despite different resolution and viewing geometry. So the time scale for the search of change is larger than the mission duration: EnVision's investigations will seek to address the timescales of months; longer timescales of years to decades can be addressed through comparison between EnVision's map (to be obtained between 2035 and 2039) and those of the Magellan radar orbiter active imaging data obtained in 1990-1992.

Climate - How are Venus' atmosphere & climate shaped by geological processes?

EnVision will **characterise** regional and local geological units, to better assess whether Venus once had condensed liquid water on its surface and was thus perhaps hospitable for life in its early history. It will (1) determine the role of geological activity, including both volcanism and surface-atmosphere chemical reactions, in sustaining the volatile and cloud content of the lower atmosphere; (2) assess intrinsic variability and transport of geophysically important volatile species through the atmosphere and clouds of Venus, through measurements below, within, and above the cloud layer, so as to be able to identify signatures of geophysical activity.

If Venus were a newly discovered exoplanet, it would be arguably one of the most Earth-like one yet identified. Not only are its size and bulk density similar to those of Earth; its equilibrium temperature of 227 K is remarkably close to Earth's 255 K, and gives no clue to the hellish temperatures below the clouds. Transit spectroscopy would reveal its CO₂-rich atmosphere and lack of water but otherwise would suggest a very Earth-like world, perhaps similar to what the Earth itself might look like after a runaway greenhouse warming. Understanding how and why the atmospheres of Venus and Earth have evolved so differently is one of the compelling reasons to study Venus, as it directly addresses the question of how our own planet became habitable.

Understanding the evolution of Venus' climate requires understanding of its exchanges with the interior, with the surface and with space. The latter was studied extensively by the Analyzer of Space Plasmas and Energetic Atoms (ASPERA) instrument onboard Venus Express, so EnVision will focus instead on exchanges with the surface and interior. The volatile content of Venus' interior is unknown, but the existence of Venus' sulphuric acid cloud deck (Figure 2.1.6) may indicate that it is still outgassing SO₂ and/or water, or has done so within the past tens of millions of years (Bullock & Grinspoon, 2001). The input of H₂O and SO₂ required by the Bullock & Grinspoon model to maintain the cloud deck corresponds to a magma effusion rate



Figure 2.1.6 – The lower/middle clouds of Venus as imaged by Akatsuki IR2 camera. Dark areas represent thicker clouds; some of these could may result from volcanic plumes of ash or sulphate particulates of present-era volcanic activity. Understanding the evolution of Venus' climate requires understanding of its exchanges with the interior, with the surface. Volcanic effects cannot be identified without understanding the intrinsic background variability of the atmosphere, which will be addressed by EnVision. Surface-atmosphere interactions are therefore a vital boundary condition on the evolution of Venus and its habitability through time. Image credit: JAXA/ISAS/DART/D. Bouic

of only $0.5 \text{ km}^3 \text{ yr}^{-1}$ (assuming a saturated magma source). Sulphur dioxide and water are both seen to be highly variable in Venus' atmosphere (Marcq et al., 2013, 2020; Shao et al., 2020; Encrenaz et al., 2020), but this variability has not yet been linked to volcanic emission. The detection of both H_2O and HDO in volcanic plumes is of particular interest; elevated D/H ratios on Venus have been interpreted as indicating escape of large amounts of water (Donahue et al., 1982), but the D/H ratio of mantle outgassing would affect those calculations. In summary, direct detection of the volatile content of volcanic emission, then, would not only be important for understanding volcanism, but also for understanding the evolution of Venus climate.

The geological record may itself contain clues as to the history of Venus' climate. In particular, rocks such as granite can form only in the presence of liquid water (e.g. Campbell & Taylor, 1983); detection of such rocks in tessera highlands, as hinted at by Venus Express, would suggest that these terrains date back to a time when Venus had extensive liquid water in its mantle and that the Venus' surface was subjected to stronger erosive processes to reveal this rock type at the surface (Khawja et al., 2020), before developing its runaway greenhouse effect. Obtaining compositional data from these areas is therefore critical along with searching for evidence for fluvial or marine processes, including shorelines. Beyond the coupling and

interactions discussed above, though, the most important unknown factor in determining the long-term history of Venus' atmosphere and indeed its habitability, is the history of the solid planet, as it represents the all-important lower boundary condition for the atmosphere. Therefore, all of EnVision's results regarding the history of Venus' geological activity will be important inputs for the reconstruction of Venus' atmospheric history.

2.2 Scientific Objectives

EnVision will investigate both present and past geological activity on Venus, and how its atmospheric, surface and interior processes are linked. The background for EnVision's scientific investigations and strategic knowledge gaps is presented in this section following the lines of three top-level science questions (Activity, History, Climate); expanded in eight science objectives, all of equal priority. A full science traceability matrix is given on pages 40-41.

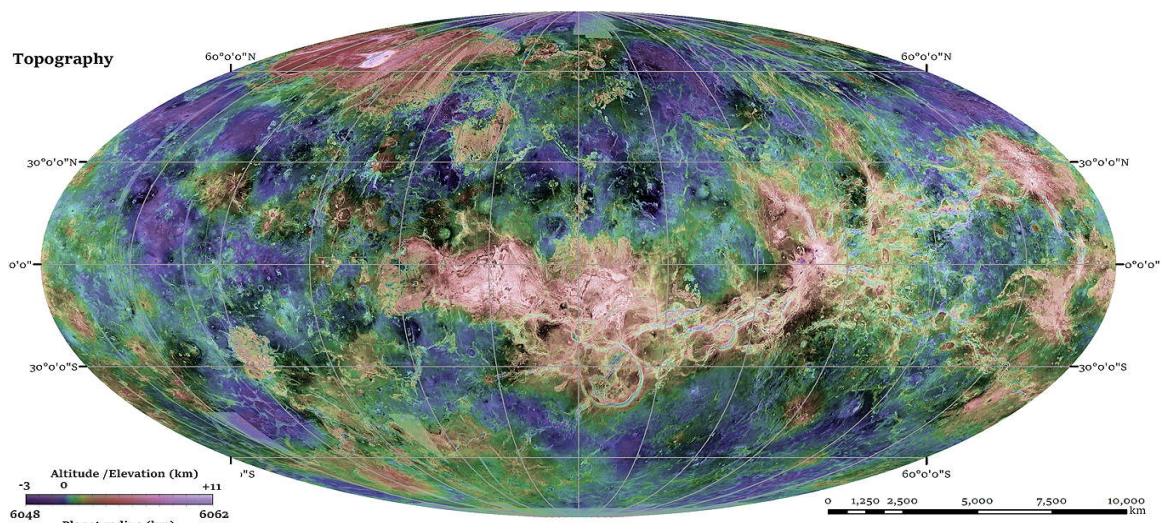


Figure 2.2.1 – Venus global topographic map from Magellan. Like Earth, Venus hosts continent-like structures, volcanic plains, tectonic rifts and mountains. Altimeter derived colour-coded topography is overlain on SAR backscatter image. The majority of what is known about the surface of Venus, its geology and geomorphology, has been derived from this mosaic.

SUMMARY OF ENVISION SCIENCE OBJECTIVES

2.2.1: Understanding Venus' magmatic history

What are the **compositions of volcanic rocks**? Are they all basaltic, or are there substantial volumes of more granitic rocks that would indicate magma formation in the presence of liquid water? Has volcanism been continuous or episodic? What are the **styles of magma emplacement**, and what do they imply about the range of magma emplacement rates?

2.2.2: Understanding Venus' tectonic history

How did the **various types of tectonic structure form**? What is the nature of the forces that produced these features, and what are the magnitudes of the deformation? What do these structures imply about the **evolution of lithospheric thickness and heat flow as a function of time**?

2.2.3: Assessing Venus' surface modification processes

How has the **surface of Venus** been modified since it was formed? In particular, what are the **processes** that have modified and partially filled impact craters? What are the causes of the low emissivity material in some highlands, and what does this imply about weathering processes and possible volatile transport?

2.2.4: Understanding how Venus' interior and surface have evolved

How does the **interior structure of Venus**, with its most important compositional layers, core, mantle and crust, differ from Earth's? What is the **size and physical state** of the core? What is the geodynamic and thermochemical evolution of Venus, the crustal and lithospheric structures of the main volcano-tectonic features (coronae, large volcanoes, ridges, tesserae, rifts)?

2.2.5: Understanding Venus' volcanic activity in the present era

Is Venus the only other terrestrial planet beside Earth that is still **volcanically active** in the present era? What are or have been the styles and distribution of volcanism? Has volcanism changed over time, and is it localised or global? How does volcanism contribute to the volatile cycles on Venus?

2.2.6: Assessing Venus' aeolian activity and mass wasting

What are the mechanisms and processes by which the planet's surface is modified and evolves? Magellan detected **mass-wasting and aeolian features**, such as landslides, dune-fields and wind-streaks; what are their distribution, abundance and geomorphology, and how do they change with time?

2.2.7: Understanding the role of geological activity in Venus' climate evolution

How are **tropospheric and geological processes** coupled on Venus? Do exchanges take place from direct outgassing of volatiles into the lowermost atmosphere, buffering of atmospheric species with surface reservoirs, or aeolian or chemical alteration of surface minerals?

2.2.8: Assessing temporal variations of the Venus atmosphere

How are volatile species, particularly water and sulphur dioxide, transported through the **cloud layers and upper atmosphere**? How much of the variability in and above the clouds is due to intrinsic dynamic variability, and how much is directly or indirectly caused by volcanic activity?

2.2.1 Understanding Venus' magmatic history

What are the **compositions of volcanic rocks**? Are they all basaltic, or are there substantial volumes of more granitic rocks that would indicate magma formation in the presence of liquid water? Has volcanism been continuous or episodic? What are the **styles of magma emplacement**, and what do they imply about the range of magma emplacement rates?

How were volcanic materials emplaced at the surface of Venus?

Volcanic eruptions form and modify much of the surfaces of terrestrial planets. While virtually all surface volcanism on the smaller planets has ended, it is likely that Venus is similar to the Earth in having continued intrusive and extrusive activity. Flow thickness, length, vent structure, and features like channels have long been used to better understand the composition of the erupted magmas and to model eruption rate and duration. These properties in turn point to the nature of heat flow and lithospheric thickness that control the ascent and eruption of gases and magma. It is probable that at least 90% of the surface was formed by effusive volcanic materials, so understanding their physical properties is crucial to the unraveling the geologic history of Venus.

The scale of the associated landforms spans the range from km-scale domes in the plains to shield volcanoes 300-400 km in diameter, vast flow fields up to 1000 km in length and hypothesized lava channels thousands of kilometres long (Figure 2.2.2). Hybrid volcano-tectonic corona features are also surrounded by flow fields hundreds of km in extent. While most of the large volcanic features have terrestrial analogs, evidence of the long-term eruption processes required to form them has often been removed by erosion on Earth. Venus also differs from the Earth in having no plate tectonic mechanism for releasing heat at present, so it is likely that effusive eruptions occur in large pulses from hot, rising mantle plumes, though possibly separated in time by long periods in different locales.

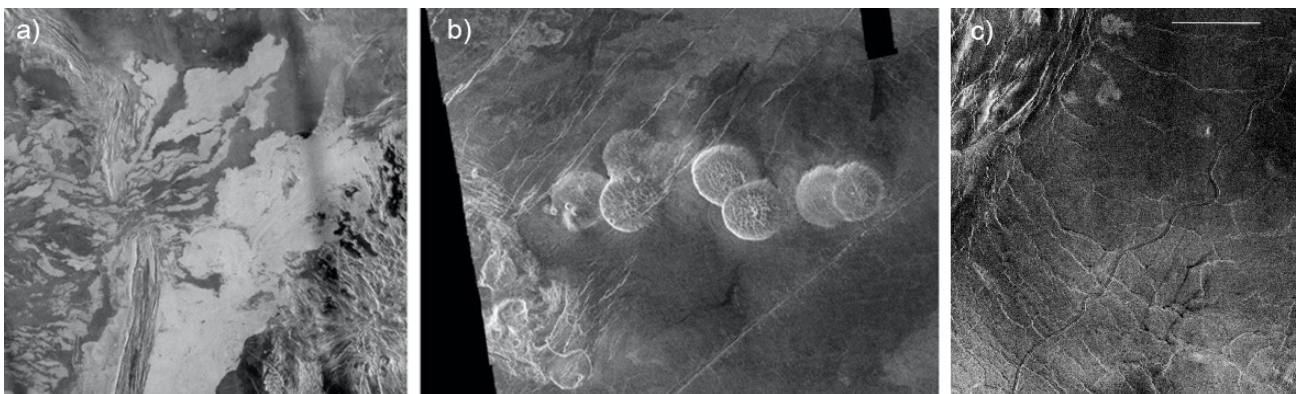


Figure 2.2.2 – (a, left): Flood lavas in Lada Terra are an example of highly fluid magma emplacement. The image is 550 km across. (b, centre): The steep-sided “pancake domes” near Alpha Regio are about 25 km in diameter and are examples of viscous magma emplacement. (c, right): A portion of sinuous canali-type channel Baltis Vallis, which has a total length of 6800 km. The scale bar is 50 km across.

What is the chemical composition of the surface?

The elemental chemical composition of the Venus surface has only been measured in three locations by Soviet Venera and Vega landers. In all three places, the rocks have SiO₂ contents of 45-49 weight %, consistent with a basaltic composition (Treiman et al., 2007). At other landing sites, only K, U, and Th were measured, which is insufficient to chemically classify the rock composition. The presence of basalt on Venus is expected, as basalt is the most common type of igneous rock on Earth, Mars, and the Moon. An important unanswered question is whether Venus has rocks of more evolved composition, such as granites, at its surface (SiO₂ ≥ 56 weight %). This is an important question, because such rocks on Earth form primarily in the presence of liquid water at subduction zones. This is considered a critical question for Venus because finding large volumes of granitic rock would therefore indicate that formation of such rocks by magmatism once occurred in the presence of abundant liquid water (Campbell and Taylor, 1983), which would be an extremely important constraint on the geological and climatological evolution of Venus. Because granite is less dense than basalt, regions with substantial granite in the crust would most likely be topographically elevated. Thus, regions of tesserae, as well as the mountain belts of Ishtar Terra, are widely considered as the most likely places to search for granitic rocks on Venus (Dyar et al., 2020).

Composition of the surface is also essential to understand weathering and oxidation mechanisms that could have an important effect on the evolution of the atmosphere and climate of Venus. At present, those effects may be considered as secondary, due to the purported low diffusion speed of oxygen into solid basaltic material (Wendlandt, 1991). However, the entire mechanism is poorly constrained and a number of parameters (i.e.

morphology of lava flows, cooling times, volume of produced lava) can greatly improve our understanding of weathering and oxidation mechanisms (Gillmann et al., 2020).

2.2.2 Understanding Venus' tectonic history

How did the **various types of tectonic structure form**? What is the nature of the forces that produced these features, and what are the magnitudes of the deformation? What do these structures imply about the **evolution of lithospheric thickness and heat flow as a function of time**?

How do tectonic structures form on Venus?

Earth has three fundamental types of tectonic structures: compressional, extensional and strike-slip. Predominantly vertical motions can be due to compressional deformation, forming thrust faults and folds, as exemplified by terrestrial mountain belts. Vertical motions can also be due to extensional deformation, producing rift systems such as the East African Rift. Finally, predominantly horizontal motions produce lateral motion at strike-slip faults, such as the San Andreas Fault in California. All three types of structure are present on Venus. Mountain belts occur in Ishtar Terra and reach elevations of 8-11 km, the highest on Venus. They are likely a product of compressional deformation producing thick crust and reflect an epoch (possibly in the geologic past) when Venus had a mobile surface. Tesserae are characterised by highly elevated topography, small-scale surface roughness and multiple sets of cross-cutting tectonic structures (Figure 2.2.3) and appear to represent areas of intense, past tectonism. The formational models to explain such high, complex and strained terrain are still the subject of much debate and uncertainty: horizontal convergence, extension, mantle upwelling, sub-crustal flow, crustal underplating, sub-crustal rejuvenation, crustal plateau formation, diapiric intrusion, gravitational sliding and relaxation, or all of these? (Hansen & Willis, 1996; Ivanov & Head, 2011).

Lesser amounts of compression are found in the ridge belts and wrinkle ridges of the vast plains on Venus. Extension has produced rift systems in several places on Venus, including Guor Linea in Western Eistla Regio and Devana Chasma in Beta Regio and is likely associated with regions of upwelling mantle convection (e.g., Kiefer and Swafford, 2006). Although the Magellan

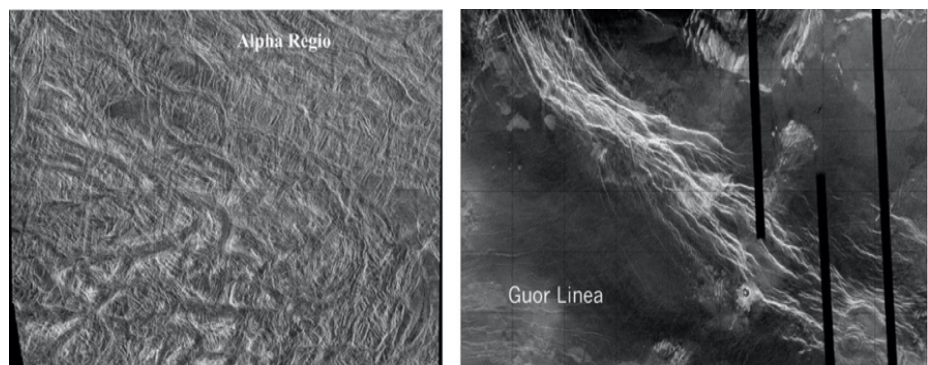


Figure 2.2.3 – (a, left): A tessera in Alpha Regio. Image is 290 km across. (b, right): Guor Linea in Western Eistla Regio is a rift system formed by extension and stretching of the crust. Image is 900 km across.

mission provided a first-order overview of the types of tectonic structures on Venus, the limited resolution of its radar imagery and topography inhibits our ability to quantitatively interpret the tectonic evolution of Venus. EnVision's much sharper view is the necessary next step to understanding the geologic evolution of Venus.

How has lithosphere thickness affected tectonism? What does thickness imply about heat flow?

The lithosphere is the outermost mechanical layer of a planet; it is colder and therefore stronger than deeper layers. The thickness of the lithosphere has a strong effect on the style of tectonic deformation, including the characteristic spacing between tectonic structures. Tesserae have closely spaced fault systems (Figure 2.2.3a), indicating that the lithosphere was thin and the heat flow out of Venus's interior was high when the tesserae formed (Brown and Grimm, 1999). Other tectonic units have more broadly spaced tectonic structures, implying thicker lithospheres and lower heat flow.

2.2.3 Assessing Venus' surface modification processes

How has the **surface of Venus** been modified since it was formed? In particular, what are the **processes** that have modified and partially filled impact craters? What are the causes of the low emissivity material in some highlands, and what does this imply about weathering processes and possible volatile transport?

What are impact crater modification processes?

The impact of asteroids and comets on the surface of Venus produces impact craters. Venus has only about 950 recognizable craters on its surface, far fewer than on the Moon or Mars. This indicates that Venus has been resurfaced relatively recently in its history. However, there is considerable debate about the timing and nature of this resurfacing process, with proposals ranging from a short, catastrophic resurfacing event a few hundred million years ago to gradual and continuous resurfacing (see review by McKinnon et al., 1997). Indi-

vidual craters show a range of morphologies ranging from pristine to degraded (Figure 2.2.4). More detailed imaging, SRS sounding and higher resolution topography data will constrain the processes that have modified or obliterated craters on Venus and the thickness of material that have apparently filled them.

What do low microwave emissivity/radar-bright terrains reveal about Venus' modern environment?

The Magellan radar has revealed that some areas on Venus display anomalously low microwave emissivity and high radar reflectivity. These regions are primarily located at high elevations (> 2 km) (Pettengill et al., 1992, 1996), but not all highlands show this anomalous behavior. The low emissivity may be related with very large dielectric constants, as high as 80 (for comparison, most planetary crusts have dielectric constant from 3 to 10 and Venusian plains, the most extensive geologic unit on the planet, exhibit a dielectric constant in the range 4-5, consistent with a moderately dense basalt surface layer). In the absence of liquid water (which is known for its high dielectric constant) such high values are puzzling; possible explanations for the high-altitude "snow-line" in Venus include cold trapping of exotic volatile species, or yet unidentified weathering reactions.

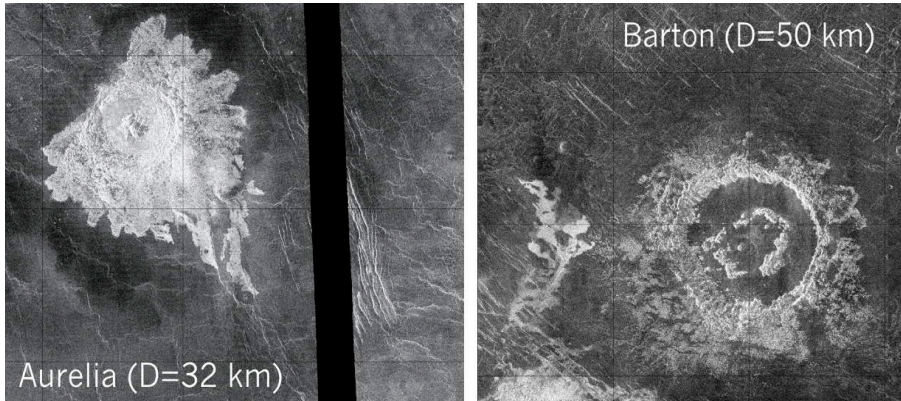


Figure 2.2.4 – (a, left): Crater Aurelia (diameter 32 km) is interpreted as a pristine impact crater. It has a rough (radar bright) floor and ejecta blanket. (b, right): Crater Barton (diameter 50 km) is interpreted as a modified crater. It has a smooth (radar dark) floor suggestive of post-impact volcanic filling. The ejecta blanket is also embayed with later radar dark material, which is also consistent with post-impact lava flooding outside the crater rim.

Among the proposed unusually high dielectric material candidates are ferroelectric substances (e.g. chlorapatite) (Arvidson et al., 1994; Shepard et al., 1994; Treiman et al., 2016) and "metallic frosts" (e.g. volatile metal halides and sulfides) transported from the "hot" plains to the "cool" highlands where they condensate forming a surficial coating (Brackett et al., 1995).

It is important, however, to highlight that the estimation

of the dielectric constant of highlands from the measured backscatter and emissivity relies on models that do not account well for multiple and volume scatterings. While it is true that many arguments are in favor of the dominance of surface scattering in the highlands, volume scattering due to inclusions embedded in a low-loss substrate could also well explain the observed anomalous microwave properties without requiring the presence of a high dielectric constant material. Furthermore, some highlands across Venus (e.g. Ishtar, Ovda and Maat) do not display anomalous backscatter and emission properties. In particular, some lava flows on Maat Mons (1.5°N, 1.94°E) do not exhibit a clear "snow-line" (Campbell, 1994). This may reflect different rock or atmosphere compositions perhaps implying a slow reaction process (or infrequent frosting) that has yet to affect these flows. Better characterising the highlands and, particularly, improving the topographic resolution of the bounding elevations, will provide insights into rock mineralogy and atmospheric sinks in the modern Venus environment.

2.2.4 Understanding how Venus' interior and surface have evolved

How does the **interior structure of Venus**, with its most important compositional layers, core, mantle and crust, differ from Earth's? What is the **size** and **physical state** of the core? What is the geodynamic and thermochemical evolution of Venus, the crustal and lithospheric structures of the main volcano-tectonic features (coronae, large volcanoes, ridges, tesserae, rifts)?

The interior structure of a planet and the driving forces of tectonism and volcanism are all connected by its inner thermal 'engine'. The effectiveness of this engine determines the cooling behaviour of a planet and controls the planet's heat budget, which in turn has a strong influence on the evolution of the magnetic field, the atmospheric evolution through volatile outgassing during volcanism and finally the time of volcanic activity; phases of strong cooling and volcanic activity cause the temperature of the silicate to fall below its melting point. There is a longer phase of inactivity until the system can heat up again through radioactive heat sources - or not. The thermal engine seems to be particularly complex in the case of Venus as can be seen at the surface with its various tectonic and volcanic features. A better understanding of the interior structure and the dynamic processes will help us to better understand the planetary thermal engine as a whole and how it can influence a planet's habitability.

The heat engine in Venus' interior: what are the driving forces for volcanism and tectonism?

On Earth, plate tectonics is the dominant present-day heat loss mechanism. On Io, and possibly on the early Earth, heat was predominantly transported by magmatic eruptions. Indeed, crust formation is another process associated with effective heat transport that cools the interior of the planet. However, at the root of these distinctions, it is interior dynamics that essentially governs the cooling of a planet. Typically, a distinction is made between two different mantle dynamic regimes on terrestrial planets: on one hand, the so-called stagnant lid convection, and on the other, mobile lid convection or plate tectonics that allows much more efficient heat transport. Stagnant lid convection represents a heat transport mechanism much less effective. It shows different tectonic characteristics than the plate tectonic regime on Earth. Internal dynamics can also cause surface stresses and thus tectonic structures on the planetary surface. Different convection regimes will lead to different tectonic characteristics. As a result, it is expected that planetary surfaces reflect their inner dynamics.

On Venus, mode(s) of heat transport and their possible evolution over time remains poorly understood (Figure 2.2.5). Its surface indicates that the tectonic regime could be much more complicated than a simple stagnant lid or may have changed over the course of evolution. The present dynamic regime of Venus seems to be consistent with convection underneath a stagnant lid. However, in some locations, this lid does not seem to be entirely 'stable'. Instead, a so-called sluggish lid could be formed in some places, which may be an instability of the lower crust like a delamination or the beginning of a subduction event (akin to plate tectonics), possibly connected to upwelling mantle plumes (Gerya et al., 2015; Davaille et al., 2017). Analyses of gravitational and topographic data suggest that Venus has a comparable number of active large mantle plumes as Earth, as well as many hundreds of smaller active plumes (Smrekar and Phillips, 1991). This mechanism – if existent on Venus - would also support the hypothesis of plume-induced subduction, which is being discussed for the initiation of plate tectonics on early Earth (Gerya et al. 2015).

In addition to these mantle dynamics features, the surface of Venus seems to have been resurfaced by volcanism within the last 500 million to a billion years. The nature and duration of this volcanic activity and the associated tectonic style(s) are however unclear. Currently discussed evolution scenarios in the literature include (i) episodic catastrophic resurfacing (Parmentier and Hess, 1992; Turcotte 1993, 1995; Armann and Tackley, 2012), (ii) gradual decay of volcanism over time in a stagnant lid regime but also (iii) mixed forms and transitions between the different tectonic regimes, i.e. stagnant lid regime, mobile lid regime, episodic regime and transitional regime (e.g., Gillmann and Tackley, 2014; Weller and Lenardic, 2018; Weller and Kiefer 2020). In this latter case resurfacing is likely limited to certain regions, i.e. it is not global but results in multiple localised resurfacing and melting events (Noack et al., 2012; Weller and Kiefer, 2020). A key parameter controlling the tectonic regime may be surface temperature, which is influenced by the atmosphere evolution and thus by the coupling between interior and the atmosphere (Gillmann and Tackley, 2014).

How does the interior structure of Venus differ from Earth's?

Knowledge of the interior structure with its most important compositional layers, i.e. core, mantle and crust, is essential for a better understanding of the formation and evolution of a planet. For one, the size of these layers provides constraints about the bulk composition of Venus. Previous models about the bulk mantle and crust composition are based on cosmochemical assumptions (Fegley, 2014 for review) and show a 500 km uncertainty in the size of the core to fit the observed mass and radius of Venus (Dumoulin et al., 2017). The uncertainty is even greater if one assumes that the core of Venus can also have a different composition than the Earth's core, in particular in the concentration of its light-alloying elements. The size of the core, however, can influence the convection structure in the mantle and thus also the distribution of volcanism at the surface (Breuer and Moore, 2015). On the other hand, the present-day interior structure with its main chemical layers shows the product of the processes that have shaped the planet so far. This starts from early metal-silicate

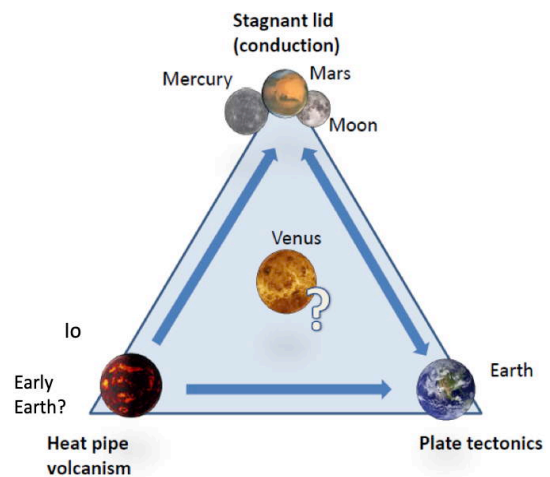


Figure 2.2.5 – Heat loss on the terrestrial planets occurs in three basic ways. Mars, Mercury, and the Moon lose their heat by thermal conduction through a thick lithosphere. On Earth, mantle convection and plate tectonics is the dominant present-day heat loss mechanism. On Io, and possibly on the early Earth ("Hadean"), heat transport was predominantly by magmatic eruptions. On Venus, the mode(s) of heat transport and their possible evolution over time remains poorly known. A better understanding of the interior structure and the dynamic processes will help us to better understand the planetary thermal engine as a whole and how it can influence a planet's habitability.

differentiation to form the iron-rich core and continues with silicate-silicate differentiation to form the silicate crust by magmatism. Core formation is expected to have occurred very early in the first ten million to hundred million years (e.g., [Kleine et al., 2002](#)) and provides also the link to an internal magnetic field that can be generated in an iron-rich fluid core. For Venus core, previous measurements do not even allow us to determine the state of the core, i.e. whether it is solid or liquid today ([Dumoulin et al., 2017](#)) – an important piece of information for the understanding of both thermal and magnetic field evolution. Crust formation on the other hand is typically a longstanding process that can last throughout the entire planetary evolution as it is observed on Earth or is limited to certain periods during the evolution as suggested for instance for Mercury, Mars and the Moon.

2.2.5 Understanding Venus' volcanic activity in the present era

Is Venus the only other terrestrial planet beside Earth that is still **volcanically active** in the present era? What are or have been the styles and distribution of volcanism? Has volcanism changed over time, and is it localised or global? How does volcanism contribute to the volatile cycles on Venus?

How does volcanic activity contribute to the planetary heat budget?

As on Earth, internal heat is expected to drive mantle convection, and thus the associated volcanism and tectonism, but a lack of understanding of how the driving forces are organised coupled with a lack of observations over time, makes estimating of the planet's heat budget challenging. Venus' apparently uniformly young surface suggests extensive volcanic resurfacing, although it is not clear whether resurfacing is periodic and catastrophic, or semi-continuous and localised, and this hinders estimation of the levels of activity and volcanic eruption. The detection and better characterisation of current volcanic and tectonic activity should help distinguish between these styles and inform models of heat exchange.

The current rate of volcanic activity on Venus is unknown; only crude, highly underconstrained estimates have been proposed. More specifically, measurements from VEx/VIRTIS weakly constrained the Venus extrusive volcanism rate to $<300 \text{ km}^3/\text{yr}$ ([Mueller et al., 2017](#)) – an improbable factor of more than ten times larger than Earth (*ca* $20 \text{ km}^3/\text{yr}$) chiefly because VEx/VIRTIS coverage was not optimised for detection of volcanic activity. [Mueller et al., \(2017\)](#) also estimate that a new imaging dataset that has 20 times higher SNR than VIRTIS and similar total coverage as VIRTIS – both conditions which will be satisfied by the EnVision VenSpec-M investigations – would have a high likelihood ($>75\%$) of observing at least one eruption at rates of volcanism of $10 \text{ km}^3/\text{yr}$ with conservative assumptions on flow brightness. This calculation relies on a great many assumptions about eruptive magnitude, duration and style but in any case provides a framework for interpreting any observations of volcanic activity, which will be updated and refined using EnVision's observations of past volcanism.

The absence of reported change detection in Magellan imagery has been interpreted as indicating a volcanism rate smaller than $10 \text{ km}^3/\text{yr}$ ([Lorenz, 2015](#)) but this estimate remains a weak constraint because Magellan repeat imagery was not optimised for change detection, having widely varying look angles between repeat observations. EnVision will obtain repeated radar imagery either with the same look angle, or a small look angle difference of typically 5 deg between stereo pairs used for topography determination; this repeat imagery with small look angle difference (and higher spatial resolution) will offer far better sensitivity to surface change than was obtainable with Magellan.

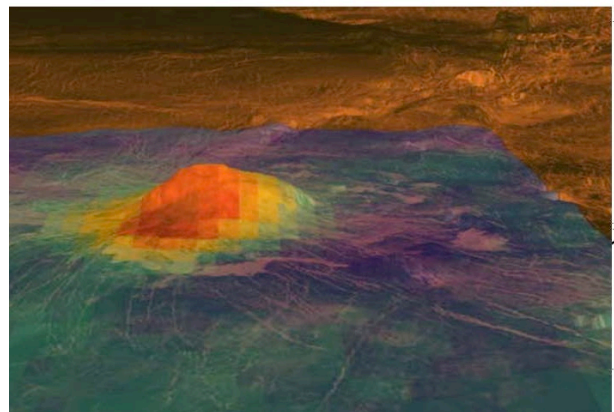


Figure 2.2.6 – Surface brightness temperature measured by VIRTIS/Venus Express on the volcanic peak Idunn Mons in the Imdr Regio area of Venus. High emissivity (in red-orange) corresponds to compositional variations possibly caused by less-weathered lava flows, which appear against the blue-purple background of lower emissivity rocks. Image: © NASA/JPL-Caltech/ESA.

There have been several relatively recent studies of transient hotspots in data from Venus Monitoring Camera (VMC) and VIRTIS/VeX data, see [Figure 2.2.6](#). Additionally, Magellan imagery of parts of Ganiki Chasma and Sitwell Crater show parabola of radar-dark (fine grained) material where there are also transient bright spots. These areas show evidence of lava flows which have flowed over rift fractures and faults, as well as faults cutting across very young lava flows, and lava flows on top of dark parabola materials. Such observations strongly support the interpretation of currently active volcanic eruptions.

Improving estimates of the current rate of volcanic effusion, even to an order of magnitude better than current understanding (i.e. to within $1 \text{ km}^3/\text{yr}$), would help to address the outstanding question of whether resurfacing on Venus is continuous, or episodic. For instance, in an equilibrium resurfacing model, proposed volcanism rates could vary widely from a minimum of $0.5 \text{ km}^3/\text{yr}$ to $200 \text{ km}^3/\text{yr}$ (Turcotte 1989). If resurfacing instead occurs in episodic, catastrophic episodes, then periods of much smaller or much greater volcanic activity are possible. Importantly, such assessments of volcanic activity would also help to understand the volatile budget of the Venus atmosphere. Nine large volcanic topographic rises have been studied (Stofan et al., 1995), each typically 1000 km in diameter, and are thought to be associated with large-scale mantle upwellings; such rises are expected to have increased rates of volcanism, and this makes them an important focus in search for active volcanism. Several studies have presented compelling evidence that volcanism (and tectonic) processes, at Imdr, Themis, Dione and Atla Regio, are geologically recent, possibly as young as $250,000 \text{ yr}$ (D’Incecco et al. 2020, Filiberto et al. 2020, Smrekar et al., 2010). Such areas (and possibly others) are thus expected to be currently active. Repeat imaging and emissivity measurements, and high-resolution imaging, are needed across such key sites to assist in constraining levels of activity and informing current models of the Venus heat budget.

Venus lacks a system of plate tectonics comparable to Earth and therefore, must have a thick lithosphere to support its range of topography. If Venus has similar radiogenic heat production rate as Earth, the heat would require either a transport mechanism other than plate tectonics and conduction or accumulation in the interior. The rate of magmatism required to transport this heat through the lithosphere is on the order of $200 \text{ km}^3/\text{yr}$. Fractionation of heat producing elements into the crust may reduce the required rate of magmatism to $90 \text{ km}^3/\text{yr}$ (Spohn, 1991). Armann and Tackley (2012) include the heat budget in a numerical model of mantle dynamics allowing for episodic behavior. They find rates of magmatism on the order of $10^3 \text{ km}^3/\text{yr}$ in 150 Myr long episodes of foundering lithosphere and rates on the order of $50 \text{ km}^3/\text{yr}$ in periods of stable lithosphere lasting approximately 0.5 Gyr . It is unclear how much of this magmatism contributes to extrusive, directly observable volcanism. The ratio of intrusive to extrusive volcanism is estimated to be 5 to 1 for basaltic crust on Earth, but this might be different for the higher temperature and less mobile lithosphere of Venus.

How does active volcanism contribute to the volatile cycle on Venus?

The presence of CO_2 , N_2 , SO_2 , HCl and HF gases in the Venus atmosphere is taken as key evidence of active volcanism and degassing (Figure 2.2.7). The cycling of such volatiles, between interior and Venusian atmosphere, may be episodic and is thought to be closely related to resurfacing events. Some volatiles (S, Cl) may decline in content over time, through weathering and escape from the upper atmosphere, until the next resurfacing event. Others that do not react with rocks (C, N, and Ne), or are not lost from the clouds, may accumulate over time. Multi-temporal and detailed atmospheric characterisation carried out by the VenSpec suite, will provide better understanding of Venusian volatile cycles, including the potential link to volcanism.

The main obstacle in the search for active volcanism with VIRTIS was the low signal-to-noise ratio of the imaging instruments of Venus Express. Improved signal-to-noise

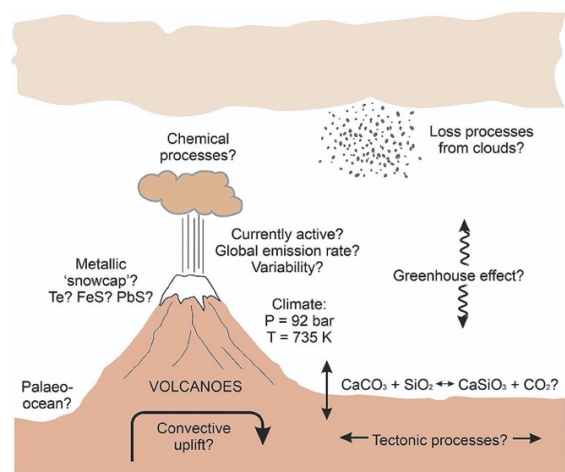


Figure 2.2.7 – Chemical cycling of volatiles in the Venus system between interior, surface and atmosphere (modified after Coustenis et al., 2018).

ratio could detect less intense eruptions, because the signature is proportional to effusion rate. Thus, increasing the signal-to-noise ratio from 16 (VIRTIS) by a factor of at least 20 could possibly detect flows with $50 \text{ m}^3 \text{ s}^{-1}$, a value more frequently achieved by Earth eruptions. Multiple observation of the same surface per day provides repeat coverage for short-lived thermal signatures, therefore greatly increasing the reliability of any detection.

2.2.6 Assessing Venus' aeolian activity and mass wasting

What are the mechanisms and processes by which the planet's surface is modified and evolves? Magellan detected **mass-wasting and aeolian features**, such as landslides, dune-fields and wind-streaks; what are their distribution, abundance and geomorphology, and how do they change with time?

After formation, any terrestrial planet's surface interacts with the atmosphere (and other volatiles present) and responds to a variety of stresses; it is then modified by a range of processes, such as gravity-driven mass-

movements (e.g., landslides and slumps), erosion and deposition, and by active chemical weathering, and evolves over time. Providing constraint on the distribution, scales and effects of these processes is vital to understanding the mechanisms and rates of interior, surface and atmospheric interactions on any planet, and is critical for understanding Venus' geological timeline.

What evidence is there of active physical and chemical landscape change?

Landscape evolution refers to processes which modify the morphology of a planet's surface, in particular gravity-driven mass-wasting processes such as landslides and slumps. Mass-wasting is a ubiquitous geomorphological process operating on any planetary body with gravity, and such features are observed on Earth, the Moon, Mercury, Venus, Mars, icy satellites, comets and asteroids. Magellan's low-resolution radar imagery provided the first evidence of mass-movement on Venus in the form of large-scale slope failures: "rock slumps, rock and/or block slides, rock avalanches, debris avalanches, and possibly debris flows are seen in areas of high relief and steep slope gradients" (Malin, 1992, Figure 2.2.8a). However, the different view angles of repeat passes made correlation difficult and these detections are in some cases tenuous. Multi-temporal observations of mass-wasting are essential for time constraints but are limited to Earth and a handful of cases on Mars. This lack prevents the understanding of the rates, frequencies and triggers of mass-wasting occurrences in our Solar System. Repeated imaging at higher resolution, over short time-scales (years to decades) is needed to improve understanding of the scales and character of geodynamism on Venus.

Magellan's imagery also provided evidence for two dune fields (Greeley et al., 1992; 1995) and indirect evidence for putative 'micro-dunes' (Weitz et al., 1994) that were not resolved by the 100 - 200 m spatial resolution of Magellan's imagery. The surface winds evidenced by these dune fields and by wind streaks and debris fans (downwind of impact craters) are likely to be important agents of aeolian geomorphological change, but data of higher spatial and temporal resolution, and the ability to distinguish loose from consolidated surface materials, are needed to characterise them. Planetary bodies (Earth, Mars, Titan and Venus), including those with extremely tenuous atmosphere, such as Pluto and comet 67P, have been shown to exhibit many aeolian landforms, such as dunes and wind-streaks (see Figure 2.2.8a) but the significance of aeolian landscape change in planetary sciences has, until recently, been under-appreciated. In particular, comparison of dune migration rates on Earth and Mars, made possible by multi-temporal, very high-resolution imagery (cm to m), has revealed that these are, in general, lower by up to 1 m yr⁻¹ on Mars than on Earth (Bridges et al., 2012).

Lastly, near infrared (nIR) thermal emissivity mapping, from Venus Express, detected anomalously high emissivities near suspected active volcanoes, and these have been interpreted as relatively fresh, as-yet unweathered lava flows, but the nature of the mineralogy and the weathering processes are still unknown.

What are the nature, distribution and range of sedimentary surface modification processes?

On Venus fine-grained sediments are likely produced by impact cratering and weathering. Even if these are not volumetrically large, sediments are likely widespread, covering a large fraction of the surface; aeolian erosion and deposition may be important processes at the Venus surface.

Indeed, despite low surface wind velocities (0.25-1.0 ms⁻¹), as recorded by probes (Lorenz, 2016), and thanks to the high atmospheric pressure (~90 bars), the transport of clastic material is possible by creep and saltation processes (e.g. Marshall & Greeley, 1992; Greeley & Ardvison, 1990), and thus dunes may be widespread on Venus but with typical feature sizes < 100 m, below the limit of Magellan's SAR image resolution. From

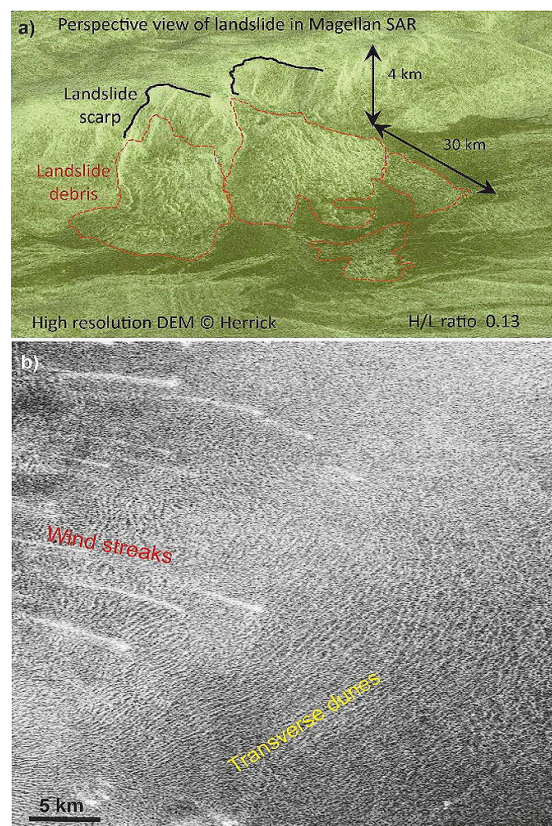


Figure 2.2.8 – Surface geomorphological features imaged by Magellan. (a, top): Perspective view of two large landslides or rock/block avalanches projected on DEM data generated by R. Herrick, Malin (1992); and (b, bottom): lowlands of Al-Uzza Undae showing subtle NE-SW-trending curvilinear features interpreted as transverse dunes, and bright SE-NW-trending wind-streaks. Kreslavsky and Bondarenko (2017).

experimental modelling, Venus' aeolian landforms are expected to form under conditions which lie between 'sub-marine' and 'desert' environments on Earth (Figures 2.2.9b & 2.2.9c) (Claudin et al., 2006, Neakrase et al., 2017). Venus' plains may also harbor many 'micro-dunes' or small-scale ripple-like aeolian landforms. Fine grained material may also be trapped behind topographic obstacles, forming wind-streaks, and may also cause abrasion leading to wind-faceted pebbles or ventifacts. Wind-streaks and debris-fans (downwind of impact craters) are relatively large-scale features on Venus (km to tens of km in length) and they are commonly observed in Magellan images (Figure 2.2.8b) (Greeley et al., 1992, 1995; Kreslavsky and Bondarenko, 2017).

Whilst impact cratering is likely the main process behind sediment production on Venus, the planet's hot, dense and highly oxidizing atmospheric conditions are likely to cause intense chemical weathering of surface materials, making them vulnerable. Associated with impacts, landslides and tectonic activity, these fragmented and unconsolidated weathered materials are seen to accumulate at the bases of slopes and are locally redistributed by winds into lowlands where they may form dune-fields, for example.

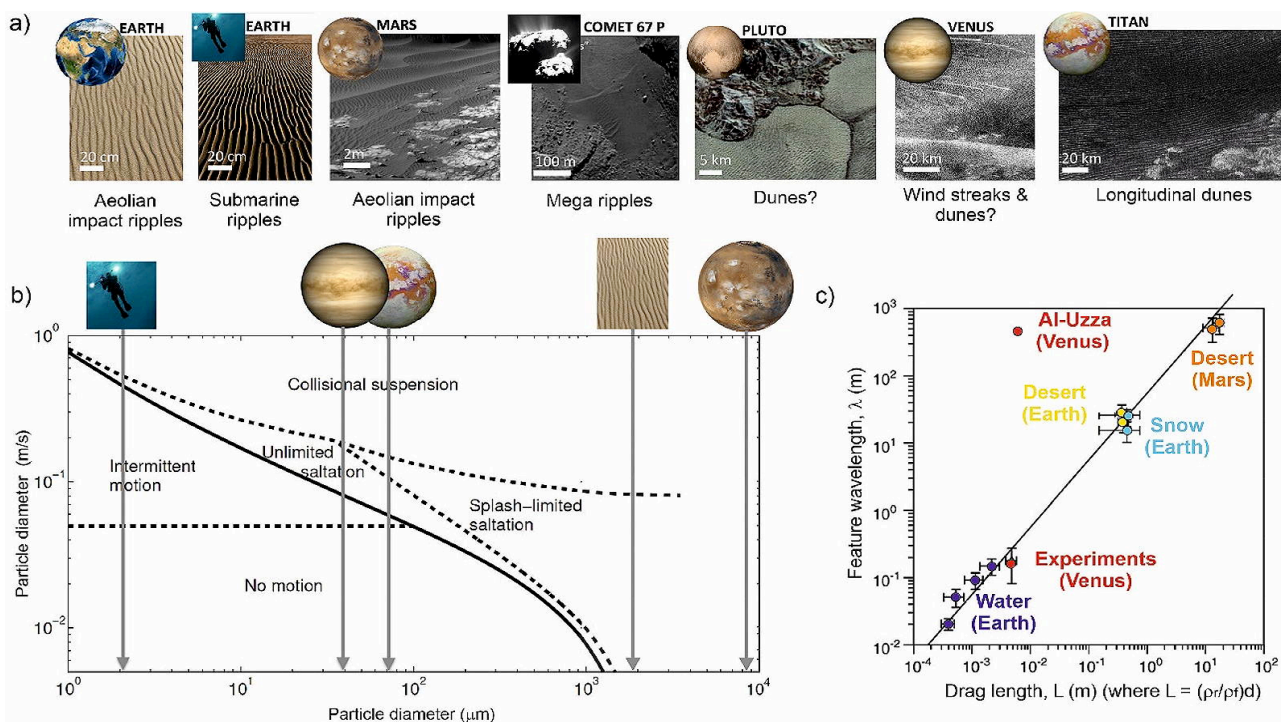


Figure 2.2.9 – (a, top): Examples of sedimentary bedforms on various planetary bodies; (b, bottom left): Regimes and processes of sedimentary transport placing likely Venus aeolian environment in its context between submarine Earth and aeolian Earth and Mars; and (c, bottom right): scales of various sedimentary transport regimes in operation, showing expected scales of dune formation on Venus. Modified after Duran et al., (2019), Claudin and Andreotti (2006), Greeley et al. (1984), Neakrase et al. (2017) and Carpy et al. (2020).

Lastly, the existence of sedimentary or volcano-sedimentary (i.e. pyroclastic) rocks is not excluded on the Venusian surface. We would assume that potentially large accumulations of clastic material, derived from impact ejecta, explosive volcanism and landslides, are subject to diagenesis due to burial or by sintering of fines under the high temperatures at the Venus surface. Many of the Venera landers images indicate a planetary surface of flat-lying, layered rocks. *In-situ* Unconfined Compressive Stress (UCS) testing measurements from Venera 13 & 14 and Vega 2 suggest strengths of less than half of an average basalt and more like those of a sandstone (Basilevsky et al., 1985). Active research on the Venus weathering environment (Marshall et al. 1991, Waltham et al., 2008, Treiman et Schwenger, 2009; Aveline et al., 2011; Nealley et al., 2017; Port et al., 2020) leads us to expect the lava flows of the Venus plains to be accompanied by sedimentary deposits and that these are likely to be in various states of consolidation.

2.2.7 Understanding the role of geological activity in Venus' climate evolution

How are **tropospheric and geological processes** coupled on Venus? Do exchanges take place from direct outgassing of volatiles into the lowermost atmosphere, buffering of atmospheric species with surface reservoirs, or aeolian or chemical alteration of surface minerals?

Venus, Earth and Mars started life as siblings, born at around the same time in similar parts of the protoplanetary disk. After accretion, during the magma ocean phase, they would have acquired a dense protoatmosphere dominated by carbon dioxide and steam (see Figure 2.1.2). Venus has a highly enriched D/H

ratio, which suggests that it has lost a lot of its primordial water; however, it is not clear whether this water was lost from a steam atmosphere phase or from a liquid ocean phase.

To understand the long-term climate evolution of Venus we need to establish (1) whether there is any morphological and compositional evidence of an epoch with abundant liquid water on the surface; (2) whether Venus is geologically active now, and whether this is a continuous or episodic style, to constrain interior-atmosphere exchange throughout history; (3) search for atmospheric evidence of present day volatile sources and sinks at the atmosphere of Venus, including potential active volcanic sources; (4) determine how volatiles, in particular sulphur- and water-related, are transported through the atmosphere and how they interact with cloud layers (Figure 2.2.10). The first two investigations above - the search for morphological or compositional evidence of a water-rich epoch and the study of Venus' geological activity - have already been discussed in §2.2.5; here we will discuss the other two points below.

How do volatile delivery and loss couple tropospheric and geological processes over geological time scales?

The most variable species in the atmosphere of Venus are sulphur dioxide and water vapour. Both play a crucial role in determining climate on Venus as on Earth or Mars, and are key magmatic volatile species. Therefore, they will be a particular target of investigation for EnVision. On a geological timescale, SO_2 is thought to originate from volcanism and to be lost through reactions with surface minerals (Fegley et al., 1997; Hashimoto and Abe, 2005). Data from Vega 1 and 2 probes suggest SO_2 in the lower atmosphere of Venus is present at abundances significantly higher than predicted by the thermochemical equilibrium models (Bertaux et al., 1996). Halogen species such as HCl and HF may also play an important role throughout the atmosphere.

There may be high-temperature condensate clouds of exotic composition only 1-2 km above the surface, at temperatures in excess of 400°C . This is hinted at by the radar-bright/low emissivity deposits found consistently at high altitude regions around the planet, and by particulate layers detected by Venera 13 and 14 descent probes (Grieger et al., 2003). These could be explained by condensing metal halides and chalcogenides – similar to those found emitted from volcanic vents on Earth (Brackets et al., 1995; Port et al., 2020). Searching for variations in deep atmospheric species will help constrain geophysical sources and sinks including potential active volcanic sources.

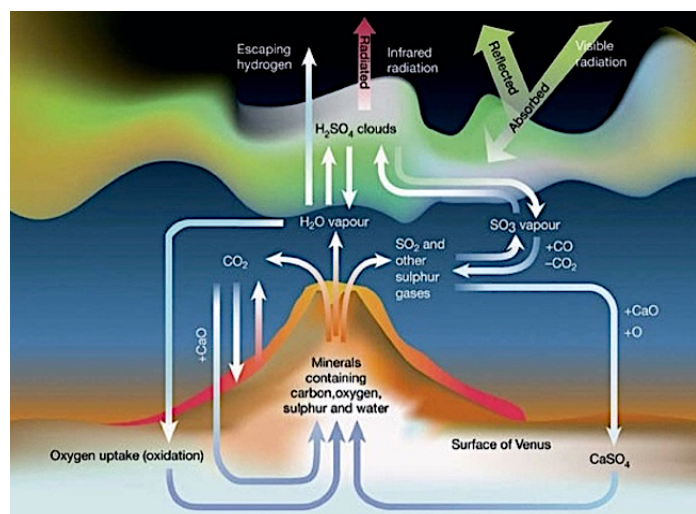


Figure 2.2.10 – Venus has an atmosphere of 96.5% CO_2 which is primarily responsible for its greenhouse effect and high surface temperature. Venus also has a thick layer of sulphuric acid (H_2SO_4) clouds that reflect sunlight away from its surface, helping to cool it. The greenhouse warming is greater than the cooling effect of the clouds, making the surface of Venus much warmer than of Earth. Numerical models suggest that over the past 1 billion years the climate on Venus has experienced periods of both cooling and warming, largely triggered by global volcanic activity spewing out large amounts of sulphur dioxide (SO_2) and water vapour (H_2O) (Bullock and Grinspoon, 2001).

What drives present day sulphur and water chemical cycles, and what are their links to active volcanism?

Sulfur dioxide is the third most abundant gas in the atmosphere of Venus after CO_2 and N_2 , with an abundance of some 150 ppm below the clouds, but its mesospheric abundance above the clouds is highly variable, ranging from < 1 to > 1000 ppbv (Encrenaz et al., 2012, 2016, 2019, 2020; Esposito et al., 1988; Marcq et al., 2013, 2020; Vandaele et al., 2017a, 2017b). The proximate cause for these variations is related to spatial and temporal fluctuations of the SO_2 supply through vertical mixing within the cloud region, since (i) SO_2 is more than three orders of magnitude more abundant below the clouds compared to cloud top level, so that the lower atmosphere acts as a large reservoir; and (ii) SO_2 exhibits, at least on the day side, a very short photochemical lifetime that allows for large horizontal and temporal contrasts to occur. However, the origin of these vertical mixing fluctuations is barely understood: purely atmospheric phenomena such as momentum deposition from upward propagating atmospheric gravity waves, induced e.g. by topography (Kitahara et al., 2019), or diurnal variations of cloud top convection through solar absorption certainly play a role, but thermal destabilization of the atmospheric column through hot volcanic outgassing has also been suggested (Esposito 1984). In the region around the cloud tops photochemical reactions between CO_2 , SO_2 , H_2O , and chlorine compounds lead to the formation of sulfuric acid, which is the main component of the cloud particles. The chemistry of the lower

atmosphere is dominated by thermal decomposition of sulfuric acid, and thermochemical cycles that include sulfur and carbon species and water vapour.

Water vapour exhibits a similar, albeit less dramatic behavior, with a bundance of ~ 30 ppmv in the lower atmosphere and variable abundance of 1 to 10 ppmv above the clouds (Cottini et al., 2015, Fedorova et al., 2016, Chamberlain et al., 2020). Water vapour also plays an important role in the transfer of heat and energy, which helps to maintain the massive greenhouse effect and drives the atmospheric superrotation (Lebonnois et al., 2010; Lee et al., 2007; Herrnstein and Dowling, 2007). The latter is also to the key element of chemical models through the release, transport and sequestering of volatiles that drive climate changes (Bullock and Grinspoon, 2001).

2.2.8 Assessing temporal variations of the Venus atmosphere

How are volatile species, particularly water and sulphur dioxide, transported through the **cloud layers and upper atmosphere**? How much of the variability in and above the clouds is due to intrinsic dynamic variability, and how much is directly or indirectly caused by volcanic activity?

What is the clouds relationship to long-term climatology and active volcanism?

The high-resolution images of Venus' cloud deck acquired a decade ago by the Venus Monitoring Camera on board Venus Express showed, as never before, the details of convective structures and gravity waves, and how crucial those small-scale phenomena are for understanding the Venusian climate (Markiewicz et al., 2007). Our current understanding of the clouds suffers from the limitations of the available data (very little in situ observations are available within the cloud layers), and the lack of complete models to interpret the observations. One- and two-dimensional modeling studies on Venus clouds have been published since late 1990s (James et al., 1997; Imamura and Hashimoto, 1998, 2002), one advanced cloud model has been extensively used and developed further to study the clouds and interpret the data (McGouldrick & Toon, 2007, 2008a, 2008b). Latest microphysical models include all the main microphysical processes: homogeneous nucleation of sulfuric acid solution particles (Määttänen et al., 2018), heterogeneous nucleation through a simple parameterisation (James et al., 1997), condensation/evaporation processes and Brownian coagulation (Pruppacher & Klett, 1997). The clouds of Venus play a large role in atmospheric chemistry (serving as reservoirs of water and sulphur in the form of sulphuric acid), radiative balance (reflecting away 70% of the light falling on Venus, and absorbing much of the rest), and therefore also in the atmospheric dynamics. In the 45-65 km altitude range, sulfur and water chemical cycles are coupled through the formation of H_2SO_4 -rich cloud droplets. EnVision's investigation will focus on understanding the chemical cycles and transport of SO_2 , H_2O and H_2SO_4 involved in cloud forming processes.

How are interannual variations of mesospheric SO_2 linked to volcanic processes?

The interannual variations of mesospheric SO_2 – sharp rises followed by gradual declines in following years – are suspected as one of the potential signs of active volcanism (Esposito, 1984, Marcq et al., 2013; Figure 2.2.11). As previously mentioned, these enhancements are associated with increased vertical mixing rather than direct volcanic injection. EnVision will carry out mapping of SO_2 , H_2O and related compounds both below and above the clouds, to characterise as extensively as possible (wrt. latitude, local solar time, longitude) their spatial and temporal distribution, and thus help in determining whether at least some of these increases in vertical mixing are caused by transient thermally buoyant volcanic plumes.

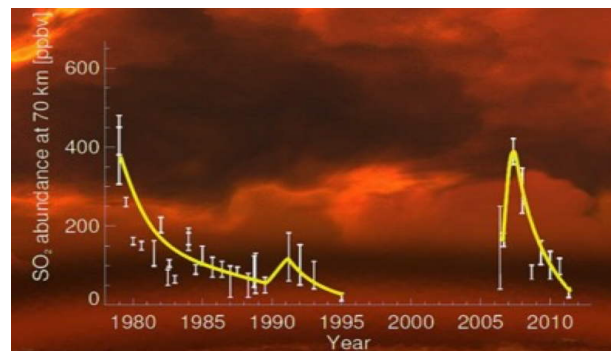


Figure 2.2.11 – Sulphur dioxide above Venus' clouds shows episodic variations which may indicate active volcanism – but proving this link conclusively requires further data on chemical abundances in and below the clouds. Left: Variation of the abundance of sulphur dioxide (SO_2) in the upper atmosphere of Venus over 40 years, expressed in units of parts per billion by volume (ppbv). A clear rise in the concentration of the SO_2 concentration was observed at the start of the Venus Express mission, with a subsequent decrease. The increase in SO_2 can be interpreted as evidence for volcanic activity or for decadal-scale variations in the circulation of Venus' vast atmosphere. (after Marcq et al., 2013).

2.3 Science Investigations

We present EnVision's strategy for addressing the Scientific Objectives described in §2.2: the observations necessary to provide answers to those questions; which features will be searched for; and which observables and physical parameters will be mapped and described by EnVision's datasets. A full science traceability matrix is given on page 40-41.

2.3.1 Establish the magmatic history of Venus: changes in style and volume with time, range of magma compositions

Geologic mapping of volcanic features, their surface morphology and dielectric constant

Geologic mapping of volcanic features and their surface morphology and dielectric constant is a cornerstone of Magellan data interpretation (Campbell and Campbell, 1992; Campbell, 1994). There is a need to carry this work to finer spatial scales and into the subsurface to answer fundamental questions of localised stratigraphy (from subsurface profiles and geologic mapping from images), magma composition (from morphology, roughness, and dielectric properties), surface mineralogy, order-of-magnitude eruption rates and volumes (from morphologic features and subsurface profiles), and post-emplacment weathering (from morphologic features and dielectric properties). EnVision will accomplish this objective in part through SAR imaging at 10 m resolution and polarimetric imaging at 30 m resolution, along with VenSpec-M surface investigations.

EnVision 30-m SAR imagery will dramatically enhance our understanding of volcanic surface features. At the >120 m resolution of Magellan (120 m azimuth resolution and 93 m best case range resolution), features like flow channels are visible only where they are at the highest end of those typically seen in terrestrial flow fields, vent locations and associated ash or rugged clinkers are too small to observe, and collapsed tubes or skylights are unseen. Within any single major shield volcano, there are often a wide range of features indicative of magma storage beneath calderas, rapid eruptions that form rugged, channelised flows, fine-grained pyroclastic ash from volatile-rich eruptions, and steep-sided constructs linked with higher-viscosity magma (Campbell and Rogers, 1994; Figure 2.3.1). Targeted observations at 10 m resolution will bring out crucial details in the stratigraphic relationship between flows, their likely thickness, and the range of scales in flow fields (i.e. short high-volume eruptions or long-term, tube-fed complexes).

Radar backscatter is sensitive to surface roughness on horizontal and vertical scales comparable to or larger than one tenth of incoming wavelength. For the primary HH-polarization mode of EnVision, both small-scale roughness and larger-scale topography play a role, with surfaces tilted toward the radar returning a much stronger echo than those areas which slope away from the sensor. EnVision also collects data in HV mode, which is much less sensitive to local slopes. Taking the two polarizations together, often as a ratio value, to complement the HH image, will yield significant information on surface texture not available from the HH- and VV-polarized Magellan data. The proof of concept for these observations comes from Earth-based polarimetric mapping using the Arecibo radar, which shows that information on small-scale roughness correlates Venus lava flows with those in terrestrial settings (Campbell and Campbell, 1992), and can reveal deposits formed during recent, volatile-rich

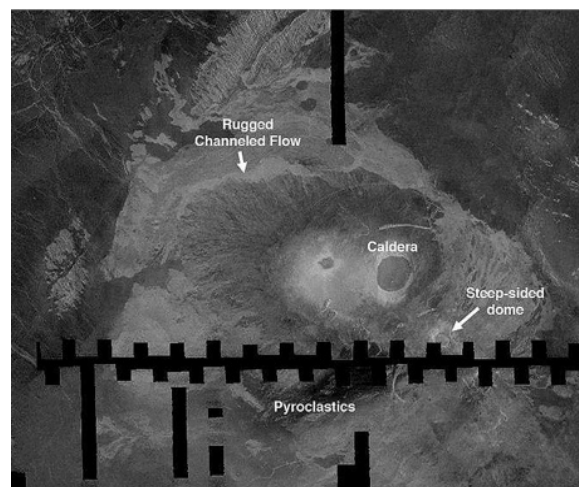


Figure 2.3.1 – Magellan radar image of Tepev Mons, showing the range of volcanic features and eruption history within one major shield volcano.

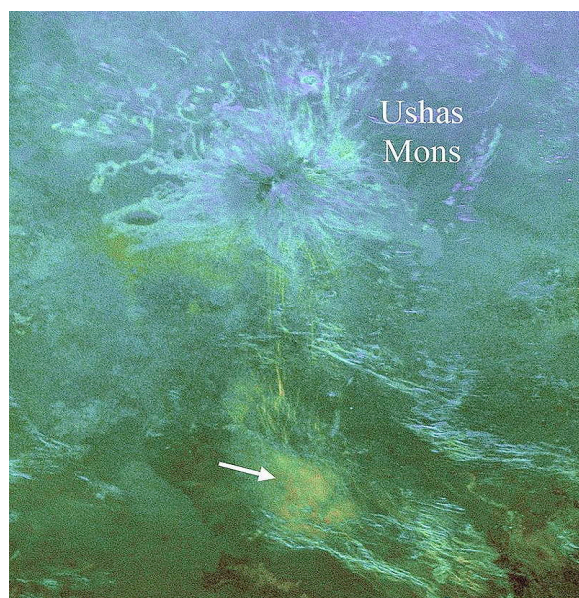


Figure 2.3.2 – Surface roughness mapping from Earth-based polarimetric 12.6-cm radar image of Ushas Mons (400 km across) and ridge belts to the south. The colour overlay is similar to the HV/HH ratio to be obtained with EnVision. Warmer colours and higher brightness represent rougher surfaces, showing differences among flow fields on Ushas. White arrow is rough debris associated with an explosive event during a geologically recent period of renewed volcanism.

eruptions (Campbell et al., 2017; Figure 2.3.2). While ~ 7 km resolution Arecibo data collect same-sense (SC) and opposite-sense (OC) circular echoes, there is a high degree of correlation between the HV-to-SC and HH-to-OC power. Radiometry performed at a nadir but also off-nadir, in H and V polarizations, will also bring insights on the composition and surface roughness.

Rock Composition: Does Venus Have Granitic Rocks?

The Venus atmosphere is semi-transparent across a series of narrow atmospheric windows near 1 micron wavelength in the near infrared. Spectral analysis, using emissivity measured at these wavelengths can be used to detect and map the composition of exposed surface materials surface (Figure 2.3.3). A variety of iron-bearing minerals in various oxidation states are expected in Venus surface materials, either in fresh basalt or as chemically weathered products of basaltic rocks. Basalts on Venus are likely subject to rapid chemical weathering on exposure to the atmosphere, transforming pristine igneous silicate minerals such as pyroxene and olivine with ferrous iron (Fe^{2+}) to oxide minerals such as hematite and magnetite containing ferric iron (Fe^{3+}) (Filiberto et al., 2020). Emissivity spectral mapping allows effective discrimination of these minerals. (Gilmore et al., 2015, Ferrara et al., 2020).

In contrast, rocks exposed at the surface which lack iron-bearing minerals are interpreted to have a felsic composition (SiO_2 -rich rocks such as granite). These point to a more evolved magma source and, importantly, to the presence of water in the mantle where melting occurred which, in turn, hints at the potential presence of water at or near the planet's surface, and its likely influence in chemical and physical processes there. Mapping the distribution of felsic rocks across the surface of Venus will help reveal whether and how Venus was different in the past; whether liquid water was capable of condensing on the surface or near-surface, or whether Venus was even hotter, and once experienced a steam-atmosphere phase (Dyar et al., 2020).

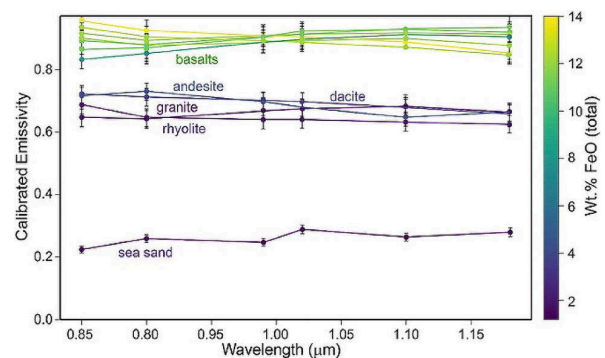


Figure 2.3.3 – Emissivity data from high-temperature laboratory experiments performed at the Planetary Spectroscopy Laboratory of DLR in Berlin (Germany) downsampled to the resolution of surface filters used by the VenSpec-M. Error bars represent a conservative estimate of the uncertainty of $\pm 4\%$ for the retrieval of emissivity from orbit including instrumental and atmospheric effects, and show that VenSpec-M can determine variations in rock composition from orbit.

Variations in morphologic characteristics, stratigraphic relationships, and dielectric properties of plains

The volcanic plains cover around 80% of Venus. Far from being uniform, they exhibit signs of extensive geological activity, from volcanic and tectonic to aeolian and weathering processes. Did the plains form rapidly, with few flow boundaries (like lunar mare) or are they constantly reformed by small-scale volcanism, below the resolution of Magellan? Understanding and mapping stratigraphic boundaries is important in distinguishing geologically old and young units, and between directional and equilibrium surface histories.

Because of the huge area covered by the plains units (> 300 million km^2 , more than twice the land area on Earth), it is not planned to target all of the plains for detailed characterisation. Global coverage will be obtained for those data types which have not been obtained before at Venus (multispectral near IR spectroscopy, and subsurface sounding). However, as we already have global imagery maps from the Magellan radar mission at low resolution (> 120 m resolution), EnVision need only target a subset ($\sim 10\%$) of the plains, chosen to include representative samples of all known features and terrain types. The targeting strategy is explained in §3.2.

The Subsurface Radar Sounder will be used to look for layering in the plains and elsewhere on Venus, as has been successfully done on both the Moon and Mars. Indeed, Lunar Radar Sounder (LRS) has successfully revealed and mapped several periods of flood basalts in the Lunar subsurface (Ono et al., 2009; Kobayashi et al., 2014). The sub-horizontal parallel layers of materials of differing densities, at multiple depths and different thicknesses, observed at several locations, have allowed the establishment of a series of volcano-stratigraphic units related to distinct flood-basal eruption periods. The SHallow RADar (SHARAD) instrument has been used to similar effect on Mars (Ganesh et al., 2020; Watters et al., 2006), to interpret the organisation of stacked lava flows and pyroclastic deposits, from their differing densities and 3-dimensional organisation (Figure 2.3.4). Analyses of this type enable a far better understanding of Venus's recent geological past and reveal vital information about the character, thickness and mode of resurfacing on Venus. For example, catastrophic resurfacing models for Venus (Strom et al., 1994) predict that the plains were resurfaced in a brief epoch several hundred million years ago. In such a model, there might not be sufficient time between lava flows to

develop thick weathering layers that would produce discrete layered returns in SRS data. If SRS does detect clear layering in the plains, it would tend to favor more gradual resurfacing models for Venus.

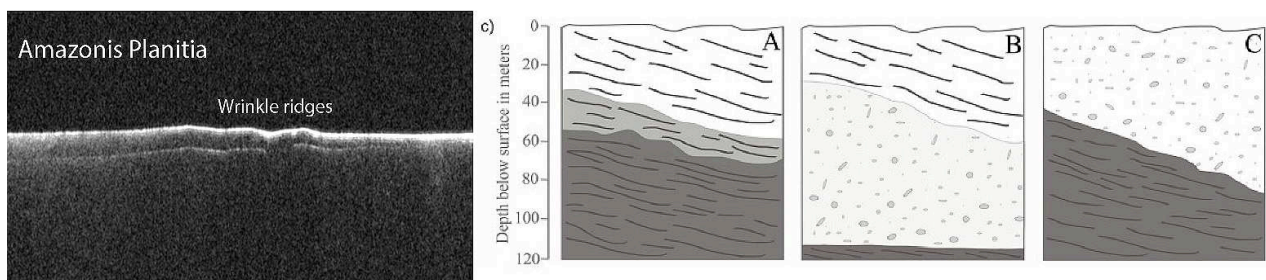


Figure 2.3.4 – (a, left): A SHARAD radargram showing layering about 100 metres thick in Amazonis Planitia warped by wrinkle ridges. The image is 400 km across (Campbell *et al.*, 2008). (b, right): Schematic representation of the three potential scenarios of subsurface stratigraphy interpreted from SHARAD radar sounding of volcanic layering in the Arsia Mons caldera (A - stacked lava flows with vesiculated and less dense flows overlying very dense lava, B - less dense lava-flow and a thick tephra deposit overlying denser bedrock, C - pyroclastic or other low-density material deposited over dense lava-flows in the southern part of the caldera, adjacent to the wall (Ganesh *et al.*, 2020; Watters *et al.*, 2006).

This investigation will be carried out using VenSAR imaging, polarimetry and radiometry, working closely with surface composition from VenSpec-M, subsurface structures from SRS and gravity mapping from radio science.



2.3.2 Establish the tectonic history of Venus: magnitude of deformation, implications for lithospheric thickness and heat flow

Mapping of tectonic structures

Magellan observations provide a valuable overview of tectonic processes on Venus (Solomon *et al.*, 1992), but are limited by the resolution of the radar images and especially the topography (10-30 km). EnVision's much higher horizontal resolution: 10-30 m imagery, 300 m horizontal resolution of the SAR stereo Digital Elevation Model (DEM) will enable much clearer definition of the styles of tectonic deformation and of the superposition and cross-cutting relationships used by geologists to map the sequence of deformation in a given region.

High resolution radar data is particularly essential in understanding the tessera of Venus, which contain fine-scale, complex patterns of deformation (Figures 2.1.3, 2.2.3). We need to understand whether the tesserae represent thick, ancient remnants of deformed and deep-rooted continental crust. The tesserae may also hold clues to the nature of past resurfacing; particularly whether there have been periods of enhanced crustal mobility, or whether Venus has been in its current state for most of its history. We expect that tesserae represent the oldest terrain, locally, but they may not have all formed at the same time; better understanding of their structure and arrangement, their relationship with volcanic terrains and their correlation from one place to another would help to unravel these temporal and structural conundrums. Magellan imagery revealed very varied tesserae interiors often with complex arrangement of solid and deformed rocks, blanketed by finer grained or smoother materials (Hansen & Willis, 1996, Ivanov & Head, 2011) but without greater spatial resolution and better topographic detail, the nature of the materials and their origins could not be resolved. Multi-polarimetry observations (HH and HV) are needed to better understand their surface textures and physical structures, to reveal emissivity variations of solid lithologies and to discriminate them from unconsolidated materials.

Relative age dating is particularly important and helpful, in the absence of independent absolute age data, in understanding the mode and sequence of formation of near-surface layers and structures. We ask whether the tesserae are always the oldest terrain, overlapped and overlain by plains materials, for instance? Or, what are the stratigraphic relationships between all the terrain types? Does Venus have a global stratigraphic, sequential organisation, or many different sequences in different regions? This science objective thus has significance across many of the other objectives because the relationships between terrain types are poorly constrained.

To assist this effort, high-resolution imagery is placed within the context of larger contiguous areas imaged at medium resolution. This approach is known to be successful in establishing the morphological details of inter-relationships between spatially separated strata and other geological units. These goals will be achieved by regional mapping at 30 m (to resolving features < 100 m in scale over >100s km in extent), targeted mapping at 10 m (resolving features > 30 m in scale), measurement of surface topography (through stereo radar imaging and near-global nadir altimetry), characterising of polarimetric reflection properties of surface materials, and by subsurface imaging of material boundaries (within upper 1000 m of the crust). Since this science objective

focuses on the boundaries and physical, chronological relationships between terrain types, attention will be aimed at regions where multiple terrain types are in close association.

Quantitative modeling of deformation caused by faulting and folding

The combination of high-resolution radar imagery for mapping structural geology and high-resolution topography for quantitative modeling of tectonic processes will be particularly valuable. Quantitative modeling of deformation caused by faulting and folding can constrain the physical processes that produced the observed landforms, the magnitude of the deformation, the orientation of the stress field that created the deformation, and the mechanical structure of the crust and lithosphere in the vicinity of the tectonic structure. In turn, mechanical structure can be interpreted in terms of chemical layering (crust and mantle) and temperature (thermal gradient and heat flow). Figure 2.3.5 shows an example of such modeling (Moruzzi and Kiefer, 2020), which is only possible in a limited number of regions of Venus using Magellan data. Higher resolution EnVision data will permit such modeling for representative examples of all major types of tectonic structure.

Comparing results for geologic regions of different relative ages may give insight into the temporal evolution of Venus, for example changes in the rate of heat loss and possible variations in the style mantle convection with time. Sounding radar observations may directly image structural offset in the crust which can be compared with inferences from gravity models. For example, Figure 2.3.4a illustrates subsurface structural offset of a wrinkle ridge on Mars.

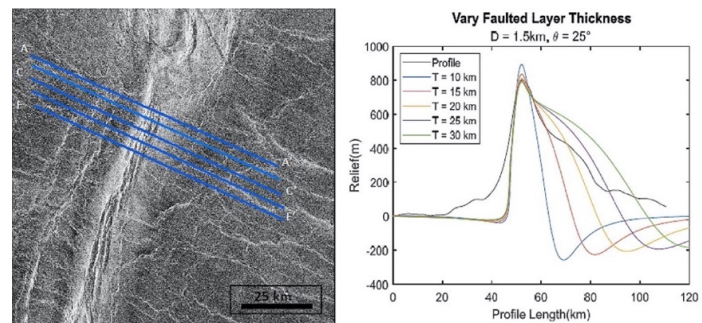


Figure 2.3.5 – (a, left): A Magellan radar image across the Vedma Dorsa ridge belt. (b, right): Elastic dislocation modeling of thrust faulting in Vedma Dorsa. The black line is the observed topography (averaged for the 5 profile lines on the left image). The various colour lines represent the topography produced by thrust faulting terminating at various depths below the surface (Moruzzi and Kiefer, 2020).

This investigation will be carried out using VenSAR imaging, polarimetry and radiometry, working closely with surface composition from VenSpec-M, subsurface structures from SRS and gravity mapping from radio science, in order to understand the evolution of lithospheric thickness and planetary heat flow with time.



2.3.3 Characterise surface modification processes: impact crater modification, low emissivity/radar bright highlands

Impact crater modification

The only method for determining the absolute age of a surface, in the absence of measurement of radioactive isotopes, is through the use of crater counts. Because Venus has so few craters it is difficult, or impossible, to distinguish the age of different geological units using craters alone. However, craters on Venus are modified to varying degrees, first by loss of radar-dark halo, and then by infilling, causing dark floors. Some are also modified volcanically or tectonically (Izenberg et al., 1994). Because initial crater depth depends on crater diameter, the extent to which a particular crater deviates from the expected depth-diameter relationship provides a guide to post-impact infilling by lava or sediments at that crater. The height of the crater's rim above the surrounding terrain similarly provides a guide to the thickness of post-impact fill in the crater's ejecta blanket. Initial estimates of crater fill with Magellan data (Herrick and Rumpf, 2012) was limited by the accuracy of the available stereo topography digital elevation model. In contrast, VenSAR observations will be optimised to produce high resolution DEMs (§3.3.2), and nadir altimetry profiling will provide global topographic data. Possible direct measurements of crater infilling with sounding radar will be complementary to topography-based estimates of crater fill thickness. Craters are globally distributed, so such measurements can provide important new information about the global resurfacing history of Venus.

Low emissivity/radar bright highlands

The low microwave emissivity and high radar brightness of some highlands is an enduring puzzle about Venus. It is not yet established whether these anomalous microwave properties are due to a locally extremely high dielectric constant or to volume scattering in the subsurface. It is even less clear whether they are due to rock chemistry or the deposition of atmospheric precipitates made possible by the cooler temperatures of the highlands. These anomalies radar properties have a strong dependence on altitude (Figure 2.3.6), suggesting a possible relationship to atmospheric temperature.

Two possible explanations for the unexpected low emissivity values (and concurrent high radar reflectivity) of Venusian highlands have been advanced (Pettengill et al., 1992): (1) emission from a highly reflective surface having a bulk dielectric permittivity of the order of 80; or (2) emission from a low-loss medium having a usual permittivity (of order 5) but containing many voids and/or heterogeneities responsible for efficient scattering in the subsurface volume and therefore for the observed decrease in emissivity. The EnVision mission will distinguish between these hypotheses thanks to radar polarimetry, both active and passive. Polarimetry radiometry, in particular, will provide a direct measurement of the effective dielectric constant of a set of Venus highlands that are included in the RoIs of the mission. Associated to active polarimetry, it will bring key insights into the surface roughness and degree of volume scattering in the subsurface of these regions. The composition of the highlands will also be globally characterised in terms of near-IR and microwave emissivities; their variations will be investigated as a function of topography which will be available nearly globally by means of nadir altimetry and/or regionally with stereo radar imaging. All these measurements together will help identify the alteration mechanism(s) at play at high altitudes on Venus.

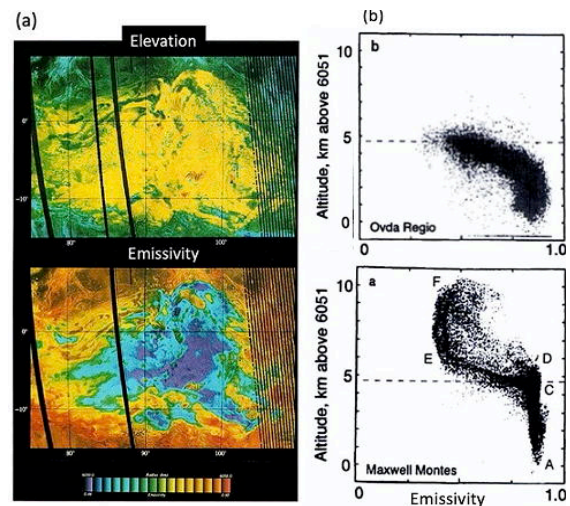


Figure 2.3.6 – (a, left): Magellan SAR image of Onda Regio, overlain (in false colour) with the relief (top) and the emissivity (bottom). Onda Regio displays anomalously low values of emissivity. Figure from Pettengill et al. (1992). (b, right): Scatterplots of emissivity vs altitude for two mountainous regions on Venus (Maxwell Montes and Onda Regio). Adapted from Klose et al. (1992).

This investigation will be carried out using VenSAR imaging, polarimetry, radiometry and altimetry/SAR stereo, working closely with surface composition from VenSpec-M, and surface and subsurface properties from SRS. Detailed imaging, SRS sounding and higher resolution topography data will constrain the processes that have modified or obliterated craters on Venus and the thickness of material that have apparently filled them.

2.3.4 Constrain the size of the major internal layers (crust/lithosphere, mantle, core), and the physical state of the core

The Lithosphere and Crust

Measurements of the lateral variations in the strength of a planet's gravity field is an important tool in probing the subsurface structure of a planet. Regional differences in elevation can be supported by differences in crustal thickness, by flexure of the elastic lithosphere, or by convective flow in the mantle. These mechanisms can in turn be distinguished by their expected gravity signatures, resulting in estimates of the thickness of the crust and lithosphere in different regions of Venus. Crustal thickness variations can measure the integrated amount of volcanism over time and thus provide tests of thermo-chemical evolution models, but can also sometimes be the product of extensional or compressional tectonism. Crustal thickness also affects the stratification of mechanical strength in the lithosphere and thus can also affect the style of tectonic deformation.

The lithosphere is the outer rigid shell of the planet and is a particularly important parameter in both gravity models and in thermal evolution studies. If the lithosphere is thin, topographic elevation can be supported by crustal thickness (thick crust tends to “float”, producing high topography). On the other hand, if the lithosphere is thick, it can support topography by its mechanical strength. Because the thickness of the lithosphere is controlled by temperature, this also serves to probe the thermal state and heat transport of a planet. If the lithosphere is thin then the heat transport is efficient, if it is thick then it is ineffective. The analysis of the lithosphere thickness and its lateral variation is therefore an important component to understand the mechanism of heat transfer. EnVision will address the different scenarios of thermo-chemical evolution, by better constraining, among other things, the lithosphere thickness.

Determining lithospheric thickness with gravity data is particularly sensitive to data with wavelengths less than 500 km. Unfortunately, the Magellan solution of the Venus gravity field is poorly resolved in large areas, in particular in the Southern hemisphere (Figure 3.9) which has limited our ability to assess the thermal evolution of Venus. Combining Magellan and EnVision gravity data would allow determination of the gravity field over at least 95% of the planet, with an average spatial resolution better than 200 km, and an accuracy better than 20 mGal. Such spatial resolution and global coverage are required to better understand the crustal and

lithospheric structure of the main volcano-tectonic features of Venus (coronae, large volcanoes, ridges, tesserae, rifts etc), using both gravity and topography fields (Figure 2.3.7).

The Deep Interior

The understanding of the thermo-chemical evolution of Venus requires knowledge of the internal structure and thermal state. Our current knowledge of the internal structure of Venus is based on a limited set of data such as mass, radius, gravity and topography. A directly existing constraint on the internal structure and thermal state is provided by the tidal Love number k_2 estimated from the Doppler tracking of Magellan and Pioneer Venus Orbiter ($k_2 = 0.295 \pm 0.066$ after Konopliv and Yoder, 1996). Due to uncertainties, however, even the distinction between liquid and solid core cannot be determined (Dumoulin et al., 2017). The absence of a current internal magnetic field is not a limitation, since both a liquid and a solid core are compatible with this observation (Stevenson, 2003). Most current models of internal structure therefore consider Venus to be only a rescaled Earth, although these two planets have followed very different geological and climatic evolution.

For the thermal state, estimates of the current temperature distribution in the interior of Venus vary widely and the published temperature profiles for the interior of Venus differ by up to 500 K in the upper mantle and 1000 K in the lower mantle (e.g. Steinberger et al., 2010; Armann and Tackley, 2012) with different implications for cooling and volcanic history (see Figure 2.2.5). Indirect information about the thermal state of Venus is obtained from its volcanic activity or when it has subsided - today's high temperatures mean a greater probability of ongoing volcanism, while low temperatures may suggest that Venus is not volcanically active. This relationship is ambiguous, since the volatile content in planetary interiors strongly influences the melting temperature. A further independent indication is given by the mantle viscosity, which is strongly related to the temperature and water content in the mantle (both of which reduce viscosity).

EnVision will provide accurate gravity measurements to better constrain the potential Love number k_2 (Figure 2.3.8). These parameters are related to the deformation reaction to the tidal force of the Sun. The potential Love number helps to determine the state of the core and, in the case of a liquid core, also its size. On other space missions to Mercury, Mars and the Moon, these parameters have already been determined with varying degrees of accuracy, and it has been shown that they can be used to delimit the internal structure: the measured k_2 is an indicator of a liquid (or partially liquid) core for Moon (Williams et al., 2014), Mercury (Margot et al., 2018) and Mars (Yoder et al., 2004). Furthermore, for Mars the core size and the amount of volatile components such as sulphur were restricted (Rivoldini et al., 2011) and via the phase lag also the viscosity profile in its mantle (Plesa et al., 2018).

The estimate of k_2 is important for the state of the core and its size. Dumoulin et al. (2017) investigated the viscoelastic tidal response of Venus, taking into account different compositional, temperature and viscosity profiles for the interior. They show that the determination of k_2 with an error of less than 0.01 allows to distinguish between different classes of interior conditions. Potential Love numbers higher than 0.27-0.28 would

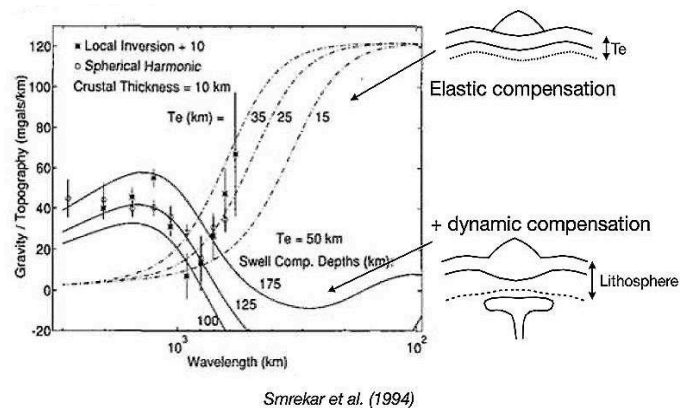


Figure 2.3.7 – Example of gravity/topography (G/T) analysis over Bell regio assuming a given crustal thickness and different types of surface load compensation (purely elastic or elastic and dynamic). Dots with error bars show the current knowledge of G/T ratio (Smrekar et al., 1994).

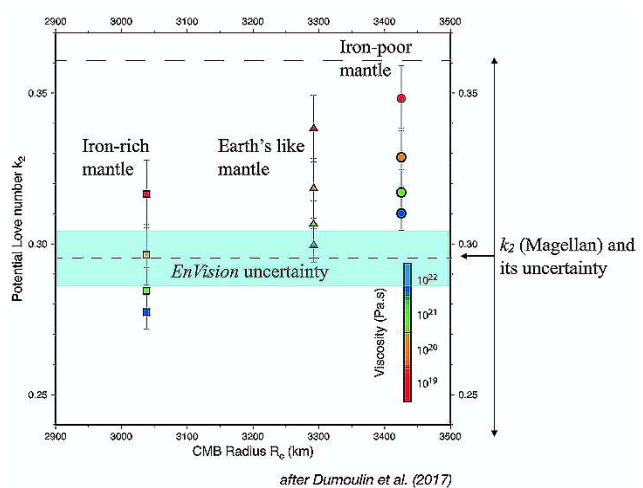


Figure 2.3.8 – Expected k_2 Love number in function of core radius for different models of mantle composition and viscosity. The actual value with its uncertainty is displayed on the right side. The expected accuracy for EnVision is shown with the blue area, assuming the same k_2 value (Dumoulin et al., 2017).

indicate that the core is partially or completely liquid. A high value of k_2 (>0.34) indicates the existence of a large core ($R_c > 3300$ km) and favours an Earth-like composition or a low FeO content.

The investigation of the interior depends largely on gravity mapping, achieved using precise radio tracking of the spacecraft, combined with high accuracy altimetry achieved with SAR and SRS instruments. EnVision will better constrain the interior structure and the state of the core by measuring the gravity field including the k_2 Love number.



2.3.5 Constrain styles and occurrence of recent volcanism on Venus

The EnVision mission's investigations will seek to address changes on the timescale of months; changes over longer timescales, from years to decades, can be addressed by comparison between EnVision's feature mapping (to be obtained 2035-2039) and those of the Magellan radar orbiter active imaging data (obtained 1990-1992). Answers will be provided by searching for its morphological, thermal and volatile signatures in repeated observations of the surface and of the atmosphere.

Detecting volcanic activity in repeated SAR images

Detecting and characterizing of relatively large eruptions over the past 40 years will come from three sources in the SAR image data: i) any new, large lava flows (>200 m wide and 100s m long) erupted since the Magellan mission and within EnVision's mapped area will be revealed in the imaging cycles of the EnVision mission; ii) any large scale changes in the morphology of volcanic edifices will also be revealed within EnVision cycles; and iii) any new, small lava flows (>60 m wide and at least a few hundred metres long) erupted in the 4-year duration of the EnVision mission. Detected changes (or non-detection) will be used to place bounds on the volcanic activity rate as described in Lorenz et al. (2015).

Searching for surface and near-surface temperature changes

In addition to SAR imaging, temperature signatures associated with volcanic activity from both hot lava and hot volatile gases will be detected and monitored in the infrared (IR) and microwave domains. Temperatures associated with volcanic eruptions can range from only 500°C for low viscosity carbonatite lava to well over 1000°C for ultra-mafic lavas. Such young, hot lavas will be directly detectable by their signature in IR emissivity data, (provided lava outflows cover an area of at least 0.1 km^3). Cooling rates at the surface are estimated to be on the order of hours (Mueller et al., 2017), but microwaves offer the prospect of sensing the shallow subsurface and thus may detect warmth from old lava flows, i.e. lava flows which have cooled at the surface possibly years ago and thus have no more IR emission signature but are still hundreds of K above ambient at depth (Lorenz et al 2016). Polarimetric radiometry measurements (used to determine whether candidate areas have anomalous emissivity rather than high physical temperature) and a better knowledge of the topography (and therefore of the altitude-dependence of the surface physical temperature) will greatly enhance the reliability of the volcanic detection and monitoring.

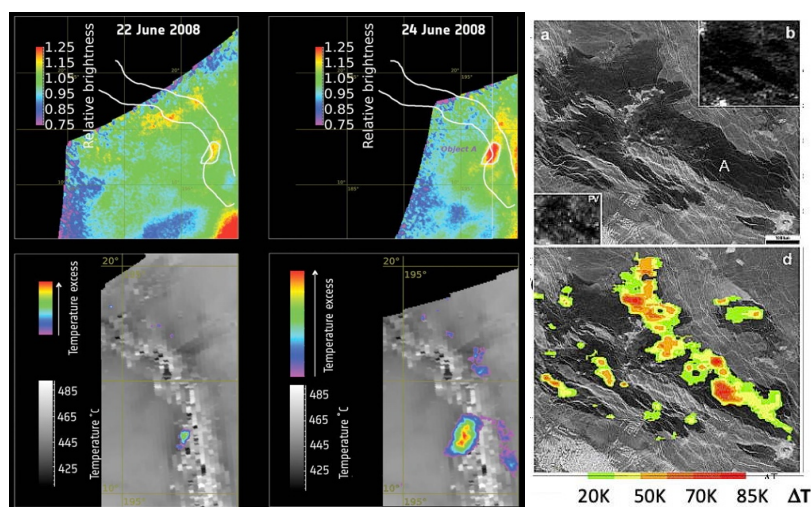


Figure 2.3.9 – (a, left): Four transient hotspots were detected by Venus Express in the Ganiki Chasma rift zone in Atla Regio. Changes in relative brightness (top row) and changes in temperature (bottom row) are shown between 22 and 24 June 2008. The bottom row shows the temperature excess compared with the average surface background temperature. Taking into account atmospheric effects, hotspot is likely about 1 square km with a temperature of 830°C (Shalygin et al., 2015). (b, top right): Magellan SAR image of Bereghinia Planitia. (c, bottom right): calculated ΔT overlain on Magellan SAR image. Using Magellan microwave radiometry observations (Bondarenko et al., (2010) identified a large lava flow in Bereghinia Planitia that is radiometrically warmer than its surroundings, by some 60–80 K and they suggest that this flow was already present in Pioneer Venus data, acquired around 15 years before Magellan. However, this detection is still debated as it could be due to regionally high emissivity.

Detection of volcanogenic gas and particulate plumes

Sulphur dioxide variations in the mesosphere have been attributed as possible evidence of volcanic activity (Esposito, 1984), but they also could be due to intrinsic dynamic variability of the atmosphere, associated with temporal changes in transport of SO_2 from troposphere (where it is highly abundant) to mesosphere (where it

is detected). On the other hand, volcanic gas plumes in the troposphere (below the clouds) would have quite a distinct signature, with distinct plumes advecting with the prevailing East-to-West winds. Water vapour is likely to be a better tracer of volcanic activity than sulphur dioxide, because it is less abundant in the Venus atmosphere than SO_2 , and because it can be mapped at three different altitudes in the troposphere using different spectral bands on the nightside. Analyses of Venus Express data found no evidence of tropospheric water vapour variations (Bézar et al 2009, 2011), but these analyses represent data only from a few days and, due to low spectral resolution, could only determine water vapour to a fairly wide range of 25 – 40 ppmv.

The nominal column mass of volcanic gases in the Venus atmosphere, integrated from surface to space, is $\sim 200 \text{ kg m}^{-2}$ for SO_2 , $\sim 10 \text{ kg m}^{-2}$ for H_2O and $\sim 0.1 \text{ kg m}^{-2}$ for HDO. If the composition of Venus volcanic gases is the same as on Earth - provided that plume dispersion does not exceed 10^4 km^2 , the limiting spatial resolution induced by cloud scattering - then a large, Pinatubo-size eruption would change H_2O abundance, D/H ratio, and SO_2 abundance, respectively, by $\sim +30\%$, -30% , and $+1\%$. The latter effect may be underestimated with respect to the others, both because the Venusian interior may be much drier than Earth's, and because the outgassed $\text{SO}_2/\text{H}_2\text{O}$ ratio is expected to be higher for a given magma volatile content due to Venus' high atmospheric pressure (Gaillard & Scaillet, 2014).

Search for volcanic activity will be carried out using a combination of repeated SAR imaging, repeated microwave and infrared thermal emission mapping, and repeated tropospheric gas & cloud monitoring. Non-detections as well as detections will narrow the possible volcanism rates for Venus.



2.3.6 Characterise geomorphological changes by mass-wasting and aeolian processes

Understanding the range and scope of mass-wasting processes (landslides)

Though Magellan imagery showed us evidence of mass-wasting and aeolian features, it was not able to reveal their temporal changes during the mission's lifetime, so their geomorphological and temporal properties remain unknown, and we have almost no information about weathering, surface alteration or other aeolian processes. Since there is currently no constraint on the mechanisms and rates at which these processes might be occurring, better topography and nested imaging at multiple resolutions, and repeated imaging during the mission, are needed.

Malin (1992) estimated that at least one large landslide (5–10 km runout distance) should, somewhere on the planet, occur per year if activity rates on Venus are comparable to those on Earth. That such activity was not detected in Magellan data may be a consequence of differing imaging geometries and limited spatial resolution from each cycle, and not a lack of landslides. Higher resolution, VenSAR observations, with consistent geometry, should reveal many smaller features and better resolve the morphology of features, that were not resolved by Magellan. Repeated observations of regions expected to be active, e.g. along rifts, will help to characterise processes operating at decadal (Magellan-EnVision comparison over 40 yrs) and yearly (EnVision inter-cycle comparison) time scales.

In the absence of near-surface water which, on Earth, affects material bulk density, shear strength and pore-pressure, and thus lead to slope instability, the mechanisms of slope instability and failure on Venus are unclear, and it is likely that landslides require triggering by external forces, such as earthquakes. Magellan imagery revealed a very strong spatial relationships between the locations of large-scale mass-wasting features and steep slopes related to rift zones and volcanic edifices, which may in turn point to them being geodynamically active in the recent geological past. EnVision's proposed Regions of Interest (RoIs, see also §3.2) and higher resolution imaging offer excellent coverage of known mass-wasting features and increase the likelihood of imaging new or previously undetected smaller features. The planned VenSAR investigations will include detailed characterisation of mass-wasting geomorphological properties and features with stereo imagery, and of their surface conditions with multi-polarimetry.

Detecting and characterising Aeolian activity

Evidence of dune-fields, debris fans and large ripples are scarcely resolvable in the $> 120 \text{ m}$ spatial resolution Magellan imagery. The surface winds evidenced by these features, downwind of impact craters, are likely to be important agents of geomorphological change, but higher resolution repeated imagery, and improved surface investigation to distinguish loose from consolidated materials (from polarimetry) are needed to characterise them.

Wind-streaks are widespread across the Venus's surface and the locations of two dune-fields and possible fields of microdunes are also known (Greeley et al., 1992). Detection of aeolian processes, via features of

erosion, transport and deposition (sedimentation), will be attempted by repeated imagery at high spatial resolution (decametre scale), and will help to constrain rates of such processes on decadal (Magellan- EnVision comparison over 40 yrs) and yearly (EnVision inter-cycle comparison) time scales. Planned VenSAR investigations will also include detailed characterisation of geomorphological features with stereo images, and of their surface material properties using multi-polarimetric observations. EnVision will search for features of aeolian activity beyond what we know from Magellan and will attempt to detect any temporal changes to these features for the first time.

The search for geomorphological changes will be carried out by searching for changes in repeated SAR imagery at 30 m and 10 m resolution, far more powerful than the > 120 m resolution available from Magellan. The analysis will be complemented by SAR radiometry & polarimetry, and Near-IR emissivity mapping, all of which work together to constrain surface composition and physical properties.



2.3.7 Assess tropospheric trace gases spatial and temporal variability

The established most variable atmospheric species on Venus - SO_2 , SO , H_2O , CO , COS , H_2SO_4 - are often associated with volcanic emissions on Earth. The goal of EnVision is to understand the intrinsic atmospheric variability, and to establish to what extent it can be associated with extrinsic inputs such as geological activity. Several key gases can be mapped below the cloud deck, at 0-50 km altitude: water vapour (H_2O and HDO) (Bézar *et al.*, 2009), sulphur compounds (SO_2 , COS) and carbon monoxide (CO) (Marcq *et al.*, 2008; Arney *et al.*, 2014) - these are all potential volcanic volatile gases. In particular, discovering spatial variability of the D/H ratio – whether associated with volcanic plumes or other fractionating processes – would be fundamental for understanding the history of the water on Venus. The atmosphere is known to be variable on a range of time scales from minutes to years, so measurements over a wide range of timescales are required.

The high surface pressure of Venus is maintained through surface-atmosphere chemical buffering reactions which are as yet unidentified. Buffer systems proposed have included Calcite-Anhydrite and Pyrite-Magnetite systems, but there is little evidence constraining these claims, and several of the relevant minerals including pyrite are not stable in Venus surface conditions (Hashimoto & Abe, 2005). Latitudinal gradients have already been observed in CO and OCS so these species act as tracers for the meridional circulation and provide a glimpse into some of the chemical cycles of the troposphere. The water vapour vertical gradient in the deep atmosphere is not known and may exhibit a steep gradient due to surface-atmosphere reactions (Ignatiev *et al.* 1997). Studying how trace gas abundances change over terrain of different compositions and/or elevations may yield insight into the surface-atmosphere exchange occurring.

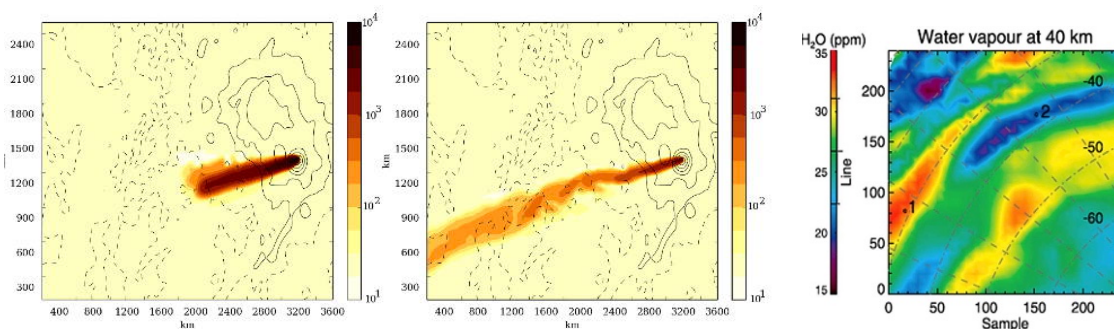


Figure 2.3.10 – Simulated advection of a volatile gas plume emitted from Imdr Regio. Black contours represent topography. Colours show excess water vapour (in arbitrary units) after 72 hours of outgassing, at (a, left:) 10 km altitude and (b, centre:) 35 km altitude. (Wilson & Lefèvre, 2020). (c, right): Variations of water vapour at 40 km altitude (Tsang *et al.*, 2010). This result was later found to be potentially attributed to degeneracies between cloud and water vapour retrieval. The higher spectral resolution of VenSpec-H, compared to VIRTIS-M, will enable unambiguous disentangling of these signals.

Radar-bright highland regions may occur due to deposition of airborne particulates or volatiles, or may indicate chemical interaction between surface and atmosphere. Observation of the composition and physical properties of these terrains, along with mapping of tropospheric gases and particulates, are necessary to study this phenomenon. The atmospheric observations required for this are global in scope, and not targeted to particular volcanic regions, because an understanding of global atmospheric variability is needed. The only technique available for mapping tropospheric gases from orbit is to exploit spectral windows on the nightside of Venus, centred near 1.18 μm , 1.74 μm and 2.3 μm ; these spectral windows probe gases at ~5 – 25 km, 20 – 30 km, and 30 – 40 km respectively. Water vapour can be mapped in all three of these windows, allowing mapping at three different heights, making it an ideal candidate for 3-D volcanic plume mapping. Further gases in one or more of the spectral windows include HDO , SO_2 , OCS , CO , HCl and HF – see Table 4.5.1 below.

The only previous orbiter equipped with spectrometers capable of probing these spectral windows was Venus Express; its observations demonstrated the viability of mapping gases at these wavelengths but their relatively low spectral resolution (VIRTIS, with resolving power $\lambda/\Delta\lambda \sim 70$, and SPICAV-IR with resolving power $\lambda/\Delta\lambda \sim 1700$) led to low retrieval precision, of typically 5 – 10 ppm for water vapour (Bézar et al., 2009, 2011). Water vapour variations were tentatively reported in the 2.3 μm band (Tsang et al., 2010), as shown in Figure 2.3.10 right panel, but it was later shown that, due to low spectral resolution, there was a degeneracy between water vapour and liquid water content in the cloud (Barstow et al., 2012). EnVision will repeat these measurements, but with higher spectral resolution in order to allow much higher sensitivity to these key trace gas species and with a much greater temporal and spatial coverage. EnVision's investigations will be discussed in greater detail in §3.4 below.

The principal instrument for trace gas mapping is VenSpec-H, designed to map key gases including water vapour at three different altitude ranges in the troposphere, as will be described in §3.4.1 below. These observations also provide validation for simultaneous and co-located VenSpec-M multispectral observations that provide wider mapping of H₂O variability at 5-25 km altitude.



2.3.8 Measure variability of sulphuric acid in the clouds, in both vapour and liquid form, and map variability of related species at the cloud-tops

Explore the main constituent of the cloud, H₂SO₄, in both vapour and liquid form

The main constituent of the clouds, H₂SO₄, in both vapour and liquid form, can be monitored near the cloud base altitude, yielding clues as to cloud formation and convection processes. Geological activity can affect clouds in several ways: (1) volcanic ash can contribute to cloud and haze layers; (2) volcanic sulphur dioxide emissions can contribute to formation of sulphate cloud & haze layers and to the as-yet unidentified UV absorber seen at cloud-tops; (3) volcanically emitted volatiles can form condensate layers, as discussed in §2.3.5; (4) heat from volcanic activity can cause changes in atmospheric circulation (Esposito et al., 1984); (5) near-surface winds in Venus' dense atmosphere can lift dust & other particulates from the surface into airborne suspension. Understanding the dependence of the cloud layer on outgassed mantle volatiles is critical for understanding the long-term climate evolution of the planet. All of these effects can be studied by monitoring the spatial and temporal variations of clouds and hazes. Characteristic timescales of cloud formation and dissipation have been measured to be of the order of hours to days, therefore observations on such timescales are required.

Measurements of the vertical profile of temperature, pressure and number density in the troposphere and mesosphere (35-90 km) of Venus will help to understand the processes driving the short & long-term variability of the cloud-level composition, as well as convection and global circulation (Figure 2.3.11). These processes are fundamental to understand the transport of momentum and the variable distribution of atmospheric constituents in the Venus atmosphere. Measurements of vertical atmospheric profiles with the required high vertical resolution is only possible through radio occultations. Coverage at a wide range of latitudes and local solar times is needed to parameterise cloud-level convective as well as dynamical processes. Measurements in consecutive orbits allow to monitor the short-term variability caused e.g., by atmospheric waves. Observations should be as widely spread in latitude, longitude and local solar time, to build up a climatology of atmospheric observations. Measurement of sulphuric acid vapour abundance profiles by exploiting the absorption of X-band radio signals has been demonstrated from previous Venus orbiters. EnVision will repeat these measurements, with more frequent occultations due to its lower orbital period (94 minutes for EnVision, compared to 24 hours for VEx and 10 days for Akatsuki), allowing shorter-period variability to be studied;

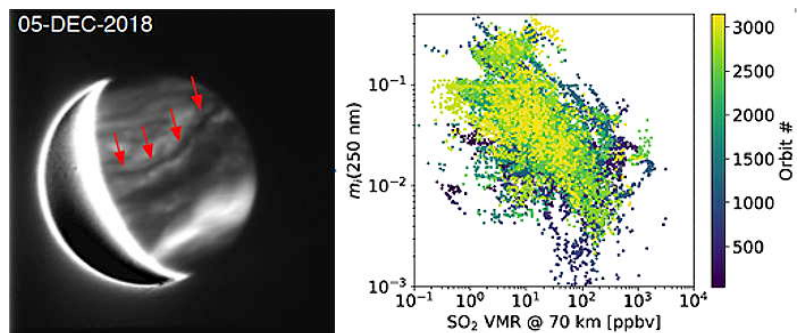


Figure 2.3.11 – (a, left): Dark streak of thicker cloud or particulates, imaged on the nightside of Venus using IRTF/SPEX (Young et al., EPSC, 2019). Could this be a volcanic plume? (b, right): Scatter plot between imaginary index of mode 1 particles at 250 nm and SO₂ mixing ratio at 70 km as measured by SPICAV-UV, hinting at a conversion between SO₂ and a sulfur-bearing UV absorber. Figure from Marcq et al. (2020).

furthermore, EnVision will also measure sulphuric acid *liquid* abundance, for the first time, using its *Ka* band radio signals. Further information is given in §4.7 below.

Constrain mesospheric composition and its variability

EnVision will measure gas abundances in the mesosphere (70-100 km altitude) above the clouds. Mesospheric abundances of carbon monoxide (CO), sulphur dioxide (SO₂), sulphur monoxide (SO), and water (H₂O) have been shown to be highly variable (Vandaele et al., 2015, 2016; Marcq et al., 2013, 2020; Chamberlain et al., 2020). Mesospheric variability may be driven by variations in vertical transport, temperature, local solar flux, and coupling among components of the SO₂-H₂O-H₂SO₄-aerosol system. Previous measurements of these species could not constrain the physical origin of this variability: ground-based observations by e.g. Encrenaz et al. (2019; 2020) are global, low spatial resolution “snapshots” acquired only during maximal elongations of Venus as seen from Earth, large scale images from Venus orbiters (e.g. VMC/VEx, UVI/Akatsuki) lacked spectroscopic capabilities, whereas orbiter-borne spectrographs (e.g. VIRTIS-H/VEx, SPICAV-UV/VEx) lacked extensive spatial coverage (Figure 2.3.12). As the mesospheric composition is variable on a range of time scales from hours to years, measurements over a wide range of latitude, local time, longitude and timescales are required. According to known spatial variability in cloud top albedo and sulphurous gases (Titov et al., 2012; Piccialli et al., 2015; Vandaele et al., 2017a,b), the investigated spatial scales should range from about 10 km to several thousand km (planetary scale).

EnVision will resume the observations of trace gases in the mesosphere conducted by these previous missions, in both UV and IR wavelengths, but with higher spectral resolution. In the UV range, this will allow separate retrieval of SO and SO₂ species, as was demonstrated using HST observations; simultaneous and co-located IR observations will allow simultaneous retrieval of water vapour, carbon monoxide and further key tracer species. Together, these observations will give an unprecedented view of transport and chemical processes at the cloud-top, in order to provide a better understanding of volatile transport through the atmosphere.

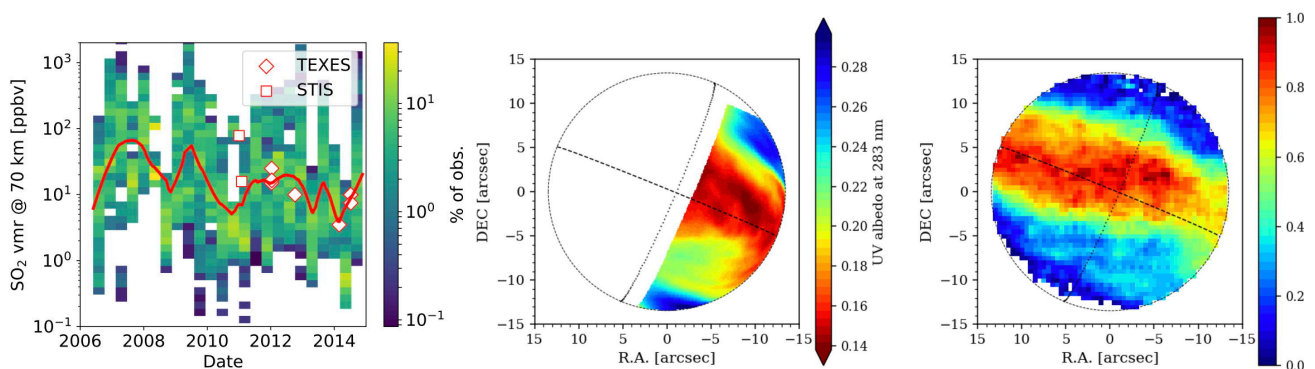


Figure 2.3.12 – (a, left): Temporal evolution of SO₂ mixing ratio at 70 km for latitudes lower than 30° as measured by SPICAV-UV. The red line stands for the moving median value, and white diamonds/squares show other SO₂ measurements in the same time interval. Figure from Marcq et al. (2020). (b, center): UV albedo map derived from the Akatsuki UVI data recorded on January 21, 2017, at 01:46 UT. Dashed lines represent the equator and the evening terminator. (c, right): TEXES map of the SO₂ volume mixing ratio at the cloudtop, inferred from the SO₂/CO₂ line depth ratio at 7.4 μm on January 21, 2017, at 03:43–04:18 UT. Figure from Encrenaz et al. (2019).

This investigation relies on dual-band radio occultation to obtain vertical profiles of sulphuric acid liquid and vapour in the clouds, as well as temperature profiles to assess where convective transport is occurring. Lower cloud distribution and properties are monitored by VenSpec-M nightside IR hyperspectral imager, and cloud-top properties and gas abundances are monitored using UV and IR dayside spectroscopy.



2.4 Complementarity of other Venus missions under study to EnVision

In this section we present both the uniqueness of EnVision, and the synergy and complementarity of other Venus mission concepts under study with EnVision.

At least three other Venus mission concept orbiters are currently under study: the VERITAS orbiter, a step 2 finalist in NASA's Discovery-class mission, under consideration for launch in 2026; the orbiter component in the Venus flagship of Russia's proposed Venera-D mission; and ISRO's planned Venus Orbiter (Shukrayaan). In addition, there are two Venus probe/lander concepts in competition: DAVINCI+, which is a step 2 finalist (like VERITAS) in NASA's current Discovery-class mission, under consideration for launch in 2026; and Venera-D flagship lander with a long-lived station.

VERITAS

The EnVision and VERITAS missions support both overlapping and distinct science objectives and have configured their payloads to best achieve their respective science objectives. VERITAS was down-selected after the first round of a competitive mission selection process in NASA's Discovery programme, approaching a final selection decision in 2021. VERITAS' instrument suite includes an X-band Venus Interferometric Synthetic Aperture Radar (VISAR) that is configured as a single pass radar interferometer to acquire global imagery and topography of the surface (Hensley, 2020). VERITAS also hosts an infrared spectroscopy instrument similar to that foreseen on EnVision. VERITAS and EnVision are two orbiter missions that leverage advances in radar technology and imaging techniques in interferometry and polarimetry since Magellan to provide greatly improved data products for the study of Venus.

VERITAS is designed to enable global topographic mapping, so it is naturally complementary to EnVision's strategy of regional observations using a broad range of synergistic techniques. Whereas VERITAS observations would provide foundational datasets important for comparative planetology, and support science studies requiring global coverage (e.g., obtaining a complete inventory of crater characteristics), EnVision's multi-messenger geophysics strategy uses combinations of observations at wavelengths from UV to radio-frequency waves to study the coupling of different processes associated with geological activity.

If selected, EnVision would collect targeted high-resolution dual-polarization radar imagery (30 m for up to 30% of surface and 10 m for 2-3% of surface) and generate topographic data via radar stereo techniques (300 m spatial resolution with 30-50 m height accuracy) over these regions. Data with nearly global extent are acquired by the VenSpec suite of optical instruments, the radar altimeter and radiometer, and the high-frequency (HF) radar sounder designed to penetrate into the subsurface. VERITAS which carries only two instruments has mission science that is almost completely focused on the surface and interior of Venus whereas by contrast EnVision's more comprehensive suite of 5 instruments has science objectives that include the surface, interior, and atmosphere. If selected, VERITAS would create global imagery (30 m radar imagery in a single polarization and 50 km infrared emissivity maps) and high-resolution topographic data (250 m spatial resolution and 5 m height accuracy) via single pass radar interferometry and conduct repeat pass surface deformation studies for a small fraction of the surface (<0.2%).

Because of EnVision's more extensive measurement suite, the atmospheric science objectives, geologic stratigraphy enabled by the HF radar sounder, and the radar radiometry and polarimetry measurements enable enhanced surface property characterisation and to study the coupling of different processes associated with geological activity, beyond that possible with VERITAS.

The nearly decade gap between the science phases of these two missions would provide a multi-temporal, multi-sensor dataset that could be of profound importance to understanding the short time-scale temporal dynamics of Venus surface. Comparable datasets for Earth and Mars have yielded deep insights on the processes and temporal scales at which they operate on these bodies. The combined science return of these two proposed missions would help advance Venus science toward a level of maturity comparable to the Moon and Mars.

Shukrayaan

A Venus Orbiter Mission is also in development at ISRO, targeting a launch date which may be as soon as 2025/6. We understand that the orbiter will carry a SAR instrument, for mapping the surface. Two further confirmed instruments to date are a Swedish-contributed instrument measuring escaping neutral and ionised particles, and a French-provided Venus InfraRed Gases Linker (VIRAL) solar occultation spectrometer, both of which are complementary to the investigations of EnVision (source: CNES & IRF press releases, 2020). Seventeen further potential science instruments have been shortlisted, including a subsurface sounder and a number of spectrometers targeting the atmosphere, however, it is not known how many of these will be finally implemented (Antonita et al., 2020). In summary, the Shukrayaan mission has not yet been confirmed but its investigations are likely to be complementary to those of EnVision.

DAVINCI+

DAVINCI+ (Deep Atmosphere Venus Investigation of Noble gases, Chemistry, and Imaging+) is a step 2 finalist (like VERITAS) in NASA's current Discovery-class mission, under consideration for launch in 2026. Two flybys will provide remote imaging followed by the probe descent over Alpha Regio. Additional orbital imaging would be performed for a six-months period in 2028-2029.

The DAVINCI+ probe would conduct scientific measurements during its atmospheric descent phase, which would be complementary to EnVision in three ways. Atmospheric composition measurements from entry probes allow high sensitivity and excellent vertical profiling complementary to global mapping of key volatile constituents from an orbiter like EnVision. Measurements of noble gas abundances and isotopic composition constrain formation and evolution scenarios of Venus, in a way impossible to achieve from orbit. Finally, optical imaging of tessera terrain obtained during the descent phase will be highly complementary to radar imagery, topography and composition mapping obtained from orbit. EnVision would provide geological context for the descent/landing site of any descent probe/lander critical for extrapolating information to a global scale.

VENERA-D

Russia's VENERA-D flagship mission would include an orbiter, whose payload is mainly focused on the atmosphere with instruments such as a thermal infrared Fourier transform spectrometer, which would recover some of the science lost from the failed PFS instrument on Venus Express. This would complement the volatile mapping carried out by EnVision, without addressing the geophysical studies which are at the heart of EnVision's science questions. The Venera-D lander would not only perform descent phase measurements but would also analyse surface composition. This would of course provide invaluable "ground truth" for EnVision's surface composition mapping, as well as contributing to understanding of geophysical evolution (Venera-D Joint Science Definition Team, 2019).

EnVision has a unique and compelling science investigation, irrespective of mission selections by other agencies. The varied investigations proposed are complementary and would add new perspectives to our understanding of the richly varied and complex system that is Venus.

3 Scientific requirements

3.1 Science Traceability Matrix

The EnVision Science Traceability Matrix (STM) traces how top level science questions are realised through scientific objectives, investigations, and finally observation, instrument and mission requirements. Numbers refer to corresponding sections of this document.

| | Scientific Objectives | Science Investigations (SI) | | Observation Requirements (OR) | Instrument Requirements | Venus Surface Coverage | | |
|---|---|---|---|--|--|---|--------------------|----------|
| | pp. 16-26 | pp. 27-37 | | pp. 42-52 | Parameter / Performance / Capability | Required / Alter 6 Cy. / Strategy | | |
| How have the surface and interior of Venus evolved? | 2.2.1 Understanding Venus' magmatic history | 2.3.1 / SI-1 Establish the magmatic history of Venus: changes in style and volume with time, range of magma compositions <i>Children: OR-1.1; OR-1.2; OR-2; OR-3.1; OR-3.2; OR-3.3; OR-3.4; OR-4</i> | 3.3.1 | OR-1.1 - Obtain regional surface mapping, resolving features < 100 m in scale over >100s km in extent. <i>Parents: SI-1; SI-2; SI-3; SI-6</i> | VenSAR SAR Standard Imaging 30m Sensitivity (NESO) | -20dB 20% 30.1% | Targeted | |
| | | | | OR-1.2 - Obtain targeted surface mapping, resolving features <= 10 m in scale over > 10s km in extent. <i>Parents: SI-1; SI-2; SI-3; SI-6</i> | VenSAR SAR Standard Imaging 30m Sensitivity (NESO) | -20dB 20% 30.1% | Targeted | |
| | | | | | 30-m SAR Stereo Imaging Horizontal resolution Vertical resolution | 250 m 20 m | 18% 28.3% | Targeted |
| | | | | | High-Res Spatial resolution | 10 m | 2% 2.4% | Targeted |
| | 2.2.2 Understanding Venus' tectonic history | 2.3.2 / SI-2 Establish the tectonic history of Venus: magnitude of deformation, implications for lithospheric thickness and heat flow <i>Children: OR-1.1; OR-1.2; OR-2; OR-3.2; OR-3.3; OR-3.4; OR-4; OR-5</i> | 3.3.2 | OR-2 - Measure surface topography (1) regionally by means of stereo radar imaging; and (2) globally by means of nadir altimetry. <i>Parents: SI-1; SI-2; SI-3; SI-6</i> | VenSAR 30-m SAR Stereo Imaging Horizontal resolution Vertical resolution | 250 m 20 m | 18% 28.3% | Targeted |
| | | | | | SAR Nadir Altimetry Vertical resolution Along-track resolution Average density | 10 m 6 km 2 per deg. of longitude at Equator | 65% 68% | Global |
| | | | | | SRS Low-density SRS acquisition Along-track resolution Across-track resolution Average density | 3 km 11 km 2 per deg. of longitude at Equator | 65% 68% | Global |
| | 2.2.3 Assessing Venus' surface modification processes | 2.3.3 / SI-3 Characterizing surface modification processes: impact crater modification, low emissivity/radar bright highlands <i>Children: OR-1.1; OR-1.2; OR-2; OR-3.1; OR-3.2; OR-3.3; OR-3.4; OR-4</i> | 3.3.3 | OR-3.1 - Map locally microwave emissivity in V and H polarizations using passive off-nadir radiometry. <i>Parents: SI-1; SI-3</i> | VenSAR Off-nadir Microwave Radiometry Both H and V polarizations Precision on short-term varia< 1 K Absolute accuracy | 2 K | 1% 2.6% | Targeted |
| | | | | OR-3.2 - Characterise surface polarimetric reflection and emission properties. <i>Parents: SI-1; SI-2; SI-3; SI-6</i> | VenSAR Dual-Polarimetry 30-m SAR Sensitivity (NESO) Spatial resolution | -20dB 30 m | 5% 6.8% | Targeted |
| | | | | OR-3.3 - Obtain a global map of the microwave emissivity using passive radiometry. <i>Parents: SI-1; SI-2; SI-3</i> | VenSAR Brightness temperature Precision on short-term varia< 1 K Absolute accuracy Surface temperature range Spatial resolution | 2 K 650-1200 K 50 km | 75% 93.2% | Global |
| 2.2.4 Understanding how Venus' interior and surface have evolved | 2.3.4 / SI-4 Constrain the size of the major internal layers (crust/lithosphere, mantle, core), and the physical state of the core <i>Child: OR-5</i> | 3.3.4 | OR-3.4 - Characterise near-IR emissivity of surface targets over 60% of the planet surface. <i>Parents: SI-1; SI-2; SI-3; SI-5</i> | VenSpec-M Near-IR Thermal Mapping Spatial resolution nIR spectral channels Thermal emission range SNR | 50 km 0.8-1.5um 650-1200 K 300 | 60% 76.6% | Global | |
| | | | OR-4 - Search for subsurface material boundaries within top 1000 m of crust over 70% of the planet surface. <i>Parents: SI-1; SI-2; SI-3; SI-5</i> | SRS Low-density SRS acquisition Along-track resolution Across-track resolution Average density | 3 km 11 km 2 per deg. of longitude at Equator | 65% 68% | Global | |
| | | | OR-5 - Measure the gravity field of the planet with spatial resolution of < 270 km; accuracy of < 0.2 mm/s2 globally; improved higher spatial resolution of < 200 km; accuracy of < 0.1mm/s2 over 40% of the planet; and the k2 Love number with an accuracy of 0.01. <i>Parents: SI-2; SI-4</i> | RSE S/C tracking using the TT&C Transponder Tracking using 2-way coherent carrier Doppler link, X (up) / X-Ka (down) Freq. stability (ADEV) better than 10e-12 between 1- 1000s integration. EIRP on the Ka-band downlink at least 102 dBm and 93 dBm on X-band. Gravity field with spatial resolution of < 270 km At least 95% of the planet with an altitude < 520 km Accuracy of < 0.2 mm/s2 (20 mGal) globally At least 40% of the planet with a spacecraft altitude < 260 km Accuracy of < 0.1 mm/s2 (10 mGal) | | | Global Targeted | |

Surface & subsurface mapping observations

Interior observations

Table 3.1 – EnVision Science Traceability Matrix. The table traces how top level science questions are realised through scientific objectives, investigations, and finally observation, instrument and mission requirements. Part 1: History: How have the surface and interior of Venus evolved? Numbers refer to corresponding sections of this document.

| | Scientific Objectives pp. 16-26 | Science Investigations (SI) pp. 27-37 | Observation Requirements (OR) pp. 42-52 | Instrument Requirements Parameter / Performance / Capability | Venus Surface Coverage Required / After 6 Cy. / Strategy |
|---|--|--|---|--|---|
| How geologically active is Venus? | 2.2.5 Understanding Venus' volcanic activity in the present era | 2.3.5 / SI-5 Constrain styles and occurrence of present-era volcanism on Venus Children: OR-1.1; OR-3.4; OR-4; OR-6; OR-7 | 3.4.1 OR-6 - Detect and characterise spatial and temporal anomalies of the surface and near-surface temperature with a precision of 1 K over time scales from hours to years and spatial resolution better than 100 km. Parents: SI-5; SI-7; SI-8 | VenSAR Brightness temperature Precision on short-term variation < 1 K Absolute accuracy 2 K Surface temperature range 650-1200 K Spatial resolution 50 km Repeated 30 m/pix SAR Standard Imaging Spatial resolution 30 m / pix 2% Sensitivity (NESO) -20dB same look direction with a look angle within +/- 5 degrees of standard or stereo observations, focusing on volcanic provinces. | 75% 93.2% Global 9.4% Targeted |
| | 2.2.6 Assessing Venus' aeolian activity and mass wasting | 2.3.6 / SI-6 Characterise geomorphological changes by mass-wasting and aeolian processes Children: OR-1.1; OR-1.2; OR-2; OR-3.2; OR-7 | 3.4.2 OR-7 - Detect and characterise changes in surface radar imagery in selected regions of interest that include the areas with high probability of volcanic and seismic activity. Parents: SI-5; SI-6 | VenSAR Repeated 30 m/pix SAR Standard Imaging Spatial resolution 30 m / pix 2% Sensitivity (NESO) -20dB same look direction with a look angle within +/- 5 degrees of standard or stereo observations, focusing on volcanic provinces. | 9.4% Targeted |
| How are Venus' atmosphere & climate shaped by geological processes? | 2.2.7 Understanding the role of geological activity in Venus' climate evolution | 2.3.7 / SI-7 Assess tropospheric trace gases spatial and temporal variability Children: OR-6; OR-8; OR-9.1; OR-9.2. | 3.5.1 OR-8 - Map tropospheric gases at 0-60 km (SO2, H2O, HDO, CO, OCS); map lower cloud properties & opacity and their variations. Parents: SI-7; SI-8 | VenSpec-M Near-IR Spectral Mapping center/width 0.86/0.04; 0.91/0.06; 0.99/0.03; 1.02/0.015; 1.11/0.02 Uncertainty on rel. emissivity 4% VenSpec-H Near-IR investigations of nightside atmosphere Horiz resolution 100x100 km Spectral ranges 1160-1180 nm; 2350-2470 nm Resolving power 8000 SNR 70 | 60% 76.6% Global 86.5% Global |
| | 2.2.8 Assessing temporal variations of the Venus atmosphere | 2.3.8 / SI-8 Measure variability of sulphuric acid in the clouds, in both vapour and liquid form, and map variability of related species at the cloud-tops Children: OR-6; OR-9.1; OR-9.2; OR-10 | 3.5.2 OR-9.1 - Measure vertical profiles of sulphuric acid vapor and liquid, from 35-55 km altitude. Parent: SI-8 OR-9.2 - Measure vertical profiles of atmospheric density, temperature and pressure from 35-90 km altitude. Parents: SI-5; SI-7; SI-8 | RSE Radio-occultation: radio link mode Temperature 10 K@90 km, 0.1K at 35 km Pressure 3-4 Pa@35 km; at least 2 passes/ 24h H2SO4 (liquid and gaseous) 1ppm (gas), 1mg/m3 (liquid) Vertical resolution 100 m RSE Radio-occultation: radio link mode Temperature 10 K@90 km, 0.1K at 35 km Pressure 3-4 Pa@35 km; at least 2 passes/ 24h H2SO4 (liquid and gaseous) 1ppm (gas), 1mg/m3 (liquid) Vertical resolution 100 m | 50% 63.9% Global 63.9% Global |
| | | | 3.5.3 OR-10 - Map mesospheric gases at 65-75 km (SO2, SO, H2O, HDO, CO); Map upper cloud properties and their variations. Parent: SI-8 | VenSpec-U UV investigations of dayside atmosphere HR channel Horiz sampling 24 km Spectral range 205-235 nm Spectral Resolution 0.2 nm LR channel Horiz sampling 5 km Spectral range 190-380 nm Spectral Resolution 2 nm VenSpec-H Near-IR investigations of dayside atmosphere Dayside Horiz resolution 100x100 km Spectral ranges 1.37-1.39 um; 2.40-2.47 um Resolving power 2000; 4000 | 60% 91.8% Global 91.8% Global 85.5% Global |

Surface change search

Atmospheric observations

Table 3.1 (cont'd) – EnVision Science Traceability Matrix (cont'd). Part 2: Activity: how geologically active is Venus? - Climate: how are Venus' atmosphere & climate shaped by geological processes? - Numbers refer to corresponding sections of this document.

3.2 EnVision Observation Strategy

Our current understanding of Venus' geology comes almost entirely from the Magellan orbiter's near global SAR image dataset, at > 120 m to 300 m spatial resolution (75 m pixel size), and its topographic data at 10 – 30 km (horizontal) and 50 – 100 m (vertical) resolution (Figure 2.2.1). Ground-based radar observations from Arecibo add polarimetric information at spatial resolutions of ~1 – 2 km, which yield broad diagnostic surface properties and surface roughness. Near-IR emissivity mapping has also been achieved, at ~50 km spatial resolution, using the VIRTIS mapping spectrometer onboard Venus Express, but this mapping was performed at one wavelength only and covers only around 40% of the planet, all in the southern hemisphere. These datasets have enabled a very broad classification of the Venus surface into different regions and terrain types; and have allowed, for example, the identification of some 900 impact craters and almost two thousand large volcanoes. These important datasets have provided a global geological context and a rich catalogue of targets which need studying in greater detail.

What is needed now is a more focused observation strategy; to collect nested image products, in a holistic way, from global down to local scales, from the cloud-tops down to the subsurface, as provided by EnVision's instrument suite. This focused investigative approach is broadly twofold: for observation types not obtained before at Venus (i.e. spectroscopic characterisation of surface composition and subsurface sounding), a global (or near-global) mapping strategy will be employed. For VenSAR observations, EnVision will focus on its Regions of Interest (RoIs) which intersect all major geologic terrain types and the boundaries between them.

Table 3.2 – Scales of surface observations for VenSAR imagery. It is not necessary to repeat Magellan's global low-resolution imagery, thus EnVision will instead focus on obtaining higher-resolution regional and targeted VenSAR observations with spatial resolutions ranging from 30 m down to 10 m. Context for these observations is also provided by VenSpec M's surface spectroscopy, Subsurface Radar Sounder investigations and from radar altimetry.

| Mapping scales: | Global | Regional | Targeted |
|--|------------------------------|-------------------------------------|-----------------------------------|
| EnVision coverage (% of global) | >95% | > 20% (Req.) 30.3% (after 6 cy.) | > 2% (Req.) 2.4% (after 6 cy.) |
| EnVision imaging coverage | Use Magellan | > 92,000,000 km ² | > 9,200,000 km ² |
| EnVision spatial resolution | 150 m | 30 m (Standard) | 10 m (High Resolution) |
| Approximate feature extents | 1 – 100s km | 100s -1000s m | 10 – 100s m |
| Examples of observable geomorphological features at these scales: | | | |
| Structures | Terra 'continents', Planitia | Chasmata, Dorsa | Folds, graben |
| Volcanoes | Volcanic rises (Regio) | Volcanic edifices | Lava Flows |
| Sediments | 'Featureless' plains | Parabolas, halos | Landslides |
| EnVision SAR observations | | | |

More specifically, coverage over a majority of the planet¹ will be provided by EnVision's altimeter, its radio science experiment (gravity field), VenSpec (-M, -U and -H) and SRS instruments (see also Figure 5.4.6). VenSAR will provide imaging at 'Regional' scales (30 m resolution) across its RoIs which cover *ca* 30% of the planet's surface, and at 'Targeted' scales (10 m resolution) across *ca* 2% of planet's surface within those RoIs (Table 3.2, see also Figures 5.4.4 and 5.4.5); thus high resolution observations will be placed in their spatial context, with all other types of observation. These RoIs will also be used to target more frequent subsurface sounding passes, so as to obtain smaller track-to-track spacing – a mode called "high density" SRS sounding.

The mission has also been designed to allow imaging at different angles (for stereo imaging) and at multiple times during the mission (for change detection) and thus the RoIs have been arranged to cover areas where we need detailed topography from stereo, where we would like to understand information from polarimetry, and/or where we expect that change may be occurring. Analysis of these complementary, multi-scale datasets, and their placement in the context of Magellan's global image framework, will allow a better understanding of large-scale geological processes at work.

A SAR imaging scenario has been developed for the EnVision study phase; this is illustrated in Figure 3.2. This was developed to illustrate the kind of science return that will be possible while satisfying all mission

¹ We note that for observations which can take place *only on the dayside* or *only on the nightside*, no polar Venus orbiter can achieve global coverage during a 4-year mission: some longitudes will remain unobserved due to Venus' spin properties. Coverage maps will be given in §5.

constraints. As illustrated in Table 3.3, the RoIs in this baseline imaging scenario will sample approximately 38% of mapped coronae (which includes 41% of coronae thought to be active by Gülcher et al., 2020), 67% of known dune fields, 71% of identified landslides, 50% of the probes/landers, 14% of volcanic rises and 29% of mapped large volcanoes. These kinds of metrics will be used to further refine the RoI selection in coming years. Table 3.3 also shows that this approach allows prioritisation of different types of observations – for example, a prioritisation of polarimetric observation for regions of suspected anomalous dielectric properties – for different target regions, as will be discussed in further subsection below. Selection of targets for the eventual mission will continue to evolve depending on inputs from the science team up to and during the mission. The mission design offers enough flexibility to adapt the observation plan to potential future changes in the mission objectives. This could include changes in the ratio of different radar modes, for example, or changes of surface targets in response to discoveries made before or during the mission.

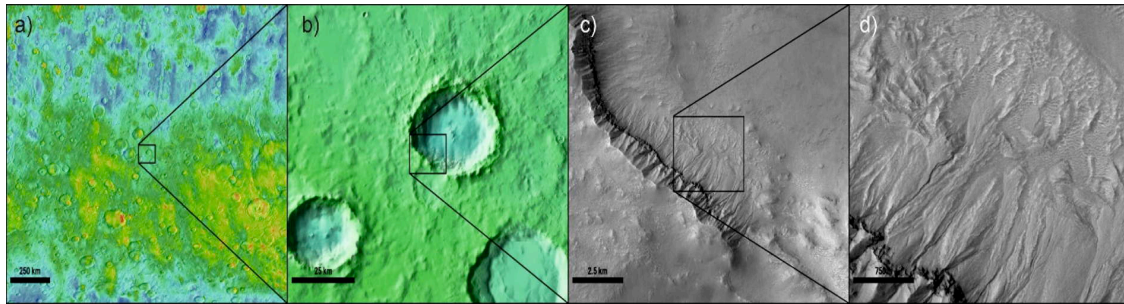


Figure 3.1 – An example from Mars showing the power of nested imaging: a) Thermal Inertia data at ~50 km/pixel (similar to spatial resolution of VenSpec-M); b) MOLA topography (232 m/px) overlain on 100 m THEMIS mosaic (equivalent to EnVision's stereo-derived global topography); c) CTX data (29 m/px), equivalent to EnVision's 30 m standard SAR; and d) CTX data (7 m/px), equivalent to EnVision's high resolution SAR. These illustrate how the progression from global coverage towards targeted imaging will allow EnVision's observations to make a significant leap forward from the understanding we have gained from Magellan data.

EnVision will employ the same strategy that has proved so successful on Mars and on Earth, and that has enabled great leaps forward in the understanding of surface and subsurface processes and their control on geomorphology and geology, as illustrated in Figure 3.1. Every time Mars has been observed at roughly an order of magnitude higher resolution, entirely new and often unexpected processes have been observed. The global context of these discoveries provides immensely important insights on a planet's evolution. This philosophy of nested, Regional and Targeted imaging is explained more fully in the following sections.

3.3 EnVision will investigate how the surface and interior of Venus have evolved to their current state

3.3.1 Regional / Targeted Surface Mapping

The surface of Venus hosts a variety of different features – volcanoes, rifts, mountain belts, etc. – that are typically on a scale of hundreds of kilometres, although some are significantly larger (e.g. Artemis at 2600 km), set in globally extensive regional lowland plains. While each feature will undoubtedly have its unique aspects, experience from Earth, Mars and the Moon shows that each class of feature (e.g. shield volcanoes, ridge belts) shares common causal processes that can be understood from a representative selection of two or three examples from each class. Therefore, to understand how Venus works, it is necessary to obtain data from a fraction of the surface. However, the ~8% of the surface classified as highlands are different and appear to be ancient, often complexly deformed terrain (tesserae) that may hold clues to conditions more than a billion year ago – perhaps to a time when liquid water was capable of condensing on the surface of Venus. Maximising the opportunities for understanding the past therefore requires a high resolution survey of some of these highland areas.

Table 3.4 – Estimates of VenSAR 30-m imaging coverage of baseline Science Operations Reference Scenario with respect to global areal extents of geological terrain types (as mapped by Ivanov & Head, 2015).

| Terrain Types | Fraction of global surface area | All observations [†] | Triple observations (change detection) [†] | Double observations (no polarimetry) [†] | Double observations (with polarimetry) [†] |
|---------------------------|---------------------------------|-------------------------------|---|---|---|
| Tessera highlands | 7% | 50% | 17% | 17% | 16% |
| Tectonically active zones | 4% | 69% | 39% | 14% | 17% |
| Impact craters | 1% | 20% | 7% | 3% | 4% |
| Lowland plains | 80% | 21% | 6% | 5% | 4% |

[†] Percentage of the global areal extent of each geological terrain type imaged with 30 m SAR in this imaging scenario.

3.3.2 Surface Topography

EnVision has three primary means for topography measurements. Topographic measurements of global extent are made by the VenSAR altimeter mode and the SRS radar sounding instrument. These instruments make spot measurements with an along-track sampling of 3 and 9 km spatial resolution, and 2.5 and 15 m vertical resolution, respectively – all of which represent a marked improvement over the topography products available from Magellan, as shown in Table 3.3. Spacing between the tracks at the equator will be roughly 40 km. These data will support science investigations such as the aforementioned crater modification and depth inventories and plain resurfacing. Higher resolution topography will be acquired through radar stereo techniques for roughly 25% of the surface in the regions of interest. By acquiring data with an incidence angle difference on the order of 5°, topography data with 300 m spatial resolution and 20-30 m elevation accuracy can be obtained for areas with sufficient scene contrast. The higher resolution topography products are essential for quantitative modeling of surface geologic processes like faulting and folding. Moreover, high resolution topography is needed to properly compensate VenSpec-M emissivity data for topographically induced atmospheric effects on surface rock type determination and to investigate microwave emissivity as a function of altitude.

Surface topography is integral to many of the EnVision science investigations, either as the primary data source for inferring the type and magnitude of geologic processes that shape the surface, or as ancillary data necessary for proper interpretation of other data. The resolution and vertical accuracy required depends on the investigation and varies from several kilometre scale resolution to roughly quarter kilometre with vertical accuracy of 10s of metres. Magellan global topographic data with its 15-20 km resolution and vertical accuracy of 50-100 m is insufficient to support these investigations (Ford, 1992).

Quantitative modeling of faulting and folding requires knowledge of topography with a vertical resolution of 25-50 m. Such models can constrain the physical processes that produce the observed tectonic landforms, the magnitude of the deformation, and the mechanical structure of the crust and lithosphere in the vicinity of the tectonic feature.

Topography from SAR stereo data for impact craters, at horizontal resolutions less than a quarter to a third of a crater diameter, i.e. less than 10 km, and vertical resolutions better than 20 m, will enable the measurement of the thickness of post-impact crater fill. Still finer spatial- and vertical-accuracy topography measurements will reduce the uncertainty in crater depth-diameter measurements and more accurate crater fill thickness estimates (Figure 3.3). Moreover, the plains of Venus are under-represented in the RoIs, and a globally distributed set of topographic measurements will be particularly important for understanding the plains resurfacing history.

Topography data are also needed for investigations other than those of the SAR. The Subsurface Radar Sounder (SRS) requires topographic information to identify likely off-nadir echoes (“clutter”) that may confuse subsurface feature identification. Knowledge of the absolute surface temperature is needed for calculation of the absolute surface emissivity from near-IR nightside observations. The variation of surface temperature is primarily dependent on surface altitude; reducing the accuracy of the surface altitude determination to ≤ 10 m also reduces the uncertainty in the absolute determination of surface emissivity.

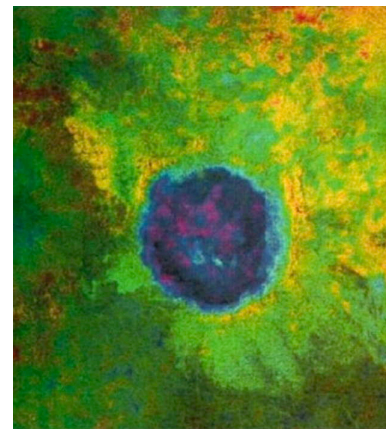


Figure 3.3 – Stereo-derived topography of Markham crater overlain on radar imagery shows that the western portion has no elevated rim and appears embayed by the corona to the west (Herrick, 2000).

3.3.3 Surface properties: passive off-nadir radiometry, surface polarimetry, microwave emissivity and Near-IR emissivity

Used in passive radiometry mode, EnVision SAR will map the thermal emission emanating from Venus surface with significantly better precision and accuracy than the Magellan radar (0.7°K against 1-2°K and 1.7°K against 15°K, respectively, see Table 3.3). Emission maps, in the form of surface brightness temperature maps, will then be used to search for thermal anomalies or, if the surface temperature is known, to map the emissivity of the surface which, in turn, provides insight into its composition (through the dielectric constant) and physical properties (roughness, density).

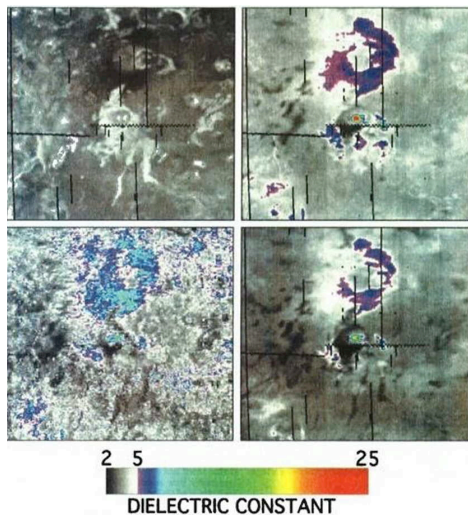


Figure 3.4 – Example of roughness and dielectric mapping from radar and radiometry data for Bell Regio, centered on the 250-km diameter volcano Tepev Mons (Campbell and Rogers, 1994). Clockwise from upper left is (1) roughness map; (2) roughness-corrected dielectric constant; (3) dielectric constant not corrected for roughness; (4) dielectric constant from Magellan radar altimeter data.

As a baseline, passive radiometry will be carried out in a near-nadir (with an incidence angle of 14°) or nadir viewing geometry, in parallel with other EnVision instruments. The surface microwave brightness temperature will be recorded globally (>75% of the surface) with repeated observations (at least 3 times) and a final resolution likely better than 10 km when using all overlapping near-nadir observations.

Nadir and near-nadir radiometry are primarily designed for the search of thermal anomalies (§ 3.4.1) but will also be used, based on assumptions on the physical temperature, to build a mosaic of the surface emissivity at 9.5-cm by dividing the measured brightness temperatures by an estimate of the surface temperature. At nadir or near-nadir the microwave emissivity of a surface is largely controlled by its dielectric constant and the surface roughness only has a second order effect. In turn, the dielectric constant is related to the bulk composition and density of the surface material and the dielectric map inferred from radiometry measurements will be used to distinguish surface units. More specifically, for dry materials, the relationship between dielectric constant and the density is generally well described by a power-law function and, with some assumptions, the dielectric map can be readily converted into a global near-surface density map (Campbell et al., 1992).

In addition to near-nadir and nadir observations, polarized radiometry measurements will be acquired in an off-nadir geometry (with a viewing angle of 25-30°) in selected regions. As aforementioned, the main advantage of nadir radiometry is to be less sensitive to roughness than off-nadir radiometry. However, the average of two orthogonally polarized emissivity values (or the polarization ratio) is also less sensitive to roughness than either individual component and can be used to provide an even more reliable estimate of the dielectric constant, requiring no assumption on the physical temperature. Such measurements will be primarily performed in Venus highlands to confirm or inform their unusually high dielectric constant and put new constraints on their composition candidates. Recording of both H and V polarization in an off-nadir geometry will distinguish between the effects of dielectric constant and roughness/volume scattering, thus offering an additional powerful tool for surface characterisation.

EnVision will acquire dual-polarization SAR imagery at 30 m resolution for about 7% of the surface after 6 cycles (Table 5.4.1) which aids surface characterisation by exploiting the polarimetric reflection properties of the surface. SAR polarimetry is essential for differentiation of surface types & properties; it is sensitive to surface roughness and structure (e.g. consolidated vs fine-grained material). EnVision employs a dual polarization mode (transmitting H and recording H and V polarizations) to enable differentiation between terrain types and make first-order surface properties characterisation. Dual polarization was chosen for data rate and swath width considerations and H polarization to match the Magellan data enhancing change detection studies.

By collecting emissivity data at a higher resolution than the radar of Magellan, with better precision and especially accuracy (by a factor ~10) and geometries (targeted off-nadir polarized measurements) relevant to the science objectives, the EnVision radar operating as a radiometer combined with the instrument high-resolution topography and polarimetric imaging will refine the mapping of Venus surface in terms of

composition and physical properties. It will thus provide key information to retrieve the geological history and age of its terrains. In particular, it will help unravel the nature and rate of alteration in Venus high-altitude low-emissivity regions, investigate impact modification in crater ejectas and maybe unveil deeply weathered regions, thick sedimentary layers or signatures of recent resurfacing. By the end of the EnVision mission (6 Cycles) we should be able to produce a radiometry map of > 90% of the surface, with a resolution of about 10 km using all overlapping measurements.

The active and passive VenSAR observations described above are complemented also by Near-IR emissivity measurements from VenSpec-M. As discussed in §2.3.1, this Near-IR spectroscopy takes advantage of narrow atmospheric windows on Venus' nightside to map surface emissivity in six spectral bands at wavelengths between 0.86 and 1.18 μm – a region which is particularly sensitive to iron-oxide content. The emissivity maps will be crucial not just in the search for felsic rocks in tessera highlands (as described in §2.3.1) but also in the constraint of surface material composition across all other surface investigations; examples include characterisation of volcanic flows (e.g. d'Incecco et al., 2017) and volcanic highlands, and the investigation of composition changes associated with wind streaks and other aeolian geomorphological features. The VenSpec-M investigation includes eight further spectral bands, most of which are used to compensate for atmospheric variability which otherwise would affect surface emissivity retrievals – the instrumental approach will be described further in §4.4 below.

3.3.4 Subsurface material boundaries

EnVision is the first mission to Venus with a confirmed sounding instrument (ISRO's proposed Venus mission is also considering a sounder, see §2.4) that will allow for the direct measurement of subsurface features. Despite some geological surface investigations that provide hints about possible existence and nature of subsurface structures, no direct measures exist. In this context the Subsurface Radar Sounder (SRS) onboard EnVision mission represents a unique opportunity to sound the great variety of geologic and geomorphic units.

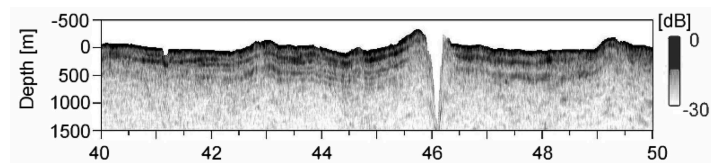


Figure 3.5 – Example of stratigraphic relationships between near-surface layers detected by LRS on the Lunar maria on the Moon (Oceanus Procellarum; depth in m., latitude in deg. (Kobayashi et al., 2014).

SRS will investigate stratigraphic and structural patterns, to test hypotheses related to the origin of structures at the surface and in the shallow subsurface and their relationships (Figure 3.5). This will enable investigation of interaction processes between surface and subsurface structures as well as subsurface structures not directly linked with surface ones.

There are many geological investigations for which the detection of subsurface boundaries may provide invaluable constraints. They include impact craters and their infilling (Figure 3.6), buried craters, tesserae and their edges, plains, lava flows and their edges, and tectonic features, and volcanic features. For those features subsurface characteristics are crucial for: the relative dating of surfaces by the analysis of stratigraphic relationships, the modelling of three-dimensional structure, the identification of boundaries between units/edges. The subsurface material boundary delineation by sounding will improve the understanding of Venus resurfacing history and geologic evolution.

These investigations will be conducted Venus wide (with an average observation density of 2 per degree of longitude at Equator) and on selected RoIs which include the mentioned features (with an average observation density of 10 per degree of longitude at Equator). The scientific investigations described in § 2 (and summarised in the science traceability matrix, §3.1) call for a penetration down to a few hundreds of metres (up to 1000 m) and about 20 metres of vertical resolution. The typical depth needed for sounding of different subsurface feature types is shown in Figure 3.7a. Calculations of SRS penetration depth, shown in Figure 3.7b and explained in greater detail in §4.3, confirm that the SRS will be able to investigate a wide variety of geological targets. The SRS penetration depth has been calculated using a large variety of different rock types and surface topologies; for a quick demonstration of the viability of HF subsurface sounding through rocks at Venus temperatures, Figure 3.8 shows an example of sounding through lava at > 600 °C of a volcanic crater floor on Earth. Further information on expected SRS performance is given in §4.3.

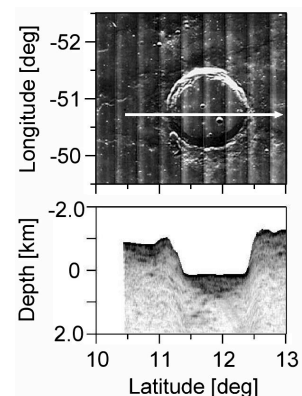


Figure 3.6 – Example of filled crater detected by the LRS on the Moon. Lunar orbiter image of Marius crater (upper) and LRS processed image (lower). LRS ground track is indicated as a white arrow. LRS image clearly shows the basalt filling the inside of the crater to completely cover its original bottom (Kobayashi et al., 2014).

An important stage in the SRS data reduction is “decluttering”, that is detecting off-nadir return echos from topography (Ferro et al., 2013; Carrer and Bruzzone, 2017). Therefore, the best quality SRS analysis will be possible in the Regions of Interest for which high-resolution Digital Elevation Models (DEMs) from VenSAR stereo topography will be available. In the EnVision VenSAR RoIs then, SRS sounding will be performed with “high density” (an average observation density of 10 per degree of longitude at Equator). Beyond this, SRS investigations with “low density” (an average observation density of 2 per degree of longitude at Equator) will be performed over the majority of the rest of the planet, using both topography from VenSAR altimetry, and techniques that do not require DEM (Carrer and Bruzzone, 2017) for clutter detection.

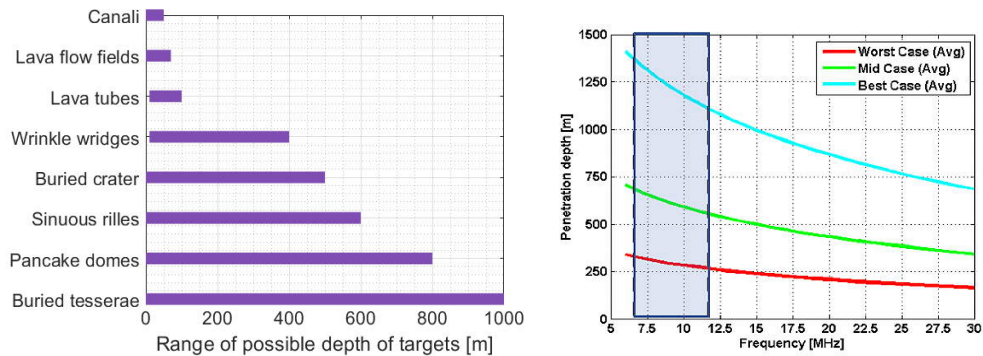


Figure 3.7 – (a, left): Typical subsurface sounding depths needed for different geological targets; (b, right): SRS average penetration depth calculated for different Venus-like samples (from measurements on Moon and Earth analogue materials at Venus temperature) versus the central frequency. The selected bandwidth of SRS is pointed out in the shaded area.

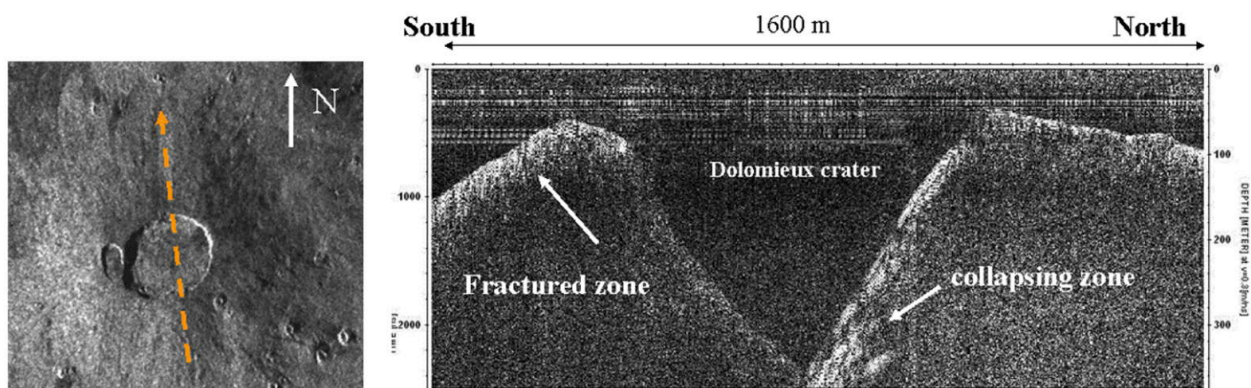
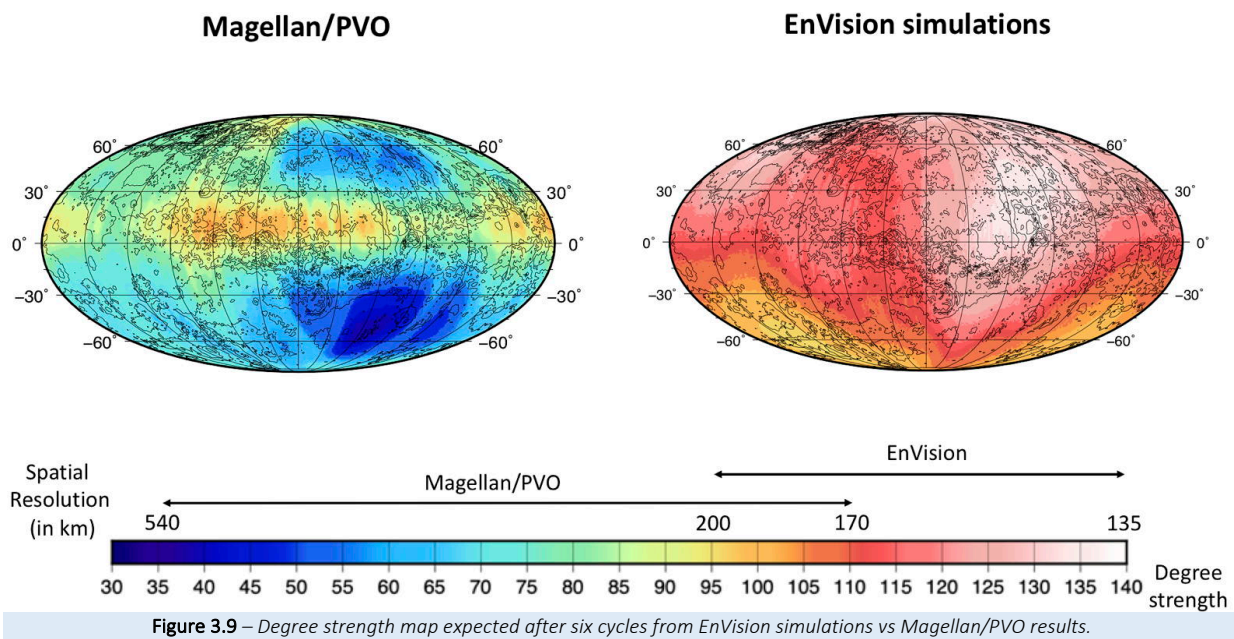


Figure 3.8 – Airborne radar sounder profile at 40 MHz central frequency (more than four times higher than the SRS one) over the Dolomieu Crater on the top of the Fournaise Volcano in the reunion Island in the Indian Ocean. Fournaise is a hot spot effusive volcano with geomorphological features and magma dynamic very similar to several Venusian volcanos (Anderson 2005). The radargram crossing from South to North the main crater on the top of the volcano show the fractured areas (white areas before and after the crater) that are materialized by the strong signal scattering resulting from the fractures. Inside the crater the radargrams shows the layering that is on the crater northern wall arising from the succession of debris flowing from the collapsing northern part. The crater depth is approximately 100 m and its width 1 km. The lava temperature ranges from 40 C at the surface to 600 C beyond the 10 m level, demonstrating the viability of HF sounding through rocks at these elevated temperatures.

The SRS will also return valuable information about the surface: The surface echo provides information on the surface and near-surface reflectivity that can be inverted for constraining the surface permittivity (Watters et al., 2006) at HF band. This information can be exploited for complementing and reducing the ambiguity derived from VenSAR due to surface roughness. Moreover, the SRS off-nadir surface echoes (i.e. clutter) when coupled with a DEM can produce HF roughness images of the surface, which also highlight otherwise undetected shallow subsurface features (Carrer et al., 2021).

3.3.5 Gravity Field

The current gravity field of Venus is, on large portions of the planet, insufficiently well resolved to allow detection of regional variations that could be related to variations in the lithosphere and crust thicknesses. Indeed, the spatial resolution of the Magellan/Pioneer Venus Orbiter (PVO) gravity solution varies from degree 110 down to 30 (170 down to 620 km spatial resolution) (Figure 3.9). Furthermore, the error on the current solution of the k_2 Love number is 22%, which does not allow determination of the mantle composition, nor the state and size of the core. The EnVision gravity experiment objective is to obtain a gravity field resolution at degree of at least 90 (210 km spatial resolution) over the entire planet and a k_2 Love number solution with an



error smaller than 3%. Both gravity field and k_2 Love number are determined from the precise reconstruction of the orbit of the EnVision spacecraft. This Precise Orbit Determination (POD) process relies on the 2-way mode Doppler tracking data and the a priori knowledge of the forces driving the spacecraft motion. Numerical simulations of the POD and gravity reconstruction process including modeling of forces impacting the orbit e.g. gravitational, solar pressure and atmospheric drag show that the EnVision gravity objectives are met with 3.5 hours of effective Doppler tracking per day, using the dual X-Ka band downlink to reduce the solar plasma effect on the Doppler measurements. The error on the k_2 Love number is estimated better than 1%. The control of the pericentre altitude (at around 220 km) and the mission duration over 6 cycles greatly helps to reach the required resolution and accuracy of the gravity field and k_2 Love number.

3.4 EnVision will investigate how geologically active Venus is in the present era

3.4.1 Search for surface temperature anomalies

Currently it is estimated that present volcanic activity can be manifested in anomalously hot surface temperatures due to lava flows, as high as 1200 K. The EnVision mission will search for and monitor spatial and temporal thermal anomalies at the surface with VenSpec-M, and in the near subsurface (with VenSAR operating as a radiometer) over time scales from hours to years and with an effective spatial resolution including cloud scattering of ~ 50 km for VenSpec-M and even better with VenSAR used in radiometer mode. More specifically, the EnVision IR emissivity mapper will inspect the surface while, depending on the surface composition and therefore on the depth to which the instrument is sensitive, VenSAR operating as a microwave radiometer should be able to probe the near subsurface and detect the thermal signature of an Etna-type eruption (producing 0.1 km^3 or 6 km^2 lava flow at six year intervals) from months to a few decades after it occurred, even if the surface itself has cooled to ambient temperature (Lorenz et al., 2016).

A search for thermal anomalies can either include spatial anomalies (regions of unusually high thermal emission) or temporal anomalies (evolution of surface temperatures in repeat temperature measurements within the mission or with respect to Magellan, Venus Express or Akatsuki indicative of volcanic activity). IR observations will be performed on the night side while microwave observations will be evenly distributed throughout the mission, to obtain coverage at all local times of day. As a start, measurements will be compared to the physical surface temperatures calculated using the adiabatic model of Seiff et al. (1985). The radiometer accuracy will be < 2 K to be compared to the 15 K accuracy of the Magellan radiometer. A precision of 1 K on the recorded brightness temperatures - both in IR and microwave - will guarantee capturing the day-to-night temperature difference at the surface, which latest models estimate to be as much as 3 K at the Equator.

The microwave radiometer will measure the surface brightness temperature at a wavelength of 9.5 cm with a typical footprint on the ground of dimension 5 km x 55 km and an expected final resolution (from overlapping footprints) better than 10 km in both directions which represents a significant improvement over Magellan - Venus surface thermal emission at 12.6 cm from Magellan has a resolution of 15 km x 23 km at periapsis (10°N) to about 85 km at the north pole (Pettengill et al., 1991, 1992). It will, as a baseline, operate in a nadir- and near-nadir (14° incidence angle) viewing geometry which is less sensitive to roughness than Magellan off-nadir observations (for reference Magellan data were collected primarily in H-polarization at incidence angles of 25-45°) and therefore more appropriate to assess the surface temperature. By the end of the EnVision science phase (6 Venus cycles, 4 years), at least 2/3 (76% for VenSpec-M, 93% for microwave radiometry, see Table 5.4.1) of the Venus surface will have been inspected for the search of thermal anomaly at least 3 times. If a thermal anomaly is detected in an area not yet included in the RoIs, the mission has the flexibility to observe it at later passes.

3.4.2 Search for changes in surface radar imagery

EnVision employs multiple methods for detecting present data geologic activity on Venus. Changes in radar imagery provide a means of detecting surface changes occurring at the kilometre scale or larger over times spans of 9 months (between Cycles of EnVision mapping) to 45 years (EnVision-to-Magellan). Change detection in radar images is complicated by radar speckle noise and by changes in the imaging geometry. Unlike Magellan, EnVision has planned repeat observations with the same imaging geometry, greatly facilitating change detection. As outlined in Table 3.3. EnVision's SAR will have lower noise levels than Magellan SAR despite its much higher spatial resolution; VenSAR is designed to use at least 8 looks (spatial averaging of radar pixels) for all its radar image products and so it has an average SNR greater than 10 dB, the speckle/thermal noise will allow more sensitivity to change detection for surface changes like new lava flows or large landslides with the same imaging geometry. Moreover, algorithms exist to efficiently reduce the speckle noise and they proved to be very valuable on the Cassini radar dataset (Lucas et al., 2014).

Decadal time-scale surface modifications will be assessed by comparing EnVision images to Magellan images acquired 45 years before. EnVision uses a radar wavelength very similar to Magellan (9.5 cm versus 12.6 cm) and hence will have similar radar backscatter characteristics. EnVision also plans to acquire its imagery looking to the east to have maximal overlap to that acquired by Magellan. However, as Magellan acquired imagery with a wide range of incidence angle (15° - 45°) and at lower resolution than EnVision, comparison will necessitate greater care to avoid false detections. By looking for changes exceeding a lower areal threshold and employing the geologic interpretation expertise of the science team we expect to eliminate most false detections.

3.4.3 Search for atmospheric changes

As discussed in §2.3.5, the search for volcanic activity is conducted not only by surface changes but also by monitoring atmospheric changes such as water vapour or volcanic ash plumes. EnVision will detect such anomalies below the clouds, by searching for water vapour anomalies in three different altitude bands; within the clouds, by characterising the attenuation in the clouds of thermal emission from the low atmosphere; and above the clouds, by investigating variations of sulphur and water vapour species and related cloud properties. For a detailed discussion of the atmospheric observation strategy, the reader is referred to §3.5 below.

3.5 EnVision will investigate how Venus' atmosphere and climate are shaped by geological processes

Envision's atmospheric science observations have been crafted based mainly on experience from precursor instruments on Venus Express; That experience has been used to create a suite of instruments with spectral ranges and resolutions tailor-made for high sensitivity to track key volatile species in the Venus atmosphere from the surface up to the mesosphere. The improved gas sensitivity of EnVision's atmospheric measurements compared to their precursors on Venus Express is summarised in Table 3.5. Solar and stellar occultation measurements from Venus Express offered higher sensitivity to trace gases but far lower spatial coverage than is possible with nadir measurements, which is why they are not included here. EnVision's observations, from low circular orbit, will be very different in spatial coverage than those from Venus Express, offering coverage with higher spatial resolution and more symmetrical latitude coverage than was obtained from Venus Express.

3.5.1 Near-IR nightside spectroscopy to measure tropospheric trace gases and lower cloud properties

Measurement of gaseous species below the clouds at altitudes of 0 - 50 km will be achieved thanks to several IR spectral transparency “windows” around 1 μm , at 1.17 μm and 2.3 μm . Through these windows, in-orbit instruments can peer below the clouds down to the lower atmosphere and surface. The thermal radiation emitted by the planet’s surface is attenuated as it passes upward through the clouds and the atmosphere. This attenuation arises both because of absorption by cloud particles themselves (nonconservative scattering), and by gaseous absorption. Because the particles are liquid and approximately spherical, and because the wavelength of the light is of the same order as the radius of the particles, one can assume Mie scattering for the calculation of their scattering properties. These measurements can only be performed during the night, when the solar radiation scattered by the clouds does not overwhelm the less intense signal from the surface. EnVision will sound the lower layers of the atmosphere close to the surface to gain information on a series of trace gases which can be related to volcanism or geological activities on Venus. EnVision will also investigate the lower cloud region to map vertically integrated total cloud opacity, cloud properties and their variations which will be investigated on time scales from hours to years and spatial resolution of ~ 100 km. The detailed windows into the nightside atmosphere, and the corresponding trace gas species and the altitudes at which they can be measured, are as follows: (1) 1.16–1.19 μm (H_2O , HDO at 0–15 km); (2) 1.72 to 1.75 μm (H_2O , HCl at 15–25 km); (3) 2.29–2.48 μm (H_2O , HDO, HF, CO, COS, SO_2 at 30–40 km). The high spectral resolution ($R \sim 8000$) coupled to the high sensitivity of the VenSpec-H instrument will be sufficient to clearly identify the absorption features of the targeted species.

| Parameter | EnVision | Venus Express |
|---|--------------------------|--------------------|
| nIR maps: H_2O@ 10-20 km | VenSpec-M | VIRTIS-M-IR |
| H_2O retrieval accuracy | 10% | $\sim 25\%$ |
| nIR spectra: H_2O @10-20 km | VenSpec-H | SPICAV-IR |
| Spectral resolving power $\lambda/d\lambda$ | ~ 8000 | ~ 1700 |
| H_2O retrieval accuracy | 3% | $\sim 25\%$ |
| HDO retrieval accuracy | 5% | not possible |
| nIR - gases @30-40 km | VenSpec-H | VIRTIS-H |
| Spectral resolving power $\lambda/d\lambda$ | ~ 8000 | ~ 2000 |
| H_2O retrieval accuracy | 3% | $\sim 10\%$ |
| CO retrieval accuracy | 1.5% | $\sim 10\%$ |
| SO_2 retrieval accuracy | 1% | $\sim 50\%$ |
| nIR - gases @ 70 - 90 km | VenSpec-H | SPICAV-IR* |
| Spectral resolving power $\lambda/d\lambda$ | 8000 | ~ 1400 |
| H_2O retrieval accuracy | 10 - 15% | 10 - 20% |
| UV - gases @ 70 - 90 km | VenSpec-U | SPICAV-UV |
| Spectral resolving power $\lambda/d\lambda$ | 1000 (HR ch) | ~ 200 |
| SO_2 retrieval accuracy | 10% | $\sim 25\%$ |
| SO: SO_2 retrieval accuracy | 25% | n/a |
| Cloudtop altitude accuracy | 0.3 km | 1 - 2 km |
| Radio Occultation | Radio science | VeRa** |
| Altitude range probed | 35 - 90 km | 40 - 90 km |
| H_2SO_4 vapour sensitivity | 1 ppm | 1 - 3 ppm |
| H_2SO_4 liquid sensitivity | 1 mg/m^3 | n/a |
| Number of profiles per year | ~ 4500 | ~ 100 |

*Both VIRTIS-H and SPICAV-IR measured this; here we have listed the latter instrument. **Akatsuki also conducted radio occultation, with broadly similar performance to VeRa.

Table 3.5 - The EnVision atmospheric gas measurements are informed by, but surpass in sensitivity, equivalent precursor measurements from Venus Express. Sensitivity to only some trace species is shown here, in order to demonstrate performance improvements.

3.5.2 Radio occultation to measure Sulphuric acid liquid and vapour

EnVision’s communication system and an onboard Ultra-Stable Oscillator (USO) will be used by the Radio Science experiment for sounding the neutral atmosphere and ionosphere of Venus, during the occultations that occur during the communications links. As the spacecraft starts to be occulted (or after, when reappearing from behind the planet during egress) the spacecraft carrier signal probes the layers of the planet’s atmosphere, causing changes in the frequency and amplitude of the carrier waves (at X- and Ka-bands). The bending of the radio-link signal, derived from the frequency shift, allows derivation of profiles of the neutral atmosphere (density, temperature and pressure) and its absorption allows estimation of sulfuric acid concentration.

The radio-occultation experiment will then determine the atmospheric structure from 35 to 100 km by deriving vertical profiles of neutral mass density, temperature, and pressure as a function of local time and season, with a vertical resolution of few 100s of metres and an accuracy of 0.1 K at 35 km. Such an accuracy will inform studies of the atmospheric dynamics (gravity waves for instance, see Figure 3.10b). Thanks to the use of the dual X-Ka band, the content in liquid phase of the sulfuric acid will be estimated for the first time. The spatial and temporal behavior of the H_2SO_4 absorbing layer (gaseous & liquid) below the cloud deck will be also investigated (at 35-55 km, with an accuracy of 1 ppm for the gaseous phase and 1 mg/m^3 for the liquid one with a vertical resolution of 100 m). As shown by Figure 3.10a, the H_2SO_4 content varies with depth and

latitude. Such an accuracy and vertical resolution, together with the frequent radio-occultations, will allow us to better understand the sulfur cycle.

As mentioned in §2.3.7, measurements of the vertical profile of temperature, pressure and number density in the troposphere and mesosphere (35-90 km) of Venus will help to understand the processes driving the short term as well as the long-term variability of the atmosphere, the cloud-level convection, and the global circulation. Observations should be as widely spread in latitude, longitude and local solar time, and throughout the nominal mission to understand both global circulation processes and transport of atmospheric constituents. As abundance of sulphuric acid in the atmosphere of Venus is linked to a) the present-day volcanic activity and b) the influence of the sulphur cycle, monitoring spatial and temporal variations of H₂SO₄ (gaseous and liquid), on time scales from hours to years with a vertical resolution of ~100 m, will therefore increase the understanding of both, a) and b). While H₂SO₄ vapour is to be detected in the altitude range between 35 and 55 km altitude with an accuracy of 1 ppm, the accuracy of 1 mg/m³ is required to detect variations of liquid H₂SO₄ around 50 km altitude.

It may be possible to use the SRS to detect the electromagnetic signatures of lightning (see Lorenz, 2018 for a review of detections and non-detections of lightning), an investigation which would contribute to the understanding of chemical and microphysical processes at work in the cloud layer. Moreover, SRS may be used for ionospheric sounding, as is conducted routinely by MEX/MARSIS (Picardi et al., 2005). These investigations are not formally among the science requirements of the mission, but their inclusion will be considered during Phase B study.

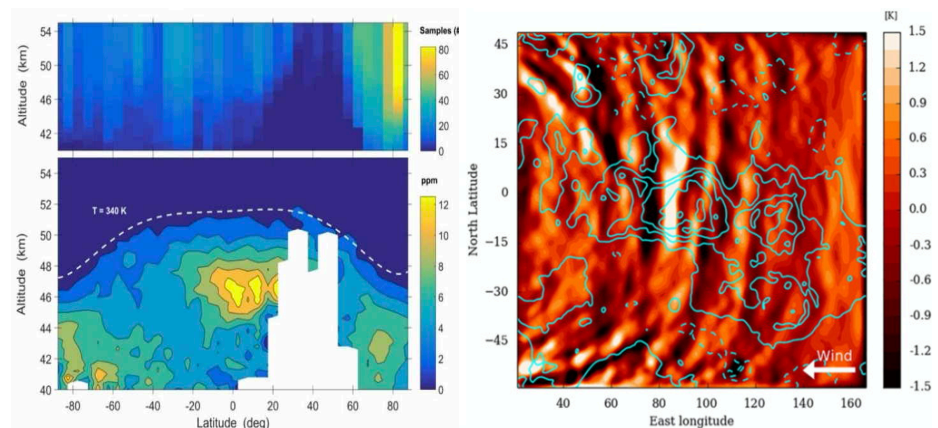


Figure 3.10 – (a, left): Gaseous H₂SO₄ content in function of latitude and altitude derived from radio-occultations by VeRa (Oschlisniok et al., 2020). (b, right): Expected temperature anomalies in a gravity wave at 70 km above Aphrodite Terra (Lefèvre et al., 2020).

3.5.3 Dayside UV and Near-IR spectroscopy to measure mesospheric trace gases and cloud-top properties

The core goal of mesospheric investigations is to map the variability of trace species, cloud and aerosol properties and to distinguish intrinsic from extrinsic (e.g. volcanic emissions) variabilities. Sensitive to the UV sunlight scattered by Venus' cloud top, absorption bands allow the detection of (SO+SO₂) near 215 nm and SO₂ at 280 nm. Similarly, different IR bands permit the observation of H₂O, HDO, CO, COS, SO₂ at 70–90 km. Observations will provide insight on the spatial distribution of trace gases essential for the understanding of the main chemical cycles on Venus. Typical spatial resolution of 100 km will help resolve most of the features, but UV monitoring will be able to reach a spatial sampling of ~ 25 km. Moreover, some campaigns with spatial sampling down to 3 km will be used for studying small-scale convection and vertical mixing processes, in particular above specific regions of interest. Typical measurement accuracy should be improved at least by a factor of two compared to previous measurements: total SO_x column density from SPICAV-UV/VEx (Marcq et al., 2013, 2020), SO:SO₂ ratio from STIS/HST (Jessup et al., 2015). Spatial coverage will also be dramatically improved compared with SPICAV-UV thanks to the much larger FOV of VenSpec-U.

EnVision will investigate the upper atmosphere using the following wavelength ranges and resolutions: (1) 205-235 nm at 0.2 nm spectral resolution (SO₂ and SO separately at 70-80 km); (2) 190-380 nm at 2 nm spectral resolution (UV absorber, total SO+SO₂ at 70-80 km); (3) 1.36–1.409 μm (H₂O, HDO at 70-90 km); (4) 2.29–2.48 μm (H₂O, HDO, CO, COS, SO₂ at 70–90 km). In the IR range, the high spectral resolution (R ~ 8000) along with the high sensitivity of the instrument will be sufficient to clearly identify the absorption features of the targeted species. In UV, a FOV>20° is required to have 4-5 successive observations over the same ground spot and assess coupling between surface (volcanic activity, topographic features) and cloud top level measurements.

3.6 Key Questions and Answers about EnVision Science

1. Why do you need another Venus orbiter mission, after Magellan, Venus Express and Akatsuki?

Magellan gave us a global map of the Venus surface, which is the basis of much of our current understanding of Venus geology. However, this map is limited by the 100-300 m spatial resolution of the radar, by the low radiometric resolution (high noise) of the radar, and the topographical information it provided is of even poorer resolution and accuracy, with errors of > 1 km in places. EnVision will not only take advantage of decades of radar development to obtain better quality measurements, but also will obtain complementary datasets, from subsurface sounding and volcanic gas plume measurement to surface temperature measurement and composition mapping through NIR spectroscopy. This combination of measurements will give a much more comprehensive view of Venus than a radar mapper alone can.

Venus Express and Akatsuki focused primarily on atmospheric science. EnVision turns its focus to the geological state of Venus today, how it evolved to its present state, and how this has affected its hostile climate, addressing some of the most compelling questions arising after these missions. EnVision's atmospheric instrument suite builds on the heritage from these missions, seeking to identify to what extent observed trace gas variations are associated with geological activity.

2. Why are you focussing your radar imaging investigations only on 30% of the planet? Is this sufficient?

EnVision's science questions are designed not only to address some of the most important questions of Venus science, but also to be achievable within the challenging constraints for an orbital sensing mission at Venus: (1) thick cloud layers require active microwave rather than passive optical imaging; (2) Venus' low planetary spin rate limits the number of revisit opportunities for any particular location; (3) lack of an equatorial bulge means that sun-synchronous orbits are not possible. This investigation strategy also takes into account that Venus is large: its surface area of 460 million km² is more than three times that of Mars, and also three times greater than the area of all of Earth's continents combined (Table 3.3; Figure 3.2). The payload reference operations scenario simulation demonstrates that all identified surface targets can be imaged with VenSAR, with a performance fully

compliant with the science requirements, with extra margin. The first two cycles allow imaging once 80% of the identified RoIs at 30 m resolution. The following two cycles are mostly devoted to acquiring 2nd observations of these areas for stereo-topography mapping and the two last cycles to perform 3rd observations of the "activity" type targets for change detection mapping. Dual polarization and high resolution SAR observations can be performed at any longitude at least once across the 6 cycles. EnVision's mission philosophy is to obtain the widest range of data types achievable from orbit and to use these in a targeted approach that enables us to put the highest resolution datasets into regional and global context. Similarly, understanding atmospheric processes requires a combination of global-scale mapping with targeted observations resolving smaller-scale processes.

Further info: §3.1; §5.4.4

3. Do you have enough observations to ensure detection of activity? What if none is observed?

Activity / change detection of targeted areas will be performed using a large number of methods:

- Thermal change detection (> 60% of surface, dozens of repeat observations)
- Volcanic gas plume detection below the clouds (repeated views on > 60% of surface)
- Volcanic activity related gas detection above the clouds (repeated views on > 60% of the surface)
- SAR image surface change from Magellan to EnVision (30% of surface, 40-year baseline)
- SAR image surface change between SAR passes of different look angle 30% of surface, ~1-year baseline)
- SAR image surface change between passes of same look angle (2% - 7% of surface)

Some hints of temporal thermal anomalies on the surface were reported by both Magellan and Venus Express, even though neither of them were optimised for these measurements. EnVision will not only have far more repeat observations, but also instruments optimised for detections of change, so have a detection probability orders of magnitude higher than previous missions, as well as the complementary measurements to characterise the nature of any detected activity. If EnVision did not detect any evidence of geological activity, that itself would place significant new constraints on geodynamic activity.

Further info: §3.2

4. Can EnVision's observations of Venus today really tell us about its climatic history?

Yes, if indirectly. The most important boundary condition for determining atmospheric state (composition, pressure, temperature) is the solid planet at its lower boundary. EnVision will provide unprecedented characterisation of the solid planet. It will constrain the geological activity of the surface for the duration of the geological record (past ~ billion years). It will search for compositional clues of felsic composition and evidence for drainage networks, both of which would indicate a water-rich past. It will directly search for volcanic plumes, which would provide evidence for current-day outgassing. Therefore, all three of EnVision's top-level science questions (Activity, History and Climate) contribute towards understanding the climatic history. A parallel programme of work in modelling the Venus atmosphere and its evolutionary pathways will be undertaken to support this work.

Further info: §2.2.7

5. If VERITAS is selected by NASA, will it address much of EnVision Science?

The proposed missions support both overlapping and distinct science objectives and have configured their payloads to best achieve their respective science objectives. VERITAS carries only two instruments, the Venus Interferometric Synthetic Aperture Radar (VISAR) and the Venus Emissivity Mapper (VEM), and the mission science is almost completely focused on the surface and interior of Venus. By contrast EnVision carries a comprehensive suite of five instruments whose science objectives include the surface, interior, and atmosphere. VERITAS will create global imagery (30 m radar imagery in a single polarization and 50 km infrared emissivity maps) and high-resolution topographic data (250 m spatial resolution and 5 m height accuracy) via single pass radar interferometry. EnVision aims to collect targeted high-resolution dual-polarization radar imagery (30 m for 30% of surface and 10 m for 2-3% of surface) and generate topographic data via radar stereo techniques (300 m spatial resolution with 20-30 m height accuracy) over these regions. Data with nearly global extent are acquired by the suite of optical instruments, the radar altimeter, and the

high-frequency radar sounder designed to penetrate into the subsurface.

The suite of EnVision's instruments will provide a complete set of information that no other foreseen mission is capable to provide. It will assess the coupling between surface and subsurface geological processes, interior geophysics and geodynamics, and atmospheric pathways of key volcanogenic gases. The atmospheric science objectives, geologic stratigraphy enabled by the HF radar sounder, and the radar radiometry and polarimetry measurements enable entirely new surface property characterisation beyond that possible with VERITAS.

Further info: §2.4

6. The data volume is very large. Does this present additional risk for the mission design?

As to the safe return of this large amount of data to Earth: this is secured through Ka-band transmission from a large high gain antenna of 2.5 m data combined with a high power amplifier and usage of 35 m antennas with cryocooling capability for an average of 9 hours per day ; The link budget has been calculated with 30% margin, a 30% margin is added on the instrument data rates, and a 5% availability margin is considered when assessing the science performance to cope with operational contingencies. Communication contingencies (e.g. missed or late passes, ground station failure) are handled by the on-board SSMM, oversized for such purpose, and the implementation of specific offline arraying slots to downlink the excess data from the SSMM. Furthermore, the predicted surface coverage is comfortably in excess of the coverage requirements, (e.g. 40% margin for standard VenSAR 30 m imaging data). Therefore the mission is resilient to unexpected problems or underperformance and is designed to fulfil the required data return requirement.

As to dealing with these datasets on the ground: the data volume of 210 Tbits is indeed large by the standard of planetary missions, but very small by the standards of Earth Observation or Astronomy missions, let alone those of the mid-2030s when this dataset will be returned.

4 Payload

The EnVision payload consists of five instruments provided by European and American institutions. The five instruments comprise a comprehensive measurement suite spanning infrared, ultraviolet-visible, microwave and high frequency wavelengths. This suite is complemented by the Radio Science investigation exploiting the spacecraft TT&C system enhanced by the Ultra-stable Oscillator. All instruments in the payload have substantial heritage and robust margins relative to the requirements with designs suitable for operation in the Venus environment. This suite of instruments was chosen to meet the broad spectrum of measurement requirements needed to support EnVision science investigations. A full science traceability matrix is given on pages 40-41.

4.1 Payload Overview

EnVision carries a robust suite of observing instruments including VenSAR, a dual polarization S-band radar, three spectrometers VenSpec-M, VenSpec-U and VenSpec-H designed to observe the surface and atmosphere of Venus and SRS a high frequency radar sounding instrument to penetrate into the subsurface. Data from this suite of instruments, coupled with gravity science based on tracking data, and radio occultation measurements will support science investigations of the surface, interior and atmosphere and their various interactions. Figure 4.1.1 illustrates how this multi-faceted suite of measurements feeds into the EnVision science objectives.

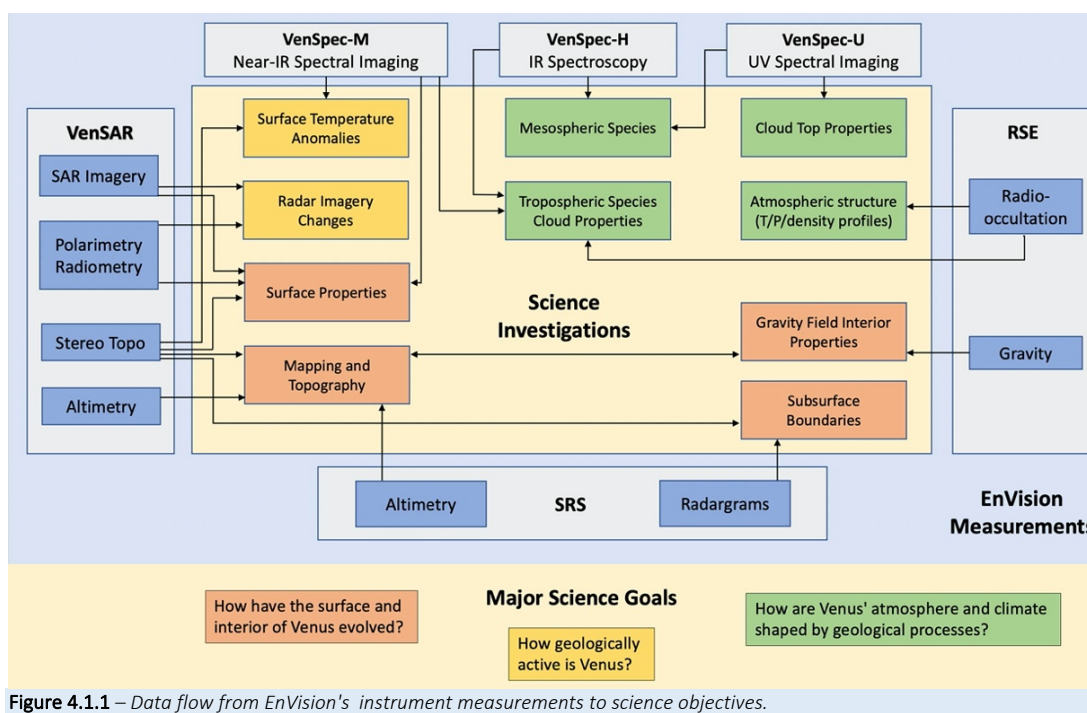


Figure 4.1.1 – Data flow from EnVision's instrument measurements to science objectives.

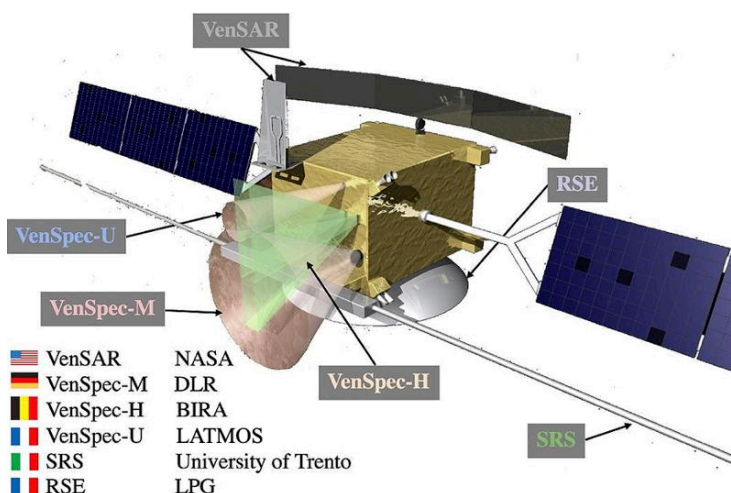


Figure 4.1.2 – EnVision payload instruments integrated onto spacecraft.

Each of the payload instruments will be developed and unit tested at the institution responsible for the payload element before being integrated and tested as a combined payload at the spacecraft provider's facility. The combined mass of the EnVision payload is 208 kg including maturity margin. Figure 4.1.2 shows the instrument payload integrated onto the spacecraft and the country and organisation responsible for each payload element.

In addition to the provided suite of instruments radio science experiment will be conducted using the spacecraft's Telemetry, Tracking and Control (TT&C) subsystem complemented by an Ultra stable oscillator (USO). Tracking data are used to determine a refined Venusian gravity field while radio

occultations provide atmospheric temperature and pressure profiles as well as variations of H₂SO₄ abundance in gaseous and particulate phases. Table 4.1.1 lists the primary science objectives, main characteristics, nominal resources, Instrument lead and lead institution for each of the payload subsystems. The EnVision suite of instruments and Radio Science Experiment are described in further detail in the following sections.

Table 4.1.1 – Science objectives, main performance characteristics and resources of the EnVision experiments. (Nominal = CBE + Contingency). Please refer to Table 5.3.1 in the following section for EnVision payload nominal resources summary.

| Payload Element | Science Objectives | Main Characteristics | Instrument Leads | Lead Institution |
|-----------------|---|--|------------------------------|--|
| VenSAR | Surface stratigraphy, altimetry, topography, properties, emissivity | Imaging and polarimetry with 30 m/px and 10 m/px. Altimetry @ 2.5m vertical & 4 km spatial resolution | S. Hensley | NASA/Jet Propulsion Laboratory, California Institute of Technology, Pasadena CA, USA |
| SRS | Subsurface structure | 9 MHz, average observation density of 2 and 10 per degree of longitude at Equator, depth ~1km, vertical resolution ~20 m | L. Bruzzone | University of Trento, Italy |
| VenSpec-M | Surface mineralogy, search for active volcanism | Imaging in 14 spectral bands at ~1 μm | J. Helbert | Institute for Planetary Exploration, DLR, Berlin, Germany |
| VenSpec-H | Composition of the lower atmosphere and above the clouds. Search for traces of active volcanism | High resolution spectroscopy at 1-2.7 μm | A.C. Vandaele | Royal Belgian Institute for Space Aeronomy, BIRA-IASB, Brussels, Belgium |
| VenSpec-U | Cloud top composition (sulfur-bearing gases, UV absorber) Search for traces of active volcanism | Spectral imaging with high resolution in UV | E. Marcq | LATMOS, Guyancourt, France |
| VenSpec-CCU | VenSpec Central Control Unit | | J. Helbert | Institute for Planetary Exploration, DLR, Berlin, Germany |
| RSE | Mapping the gravity field Atmospheric sulphuric acid abundance and temperature profile | Gravity field with 150 and 200 km (90-120 degree strength) resolution; H ₂ SO ₄ at 1 ppm accuracy | C. Dumoulin P. Rosenblatt | Laboratoire de Planétologie et Géodynamique, Nantes, France |

The Instrument teams are supported by their respective national funding agencies.

A portion of this study was carried out at the Jet Propulsion Laboratory, California Institute of Technology, under a contract with the National Aeronautics and Space Administration.

4.2 Synthetic Aperture Radar VenSAR

4.2.1 Instrument objectives and description

The EnVision VenSAR radar will contribute to addressing the key science objectives of the mission. It will image pre-selected Regions of Interest with resolution of 30 m/pixel and high resolution (10 m/px) across some RoIs. Imaging will be essential for reconstruction of the surface stratigraphy thus revealing geological and chronological relations between surface units. Imaging at two incidence angles will allow reconstruction of surface topography as Digital Elevation Models (DEM) of selected terrains. Quasi-global altimetry would enable quantification of various surface processes. Surface emissivity and roughness will be derived from the imaging in HV and HH polarizations as well as passive radiometry. Comparison to the Magellan images and within the VenSAR data set will allow search for surface changes due to volcanic, tectonic and landscape forming processes from year to decade time scales.

The EnVision VenSAR radar is designed and built by NASA's Jet Propulsion Laboratory, and is a reflectarray antenna concept consisting of a 5.8 m × 0.7 m reflector antenna illuminated by 0.85 m feed separated by a distance of 2.75 m as shown in Figure 4.2.1. Its design was motivated by mass and size considerations, the ability to support multiple modes of operation and a desire to operate with a frequency similar to Magellan thereby facilitating inter comparison of the two datasets. The antenna is a piecewise planar approximation to a parabolic reflector to achieve good sidelobe performance over the entire 60 MHz transmitted bandwidth. The radar supports two bandwidths 15.5 MHz to generate 30 m stripmap imagery with approximately 16 looks, and a 60 MHz mode to generate 10 m stripmap imagery with 8-10 looks. The radar has a noise equivalent $\sigma_{\text{e}} \leq -20$ dB (where backscatter level equals to the noise power) and operates with incidence angles between 20° and

40° depending on platform altitude (220-540 km depending on latitude, see Table 5.6.2 and Figure 5.6.3). The radar transmits horizontal (H) polarization and can receive both H and vertical (V) polarizations. Additionally, the radar can point to nadir to operate as an altimeter to provide topography and operate as a receive-only radiometer to provide brightness temperature measurements with nearly global extent for surface type discrimination and characterisation.

The VenSAR radar is composed of three primary elements which are the reflectarray antenna, radio frequency (RF) and digital assembly subsystems as shown in Figure 4.2.2. The antenna subsystem consists of the reflectarray, feed, mechanical deployment mechanisms, waveguide choke joints, and interconnect waveguide. The RF subsystem comprises the frequency synthesiser, upconverter, RF receiver, downconverter, solid state power amplifier (SSPA), energy storage subsystem (ESS) and cabling. Control and timing for the radar resides in the Digital Electronics Assembly (DEA) that includes: ADC sampling and signal filtering and decimation; data compression; the command interface from the spacecraft; and the routing of radar science data to the onboard Solid State Mass Memory (SSMM). Key parameters for the radar are shown in Table 4.2.1.

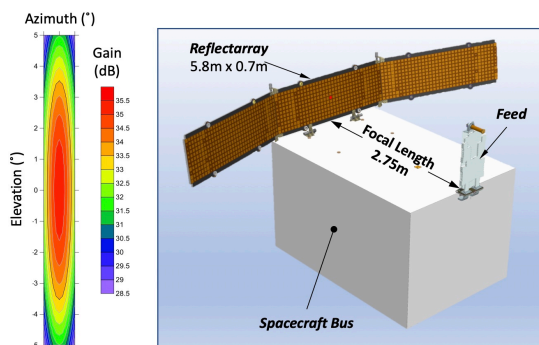


Figure 4.2.1 – VenSAR is an S-band reflectarray radar designed to image a 57-km swath on the surface with incidence angles from 20° to 40°. The antenna was designed to have sidelobes ≤ -20 dB with a short focal length of 2.75 m.

The reflectarray meets key antenna performance requirements with a low mass and power efficient design. This design concept reduces mass and cost by collecting the RF electronics into a single fixed location. A 5.8 m × 0.7 m Folded Panel Reflectarray (FPR) was selected to meet radar antenna requirements. The reflector aperture is partitioned into three 2.0 m × 0.7 m panels that use hinges to stow compactly and deploy shortly after launch.

The reflector is illuminated with a waveguide feed that can handle 2kW peak power and stows compactly against the bus. Beam pointing will be accomplished by physically rotating the spacecraft. Predicted gain is 33.9 dB, including 0.3 dB margin to cover tolerances and other uncertainties. To simplify the feed, the reflectarray separates the V-pol and H-pol focal points by a short distance while keeping the secondary beam peaks co-aligned. This eliminates the need for a complex dual polarized radiating element.

The RF electronics will be based on the architecture used for SMAP, but at different frequencies and without the chirp generator that will now be replaced with a digital arbitrary waveform generator. The Frequency Synthesiser (FS) will be based on a 10 MHz TCXO from Wenzel that will serve as the radar clock. From this master frequency we will derive a 400 MHz clock signal to serve as the clock for the DAC in the waveform generator. This signal will also be halved to provide a 200 MHz clock to the digitiser used for the H-pol and V-pol receive channels. The ESS will receive 28 VDC (or 50 VDC) from the spacecraft and will provide primary isolation and convert that voltage to the necessary voltages for the SSPA.

The Solid State Power Amplifier (SSPA) is a single H-polarization stage separated from other RF electronics for thermal reasons, and the GaN SSPA transmitter consists of six power-combined 500 W Sumitomo devices. These parts are pre-packaged; after combining losses and front-end losses they produce 2160 W of peak RF power at a power-added efficiency of 36%.

| Parameter | Value |
|---------------------------------|------------------|
| Centre Frequency | 3.20 GHz |
| Antenna Size | 5.8 m x 0.7 m |
| Transmit Power | 2 kW |
| Bandwidth | 15.5 or 60 MHz |
| System Noise Temperature | 1226°K |
| System Losses | -4.4 dB |
| Atmospheric Losses (2-way) | -1.5 dB |
| BFPQ Bits | 3 (SAR) , 2(Alt) |
| SAR Modes | |
| Incidence Angles | 20° -40° |
| Polarizations | HH and HV |
| SAR Swath Width | 57 and 20 km |
| Ground Pixel Size | 30 and 10 m |
| SAR Maximum PRF | 3300 Hz |
| SAR Pulse Length | 40 μs |
| Noise Equivalent σ ₀ | ≤ -20 dB |
| Multiplicative Noise Ratio | ≤ -18 dB |
| Number of SAR Looks | 16 and 8 |
| Radiometric Resolution | 1.1 dB |
| Altimeter Mode | |
| Altimeter PRF | 14800 Hz |
| Altimeter Presum PRF | 426 Hz |
| Altimeter Vertical Resolution | 2.5 m |
| Altimeter Footprint (Pulse) | 3 km |
| Altimeter Pulse Length | 0.5 μs |
| Radiometer Modes | |
| Brightness Temp. Accuracy | 1.7°K |
| Brightness Temp. Precision | 0.7°K |

The Digital Electronics Assembly (DEA) design and implementation draw from recently executed JPL flight radar builds to reduce cost and risk. All of the digital subsystem functionality will reside in a single assembly

with a nominal mass of ~15 kg and power consumption of 45 W. Each polarization of the SAR return signal will be digitised by an ADC sampling at 200 MSPS to capture the maximum high-resolution bandwidth mode of 60 MHz. The sampled data will be selectively filtered and decimated based on the operational mode and then compressed and formatted for transfer to mass storage on the spacecraft. The interface to the spacecraft mass storage will be WizardLink. The digital processing for the radiometer sensor application will also reside on the Digital Signal Processing (DSP) FPGA utilizing the same digitised channels as the SAR when no transmit signal is present. The Digital Subsystem will also include the waveform generation, system control and timing, telemetry acquisition and the necessary DC power conversion.

4.2.2 Interface and Resource Requirements

The VenSAR instrument has components mounted both internally and externally to the spacecraft and is designed to operate in the Venus environment.

Mechanical Interfaces and Mass Budget. The reflectarray and feed are stowed for launch and deployed shortly after launch via damped actuators. Following deployment the reflectarray and feed remain stationary with respect to spacecraft. All electronics (4 assemblies) are mounted to the interior of the spacecraft with SSPA being mounted close to the Feed location and RFES assembly close to the SSPA to reduce RF losses. The ESS also will be mounted in close proximity to the SSPA to reduce cable losses.

Thermal Interfaces. Close proximity of the high power SSPA and ESS presents a thermal challenge and heat pipes are used to dissipate the heat from these units. Thermal analysis of the reflectarray and feed both during science operations and during aerobraking show neither element exceeds its operational or allowed flight temperature limits. Paint, thermal coatings and MLI are employed to protect the exposed antenna assemblies in flight.

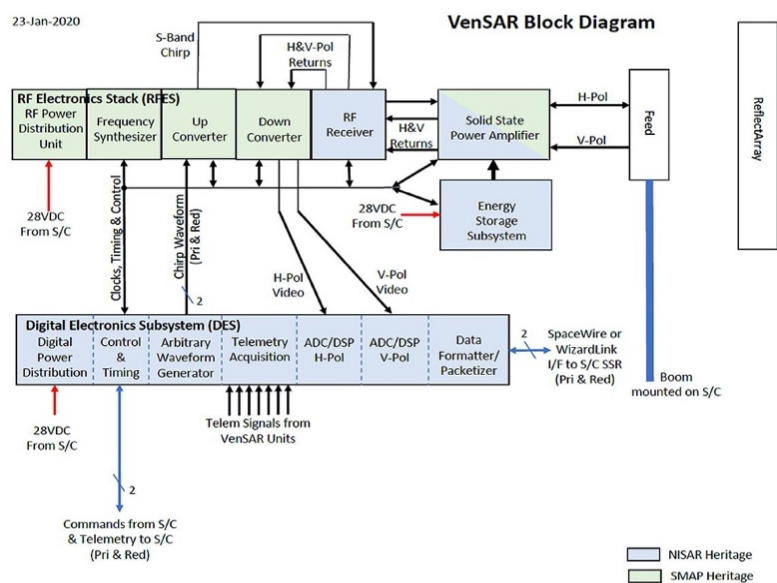


Figure 4.2.2 – VenSAR instrument block diagram with the design heritage colour-coded from other NASA flight radar programs. The radar consists of three primary subsystems which are the Antenna, RF and Digital Subsystems.

Electrical Interfaces and Power Budget.

The DC power bus provided by the spacecraft will be 28V DC. There will be 3 separate DC power bus inputs: one for the RFES, one for the DES, and one for the ESS/SSPA. The VenSAR power converters will provide isolation on the primary side of the DC power bus provided by the spacecraft.

Data Volume and Storage Requirements.

Depending on operational mode the VenSAR instrument has nominal output data rates that vary from 89 Mbs in the 30 m SAR mode, 178 Mbs in the polarimetric SAR mode, 192 Mbs for the 10 m SAR mode, 2.2 Mbs for the altimeter mode and 2 kps for the radiometer modes (nadir, near-nadir and off-nadir). The instrument is designed to operate continuously for up to 13 minutes per orbit in the 30 m SAR mode.

4.2.3 Operation Requirements

VenSAR operation is controlled by preplanned command sequences generated on the ground that are regularly uploaded. During SAR acquisition the antenna is oriented to the desired off-nadir look angle whereas during altimeter and nadir looking radiometer observations the antenna is pointed to nadir with the long axis of the antenna perpendicular to the flight track. The command sequences are transferred from the spacecraft to the radar and are executed based on time provided by the radar clock. A timing offset uploaded every couple of days compensates for along-track timing offsets from the time the commands were generated. Parameters uplinked to control the radar include PRF, timing for the data window, bandwidth and sampling frequency, pulse-length, polarization channels and the number of BFPQ bits. As the orbit is elliptical the PRF and data window commands can be updated every 100 seconds.

4.2.4 Heritage

VenSAR design is predicated on flight qualified designs and technologies used by JPL on other flight programs like the NASA/ISRO Synthetic Aperture Radar (NISAR) and Surface Water and Ocean Topography (SWOT) missions. The most novel element of the radar is the transmitter which is a solidstate power amplifier undergoing early prototyping risk mitigation activities and testing prior to MSR. Reflectarray panels, feed, hinges, HDRMs, viscous dampers, and boom designs are all based on flight proven or flight qualified designs that will require only engineering modifications for the VenSAR application. JPL has successfully used similar deployable FPR antenna technology on the ISARA (Ka-band, Earth LEO) and MarCO (X-band, Mars) missions, and recently flight qualified a 5m Ka-band FPR with a similar waveguide feed for SWOT. The SSPA is based on solid-state GaN 500W devices from Sumitomo, screened by the vendor to flight specifications. The ESS design will be based on heritage flight designs, most recently the ESS design qualified for the NISAR TR Modules. The Digital Electronics Subsystem is based on NISAR designs. Circuit designs previously implemented on REASON and SWOT are added to enable waveform generation and potentially DDR memory for data buffering if required.

4.2.5 Instrument Performance

VenSAR Modes. Two primary metrics are used to assess the utility of the VenSAR data to meet the science requirements. The radar was designed to have a maximum noise equivalent σ_0 of better than -20 dB resulting in required SNR and radiometric resolution for the 30 m SAR mode for the regions of interest (RoIs) shown in Figure 4.2.3 for Cycles 1 and 6 that have the highest and lowest altitudes during the mission. Performance is estimated on the descending passes where the orbit goes through periapsis.

Radiometric resolution measures the ability to distinguish regions of different contrast and includes speckle, SNR and number of looks effects with lower values being better. The mean SNR is 16.9 dB with a standard deviation of 3.5 dB and the mean radiometric resolution is 1.1 dB with a standard deviation of 0.05 dB that exceeds the Magellan radiometric resolution of 1.5 dB at with coarser 120 m resolution.

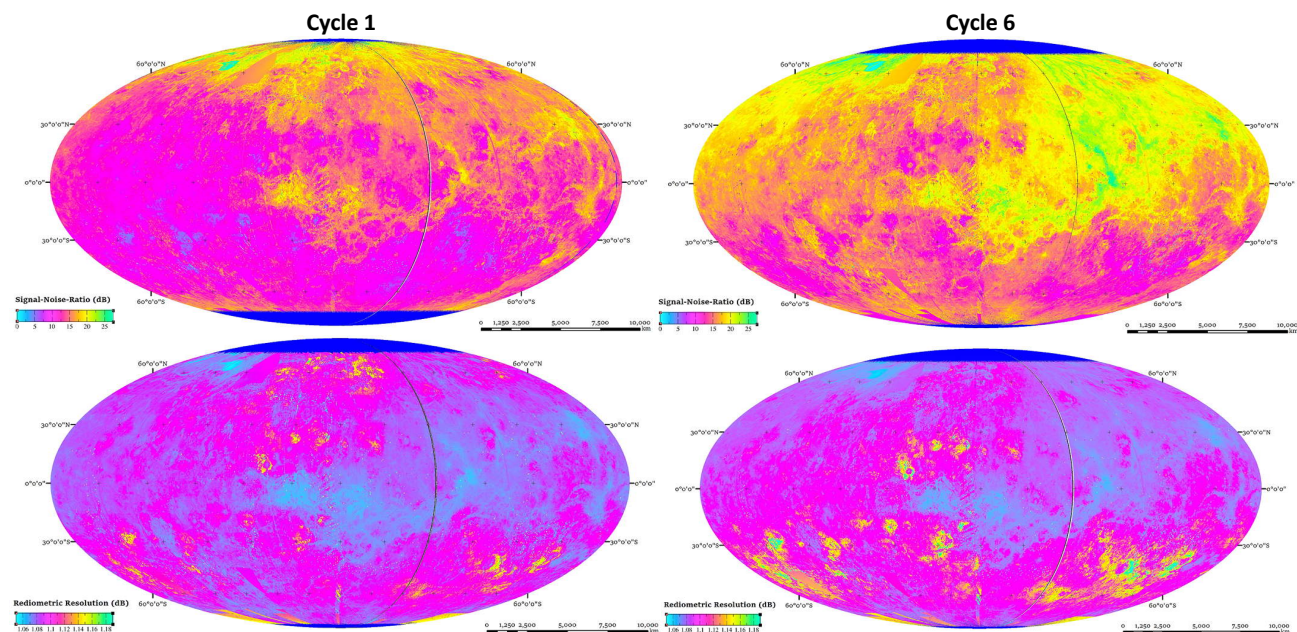


Figure 4.2.3 – (a, top): VenSAR SNR and radiometric resolution for the 30 m VenSAR mode, for Cycle 1 (left) and Cycle 6 (right). (b, bottom): The mean SNR is 16 dB with a standard deviation of 3.5 dB and the mean radiometric resolution is 1.1 dB with a standard deviation of 0.05 dB. VenSAR’s maximum noise equivalent σ_0 of ≤ -20 dB is better than that of Magellan (-26 to -15 dB). The mean SNR will be 16.9 dB (with a standard deviation of 3.5 dB) and the mean radiometric resolution of 1.1 dB (with a standard deviation of 0.05 dB) which exceeds the Magellan values of 1.5 to 1.75 dB at 120 m resolution, meaning that VenSAR will be more sensitive to features of subtle brightness contrast than Magellan.

Altimeter Mode and SAR Stereo Modes. The altimeter beam limited footprint is 50 km in the along-track direction and 6 km in the cross-track direction. By presumming the data and using Doppler beam sharpening a pulse-limited footprint of ~4 km is obtained with the 60 MHz altimeter transmit bandwidth. This results in a vertical resolution of 2.5 m providing a topographic mapping accuracy of ~20-30 m. Using two SAR data acquisitions with incidence angles separated by about 5°, radar stereo techniques can be employed to generate

high resolution topography in regions with sufficient contrast. Using a semi-empirical matching model based on local scene contrast and informed by Magellan stereo match statistics we estimated the stereo elevation precision using Cycle 3 and 4 stereo pairs. Topographic maps with 300 m spatial resolution had a mean elevation precision of 33 m with a standard deviation of 22 m as shown in Figure 4.2.4.

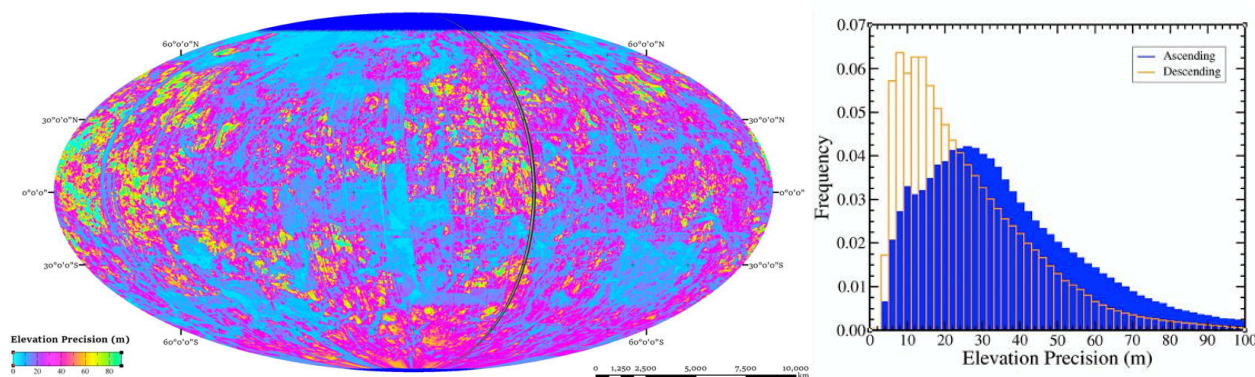


Figure 4.2.4 – VenSAR stereo elevation precision. (a, left): VenSAR elevation precision in m. (b, right): Histogram of stereo elevation precision using Cycle 3 and 4 stereo pairs (blue: ascending branch; brown: descending branch).

4.3 Subsurface Radar Sounder SRS

4.3.1 Instrument objectives and description

SRS will be the first instrument to profile the subsurface of Venus and thus will acquire fundamental information on subsurface geology by mapping the vertical structure (mechanical and dielectric interfaces) and properties of tesserae and their edges, plains, lava flows and impact craters and debris, thus providing useful data for inferring the genesis of these features. It also provides information on the surface in terms of roughness, composition and permittivity (dielectric) properties at wavelengths much longer than those of VenSAR, thus allowing a better understanding of the surface properties. SRS also obtains altimetry measurements by providing low-resolution profiles of the topography that can be integrated with the altimetric data of VenSAR.

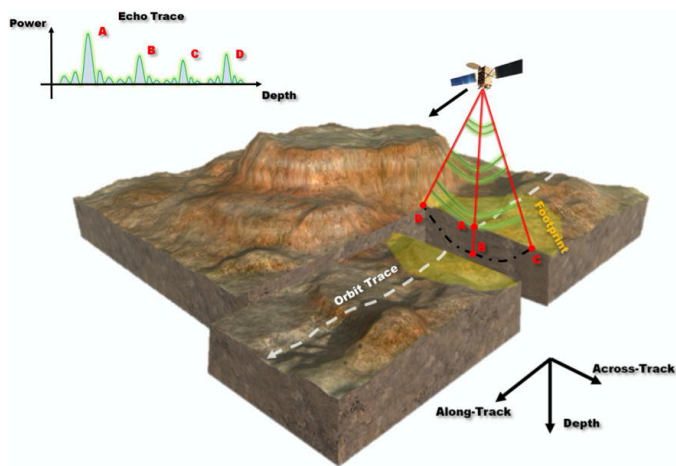


Figure 4.3.1 – SRS acquisition concept (Carrer and Bruzzone, 2017). Varying reflections are detected by the radar receiver and used to create a depth image of the subsurface (referred to as radargram) and map unexposed subsurface features.

SRS is a nadir-looking radar sounder instrument which transmits low frequency radio waves with the unique capability to penetrate the subsurface (see Figure 4.3.1). As these radio waves travel through the subsurface, their reflected signal varies through interaction with subsurface horizons and structures with different dielectric constants. These varying reflections are detected by the radar receiver and used to create a depth image of the subsurface (referred to as radargram) and so map unexposed subsurface features.

As discussed in §3.3.4, the scientific requirements call for a subsurface penetration between few tens and few hundred meters (up to 1000 m), and a vertical resolution of 20 m; this is also summarised in Figure 4.3.1. This drives the selection of SRS central frequency,

transmitted bandwidth and power. The penetration depth for SRS sounding has been calculated considering a wide range of dielectric properties at Venus temperature, corresponding to many different possibilities for the composition, and the porosity of surface material, such as basaltic (from Lunar, Terrestrial and Martian analogs), granitic and rhyolitic; these calculations are based on dielectric properties of rocks at elevated temperatures (e.g., Bruzzone et al., 2020). The operating frequency also needs to be high enough to minimise interference from the ionosphere.

This leads to adopting a central frequency of 9 MHz with 5 MHz bandwidth as the baseline SRS design. The radiated peak power is 200 W, an order of magnitude higher than that of MARSIS and SHARAD. Figure 4.3.2 shows the SRS overall architecture that includes three main units: the transmitter (TX), the Receiving Digital Subsystem (RDS) including the Digital Electronic subsystem) and the Matching Network (MN). The deployable dipole antenna with total length of 16 m will be provided by the spacecraft manufacturer.

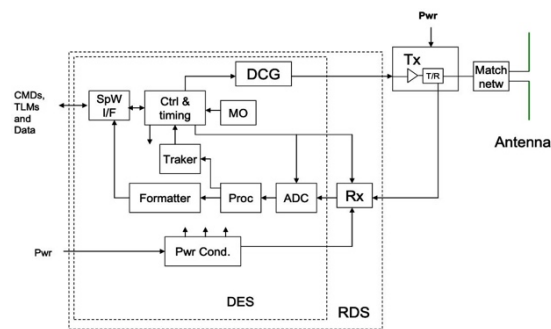


Figure 4.3.2 – SRS block diagram

4.3.2 Interfaces and resources requirements

The instrument nominal mass is 12.8 kg excluding the antenna. The SRS peak radiated power is 200 W, while the average power consumption is 115 W. The data rate for the main science modes ranges between 3.25 Mbps and 6.47 Mbps. The estimated total data volume collected over the nominal mission is 17 Tbits.

4.3.3 Operation requirements

During operations the SRS antenna shall be parallel to the ground with an absolute pointing error of ± 5 degrees. On Venus the maximum plasma frequency on the day side is 5-6 MHz, and below 1 MHz on the night side. Thus, acquisition of the SRS should be performed at night time to limit ionospheric distortions that can be corrected with consolidated techniques (Campbell et al., 2011; Restano et al., 2016). Moreover, to reduce the noise of solar electromagnetic radiation, the instrument itself shall be in eclipse. The instrument is very versatile and can be programmed in different ways. The two main science modes are: 1) SRS high-density mode is optimised for acquiring data on targets of high interest over 10% of the surface of Venus with average observation density of 10 per degree of longitude at Equator and no compression; 2) SRS low-density mode will perform measurements over 65% of the surface of Venus with average observation density of 2 per degree of longitude at Equator and lossy data compression. To meet the coverage requirement, the night time observations will be distributed over all the nominal mission.

4.3.4 Heritage

SRS benefits from rich heritage in the development of planetary radar sounders. These instruments were extensively used in planetary investigations. Two subsurface radars are currently operating at Mars: 1) the Mars Advanced Radar for Subsurface and Ionosphere Sounding (MARSIS) on-board ESA’s Mars Express spacecraft optimised for deep penetration of the Martian subsurface (Picardi et al., 2005); and 2) the SHallow RADar (SHARAD) on-board NASA’s Mars Reconnaissance Orbiter (Seu et al., 2007) optimised for high vertical resolution with shallow penetration. The subsurface of the Moon is explored by the Lunar Radar Sounder (LRS) on-board the SELENE, Kaguya mission (Ono et al., 2009). For the study of the Jovian icy moons, two radar sounders are under development: 1) the Radar for Icy Moons Exploration (RIME) on-board the Jupiter Icy Moons Explorer (JUICE) (Bruzzone et al., 2015); and 2) the Radar for Europa Assessment and Sounding: Ocean to Near-surface (REASON) on-board the Europa Clipper. SRS will be mainly based on the heritage of RIME (which operates at the same central frequency considered as baseline for SRS).

4.3.5 Instrument performance

The performance of SRS (Figure 4.3.3) has been derived by considering advanced radar sounder simulation techniques (Gerekos et al., 2018; Thakhur & Bruzzone, 2019) and by realistically modelling different target terrains on Venus. A hierarchical approach to the simulation has been followed by considering all main variables affecting the performance with an increasing level of detail. Simulations of different Venus geological scenarios (e.g., buried craters, lava flows) have been performed for assessing the detectability of subsurface interfaces under different conditions of digital elevation models (clutter) and dielectric contrast, as described in Bruzzone et al. (2020); an example is given in

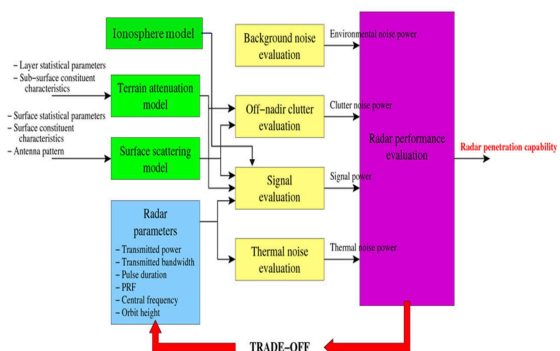


Figure 4.3.3 – Illustration of the approach used for defining the parameters and the performance of SRS.

Figure 4.3.4. The results indicate that the baseline design of SRS meets the required detection performance for important Venusian target types.

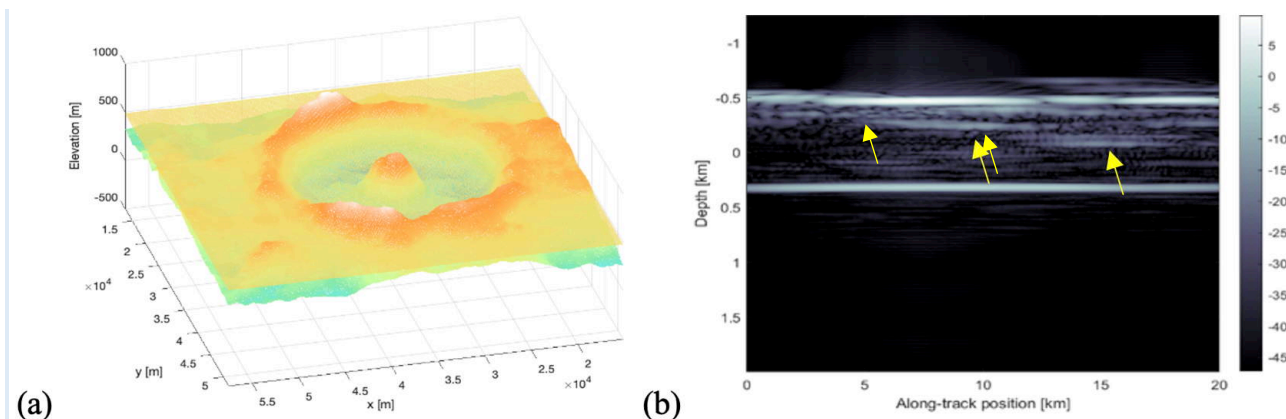


Figure 4.3.4 - Example of 3D simulation of sounding of a crater partially buried up to a depth of 200-600 m under the plains ($\epsilon_{real} = 4$ and $\tan\delta = 0.01$, with the underlying crater material having $\epsilon_{real} = 8$). (a, left): 3D model of the buried crater derived starting from Magellan stereo DEM. (b, right): Simulated radargram with the yellow arrows showing the diffused reflections from the buried crater floor. Further simulations of craters, tesserae and lava flows are described in (Thakur et al., 2020).

4.4 Near-IR mapping spectrometer VenSpec-M

4.4.1 Instrument objectives and description

VenSpec-M (Helbert et al., 2017, 2018; 2019; Smrekar et al. 2018b) is a pushbroom multispectral imaging system which will provide near-global compositional data on rock types, weathering, and crustal evolution by mapping the night-side emission of Venus surface and lower atmosphere in 14 near-IR spectral transparency “windows” at 0.86-1.18 μm (Figure 4.4.1; Mueller et al., 2008; Meadows and Crisp, 1996; Pollack et al., 1993). A total of six bands (shown in brown colour in Figure 4.4.1) sound the surface in the five atmospheric windows. The broadest “window” at 1.02 μm is covered with two filters to obtain information on the spectral slope of the surface reflectance within the “window”. Eight additional channels provide measurements of atmospheric water vapour abundance (two bands in blue in Figure 4.4.1) as well as cloud microphysics and dynamics (three bands in orange) and stray light (three bands in green) permitting an accurate correction of atmospheric interference on the surface data. Continuous observation of Venus’ thermal emission in the surface windows will place tight constraints on current day volcanic activity.

VenSpec-M will use the methodology pioneered by VIRTIS imaging spectrometer onboard Venus Express (Mueller et al., 2008, 2017, 2020; Stofan et al., 2016; Gilmore et al., 2015; Smrekar et al., 2010) but with more and wider spectral bands and the use of VenSAR-derived DEM to deliver multiband imagery of more than 60% of the surface of Venus with wider spectral coverage and an order of magnitude higher sensitivity.

Figure 4.4.2 shows the functional layout and design of VenSpec-M. The instrument consists of two main units mounted together in a mono-block structure to allow for simplified spacecraft interfaces. A telecentric optics images the scene onto a filter array. VenSpec-M uses a multilayered dielectric-coating ultra-narrow-band filter array to split the light into 14 spectral bands. Figure 4.4.1 shows the spectral assignment of each filter and their main objective. The filter array is located at an intermediary focus of the optical path. Each band is imaged by two lenses relay optic onto 33×640-pixel rows on the detector. The filter array is used to provide greater wavelength stability than a grating design. VenSpec-M is using a 640×512 pixel Xenics XSW-640 InGaAs detector. The FOV is 30°×45°; each 20- μm -pitch pixel sees a 0.07°×0.07° FOV. An integrated thermoelectric cooler is used to stabilise the working point of the detector. The detector requires no cryogenic cooling,

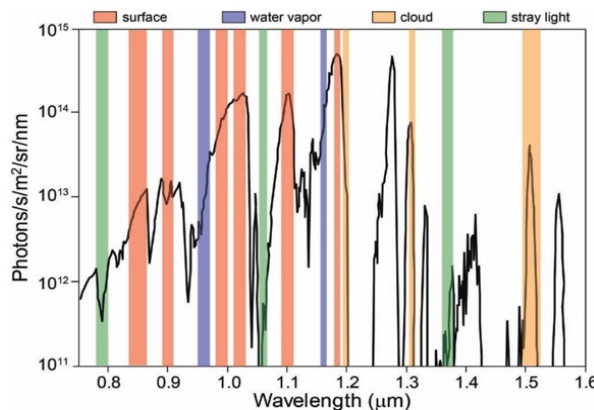


Figure 4.4.1 – Wavelengths of near-infrared bands used opportunistically around gaps in the CO₂ atmosphere of Venus. Collectively, these offer a comprehensive sampling of surface, water vapour, cloud opacity, and stray light as needed to estimate errors on surface bands. Black line is an observed night-side emission spectrum of Venus. Adapted from Helbert et al. (2018).

avoiding a single point failure. The frontend electronics use the highly integrated AFE device LM98640QML-SP, a fully qualified (radiation tolerant), 14 bit, 5 MSPS to 40 MSPS, dual channel, complete Analog Front End. Texas Instruments specially designed it for digital imaging applications.

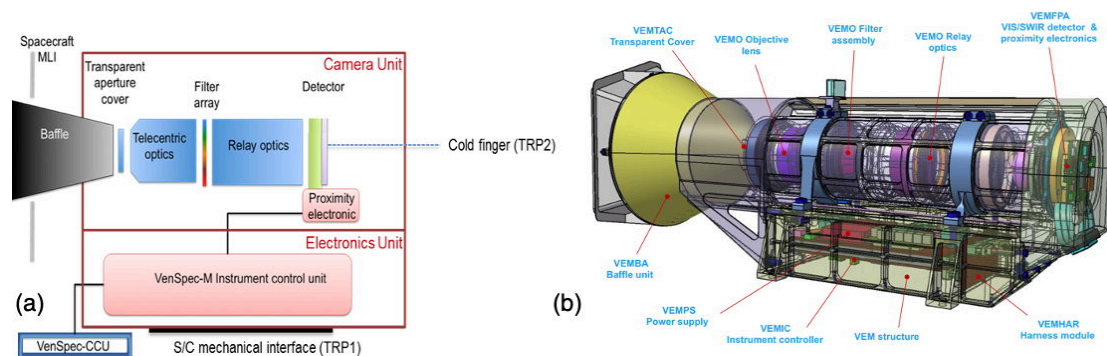


Figure 4.4.2 – VenSpec-M block diagram (a, left) and design (b, right).

4.4.2 Interfaces and resources requirements

All main interfaces are shown in Figure 4.4.2a. The three units are also the main thermal subunits of VenSpec-M supported by spacecraft interfaces according to their requirements. One Thermal Reference Point (TRP) is the instrument mounting plate, which handles the electronics thermal control in an appropriate operating range with heater maintenance as needed. It also connects the optics/detector section via thermal strap to a stabilised spacecraft interface, which is the second TRP. Thermal interference of both units is controlled by the optics mounting elements to the electronics unit. The instrument's nominal mass is 5.9 kg. Mean and peak power consumption are 11.5 W and 15 W respectively (including 15% margin). Data rate is typically 0.5 Mbps with a peak of 1 Mbps for calibration observations. Commanding, data link to the spacecraft and power supply will be provided by a dedicated Central Control Unit (CCU).

4.4.3 Operation requirements

VenSpec-M is continuously operating on the nightside of Venus to reach 60% coverage with three repeats by the end of the nominal, 6-cycles mission. To search for volcanic activity the instrument will acquire sets of five consecutive orbits, that due to sufficient overlap of orbital swaths would enable robust detection and avoiding false positives. Over the mission duration seven revisits are required to minimise the effect of atmospheric uncertainties not included in the atmospheric model used for emissivity retrieval.

4.4.4 Heritage

VenSpec-M low development risk results from a standard camera optical design, a flight proven InGaAs detector with a thermo-electric cooler, and flight-qualified support systems from MERTIS (D'Amore et al., 2019; Peter et al., 2013).

4.4.5 Instrument Performance

VenSpec-M has a mature design with an existing laboratory prototype verifying an achievable instrument SNR of well above 1000 as well as a predicted error in the retrieval of relative emissivity of better than 1% (Helbert et al. 2018). By observing through all five windows with six narrow band filters, ranging from 0.86 to 1.18 μm , VenSpec-M will provide a global map of surface composition as well as redox state of the surface. Because VenSpec-M observes each spot on the surface multiple times, both atmospheric noise and instrument noise are reduced by averaging image swaths acquired at different times. Applying the updated analysis of atmospheric error for VenSpec-M parameters (Kappel et al., 2016, Helbert et al., 2018), and taking multiple-look averaging into account, our capability for emissivity precision is better than 1.5% for all bands in most bands better than 1%. Continuous observation of Venus' thermal emission will place tight constraints on current day volcanic activity. Eight additional channels measure atmospheric water vapour abundance as well as cloud microphysics and dynamics and will permit accurate correction of atmospheric interference on the surface data.

4.5 High-resolution infrared spectrometer VenSpec-H

4.5.1 Instrument objectives and description

The aim of VenSpec-H (**V**enus **S**pectrometer with **H**igh resolution) is to monitor the composition of minor species in the lower atmosphere on the night side and above the clouds on the day side. These observations will be performed in nadir geometry. More specifically VenSpec-H will focus on the volcanic and cloud forming gases and search for composition anomalies potentially related to the volcanic activity. VenSpec-H will include four spectral bands: 1.165 - 1.180 μm (B#1), 2.34 - 2.48 μm (B#2), 1.72 - 1.75 μm (B#3) and 1.37 - 1.39 μm (B#4) that cover the infrared spectral transparency “windows”. In order to reduce the instrument complexity, B#2 will be further subdivided in two ranges: 2.34 - 2.42 μm (2a) and 2.45 - 2.48 μm (2b). Bands 1, 2a, 2b and 3 will be observed on the night side, bands 2a, 2b and 4 on the dayside. Figure 4.5.1 illustrates the different bands sounded and which main species will be measured.

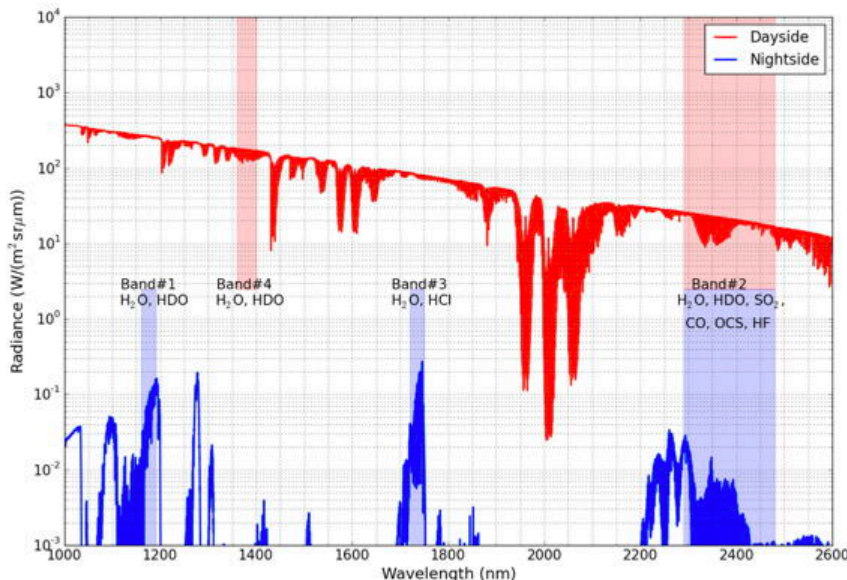


Figure 4.5.1 – Typical Venus spectra observed by the VenSpec-H for day (red) and night (blue) conditions. The positions of the bands are indicated, as well as which atmospheric species are absorbing.

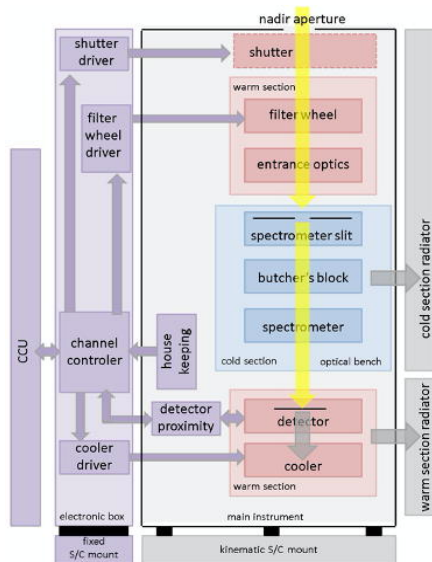


Figure 4.5.2 – VenSpec-H Functional block diagram.

The selection of the spectral band is carried out using filters on a filter wheel situated in front of the slit in the warm section, and a butcher’s block attached to the slit in the cold section. The detector is an Integrated Dewar Detector-Cooler Assembly whose window sits in the exit aperture of the spectrometer section. The focal plane array located at the focal plane of the spectrometer exit optics, is cooled by means of a cryocooler. VenSpec-H has a rectangular field of view (defined by the spectrometer slit) of 7.32° (length of slit) by 0.084° (width of slit).

4.5.2 Interfaces and resources requirements

The instrument’s estimated nominal mass is 16.6 kg. From the NOMAD/TGO experience the estimated nominal mean power (over one orbit) and peak power consumption (during detector precooling) are 24.6 W and 29.7 W respectively (including 15% margin). Data volume can be modulated depending on the available

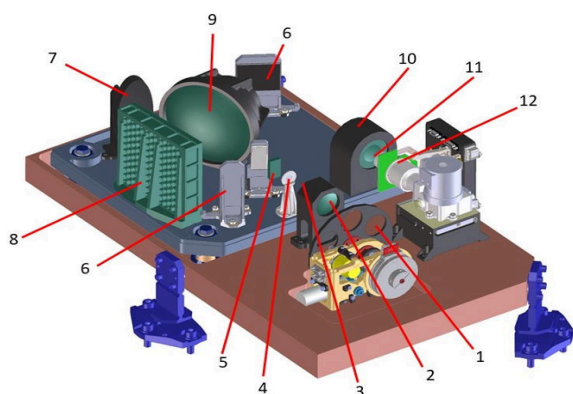


Figure 4.5.3 – VenSpec-H optical design: (1) filter wheel, (2) warm entrance optics, (3) cold section entrance aperture, (4) slit with butcher's block, (5) free form correction plate, (6) folding mirrors, (7) parabolic mirror, (8) echelle grating, (9) collimating optics, (10) detector optics, (11) cold section exit aperture, (12) detector plane.

mission resources, by on board binning, providing 6.5 and 14.2 Mbytes per orbit, for the minimum (binning on 10 lines, 20 min of science) and typical (binning on 16 lines, 30 min science) scenarios respectively, including 20 % margin. VenSpec-H consists of two units (Figure 4.5.3): the main instrument (optical bench) interfaces with three isostatic mounts to the spacecraft, and the electronic box that is hard mounted with four mounting points. The instrument has three TRPs (Thermal Reference Points), one at a foot of the main instrument (warm section), one at a foot of the cold section and one at a mounting point of the electronic box. To achieve the required signal-to-noise ratio the cold section of the instrument that encompasses optics and detector will be cooled down by passive radiator cooling. Commanding, data link to the spacecraft and power supply will be provided by a dedicated Central Control Unit (CCU).

4.5.3 Operation requirements

VenSpec-H will observe close to nadir direction on both day and night side. The requirement on the pointing is as follows: the VenSpec-H instrument shall be pointed towards the centre of Venus with an absolute pointing error (APE) of ≤ 15 mrad (along and around pointing axis) and ≤ 50.0 mrad (across pointing axis). The relative pointing error (RPE) or drift stability shall be ≤ 5.0 mrad (>60 sec; 15 sec and < 1 sec), around pointing axis, ≤ 10.0 mrad (> 60 sec; 15 sec and < 1 sec), along axis and ≤ 20.0 mrad (> 60 sec; 15 sec and < 1 sec), across axis. The Absolute Knowledge Error (AKE) is ≤ 0.54 mrad (across axis and along axis) and ≤ 5.0 mrad around pointing axis.

While VenSpec-H is capable of measuring continuously, the basic operations scenario foresees periods of four consecutive orbits of observation per cycles of 15. VenSpec-H science operations are timeline controlled. In the standby mode only the central electronics are active. Once the first command is received by the instrument it switches to precooling mode. After a second command the instrument goes in measurement mode. Precooling mode lasts for 10 minutes. Science mode duration depends on the length of the observation (a duration of 30 minutes is assumed as the typical EnVision case). During the entire period that VenSpec-H is switched on the housekeeping data will be transmitted at a rate of one frame per second.

4.5.4 Heritage

The instrument heavily builds on the LNO channel of NOMAD on board ExoMars Trace Gas Orbiter (Neefs et al. 2015; Vandaele et al. 2018).

4.5.5 Instrument performance

Performance of the instrument, i.e. the signal-to-noise ratio (SNR) per pixel element (no binning, no co-addition) reached under different observing conditions, is summarised in Table 4.5.1. These values are achieved when the cold section is at -45°C . Thanks to its high spectral resolution ($R\sim 8000$), VenSpec-H will determine the abundances of H_2O , HDO, CO and SO_2 with an accuracy of 3%, 5%, 1.5% and 1% respectively. This would allow an accuracy on the isotopic ratio D/H of 8%. Such an accuracy will enable to detect expected atmospheric variability potentially linked to volcanism. The slit size corresponds to an instantaneous FOV of 0.32×28.27 km² and 0.79×69.39 km² for an altitude of the s/c of 220 km and 540 km respectively. The maximum integration time on the nightside will be 14.4 seconds. The FOV then becomes 28.27×99.52 km² and 28.27×99.98 km² for 220 km and 540 km altitude respectively.

Table 4.5.1 – Expected performances of VenSpec-H. The SNR values are given per pixel, for an averaged value of the signal, and considering that the cold section temperature is -45°C .

| | | Spectral range (nm) | SNR per pixel (see caption) | Targeted molecules | Altitude range probed |
|-----------|---------|---------------------|-----------------------------|---|-----------------------|
| DAYSIDE | Band#2a | 2340-2420 | 780 | H_2O , HDO, OCS, CO | 65-80 km |
| | Band#2b | 2450-2480 | 1172 | H_2O , HDO, OCS, SO_2 , HF | 65-80 km |
| | Band#4 | 1370-1390 | 1197 | H_2O , HDO | 65-80 km |
| NIGHTSIDE | Band#1 | 1165-1180 | 131 | H_2O , HDO | 0-15 km |
| | Band#2a | 2340-2420 | 81 | H_2O , HDO, CO, OCS | 30-45 km |
| | Band#2b | 2450-2480 | 18 | H_2O , HDO, OCS, SO_2 , HF | 30-45 km |
| | Band#3 | 1720-1750 | 493 | H_2O , HCl | 20-30 km |

4.6 UV spectral imager VenSpec-U

4.6.1 Instrument objectives and description

The VenSpec-U experiment will map distribution and spatial and temporal variations of sulfur bearing gases (SO, SO₂) and unknown particulate absorber at the cloud tops. These measurements will support the search for volcanic activity by constraining variability of the species that can be attributed to the atmospheric dynamics.

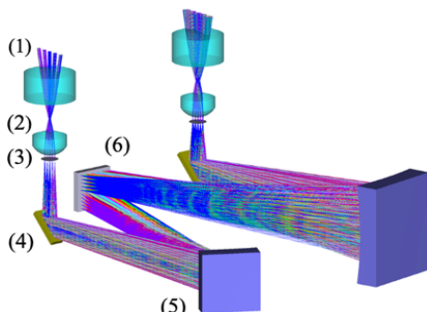


Figure 4.6.1 – VenSpec-U optical layout overview, with the HR and LR channels respectively on the left and on the right. For the HR channel: (1) Front lens; (2) Rear lens; (3) Slit; (4) Reflective filter; (5) Grating; (6) Shared sensor.

The VenSpec-U instrument is a dual channel UV spectral imager (low and high spectral resolution channels, “LR” and “HR” hereafter). Each channel consists of an entrance baffle, an objective composed of two lenses and a stop diaphragm, and a spectrometer composed of a slit and a toroidal holographic grating. It also includes a shortpass filter to reject the wavelengths above the higher limit of both channel bands and a zero-order trap to avoid straylight due to internal reflections of the grating zero-order. The optical layout is presented in Figure 4.6.1. Both LR and HR slits are parallel and the optical layout is such that both channels have the same instantaneous FoV, allowing simultaneous observations and calibrations. Each slit image is then spectrally dispersed by its respective toroidal holographic grating and is formed on a shared CMOS back-side illuminated detector.

The narrow-slit axis of the detector contains the spectral information, whereas the long-slit axis contains the spatial information along the 22.5° FOV of each slit. The spectra of LR and HR channels are dispersed one above the other on the focal plane. The remaining spatial direction is provided through orbital scrolling (“pushbroom” strategy). Binning on the spatial axis is performed on the detector. The detector will be controlled such that the integration time and the binning scheme is adjusted independently (and simultaneously) for each channel giving high flexibility and providing parameters for the optimisation of each acquisition.

4.6.2 Interfaces and resources requirements

Interfaces between VenSpec-U and the spacecraft are: (1) Thermal interface providing TRP1 (for detector cold finger) and TRP2 (electrical box and optical bench); (2) Power interface (redundant 28 V) to VenSpec-U electronics and spacecraft controlled heaters and (3) Data link (including ground debug EGSE) through SpaceWire. Commanding, data link to the spacecraft and power supply will be provided by a dedicated Central Control Unit (CCU). The instrument nominal mass is 6.8 kg. The power resources are 6.5 W in standby and 13.2 W during science operations and 18.7 W for peak power. The data rate is 44-644 kbit/s depending on the distance to the clouds and spatial sampling mode (medium or high). The data volume per orbit is 936 Mbit.

4.6.3 Operation Requirements

VenSpec-U nominal science operations will consist of four overlapping measurements of 50 minutes duration per day performed at emission angle < 30° on the day side. The observations will be interleaved with star and internal/ dark calibrations performed once-twice per month on the night side. The required pointing accuracy in Venus observations mode is: APE (3σ) = 10 mrad, RPE (3σ) = 1 mrad over 5seconds, and AKE = 1 mrad. The most stringent required pointing accuracy is in star calibration mode: APE (3σ) = 1.7 mrad, RPE (3σ) = 0.17 mrad over 1000 s, and AKE = 0.1-0.25 mrad.

The mission shall achieve coverage of 60% of the planet in local time, latitude, longitude, with no gap larger than 10%. The cleanliness status of the instrument shall be also monitored during the cruise through dedicated radiometric calibration campaigns (at least once per month) pointing towards stable stars in the ultraviolet range. In case of an instrument or spacecraft anomaly, the protective door shall be closed in less than 10 seconds before switching off the instrument.

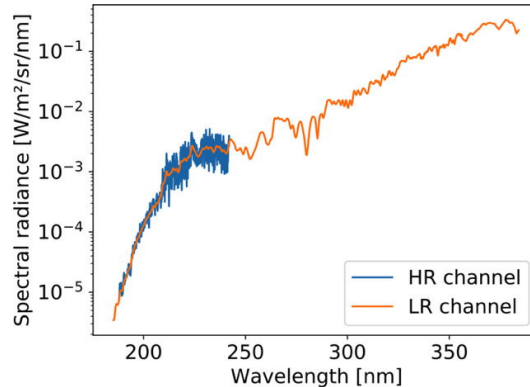


Figure 4.6.2 – Synthetic radiance factor as measured by VenSpec-U for a 25% SO:SO₂ ratio, 500 ppbv SO₂ abundance, and 0.2 imaginary index of cloud particles at 250 nm for a solar zenith angle of 30° and zero emission angle (nadir viewing). The predicted spectral structure comes from both solar spectrum and absorption by SO, SO₂ and UV absorber at Venus’ cloud top.

4.6.4 Heritage

VenSpec-U is an instrument based on a strong heritage mainly provided by PHEBUS onboard BepiColombo, a double UV spectrometer covering from 55 nm to 315 nm, (Qu  merais et al., 2020); and SPICAV-UV onboard Venus Express, an UV spectrometer covering from 118 nm to 320 nm, (Bertaux et al., 2007). Both instruments were assembled and tested in LATMOS as it is expected for VenSpec-U, so the laboratory technical expertise is also a major part of this heritage. The optical scheme of the spectrometer part of VenSpec-U is based on holographic gratings and is therefore very similar to the PHEBUS and SPICAV ones. Due to the quite large field of view required, VenSpec-U is the first ultraviolet spectrometer developed at LATMOS using lens objectives as telescope. Nevertheless, the IRAP laboratory in charge of the mechanical design of VenSpec-U can demonstrate a strong heritage on lens mounting for space projects thanks to ChemCAM on-board Mars Science Laboratory (NASA).

4.6.5 Instrument Performance

(1) The HR channel operating at 205-235 nm at 0.2 nm spectral resolution and spatial sampling not coarser than 24 km (12 km as a goal) should reach a SNR of at least 100; (2) the LR channel operating at 190-380 nm at 2 nm spectral resolution and spatial sampling not coarser than 5 km (3 km as a goal) should reach a SNR of at least 200. According to our forward model based on SPICAV-UV heritage, this shall be sufficient to measure abundance of targeted species (SO, SO₂, UV absorber) with an accuracy better than 25%. These measurements shall allow characterising variability on timescales from hours to years.

4.7 Radio Science Experiment RSE

4.7.1 Experiment objectives and description

The Radio Science Experiment relies on the recording at ground stations of the frequency of the radio-signal sent by the spacecraft. The experiment consists of two parts, described below and presented, together with the institutions involved, in Table 4.7.1.

| RSE | Analysis task | Institution of Scientific lead | Institutions involved |
|------------------------------------|---|--|------------------------------------|
| Gravity experiment | - Gravity field (global resolution of 200km) - k ₂ Love number (<3% accuracy) | LPG, Nantes University  | LPG, Nantes University, France |
| | | | CNES, Toulouse, France |
| | | | Sapienza University of Rome, Italy |
| Radio-occultation experiment (USO) | - T and P profiles (35-90 km) - H ₂ SO ₄ content (vapor and liquid, 35-55 km) - Total Electron Content (ionosphere) | RIU, Cologne University  | RIU, Cologne University, Germany |
| | | | CNES, Toulouse, France (USO) |
| | | | Boston University, MA USA |

Gravity experiment. The gravity experiment aims at mapping of the Venus gravity field with 150-200 km spatial resolution (~120 degree strength) and thus determining interior structure. The experiment will use the 2-way mode with an X-band uplink and a dual X-Ka band frequency downlink in order to reduce the noise on the frequency measured at the ground station resulting from the interplanetary plasma. The Doppler shift of the received frequency with respect to the transmitted frequency will be used to monitor the velocity variations of the spacecraft in order to precisely reconstruct its trajectory around the planet. The orbital velocity perturbations are then inverted to reconstruct the gravity field of Venus (including the tidal component, the k₂ Love number). The space segment of the experiment is the onboard transponder used for telemetry and radio-navigation and the high gain antenna. The ground segment are Earth’s based ground stations, which record the phase of the downlink signal and extract the Doppler shift of the received carrier frequency.

Radio-occultation experiment. The radio-occultation experiment aims at sounding of the temperature structure of the Venus atmosphere in the altitude range 90-35 km and abundance of sulfuric acid in gaseous and particulate phases. The experiment relies on the observation of the radio-link propagation (frequency and amplitude) through the atmosphere of Venus during radio-occultation. The experiment is performed in the 1-way mode and therefore requires an Ultra-Stable Oscillator (USO) onboard the spacecraft. The radio ray path

changes in the ionosphere and neutral atmosphere are induced by a change in the refractivity profile. This leads to a shift in the measured frequency at the ground station. These frequency changes can be used to retrieve the neutral number density, temperature and pressure profiles as a function of the planetary radius at a high vertical resolution. The recording of the absorption of the radio waves at the base of the clouds and below in both X- and Ka-band will allow to estimate sulfuric acid abundance in both gaseous (down to 35 km) and particulate (~50 km) phases.

4.7.2 USO interfaces and resources requirements

One-way radio-occultation experiment requires high frequency stability of the radio signal. This is provided by an Ultra-Stable Oscillator (USO) included in the TT&C system of the spacecraft. The USO shall provide Allan deviation ADEV less than 10^{-12} from 1 to 1000 s. The USO is designed to perform the function of providing a stable frequency reference to the spacecraft Deep Space Transponder (DST) at the time scales of interest for the atmospheric experiment. The Oscillator generates the base frequency using a high quality factor quartz crystal oscillator. This type of oscillator is already onboard terrestrial missions (Doris satellites for example).

4.7.3 Operation requirements

The spacecraft radio-tracking will be performed during each slot of communication with the ground station. It will ensure 3 to 3.5 hours of effective tracking of the spacecraft per day during the nominal science mission (six Venusian sidereal days). Radio-occultations will be performed during two to four tracking passes within 24 hours. Bending of the radio ray path in the atmosphere will have to be compensated by slewing the spacecraft with appropriate slew rates. The USO, once turned on at the beginning of the science mission, will be kept on for its entire duration in order to reduce the instability caused by the crystal aging effect. It will be unmuted during radio-occultations sequences.

4.7.4 Heritage

Both gravity and radio-occultation experiments exploit well established techniques used on many planetary missions before. The precise reconstruction of the orbit will use the state-of-the-art methods and orbitography software to reach a precision of the order of a few metres, which will allow to reconstruct the gravity field within the scientific requirements for the gravity investigation. This accuracy in orbit reconstruction is currently reached for Martian spacecraft from which high-resolution gravity field of Mars is obtained (Marty et al., 2009; Genova et al., 2016). The analysis of the radio occultation profiles uses retrieval methods developed for Venus Express radio occultations. These software packages are even capable to correct measurement difficulties resulting from multipath effects in the cloud layer (Tellmann et al., 2009).

4.7.5 Experiment performance

The gravity field will be obtained with a spatial resolution between 150 and 200 km (~90-120 degree strength) and an accuracy better than 20 mGal. The k_2 Love number accuracy will be better than 1%. This performance is due to the very favourable geometry of the Doppler link, the mission duration and the strong gravity field signal in the Doppler measurements. It will significantly improve the current gravity field solution based on Magellan data which has a spatial resolution between 200 and 500 km and a k_2 accuracy of 22%. The Radio-occultations will probe the atmosphere with a much better temporal resolution than performed so far and will perform first ever measurements of the liquid sulfuric acid content with accuracy of 1 mg m^{-3} in the cloud layer.

5 Mission design

To meet its science objectives, the EnVision mission needs to return a significant volume of science data to Earth, with a large distance-to-Earth dynamic range (from 0.3 to 1.7 AU), from a low Venus polar orbit, in the hot Venus environment (exacerbated by the operation of highly dissipative units), while operating three spectrometers in an almost cryogenic level environment. This needs to be achieved within constraints on the spacecraft mass due to launcher capability, as well as programmatic boundaries of ESA’s 5th M-class call. Achieving the science objectives under these multiple constraints without oversizing the spacecraft calls for a careful planning of science operations, making the science planning strategy a critical driver in the design of the whole mission, against which the spacecraft and ground segment are then sized. In this chapter the main mission requirements and design drivers will be first summarised, the design of the science mission profile explicated, before detailing the resulting spacecraft design. It will be shown that the mission & spacecraft design successfully meet the requirements with sufficient margins.

5.1 Mission requirements and design drivers

The main mission drivers are related to the combination of:

- The payload-accommodation requirements on the spacecraft
- The requirements on the science orbit
- The environmental constraints imposed by a deep space mission to Venus orbit
- The mission science observation requirements (e.g. surface coverage to be observed by the various experiments and instruments over the six cycles of the mission).

Note: a Venus cycle is defined as 243 Earth days. This is the Venus sidereal day, the time needed for Venus to spin 360 degrees on its axis. This Venus “day” lasts longer than the revolution of Venus around the Sun (or Venus “year”, 224 days).

5.2 Driving mission requirements

Science orbit requirements

The choice of science orbit around Venus is mostly driven by the radio science gravity experiment and the operational altitude range for the SAR and SRS instruments. The former requires a low altitude polar orbit, with at least 40% of the time spent below 260 km over at least six cycles to reach degree strength of 90 over the full Venus surface. The latter requires the observations to be done at altitudes lower than 500 km to achieve good imaging qualities with high incidence angles. The orbit shall also remain at all points during the science mission above 220 km to keep the atmospheric drag torque controllable by the spacecraft reaction wheels. There is no other imposed constraint on the orbit, and no strict orbit control requirement is derived from the science requirements. In particular the orbital ground track does not need to be repeatable from cycle to cycle, a natural track-to-track shift of around 10 km is sufficient to implement the planned SAR observations. Such a shift is naturally achieved with orbit requirements summarised in [Table 5.2.1](#).

| | |
|-----------------------------|--------------|
| Maximum apocentre altitude | 540 km |
| Maximum pericentre altitude | 300 km |
| Minimum pericentre altitude | 220 km |
| Inclination | > 85 degrees |

Launcher and Planetary Protection Requirements

EnVision is required to be launched with Ariane 6, the new generation European launcher, in its dual booster configuration (Ariane 62). Ariane 62 maiden flight being scheduled in 2022, the launcher will have reached its mid-life by the time when EnVision is launched, which means a mature launch configuration with proven flight experience. The mission shall fulfil its nominal science objectives within a maximum duration of 6.5 years from launch to spacecraft disposal. On top of these science-driven requirements, EnVision is a Planetary Protection Category II mission, in accordance with ESA Planetary Protection Requirements. A planetary protection plan will be prepared and maintained as per phase B of the mission, in accordance with the applicable planetary protection requirements.



Figure 5.2.1 – Ariane 62 launcher illustration.

5.3 Design drivers

5.3.1 Design-to-cost

The mission is designed to achieve all of the prime key science objectives with a cost-at-completion compatible with the programmatic boundaries imposed by ESA’s 5th Medium class call. This so-called 'design-to-cost' approach is a driver for key design choices for the mission architecture. It leads to:

- *prefer* a body-fixed dual band High Gain Antenna rather than a steerable HGA, to limit the on-board solid state mass memory size to 8 Tbits (at End Of Life), and generally speaking to rely on mature, high TRL technologies for all subsystems
- *discard* electric propulsion solutions which otherwise would also fulfil the mission requirements but at a significantly higher cost
- *select* the lower performance version of the Ariane 6 launcher family as baseline launcher (Ariane 6.2), limiting the total available mass for the spacecraft. In that context the use of aerobraking becomes mandatory to reach the desired science orbit, and the science orbit itself can only be coarsely controlled.
- *limit* the complexity and duration of ground operations, the mission duration being in particular adjusted to six cycles to confidently fulfil all science requirements.

5.3.2 Environment

The thermal fluxes in orbit around Venus are high, the solar flux at Venus distance is twice its value on Earth (around 2600 W/m²), and the reflected sunlight flux has a similar order of magnitude due to the albedo of 0.75. Besides, during aerobraking, a third thermal flux, the aerothermal flux, needs to be taken into account, with a similar order of magnitude as the two others. These high total thermal fluxes, together with the cold instruments requirements, high power dissipation, and low orbital period, make the thermal environment a design driver for the mission. Avoiding the aerothermal flux to fully add up to the two others thermal fluxes drives the pericentre location to be close to ecliptic, driving the whole Venus Orbit Insertion strategy and constraining the pericentre location for the science orbit, but allowing the thermal fluxes to remain within known limits for materials selection.

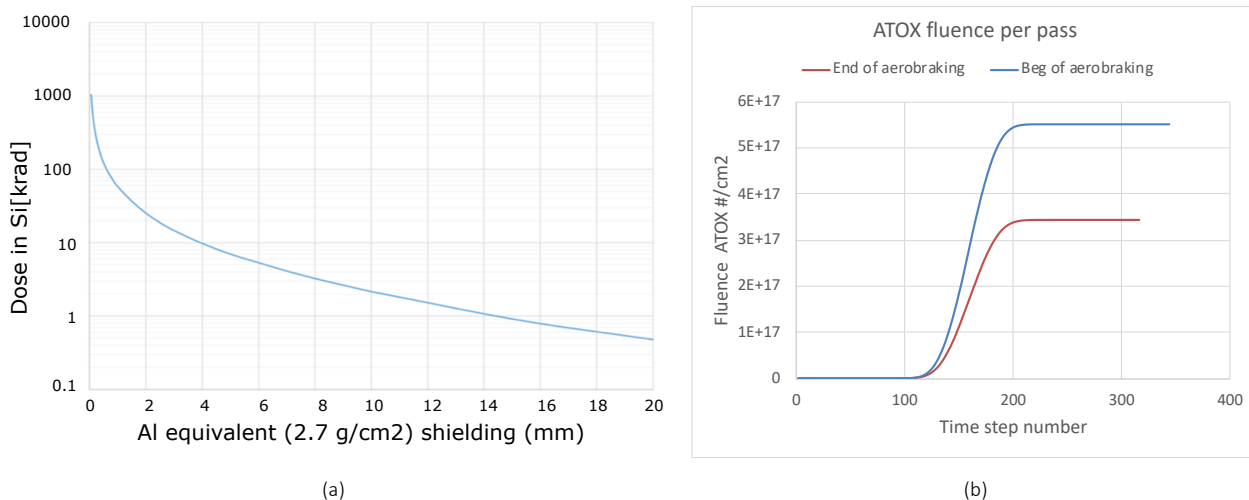


Figure 5.3.1 – (a) Total Ionizing Dose for EnVision behind Aluminium equivalent spherical shielding, without margins (b) total atomic oxygen fluence per atmospheric pass at the beginning and end of aerobraking, without margins.

The rather long interplanetary mission leads to total radiation dose requirement for the spacecraft of 37.5 kRad behind 2-mm equivalent Aluminium spherical shielding, assuming a margin of 100%, for a 6.5 years total mission duration. This is comparable to typical doses encountered for Low Earth Orbit missions.

The atmospheric environment during aerobraking needs also to be taken into account. The atomic oxygen exists in Venus atmospheres at the altitude range foreseen for aerobraking, with densities of up to 10¹⁷ oxygen atoms per cubic metres at aerobraking altitudes. Though the concentrations are small, their accumulation over up to 2000 atmospheric passes lead to total atomic oxygen fluences on the exposed spacecraft surfaces which are comparable to those encountered on classical Earth Low Earth orbiting satellites. This drives the selection of spacecraft materials e.g. Multiple Layers Insulation on the most exposed surfaces.

5.3.3 Payload accommodation and observation modes

The SAR instrument, due to its size (6 m reflectarray length) and accommodation constraints (2.75 m between reflectarray and feed array), its number of operating modes (standard, polarimetry, high resolution, altimetry, radiometry) and its associated resources (mass, power, data volume), determines the spacecraft configuration. The infrared spectrometers (VenSpec-M and H) drive the design of the spacecraft thermal control subsystem, due to their thermal requirements. VenSpec-H for instance needs to be kept at -45 degree, in its cold section, while VenSpec-M require thermal stability in the order of few degrees. This leads to the definition of a “cold” face on the spacecraft, which needs to be maintained cold whatever the sun elevation with respect to the orbital plane, requiring specific 180 degrees flip-around manoeuvres of the spacecraft twice per Venus year. The Subsurface Radar Sounder requires deployment of a 16 m tip-to-tip antenna composed of two 8 m dipole antennas, driving in particular the spacecraft configuration and attitude control requirements to avoid exciting the associated flexible modes.

Table 5.3.1 – EnVision payload nominal resources summary. (*) the nominal mass and power include design maturity margins. (**) the allocated mass corresponds in phase A to a 20% higher mass and the allocated power to 30% higher power. The SRS antenna is under prime responsibility and its mass included in the spacecraft “mechanisms” budget.

| Unit | VenSAR | Radio Science | VenSpec suite | SRS | Total |
|--|---|-----------------|--|---------------------------|--|
| Nominal Mass (*) [kg] | 149.6 | 0.55 [USO] | 34.3 [M:5.9,H:16.6, U:6.8, CCU:5.0] | 12.8 (+ 12.0 antenna)* | 197.3 |
| Allocated mass [kg] (**) | 180 | 2.4 [USO] | 41.09 | 15.34 | 239 |
| Nominal peak power (*) [W] | 1364 | 5.2 [USO] | 72.9 [M:15, H:29.7, U:18.7] | Peak: 200 | 1400 max. (sequenced operations) |
| Allocated power (**) [W] | 1773 | 11.4 [USO] | 66.2 | 149.5 | 1800 max |
| No. of units | Reflectarray, Feeder,ESS, RF electronics, Digital electronics, SSPA | USO | VenSpec-M, VenSpec-H, VenSpec-U, CCU (central control unit) | RDS, TX, MN | 14 |
| Size (cm) | see §4.2.1 | 9.9 x 8.8 x 5.5 | M: 38 x 14.4 x 17.3 H: 65.5 x 46.3 x 27.5 U: 30 x 30 x 30 | | |
| Data rate (Mbps) | 0.003-197 | -- | M: 0.5-1, H: 0.030, U: 0.04-0.64 | 3.25-6.47 | |
| Downlinked data volume (nominal mission) [Tbits] | 180 | -- | 13 | 17 | 210 |

The need for the spacecraft to follow the changing bending angle of the communication system radio ray path, during radio-occultation experiment leads to specific slew profiles which need to be provided by the spacecraft reaction wheels. The various pointing modes of the spacecraft required for instrument operations and the downlink of their data are also driving the sizing of the spacecraft power and thermal subsystems, and in general the spacecraft configuration (solar array and battery sizing, radiator area).

The various planetary coverage requirements of the payload instruments lead to a total return of 210 Tbits over the 6 cycles of the mission, the various SAR modes representing more than 80% of this data-volume. Achieving the required science data return drives the concept of operation of the mission, in particular the ground stations usage and the spacecraft communications and datahandling subsystems designs, and as a consequence also the power subsystem sizing and therefore the dry mass of the spacecraft.

5.4 Design of the science mission profile

5.4.1 Operational point for data return

The baseline mission operational point for achieving the required science data return is tuned by design optimisation at mission level, combining space and ground segments. It can be summarised as:

- At spacecraft level: use of Ka-band RF subsystem for science data downlink, Ka-band travel waveguide tube amplifier (TWTA) with high RF power (120 W), large body-fixed high gain antenna (HGA) diameter (2.5m), and on-board mass memory with 8 Tbits capacity at end of life (EOL);
- At ground segment level: use of cryocooling technology at the deep space antennas ground station receivers to maximise the G/T in Ka-band, and average daily usage of 9.3 hours of ESA’s 35 m deep space antennas for Ka-band downlink during the nominal science phase.

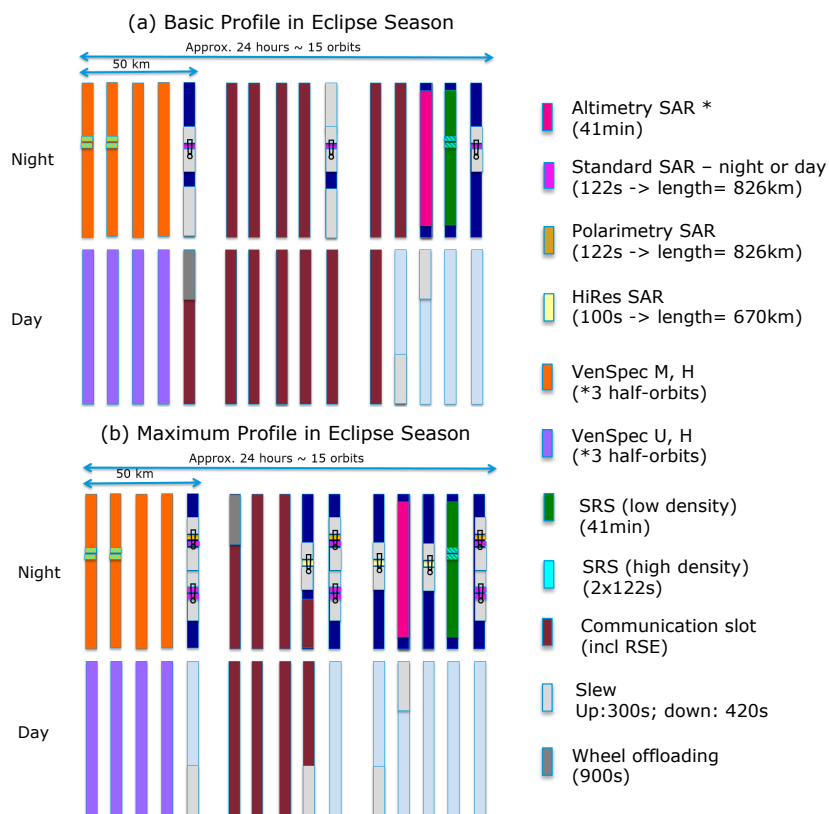
This mission-level operational point allows retrieving the required data return while minimizing spacecraft resources and for an acceptable load on the ground segment. The following paragraphs present the details of the proposed planning and operations strategy and demonstrate its feasibility on a science operations reference scenario.

5.4.2 Conceptual design

The mission design needs to accommodate the operation of the science instruments, namely VenSAR (standard, stereo, polarimetry, HiRes, altimetry, nadir, near-nadir and off-nadir radiometry modes), SRS (high and low density modes), VenSpec-M, VenSpec-H (cooling and nominal), VenSpec-U (Nominal and SNR-limited modes) and Radio Science Experiment (gravity experiment and radio-occultation experiment) such as to achieve the mission objectives in terms of surface coverage and repeated observations, while taking into account the constraints posed by the spacecraft design (e.g. wheel offloading manoeuvre duration and frequency, slew manoeuvres for pointing, mass memory capacity constraints, thermal and power constraints), the instrument design (e.g. VenSpec-M operates on the night side, VenSpec-U operates on the day side, cooling of VenSpec-H is required) and mission boundaries (e.g. the baseline science duration is six Venus cycles and starts in 1st half of 2035).

To cope with the varying downlink capacity and S/C avionics constraints (there is only a limited, discrete number of possible downlink rates due to data handling and transponder limitations), and achieve the science surface coverage requirements, several observations profiles are defined to optimise the data return. They correspond to 15-orbit patterns including observations, slews and communication slots. They are defined such that the daily science data return is as-close-as possible to the data downlink potential that day, so as to store only for a limited time the science data onboard and avoid embarking a very big SSMM which would have cost and mass implications, not affordable in the context of EnVision.

The adopted observation strategy distinguishes between measurements which need to be performed on a regular, routine basis at each cycle, to meet global coverage requirements (e.g. VenSpec, altimetry, RSE, nadir and near-nadir radiometry, SRS) or contiguous coverage requirements (e.g. VenSAR, SRS), and measurements which can be acquired on an irregular basis, e.g. when the available downlink allows it (SAR dual polarization, SAR 10 m resolution, off-nadir radiometry) and when the given target is in visibility. The first category forms the definition of the basic science operations profile, while the second category forms the intermediate and maximum science operations profiles. Each category is then declined in “seasonal” versions to take into account thermal constraints imposed by the S/C configuration.



This illustration shows two possible science operations profiles:

(a) represents the daily pattern for the basic profile that corresponds to the far Earth-Venus distances (low downlink data rates) and long eclipses; the communication slot is long and there are few observations;

(b) represents the daily pattern for the maximum profile that corresponds to close Earth-Venus distances and long eclipses; the communication slot is short and there are many observations.

Radiometry is performed together with altimetry (in a nadir geometry) and in parallel with SRS and VenSpec observations (in a near-nadir geometry).

Each orbit is divided in two parts, the top part refers to night-side, the bottom part to the day-side. For simplification purpose, daytime and night time durations are assumed equal on this figure. In the operations planning exercise, the transition from one science operation profile to another is triggered by the available downlink (Earth-Venus distance) and the season (whether in eclipse or in non-eclipse season).

Figure 5.4.1 – The science operations planning relies on the definition of science operations profiles that are 15-orbit patterns including observations, slews and communication slots. There are eight science operations profiles, created to best cover the mission requirements, while minimizing the needed mass memory capacity and taking into account the variations in data downlink rate, eclipse durations and thermal constraints.

There are eight such science operations profiles defined, created to meet the science requirements, while minimizing the needed on-board mass memory capacity and taking into account the variations in data downlink rate and eclipse / occultation durations. These profiles allow to return between 80 and 350 Gbits per day to Earth. The data downlink potential volume profile is depicted in Figure 5.4.2 in blue. The produced data volume is depicted in orange and show many variations that are due to the transitions between the various science operations profiles.

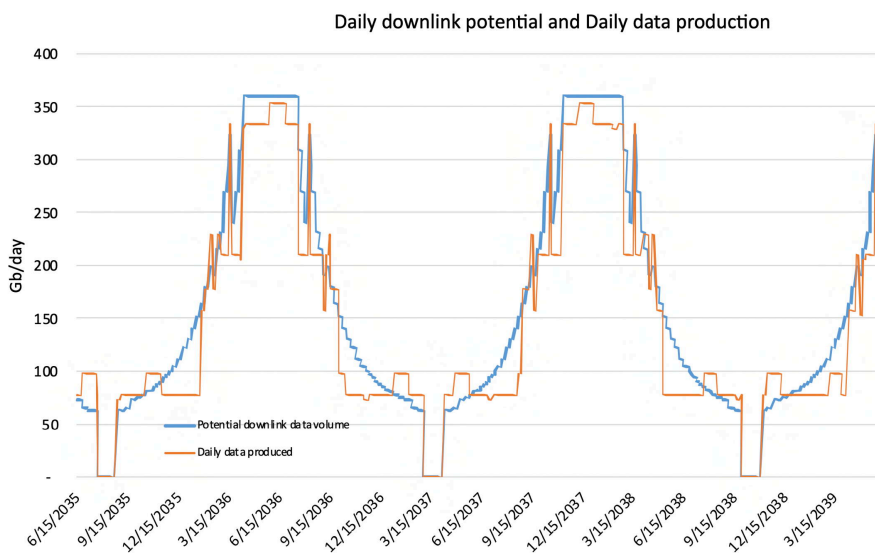


Figure 5.4.2 – Potential downlink data volume in Gb/day (solid blue). Date and EnVision daily data production (solid orange).

5.4.3 Science observations planning strategy

SAR observations planning

The SAR swath width is ~57 km. With a reference orbital ground track shift of 10 km for the reference science orbit, SAR images have to be taken every 6th orbit to ensure contiguous coverage of the observed regions of interest. As a consequence, the science observation strategy foresees three SAR 30 m observation slots every day (on 1st, 6th and 11th orbits, as illustrated in Figure 5.4.1 during the full science phase (excluding superior solar conjunction periods). The total duration of the observation per orbit is modulated between 122 s and 488 s as a function of the science operations profile being implemented. SAR observations are performed on the descending arc of the orbit which minimises the altitude and therefore maximises the image quality.

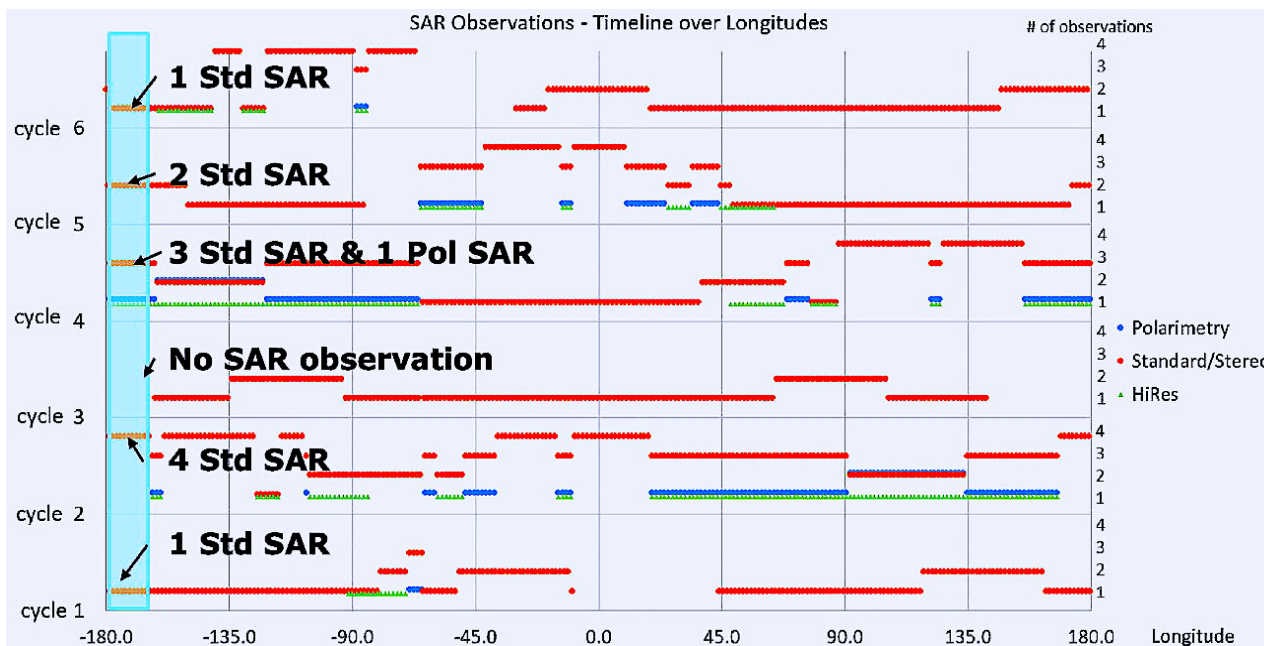


Figure 5.4.3 – Pattern of repeatable observations along the 6 cycles resulting from the implementation of the 8 science operation profiles during the 6 cycle missions, plotted as a function of longitude at the surface of Venus. For the example longitude band highlighted in the figure on the left side, it is possible to perform 1 standard SAR observation at cycle 1, 4 standard SAR observations at cycle 2, no SAR observation at cycle 3, 3 standard SAR and 1 polarimetry observations at cycle 4, 2 standard SAR observations at cycle 5 and 1 standard observation at cycle 6. One standard SAR observation in this context covers a latitude extension of 8 degrees corresponding to 122 s of continuous observation. The elaboration of the science observation strategy must fulfil the boundaries given by these longitude bands pattern, in particular for the planning of inter-cycle repeated observations. The repeatability pattern is dependent on the starting date of the science phase, and the one provided here corresponds to the science operations reference scenario, assuming a start on 15.06.2035.

A further constraint in planning arises from the need to perform repeated VenSAR observations of the identified regions of science interest over two cycles with similar viewing conditions (East-looking) to obtain stereo-topography terrain models (two observations at different incidence angles) or over three cycles with similar viewing direction (all East-looking) to search for surface changes (two observations at same incidence angles and a third one at different incidence angle).

A Venus cycle lasts 243 days and the synodic Earth/Venus period is 578 days. The spacecraft will therefore fly over a given science target at the surface of Venus once every 243 days on the descending branch of the orbit, but the possible downlink datavolume over this region will be different from one cycle to another, meaning that the possible VenSAR observation duration at a given longitude will differ from cycle to cycle. Besides, every 578 days, superior solar conjunction will occur, lasting for around 2 months, preventing any science observations over a given longitude range.

This leads to longitude-dependent possible VenSAR observation time series along the six cycles, that need to be planned carefully in order to acquire the required number of repeated observations over the desired regions of scientific interest. In practice, bands of longitudes at the surface of Venus are defined (43 bands of longitude for the example observation scenario), with for each band latitude extensions defined which can be observed once, twice or three times over mission duration, as illustrated in [Figure 5.4.3](#).

With this baseline observation strategy, the mission design allows the following:

- At all longitudes, latitude bands of cumulated extension of 31 degrees can be observed at least twice over six cycles. The maximum cumulated latitude extension is 55 degrees and the average 42 degrees;
- At all longitudes, latitudes bands of cumulated latitude extension of eight degrees can be observed at least three times over six cycles. The maximum cumulated latitude extension is 23 degrees and the average 13 degrees.

These bands and the associated latitude extensions can then be used by the science team to pre-select the regions of interest (RoIs) to be observed over the mission in an optimal way for a given date of start of science. An example of such RoIs selection based on this approach is provided in [§3.3.1](#) and [Figure 3.2](#) assuming a date of start of science on 15.06.2035. This strategy allows to progressively build up along the 6 cycles the required global and targeted measurements dataset, in particular over all pre-selected regions of interest, which represent a fraction of about 30% of Venus surface. The evolution of the observed RoIs from Cycle 1 to 6 is presented in [Figure 5.4.4](#). Any alternative RoI selection fulfilling the conditions above can be accommodated by the mission.

VenSpec H, M and U observations planning

VenSpec observations require global coverage over mission duration, as well as repeatability at short term (hours) and long term (cycle). The strategy consists of planning VenSpec observations on a daily basis, with observations over half an orbit, over four consecutive orbits, and for every cycle. This is reflected in [Figure 5.4.1](#) with a group of four orbits at the beginning of each group of 15 orbits dedicated to VenSpec observations whatever the science operations profile. This strategy allows to fulfil all VenSpec observation requirements in six cycles.

SAR altimeter and SRS observations planning

The objective is to cover the whole Venus surface with altimetry and SAR observations with an average observation density of 2 per degree of longitude at Equator. The science operations planning considers between 30 and 41 minutes of altimetry per day over the science operations phase. This allows to achieve the required density of 2 per degree of longitude at Equator at the end of the mission, by shifting, from cycle to cycle, within the 15-orbits pattern, the index of the orbit at which altimeter acquisition is planned.

Low density SRS observations need also to be planned such that an average density of 2 per degree of longitude at Equator is achieved over the science phase duration over the whole Venus surface that is accessible on the night side. This is made possible by scheduling SRS low density observations every day on one orbit for 30 to 41 minutes (when the spacecraft is in eclipse, see [Figure 5.4.6b](#)).

High density SRS observations are required over a representative fraction of the RoIs observed with the SAR at 30 m resolution, with an average observation density of 10 per degree of longitude at Equator over the science phase duration. In order to uniformly distribute SRS HD observations over the mission, 244 s-long SRS HD observations over the targeted RoIs are planned, performed on three consecutive orbits, and every day of the science mission whenever the spacecraft is in eclipse.

Radio Science observations planning

Within each observation profile, a group of orbits is reserved for data downlink, with an effective downlink duration varying between 3.5 and six hours every day. This strategy allows to naturally fulfil the gravity science requirements in terms of observability and spatial resolution of the whole surface of Venus at low altitude. When downlink periods occur during the Earth radio-occultation season, radio-occultation experiment is performed, providing at least four ingress and four egress observations per day.

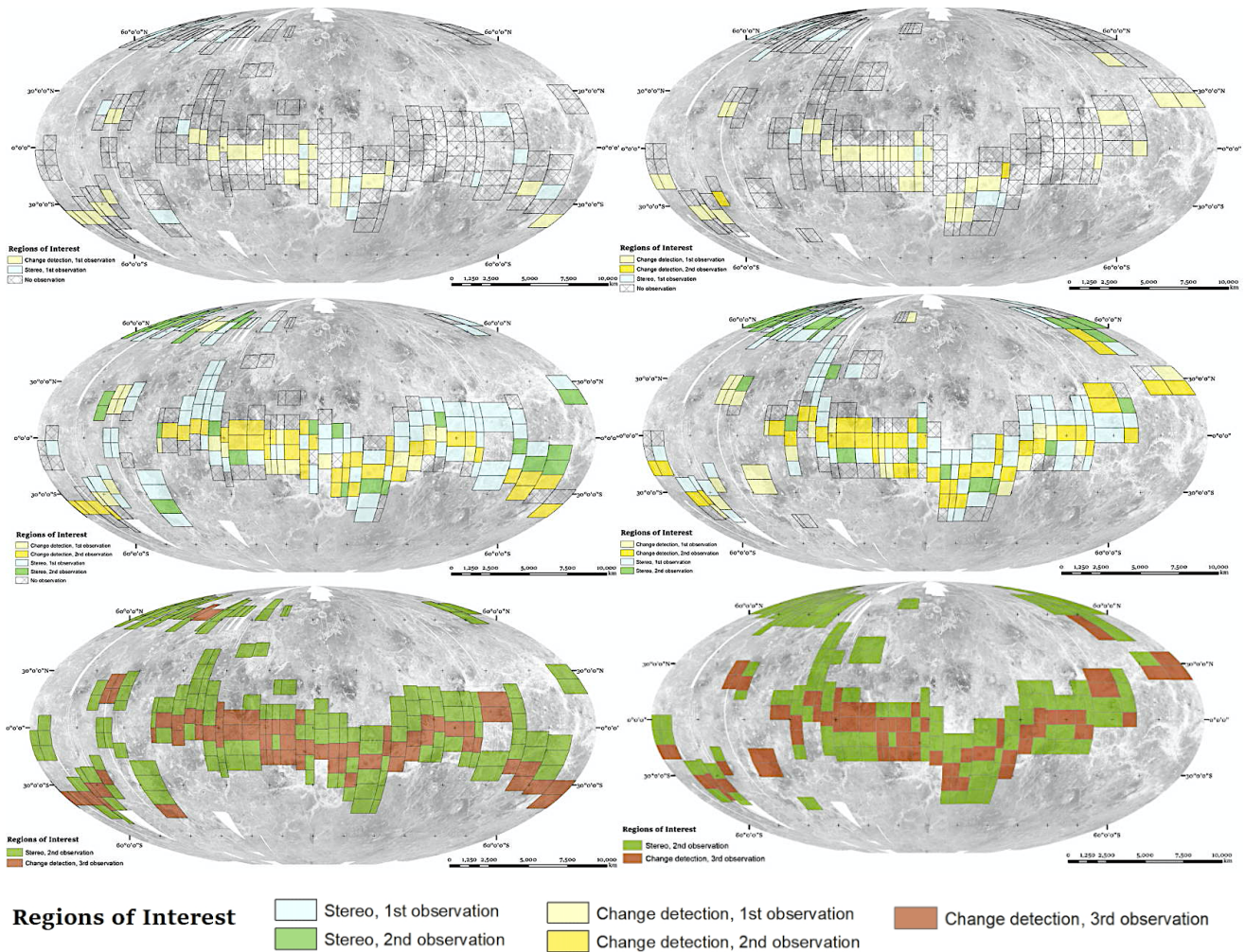


Figure 5.4.4 – Illustration of the spatial SAR 30 m Rols coverage build-up along the cycles. The mission design can accommodate any Rol selection which fulfils the repeatability pattern as described in Figure 5.4.1. Maps are presented here at the end of cycles 1, 3 and 6 and for two example Rol selections complying with such repeatability pattern for a start of science on the 15.06.2035. The brown Rol correspond to the 30 m VenSAR observations requiring 3 repeated passes. The green Rols correspond to the 30 m VenSAR observations requiring 2 observations at different angles. In both cases, the planning allows to guarantee that all identified Rol can be observed the required number of times over mission duration.

5.4.4 Payload Reference Operations scenario

To arrive at a realistic sizing of the spacecraft, in particular for its power, data handling (e.g. mass memory), communications, GNC and thermal subsystems, a reference operations scenario for the payload operations has been implemented, based on the strategy described in detail in §5.4.1-5.4.3. This scenario has been simulated by ESAC with its operational tool GMAPP, taking into account realistic operational constraints (including ground stations availabilities). The Rol scenario 1 of Figure 5.4.4 has been used for that purpose. The reference scenario assumes a start of science on 15.06.2035 which corresponds to a worst case in terms of orbit stability.

The simulation demonstrates that all identified surface targets can be imaged with VenSAR, with a performance fully compliant with the science requirements, with extra margin (Table 5.4.1; Figure 5.4.7a). The first two cycles allow imaging once 80% of the identified regions of scientific interest with the SAR at 30 m resolution. The following two cycles are mostly devoted to acquiring 2nd observations of these areas for stereo-topography mapping and the two last cycles to perform 3rd observations of the “activity” type targets for change detection mapping. Dual polarization and high resolution VenSAR observations can be performed at any longitude at least once across the 6 cycles. The strategy shows robustness in the event of an early loss

of the mission, a required 20% of Venus surface being imaged at least once at 30 m resolution after two cycles only, while the same coverage in stereo-topography would be met after four cycles.

Due to the limited difference between Venus sidereal day (243 days) and its heliocentric orbital period (224 days), the part of the planet which is visible on the night side (respectively day side) during each cycle of the mission represents about only half of Venus surface, with a shift of this zone by about 30 degrees in longitude per cycle. After 6 cycles of mission, a small portion representing about 3% of the planet, will therefore remain inaccessible for night-side (respectively day-side) observations. This impacts the instruments which have specific diurnal / nocturnal observation constraints such as respectively VenSpec-M (night-side), VenSpec-H (night-side and day-side), and VenSpec-U (day-side observations), as can be observed in Figure 5.4.6b (VenSpec-M) and Figure 5.4.6d (VenSpec-U and H). SRS and VenSAR altimetry operations have the slightly more stringent constraint to be operated only when the spacecraft is in eclipse: after six cycles of mission, a larger portion representing about 10% of the planet, will therefore remain inaccessible to such observations (cf Figure 5.4.6f). Despite these constraints, the accessible coverage during a six-cycle mission are largely sufficient to meet the related science requirements of the mission (Figure 5.4.7b, c and d).

Dual polarization VenSAR observations and 10 m resolution VenSAR observations are performed only when the downlink data rate is sufficiently high (Figure 5.4.5). Over 6 cycles, all longitudes are accessible for such observations.

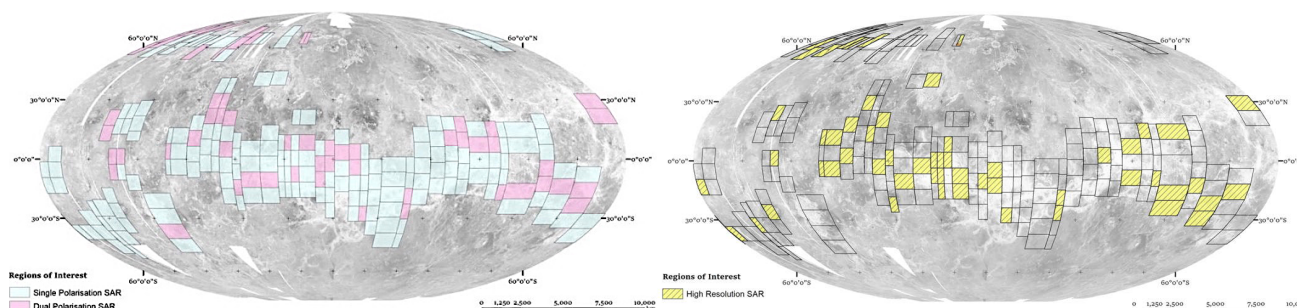


Figure 5.4.5 – Dual polarization 30 m SAR observations over 6 cycles (left) and 10 m SAR observations (right). The pale blue colour code indicates standard SAR, the pink a polarimetry observation.

Table 5.4.1 – Science performance synthesis with the science operations reference scenario, assuming a start of science on 15.06. 2035. All performance figures are provided after deduction of a 5% availability margin to cover operational contingencies and uncertainty on starting date. (*) VenSpec-M coverage with 3 repeats at long time scales (half-cycles); (**) VenSpec-U coverage without repeat; (***) VenSpec-H coverage without repeat. The requirements are met with a margin greater than 5% on top of the 5% availability margin.

| | Observation type | Science requirements (% of Venus) | Coverage in nominal mission |
|----------------------|---|-----------------------------------|-----------------------------|
| Targeted observation | SAR Standard (30 m) | 20% | 30.3% |
| | SAR Stereo (30 m) second pass | 18% | 28.3% |
| | SAR Standard (30 m) third pass observations | 2% | 9.4% |
| | SAR off-nadir radiometry | 1% | 2.6% |
| | SAR Polarimetry (30 m) | 5% | 6.8% |
| | SAR High-Resolution (10 m) | 2% | 2.4% |
| | SRS High Density | 10% | 14.2% |
| | Gravity Science (High resolution; < 260 km) | 40% at < 260 km | 50.8% |
| Global observation | SAR Altimetry | 65% | 68% |
| | SAR Near-nadir and Nadir Radiometry | 75% | 93.2% |
| | SRS Low Density | 65% | 68% |
| | VenSpec-M (*) | 60% | 76.6% |
| | VenSpec-U (**) | 60% | 91.8% |
| | VenSpec-H night (***) | 60% | 86.5% |
| | VenSpec-H day (***) | 60% | 85.5% |
| | Gravity Science (Low resolution; < 520 km) | 95% at < 520 km | 100% |
| Radio Occultation | 50%, 4 events/day | 63.9% | |

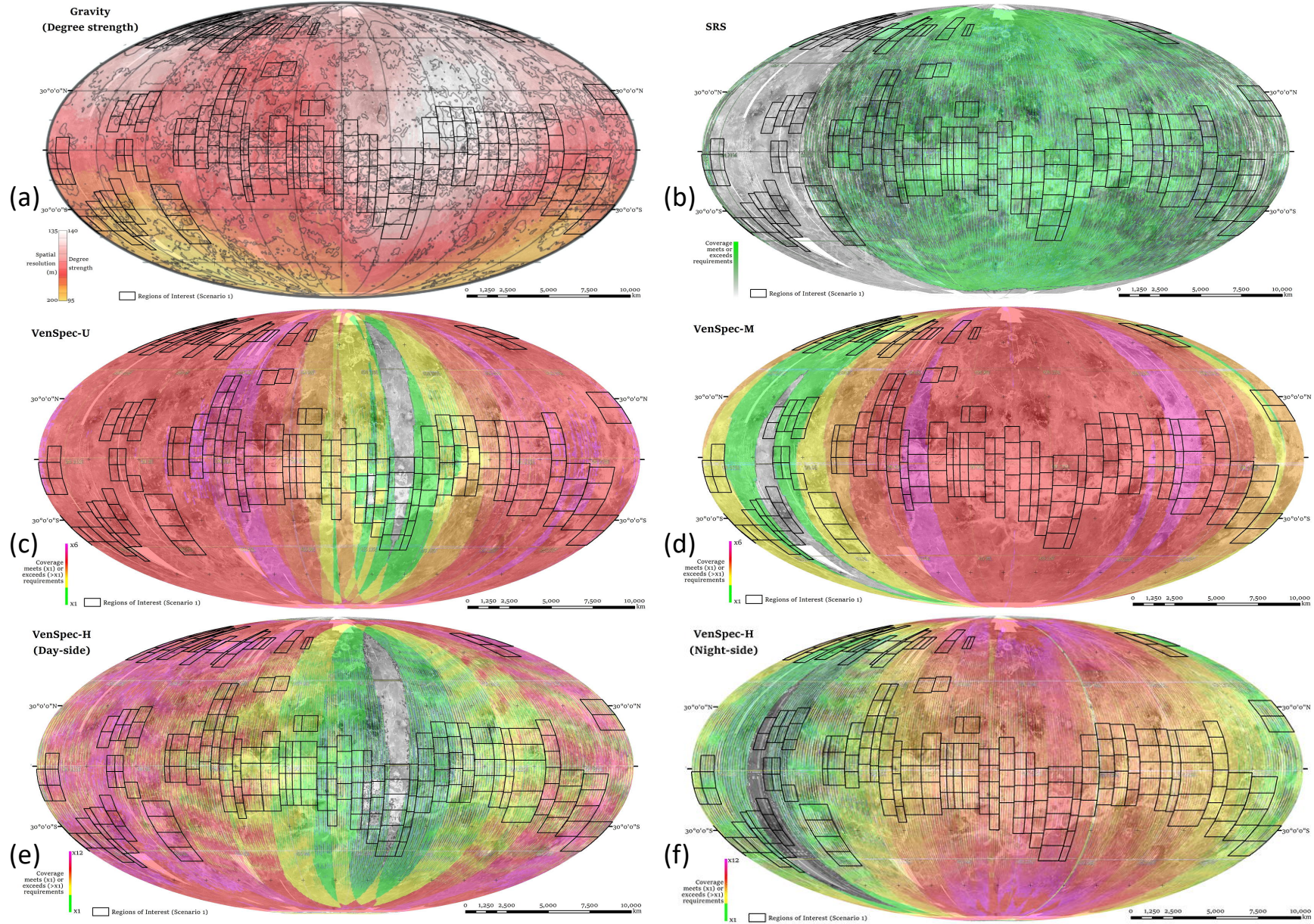


Figure 5.4.6 – Results of the science reference scenario simulation, superimposed to SAR 30 m reference scenario ROIs, assuming a starting date on 15.06.2035 (a) Gravity science (degree strength); (b) SRS LD and altimeter; (c) VenSpec-U (dayside); (d) VenSpec-M (nightside); (e) VenSpec-H dayside; (f) VenSpec-H nightside. Square boxes indicate EnVision Regions of Interest (ROIs) described in §3.1 and Figure 3.2. For (b) the green code represent regions where SRS and altimeter meet or exceed coverage requirements. For (c, d, e, f) colour code indicates the number of observations over 6 cycles, with green representing 1 observation, yellow 2, red 3, 6 or 12 observations.

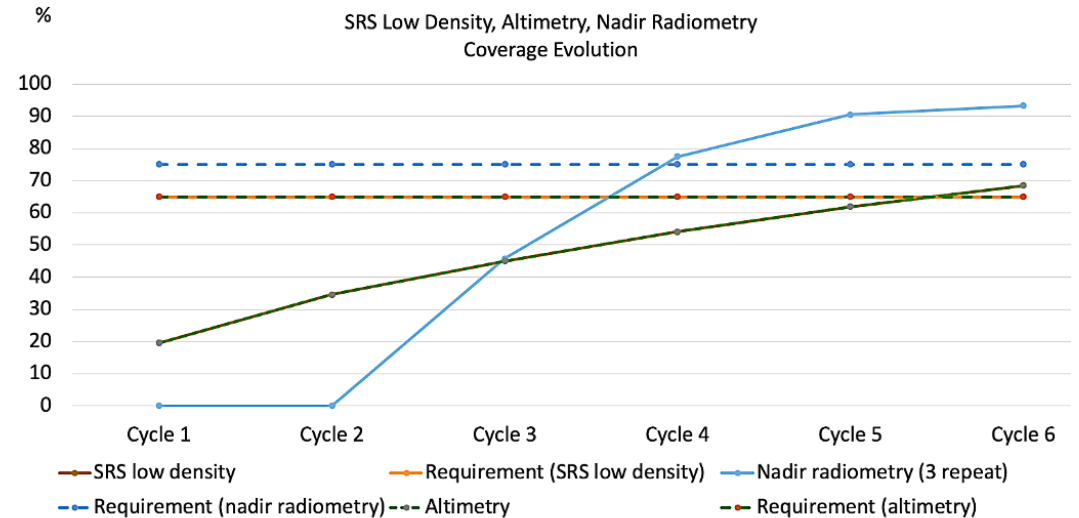
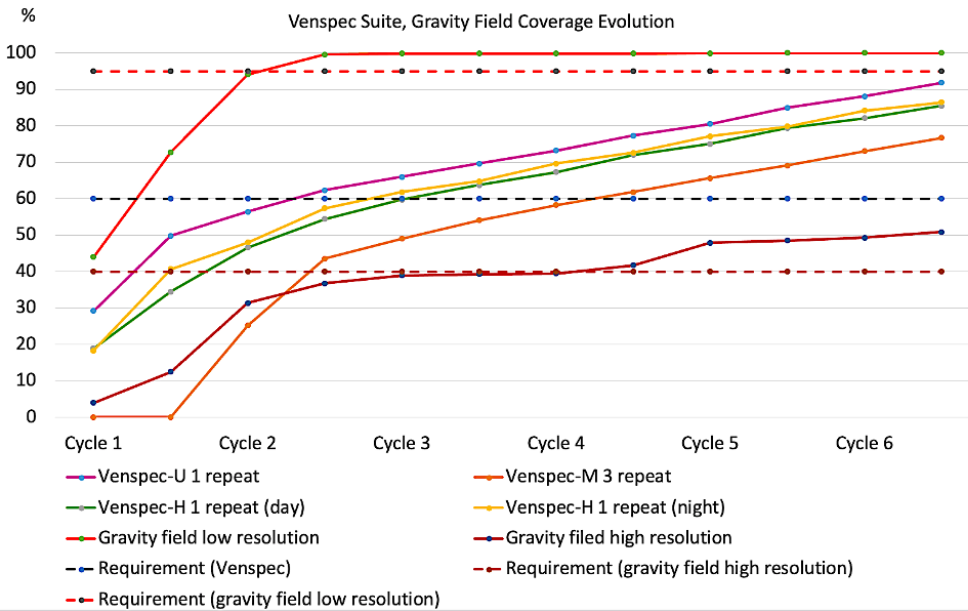
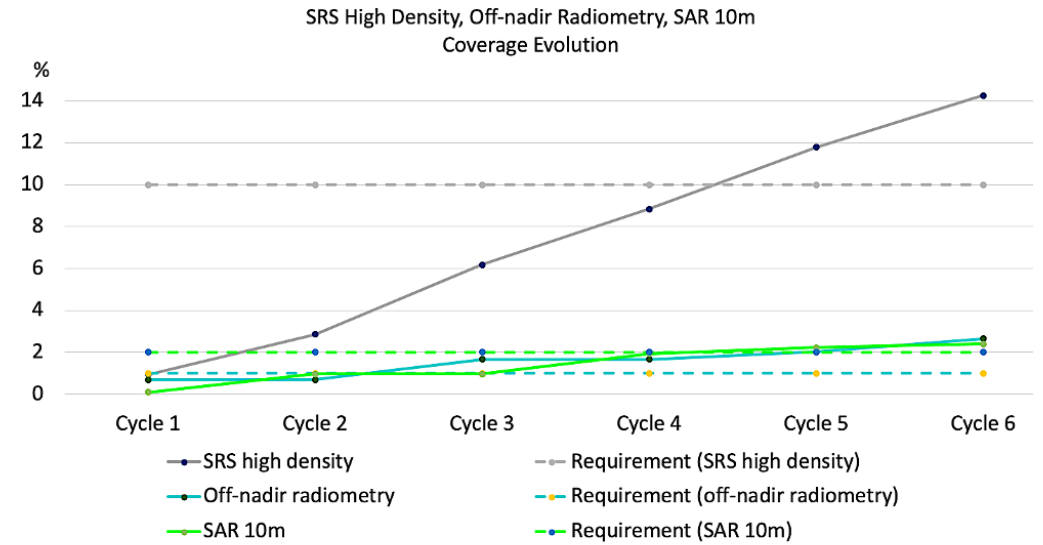
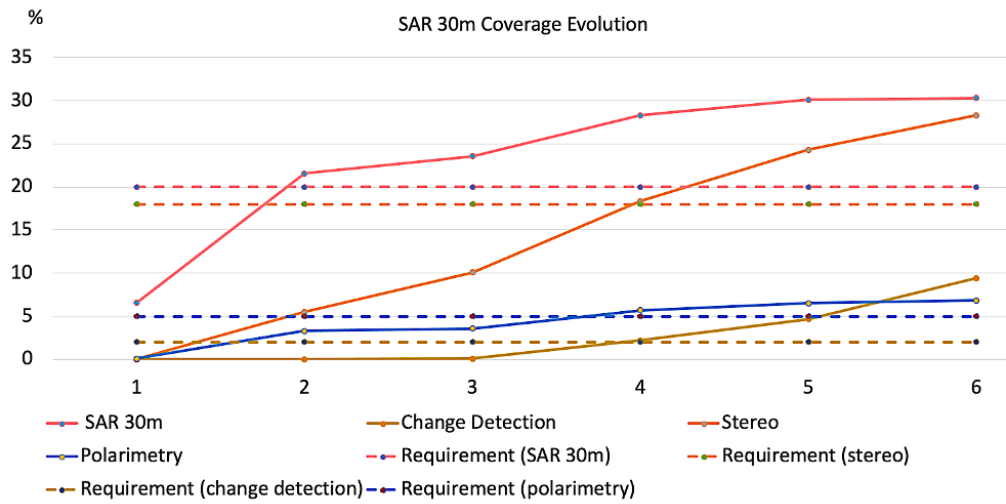


Figure 5.4.7 – Cumulative science performance metrics based on the science operations reference scenario modelling, assuming a starting date of science on 15.06.2035. Values are provided at the end of each cycle. The linear interpolation between each data point is for illustration only. All values presented are after deduction of a 5% margin for operational contingencies and uncertainty on starting date.

Radio-occultation performance is also assessed as part of the reference operations scenario (Figure 5.4.8). The requirement of 50% of the days within the mission with more than four radio-occultation events is achieved after five cycles (one event being either an ingress or egress from the atmosphere).

The simulation of the science operations reference scenario confirms the achievability of all science requirements, with margin (Table 5.4.1); it validates the overall science observation strategy. The overall

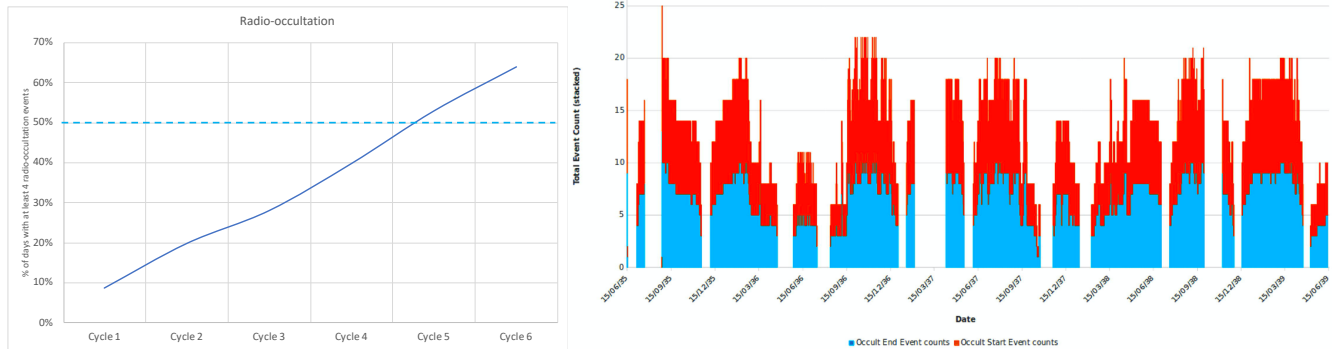


Figure 5.4.8 – Performance metrics for the radio-occultation experiment. Left: cumulated percentage of days over mission duration with at least 4 radio-occultation events. Right: counts of ROC events (blue: ingress; red: egress) per day from the science operations reference scenario, assuming a start of science on 15.06.2035.

science performance is assessed considering a 5% availability margin, which means 5% of the duration nominally available for science is assumed not to be available e.g. due to safe mode occurrence or due to uncertainty on the date of start of science.

The Science Operations Scenario presented here is an illustration to demonstrate that all the science observation requirements can be met with ample margins. The mission design offers enough flexibility to adapt the observation plan to potential future changes in the mission objectives. This could include changes in the ratio of different radar modes, for example, or changes of surface targets in response to discoveries made before or during the mission.

5.5 Strategy robustness assessment

Two main elements may influence the data return of the mission:

- The date at which the science actually starts may differ from the assumed one due to aerobraking uncertainties. The initial date influences the data return for a six-cycle fixed science mission duration.
- The actual available duration of the ground communication slots might not be as anticipated, leading to a shorter communication slot, or no communication slot at all, requiring the spacecraft to store the excess data and the mission to ensure this excess data can be later retrieved without compromising the planned observations.

The strategy for science data acquisition needs to show robustness to these events to guarantee the science return of the mission.

5.5.1 Sensitivity to starting date

The mission science performance has been simulated and verified on a reference scenario assuming a notional start of science on 15 June 2035 which provides the most eccentric orbit value over the likely period of start of science following the aerobraking, and from this point of view constitutes a worst case. The actual date of science could be different, depending on the performance of the aerobraking phase. Changing the reference date requires to adjust the definition of the longitude bands as described in Figure 5.4.3, and therefore to adapt the pre-selected list of targets in order to optimise the coverage criteria. A three months earlier date (Figure 5.5.1) would reduce the total data volume returned by less than 2%. On the other hand, a three months later date would increase the data return by close to 20%. The selected date used for the performance assessment is

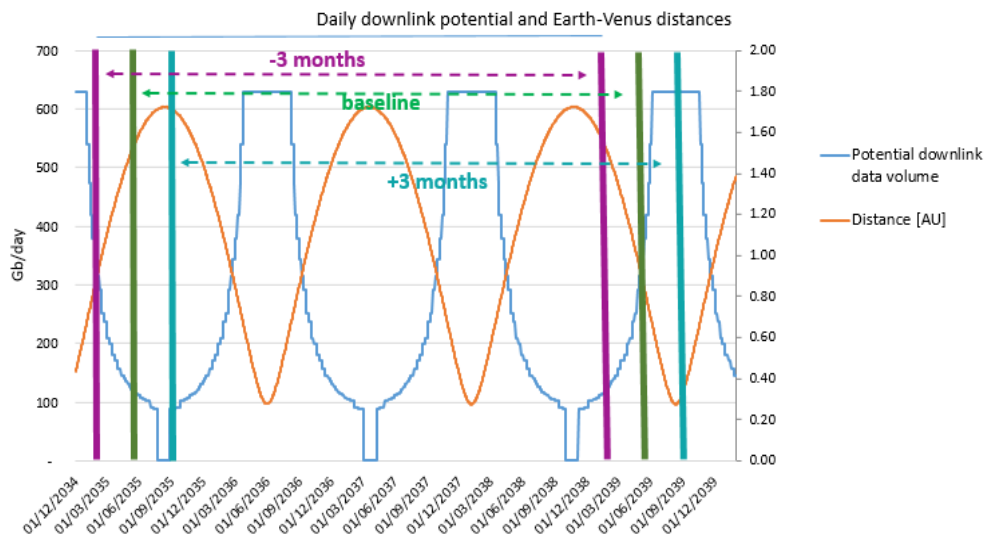


Figure 5.5.1 – Sensitivity to the date of start of science. The operations reference scenario assumes a start close to the minimum data rate (green vertical bar), and only 2 months before a superior conjunction. A three months earlier start would provide a similar data return. A three months later start would provide higher data return since in that case more than two peaks of high data rate would occur for the six-cycle mission.

therefore very close to the worst case, and the assessed science performance include a margin in particular to cover this uncertainty.

5.5.2 Resilience in degraded communication scenarios

The mass memory is sized for 8 Tbits capacity at end of life (EOL). The reference Solid-State Mass Memory (SSMM) fill state profile is presented in Figure 5.5.2 (orange curve). The mass memory sizing is compatible with two days of science data generation without any ground contact, which could occur at any point of the nominal mission. The SSMM sizing also nominally includes a 30% margin on the instruments datarates. Even with these conservative assumption, the available free memory space is higher than 80% of the SSMM capacity for 20% of the time, and higher than 20% for 90% of the time. In the worst case the free memory space represents still 6% of the EOL capacity. It needs to be checked if this is sufficient to cope with potentially reduced communication slot durations. The following contingency cases impacting the duration of the communication slot have been identified:

- a) **Planning conflict:** if a communication slot is in conflict with a SAR observation, that observation should take priority at the expense of one communication orbit. The data volume which was supposed to be downloaded in that orbit needs to be stored and downlinked later. The SSMM provides flexibility in the planning of observations in such situations. A frequency of one such conflict per month is conservatively assumed.
- b) **Missed ground pass:** if a full communication slot is missed, this means in the worst case one full day without ESTRACK ground contact. A frequency of once a year is considered for such events based on station maintenance statistical data from ESOC.
- c) **Late ground pass:** a 10 minutes late station acquisition could occur. A frequency of once per week is considered for such events, based on ESOC experience. The SSMM shall absorb such cases.

Any data which has not been downloaded and which is stored on the SSMM needs to be downlinked later, without compromising the plan. This means in particular that no additional communication orbit can be placed in lieu of an already planned observation.

In such case, offline arraying technique in Ka-band between distant antennas of the ESA's ESTRACK network will be used to regularly offload the on-board mass memory. For Malargue and Cebreros the visibility overlap is around four hours every day and this pair of stations is therefore assumed as baseline for the arraying technique. During such overlap periods the data rate can be increased by around a factor two with respect to the reception from a single antenna by using the two antennas at the same time. Offline arraying implies a significant delay between reception of the signal at the antennas and delivery of the final products to the user, as well as a channel bandwidth limitation, both due to the need to record and transfer digital raw samples

between remote locations across the wide area network. Such a significant delay (days) is acceptable for science data.

A total of 160 hours of offline arraying (corresponding to 40 slots of four hours) over mission duration, with a distribution between eight and 48 hours per six months period, is sufficient to absorb the worst case accumulated extra data on the on-board mass memory due to the described contingency cases, and is fully compatible with ESTRACK capabilities. To cover the case of loss of contact during one day per year would require between 16 hours and 84 hours of extra offline arraying per year. The data return strategy is therefore fully robust against the identified data return contingencies.

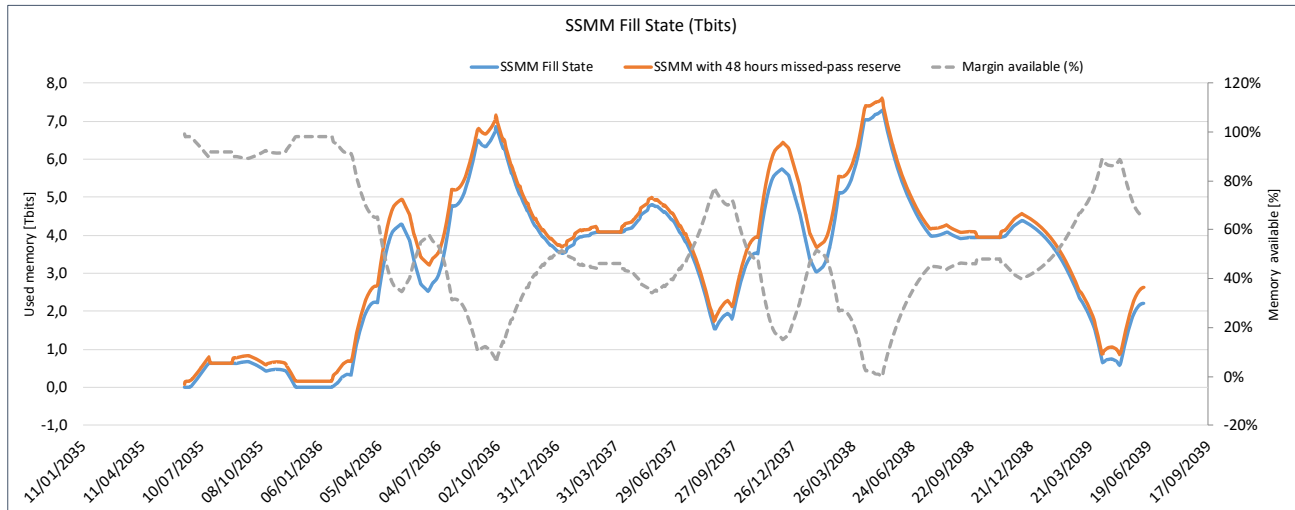


Figure 5.5.2 – This figure shows the SSMM loading profile consistent with the science operations reference scenario, assuming a starting date on 15.06.2035. The blue curve represents the nominal accumulation of science data in the SSMM. The orange corresponds to the blue line with the addition of 2 days accumulation at the current data volume generation rate to preserve the science return at any moment even with a 2 days interruption of ground contact. The gray dotted line represents in % the available free memory compared to the EOL SSMM capacity. The free memory ratio is higher than 20% for 90% of the time and 6% in the worst case.

5.6 Mission timeline

Table 5.6.1 describes the baseline EnVision nominal mission timeline, starting from opening of the launch period T0 to End of mission at T0+78 months, for a total mission duration of 6.5 years.

| | |
|---|-------------------------------|
| Launch =(T0) (opening of the launch period) | 29/05/2032 |
| Venus Orbit Insertion (VOI) | 28/08/2033 (T0 + 15 months) |
| Start of Aerobraking phase | 12/10/2033 (T0 + 16.5 months) |
| Start of in-orbit science operations | Q1 2035 (T0 + 30 months) |
| End of mission | Q1 2039 (T0 + 78 months) |
| Total mission duration | 6.5 years |

5.6.1 Launch

Ariane 62 would release EnVision spacecraft in a direct escape trajectory, with a velocity at infinity of 2.35 km/s, at an optimal declination of -4 degrees, 36 minutes after launch, following a 13 minutes long boost of its re-ignitable upper stage VINCI engine.

The baseline launch period opens on 29 May 2032 and closes on 21 June 2032 guaranteeing 21 launch opportunities (one per day, with three days excluded due to the influence of the Moon). The launch trajectory is optimised to allow full visibility from ESA ground stations during the three hours following launcher separation.

EnVision design is fully compatible with a back-up launch opportunity six months later in 2032 (December) with a short direct transfer (type 2, six months duration), with a launch period opening on 14.12.2032 and closing on 04.01.2033. In this scenario the required aerobraking duration is significantly longer than for the baseline launch date. An alternative launch date exists also in May 2033, involving a long interplanetary transfer with an Earth swing-by.

5.6.2 Interplanetary transfer phase

Right after separation, the Launch Early Operations Phase (LEOP) will start, marked by the correct deployment of solar arrays, the completion of launcher dispersion trajectory correction, the acquisition of safe attitude and nominal communications with ground. The LEOP is assumed to last no more than three days in the case of EnVision. The deployment of the SRS dipole antennas, then of the VenSAR arrays, will follow, when the Spacecraft is still in Earth vicinity.

The baseline interplanetary transfer consists in a direct transfer involving more than a complete revolution around the Sun before reaching Venus, and lasting about 15 months, with no Earth swingby. This transfer strategy has been selected as baseline despite its relatively long transfer time, because it maximises the mass at Venus and minimises the aerobraking phase duration, hence the operational cost of the mission.

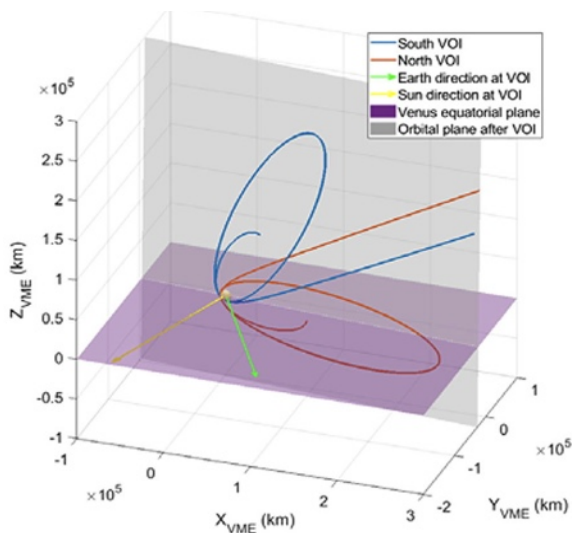


Figure 5.6.1 – Venus orbit insertion (VOI) approach possibilities for the baseline transfer.

The direction of Venus arrival from the velocity at infinity and the target orbit inclination determine the geometry of the Venus orbit insertion (VOI, Figure 5.6.1), allowing for only two possible solutions: arriving to Venus over either the North or South poles, which determines the location of the VOI manoeuvre and the pericentre of the orbit around Venus. After that, the location of the pericentre remains virtually constant until the end of aerobraking phase. The approach direction is chosen in order to place the pericentre as close as possible to the Venus orbital plane, which minimises the effect of the Sun's 3rd body perturbation and the amount of solar flux received by the spacecraft at the peak aerothermal flux encountered at pericentre. For the baseline transfer strategy, this results in performing a North insertion, with the argument of pericentre being only few degrees away of the Ecliptic plane, allowing for an efficient aerobraking.

5.6.3 Aerobraking

Aerobraking consists of a sequence of thousands orbital revolutions during which the orbit dips into the upper atmosphere around each pericentre, resulting in a progressive reduction of the apocentre altitude. The pericentre altitude is controlled to prevent the maximum heat flux, dynamic pressure and the heat load accumulated during a pass from exceeding their specified constraints. The aerobraking strategy relies on the anti-nadir panel of the S/C and the back side of the SAR reflectarray as main drag surface, complemented by specific aerodynamic flaps to minimise the ballistic coefficient of the spacecraft.

The aerobraking sequence is divided as follows:

1. An initial walk-in phase, where the pericentre is gradually lowered with a sequence of manoeuvres, at low aerodynamic regime.
2. A central phase, where the aerodynamic regime is dominated by the peak heat flux/peak dynamic pressure, according to which is dominant. These peak quantities are always achieved close to the pericentre, since the density is mostly dependent on the altitude.
3. A final phase, where the prolonged duration of the atmospheric passages make the heat load the driving quantity for the pericentre control.
4. A walk-out phase, where the pericentre is increased up to outside the atmosphere. This phase is not modelled in the current analysis.

The aerobraking central phase is assumed to start 45 days after VOI. This period is dedicated to the execution of apocentre lowering manoeuvres (assumed to be split in two manoeuvres) and the walk-in manoeuvres (7-10 manoeuvres as reference) until the full aerobraking regime is reached.

The selection of the aerobraking strategy is the result of a mission-level trade-off between mission performance (aerobraking duration), mission cost (at ground and space segments levels), and risk. A key guideline for EnVision is to rely on mature technical solutions at spacecraft level to minimise the technical risk. This calls for defining a strategy which allows the spacecraft and its payload to remain within known thermal limits of existing surface materials (MLI and Solar Arrays being the driving elements), with significant margins to cope with the largely unknown atmospheric density variability.

An aerodynamic “corridor” is defined for the spacecraft based on these considerations which guarantees that all spacecraft surface materials qualification limits are never exceeded over the aerobraking duration with high probability, considering the known atmosphere density natural variability. The aerobraking corridor, defined as a heatflux profile as a function of the orbital period and local solar time at pericentre, is dominated by MLI thermal constraints until orbital periods of few hours, and then by solar arrays thermal constraints toward the end of aerobraking.

In the unlikely case where the materials thermal limits would be exceeded, the S/C is capable of performing autonomously an emergency pericentre raising manoeuvre (so-called pop-up manoeuvre) before next

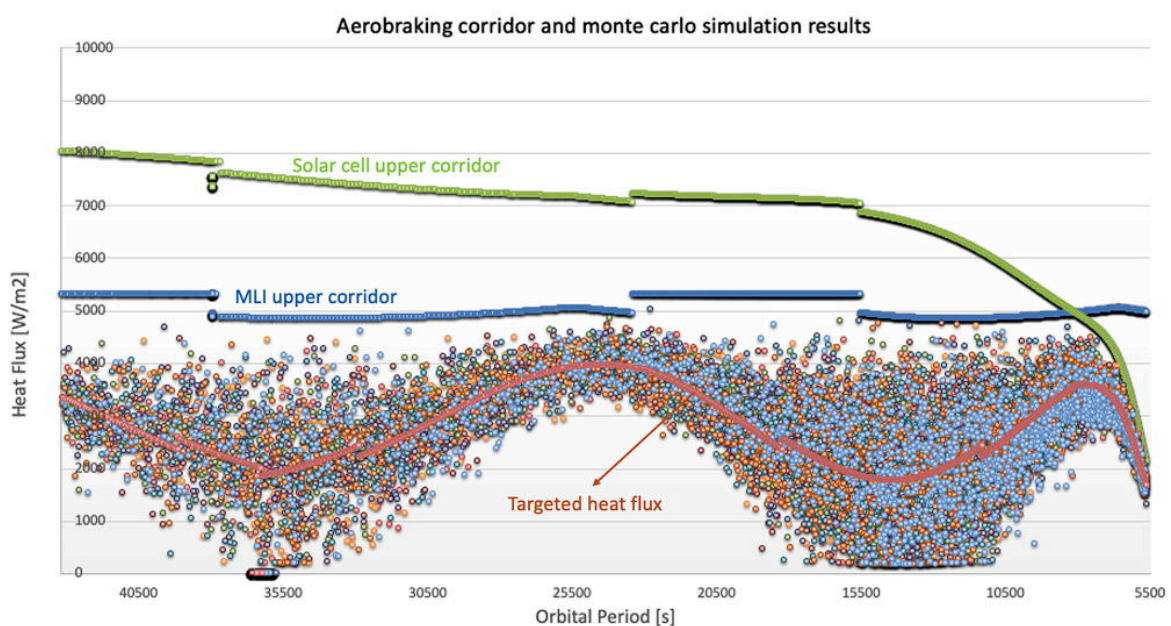


Figure 5.6.2 – Baseline aerobraking corridor and Monte Carlo (MC) results. Individual point colours correspond to different MC results. The targeted heatflux is the red line, which is dynamically adjusted to the local solar time at pericentre to cope with the expected higher density dispersions at night as observed by previous missions Pioneer Venus Orbiter and Magellan.

atmospheric pass. This approach is similar to the one implemented on ESA’s Trace Gas Orbiter which successfully achieved its science orbit around Mars after one year of aerobraking.

The baseline strategy foresees a start of Aerobraking on 11 October 2033, from a 12 hours orbital period, and stops when the apocentre has reached an altitude of 500 km (similar to NASA’s Magellan apocentre altitude at the end of its aerobraking phase). Aerobraking operations are interrupted due to the Superior Solar Conjunction between 14.12.2033 and 24.01.2034, requiring the S/C to be put on a stable orbit by raising its pericentre altitude by 100 km typically. Including this operational interruption, the expected aerobraking duration is about 500 days (16 months) and is achieved with a total of 2000 passes through Venus atmosphere.

Aerobraking involves significant ground operations to track the spacecraft, monitor the aerobraking progress, prepare the aerobraking manoeuvres sequences for the next day(s), or update the atmosphere models. In particular 16 hours daily support is required from ESTRACK’s 35m Deep Space Antennas for orbital periods above 6 hours, and 24/7 support for orbital periods smaller than six hours.

5.6.4 Transition to science orbit and nominal science phase

The baseline assumption for the science orbit is that the orbital elements are left untouched at the end of the aerobraking phase, thus driven by the interplanetary transfer, choice of VOI approach, and the actual aerobraking duration. Because of this, the transition to science orbit at the end of aerobraking requires only a

pericentre raising manoeuvre, and the apocentre can be left untouched, once aerobraking has reached the target altitude of 500 km. The aerobraking end date (combined with the actual value of right ascension of ascending node) fully define the initial longitude at the ascending node (or roughly equivalently at pericentre) at the beginning of the science orbit.

A reference orbit example is given in Figure 5.6.3, assuming a start of science on 15.06.2035, which is considered as a worst case in terms of eccentricity among the likely range of starting dates following aerobraking. The resulting science orbit has its pericentre close to the descending node at a latitude of around +5 degrees. The natural evolution of the orbit due to Venus' oblateness implies a secular decrease of eccentricity, i.e. pericentre naturally raising and apocentre lowering. Additionally, the argument of pericentre experiences a relatively quick secular drift towards the Venus' north pole. Small pericentre lowering manoeuvres are performed once per cycle to avoid a too large increase in pericentre altitude which would penalise the radio science experiment. The apocentre altitude is left uncontrolled for the full science phase: the natural decrease of altitude benefits to all instruments (improved signal to noise).

The initial latitude and longitude at pericentre defines the orbit evolution. Different initial conditions (e.g. shorter or longer aerobraking) would see similar latitude evolution of the pericentre as in Figure 5.6.3 but shifted up or down by up to 30 deg accordingly to the initial pericentre location. Rather independently of the initial conditions, the overall perturbations in the orbit are expected to be very similar at equal longitudes, therefore this variation would mainly cause a shift in time of the apocentre and pericentre altitude curves but remaining quite close to the examples in terms of altitude versus longitude in Figure 5.6.3. This dispersion in the initial conditions has a non-negligible impact on the orbit maintenance Delta-V and a conservative (enveloping) delta V allocation has been considered to cope with such dispersion.

Table 5.6.2 – Example orbit parameters assuming a start of science on 15.06.2035.

| | |
|------------------------|--------------------|
| Pericentre altitude | 220-290 km |
| Apocentre altitude | 355-527 km |
| Semi-major axis | 6372-6425 km |
| Orbital period | 93.45 to 94.62 min |
| Inclination | 87.7-88.6 deg |
| Argument of pericentre | 103-186 deg |

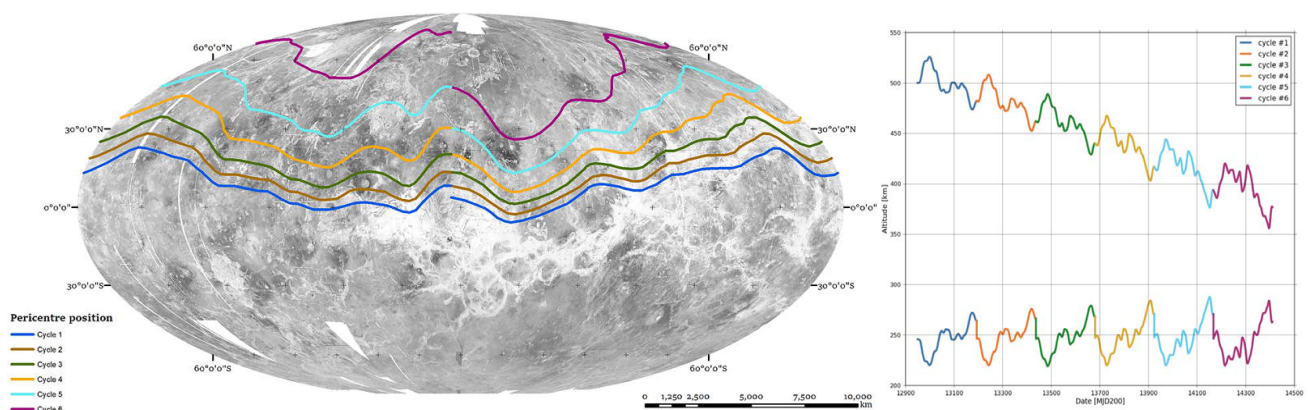


Figure 5.6.3 – Example orbit evolution assuming a start of science on 15.06.2035. The evolution of the pericentre position in Venus surface coordinates (left), and apocentre / pericentre altitudes (right) along the 6 cycles of the mission. The intra-cycle variations are due to the accumulation of local longitudinal topography effects on the orbit, while the inter-cycle variations are caused by Venus oblateness.

5.6.5 Spacecraft disposal

At end of mission, the EnVision spacecraft will be passivated, following ESA's guidelines for spacecraft debris mitigation. The spacecraft will naturally enter into the atmosphere and disintegrate in the upper atmosphere of Venus in a few months.

5.7 Spacecraft Design

5.7.1 Main modes of S/C operations

Three main spacecraft pointing modes for instruments operations are identified:

- (a) *default* pointing mode, with the long direction of the SAR antenna parallel to velocity..
 - a. When +X face is nadir pointed (Figure 5.7.1b) this corresponds to the default orientation of the spacecraft, with the central part of the SAR antenna aligned with the orbital velocity and the nadir face (+x) nadir pointed for radiometry, VenSpec and SRS observations.
 - b. When +X face is off-nadir pointed, 30 m, 10 m-resolution and off-nadir SAR observations can be performed, with the +x face of the spacecraft with angles between -50 degrees and +20 degrees degrees around the y axis to cover the range of look angles for the SAR (Figure 5.7.2).
- (b) *altimeter* pointing mode, with the long direction of the SAR antenna perpendicular to the velocity: this mode is used for altimetry observations. The SAR antenna is perpendicular to the velocity and the SAR boresight is nadir-pointed. The +x face is off-pointed by -14 degrees around y.
- (c) *communications* pointing mode, with the fixed High Gain Antenna Earth-pointed (COMMS mode).
 - a. In the comms mode the body-mounted HGA, accommodated on +Z panel, needs to be pointed to Earth for several hours. Since comms are required every day, the spacecraft attitude with respect to the Sun and Venus can take any value.
 - b. For radio-occultation (at ingress and egress of the atmosphere during seasons of Earth occultation), the spacecraft needs to follow an attitude profile to compensate for the changing bending angle of the RF signal in Venus atmosphere. This involves S/C angular rates of up to 0.07 deg/s, provided by the reaction wheels.

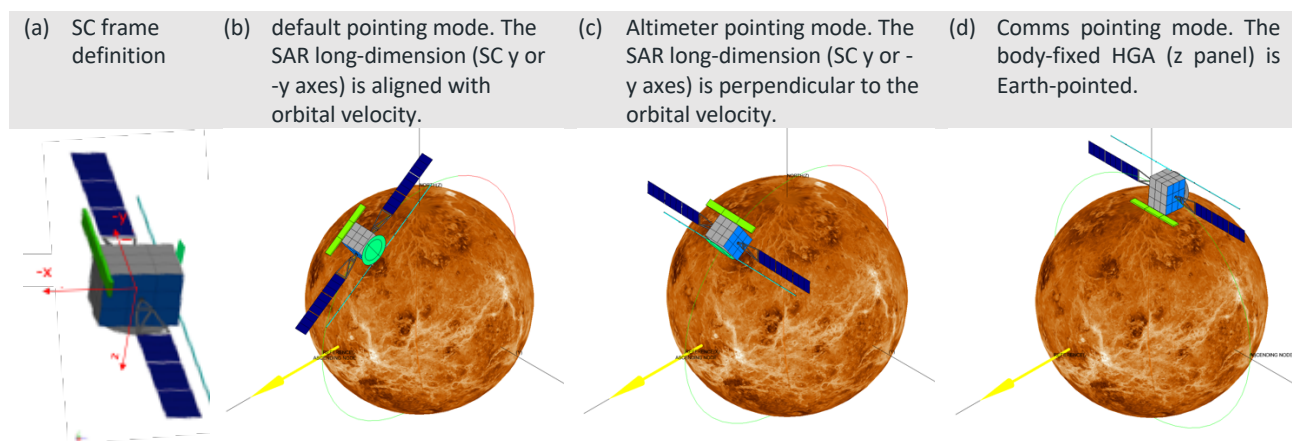


Figure 5.7.1 – This figure shows the three spacecraft pointing modes required for scientific observations. The combination of the spacecraft attitude, the Solar aspect angle and the Earth aspect angle need to be considered for the sizing of the spacecraft critical subsystems: power and thermal.

The transition between any of these modes is achieved via the reaction wheels assembly, with typical slew times of maximum 10 minutes. Outside of the science pointing modes, the main modes required to execute the operational mission and handle any contingency situation are the Cruise Mode, the Thruster Control Mode, the Aerobraking Mode, and the Safe/Survival Mode.

The Safe Mode strategy relies on star tracker, Coarse Sun Sensor and gyroscopes to automatically point the solar arrays to the Sun and the HGA to the Earth to minimise the recovery time. In the unlikely case where the star tracker would not be available), a second level of Safe Mode is activated, relying on the omnidirectional coverage of the two X-band low gain antennas (LGA). The X-band TT&C chain is sized to allow commanding from ESTRACK ground station at any attitude and any distance from the Earth, and to provide a minimum downlink signal in the form of semaphore tones. In such situations, NASA's DSN stations may be used to minimise the time of SC unavailability for science operations.

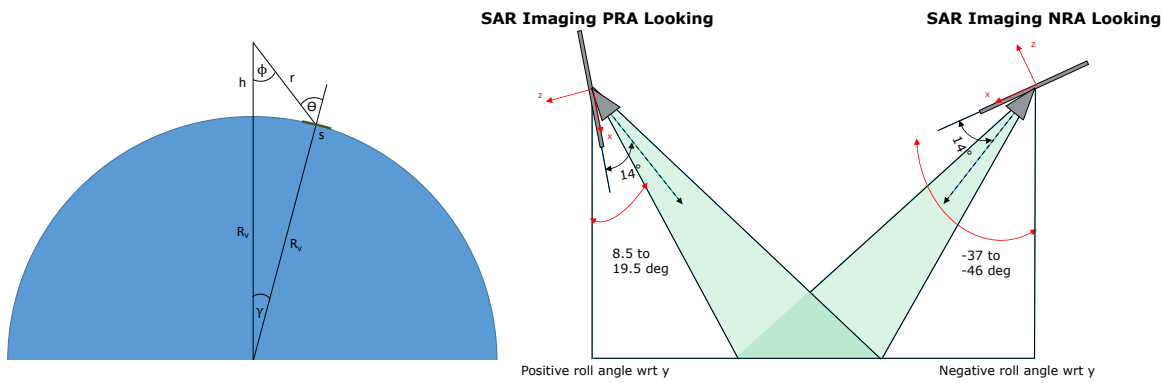


Figure 5.7.2 – (Left) The look angle ϕ for a SAR observation is the angle between the nadir direction and the direction to which the maximum gain of the antenna is beamed. The incidence angle ϑ is defined as the angle between the local vertical at the target location and the direction of the incidence SAR radiation. (Right) A positive or negative look angle can be provided by the spacecraft corresponding to respectively positive roll angle (PRA) or negative roll angle (NRA). Positive Roll observations are in general preferred as they require smaller amplitude manoeuvres and are more favourable from a thermal point of view.

| Spacecraft pointing | Orientation wrt. orbital plane | Targeted observations | Global observations |
|------------------------|--|---|---|
| Nadir | Parallel to velocity | SRS High Density | SRS Low Density VenSpec-M VenSpec-U VenSpec-H |
| | Perpendicular to velocity | | SAR Altimetry |
| | Parallel and perpendicular to velocity | | SAR Nadir and Near-nadir Radiometry |
| 29 degrees incidence | Parallel to velocity | SAR off-nadir radiometry | |
| Up 40 degree incidence | Parallel to velocity | <ul style="list-style-type: none"> SAR Standard (30 m) SAR Stereo (30 m) SAR Polarimetry SAR High-res. (10 m) | |
| Earth-pointing | Any attitude | Gravity Science (High resolution) | <ul style="list-style-type: none"> Gravity Science (Low resolution) Radio occultation |

5.7.2 Spacecraft subsystems overview

Two design solutions have been studied in the EnVision phase A, both meeting the applicable mission requirements and compliant with the payload reference operations scenario.

Configuration, structure and payload accommodation

The mechanical design consists of a central tube configuration. The Primary Structure is the main stiffness contributor, and is composed of the launcher interface ring (1194 mm diameter), the central tube itself and shear webs. The Secondary Structure mounts the platform and instrument units and adds local stiffness. The total height of the S/C is about 3 m from launcher ring interface to the bottom of the nadir panel (+x panel), for widths and depths of about 2 m for both designs in stowed configuration.

The +x panel is dedicated to nadir-looking instruments (spectrometers and SRS). The -x panel includes the ring interface to the launcher, as well as the Main Engine used in particular for Venus Orbit Insertion manoeuvre. The y and -y panels include the attachment of the two Solar Arrays wings and are mostly covered in Optical Surface Reflectors (OSR) radiators for platform and payload units. The +z panel is where the fixed X/Ka High Gain antenna is located. The -z panel is the so-called cold face where the radiators of thermally-sensitive instrument parts are located, in particular VenSpec-H, U and M.

The SC aerobraking configuration, with the -x face of the spacecraft facing the aerothermal flux, is fully compatible with the aerobraking phase: the most sensitive elements (e.g. spectrometers) are naturally protected from the flux, being located on the opposite panel of the spacecraft, while the least sensitive elements are directly exposed to the flux (e.g. Main Engine nozzle and ring adapter). The solar arrays longitudinal axis crosses the spacecraft only 50 cm below the nadir-panel to ensure the centre of pressure remains behind the centre of mass during aerobraking, guaranteeing a naturally stable aerodynamic configuration. The solar arrays, SAR back-side, the -x face of the spacecraft and the lateral side of the HGA are the main contributors to the drag surface, which totalise about 30 m², for a ballistic coefficient close to 25 kg/m² at the start of aerobraking.

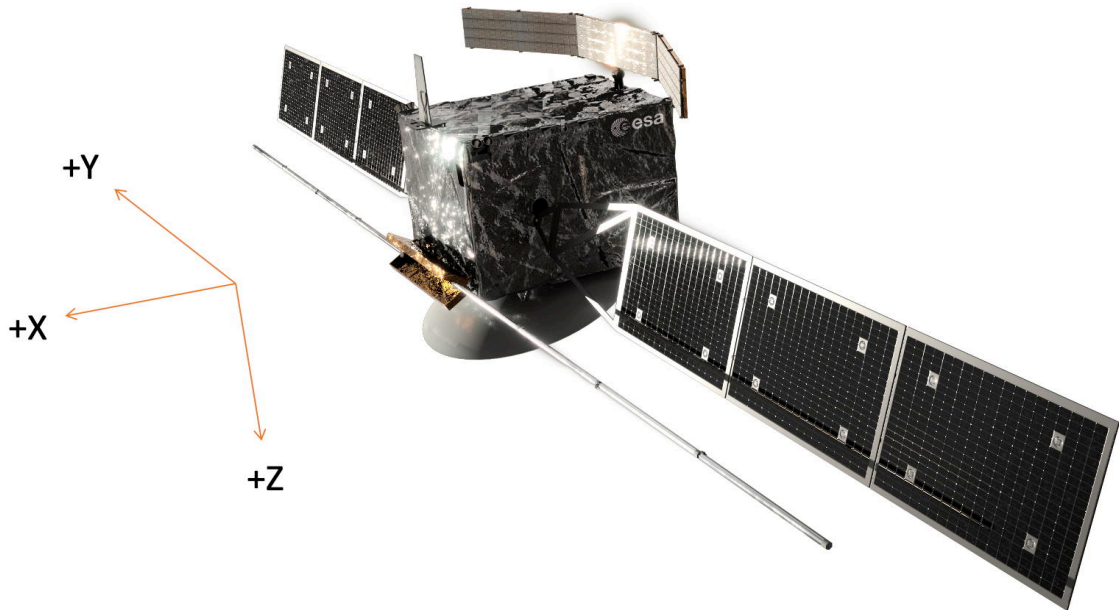


Figure 5.7.3 – Overview of the EnVision spacecraft design configuration, as studied in phase A. The -z panel of the spacecraft is the so-called cold face of the spacecraft. Specific radiator cavities (notches) are implemented on that face to avoid exposing the most sensitive radiators to the planetary fluxes (mostly albedo) and to minimise direct sun flux during communications around inferior conjunctions. Artwork: VR2Planets, Nantes, France.

Guidance, Navigation and Control and propulsion

The Guidance, Navigation and Control system relies on a classical design, with Star Tracker as the main attitude sensors, and IMU which provide 3-axis angular rates and non-gravitational accelerations measurements. Two internally redundant coarse sun sensors are used to acquire and maintain sun pointing in safe mode. The AOCS subsystem is completed by a swarm of four reaction wheels which allow to slew the S/C in any required attitude in less than 10 minutes, even in the case of one wheel failure. Wheels are offloaded once per day. The S/C pointing requirements are summarised in Table 5.7.2.

Table 5.7.2 – Summary of main pointing requirements. All values are given in mrad at 2 sigma

| | Absolute Pointing Error (APE) | Relative Pointing Error (RPE) | | | | | | | Attitude Knowledge Error (AKE) |
|---|-------------------------------|-------------------------------|----------|---------|-----------|----------|----------|----------------|--------------------------------|
| | | 90 ms | 1 s | 5 s | 10 s | 15 s | 60 s | 1000 s | |
| x | 0.7 (SAR) | 0.5 (V-M) | 5 (V-H) | 1 (V-U) | 1.4 (SAR) | 5 (V-H) | 5 (V-H) | 2.5 (V-U, cal) | 5 (V-H) |
| y | 1.5 (SAR) | 0.5 (V-M) | 10 (V-H) | 1 (V-U) | - | 10 (V-H) | 10 (V-H) | 2.5 (V-U, cal) | 0.5 (V-H) |
| z | 0.7 (SAR) | 0.5 (V-M) | 5 (V-H) | 1 (V-U) | 1.4 (SAR) | 20 (V-H) | 20 (V-H) | 0.5 (V-U, cal) | 0.5 (V-H) |

The propulsion subsystem relies on a bi-propellant MON/MMH system, with Helium as pressurant. It is composed of the LEROS-4 1 kN Large Apogee Engine currently in development, and two redundant sets of eight RCS thrusters of 10 N which are used for wheel offloadings and small delta V manoeuvres e.g. for orbit correction manoeuvres during science or aerobraking phases.. The propellants tanks are accommodated in the central tube of the structure and store more than one ton of propellant for the needs of interplanetary transfer manoeuvres, Venus Orbit Insertion, aerobraking manoeuvres, orbital control manoeuvres, and wheels offloading. The maximum total Delta v required from the system is about 1700 m/s.

Electric power and data handling

The power subsystem relies on a battery-regulated 28V bus. The Li-Ion battery provides about 10000 Wh at end of life, and is sized by the so-called maximum science operations profile in worst case eclipse conditions. The solar arrays are composed of two wings of three panels totaling 15 m² and a yoke per wing. The wings use of one degree of freedom Solar Array Drive Mechanism (SADM) to track the Sun for a significant portion of any orbit. Solar Arrays are sized to enable all planned nominal science operations in the worst orbital conditions (e.g Sun in the orbital plane). The solar arrays are also used as one of the main drag surface during aerobraking operations. The data handling system consists mainly of a Central Data Management Unit (CDMU) including the On Board Processor and a flash memory, a Remote Interface Unit (RIU), and an external large capacity Mass Memory of 8 Tbits End Of Life. The spacecraft uses file-based protocols for all its operations, simplifying the management of science data and overall spacecraft operations. The main data handling interfaces towards EnVision instruments are through WizardLink and a SpaceWire (SpW).

Communications

The communication subsystems relies on X-band uplink for simultaneous telecommand and ranging reception, on X-band downlink for simultaneous S/C telemetry and ranging transmission, and Ka-band (32 GHz) downlink for high data rate transmission of science data or alternatively for ranging. The communications subsystem relies on a fixed high gain antenna (diameter >2.5m), which is attached on the +Z panel of the Spacecraft. The HGA is the primary antenna used for S/C communication in X and Ka-band, and is completed by several Low Gain Antennas (LGA) used for X-band communications only, during LEOP and safe modes. To maximise the data return, the Ka-band communications subsystem relies on a powerful Travel Waveguide Tube Amplifier (TWTA) with an RF power output of 120W. This architecture, together with daily communication passes with 35m Deep Space Antennas of 9.3 hours in average, allow to downlink the required science data return whatever the Earth to Venus distance.

Thermal design

In the hot environment of Venus, and with the variety of possible spacecraft attitudes, the placement of the radiators on the spacecraft is constrained. Only three faces of the spacecraft are available and can be kept cold enough for the needs of the platform and of the instruments: the two faces where solar panels are attached (y and -y), and the -z face. Radiators placement for platform / payload are therefore distributed over those panels. The -z face can be maintained cold all year long during science observations, thanks to a 180 degree flip-around of the spacecraft twice per Venus year (every 112 days), allowing to obtain a cold and stable thermal environment, as required for the operations of the three spectrometers VenSpec-M, H and U.

The large dissipation power for the science payload and the communication subsystems lead to a high radiator area which means also high thermal losses in cold cases, therefore requiring significant heating power.

The altimeter pointing mode may lead +y or -y to be fully exposed to the sun. This drives the choice to perform altimetry observations only when the spacecraft is in eclipse for science operations planning.

With the help of the spacecraft configuration and its concept of operation, the thermal design is kept simple and based on reliable technology, relying mostly on passive control with radiators, Optical Surface Reflectors and Multiple-Layer Insulation, and active control through heaters only. Heat pipes are used to spread high thermal dissipation evenly on radiators when necessary. Despite the harsh Venus thermal environment, only flight-proven materials are used.

Payload accommodation

The three spectrometers VenSpec-U, H and M are accommodated on the +x panel. VenSpec-H and M are accommodated as close as possible to the -z/+x edge, to minimise distance to the cold face (-z) where their respective radiators are accommodated. VenSpec-U is accommodated as close as possible to the -y/+x edge to minimise the distance to its radiator. This allows to avoid any obstruction of the three spectrometers field of views.

VenSAR is composed of two main elements: the reflectarray antenna, accommodated on the -x/-z edge and deployed after launch, and the feedarray which is located on the +x/-z edge, 2.75 m away from the reflectarray centre to reach the required performance. Both elements are rigidly attached to the S/C bus (e.g. no dedicated boom) to minimise thermo-elastic deformations between both elements.

The SRS antenna is under the industrial prime responsibility and is composed of two identical 8 m dipole antennas that are held inside a Hold-Down and Release Mechanism (HDRM), and parallel to each other once deployed, providing 16 m tip-to-tip. The SRS antenna is accommodated on the +x panel, parallel to the -z/+x edge, allowing for a safe deployment of the two dipole antennas with sufficient mechanical clearance to the other platform and payload elements. The technology is built on ESA's heritage gained in particular on JUICE. The SRS antenna is deployed after launch, when the spacecraft is on its escape trajectory to Venus.

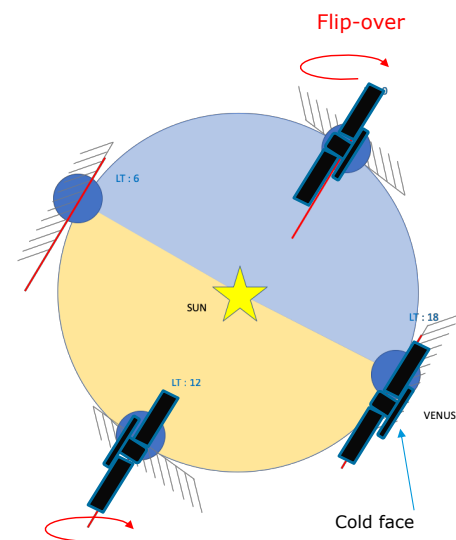


Figure 5.7.4 – Top view of the orbital geometry wrt sun during 1 Venus year of 224 days. A 180 degree fliparound of the S/C around its x axis is performed twice a year, when the Sun crosses the orbital plane. This allows to maintain the -z face always in the shadow whenever the instruments are operated in the default pointing mode. This means the S/C will be naturally right looking for half of the year, and left-looking the other half.

5.8 System Budgets

Margin philosophy

The mission design is in phase A (feasibility phase). To cope with unknowns in the future evolution of the project, the current design phase involves significant margins on key resources at various levels. The standard ESA margins apply on the dry mass of the spacecraft at payload and platform levels. The margins on dry mass include maturity margins (DMM) and system margins (SMM). A 30% system margin is also included on the power budget at payload and platform levels, and a 30% system margin is applied on the instruments data rate. Additional margins are applied to the delta V manoeuvres depending on their nature e.g. 5% for deterministic manoeuvres. A 10% additional margin is required to cope with uncertainties on the launcher design and performance.

Mass budget

Table 5.8.1 – Indicative mass budget for the spacecraft design, including all margins.

| | |
|---|---------------------|
| Total dry mass [kg] | 1350 |
| Communications [kg] | 40 |
| Power [kg] | 207 |
| Data Handling [kg] | 30 |
| Propulsion [kg] | 150 |
| Mechanisms [kg] | 43 |
| Structure [kg] | 230 |
| AOCS [kg] | 35 |
| Thermal [kg] | 85 |
| Payload [kg] | 241 |
| Harness [kg] | 65 |
| System Margin [kg] | 224 |
| Propellant including 2% Residuals [kg] | 1100 |
| Launch Adapter [kg] | 50 |
| TOTAL Wet Mass including launch adapter [kg] | 2500 |
| Ariane 62 performance [kg] | 2782 |
| Excess Launch margin [kg] | 282 kg (11%) |

Power budget

Table 5.8.2 - Indicative power budget for the main mission modes

| | Major Power Modes | | | | | |
|---|-------------------|-------------|-------------------------|---------------------------------|-------------------------------|---------------------------|
| | Cruise | Aerobraking | Mode (1) Science SAR | Mode (2) Science Venspec-SRS | Mode (3) Science Altimetry | Mode (4) Communication |
| Total Payload Power Without Maturity Margin | 0 | 0 | 1213 | 244 | 214 | 129 |
| Total Payload Power Incl. Maturity Margin | 0 | 0 | 1573 | 300 | 275 | 164 |
| Communications | | | | | | |
| Without Margin [W] | 53 | 53 | 53 | 53 | 53 | 550 |
| With Margin [W] | 58 | 58 | 58 | 58 | 58 | 605 |
| AOCS | | | | | | |
| Without Margin [W] | 85 | 288 | 85 | 85 | 85 | 85 |
| With Margin [W] | 89 | 302 | 89 | 89 | 89 | 89 |
| Chemical Propulsion | | | | | | |
| Without Margin [W] | 8 | 8 | 8 | 8 | 8 | 8 |
| With Margin [W] | 8 | 8 | 8 | 8 | 8 | 8 |
| Data Handling | | | | | | |
| Without Margin [W] | 70 | 70 | 70 | 70 | 70 | 70 |
| With Margin [W] | 84 | 84 | 84 | 84 | 84 | 84 |
| Mechanisms | | | | | | |
| Without Margin [W] | 6 | 6 | 6 | 6 | 6 | 6 |
| With Margin [W] | 6 | 6 | 6 | 6 | 6 | 6 |
| Power | | | | | | |
| Without Margin [W] | 89 | 67 | 75 | 75 | 75 | 61 |
| With Margin [W] | 107 | 80 | 90 | 90 | 90 | 73 |
| Thermal Control | | | | | | |
| Without Margin [W] | 1200 | 300 | 243 | 243 | 243 | 500 |
| With Margin [W] | 1440 | 360 | 292 | 292 | 292 | 600 |
| Total Power Without Maturity Margin [W] | 1511 | 792 | 1757 | 804 | 758 | 1412 |
| Total Power Incl. Maturity Margins [W] | 1793 | 899 | 2201 | 928 | 902 | 1629 |
| System Margin [W] | 538 | 270 | 660 | 278 | 271 | 489 |
| Total Power Incl. System Margin [W] | 2330 | 1169 | 2861 | 1207 | 1173 | 2118 |
| Total margins | 819,8 | 377,6 | 1104,3 | 402,4 | 415,0 | 705,7 |

The margins in the power budget represent more than 50% of the “raw” power budget (when assuming the system margins with design maturity margins at platform and payload levels).

5.9 Conclusions

The selected mission profile allows to robustly fulfil the science requirements of the mission with significant margins. The preliminary spacecraft design solutions studied in phase A demonstrated two feasible solutions, technically and programmatically, meeting the mission requirements and presenting good margins with respect to the launch performance requirements. In both design solutions, a suitable configuration has been found for all instruments, which satisfies the science requirements. The spacecraft designs are both compatible with the described science operations strategy, guaranteeing that the pre-selected regions of science interest can actually be observed as required. Mission-level risks are limited, understood and mitigation strategies have been put in place already in phase A.

6 Mission operations and ground segment

ESA will be responsible for the launch and operations/checkout of the spacecraft and the payload. An EnVision ground segment (GS) will be set up to provide the means and resources with which to manage and control the mission via telecommands, to receive and process the telemetry from the satellite, and to produce, disseminate and archive the generated products.

6.1 Overview

Responsibility for, and provision of the EnVision GS is split between ESA and the Instrument teams. ESA will be responsible for the Operations Ground Segment, consisting of the tracking station network (ESTRACK) and Mission Operations Centre (MOC), and part of the Science Ground Segment Science Operations Centre (SOC). The Instrument teams are in charge for the rest of SGS. A schematic drawing of the top level operational interfaces of the EnVision mission is shown in [Figure 6.1](#).

6.2 Operations Ground Segment (OGS)

6.2.1 Ground Stations

All communications and tracking with EnVision will be done at X-Band for uplink and spacecraft housekeeping telemetry downlink, and Ka-band for science data downlink. The three ESTRACK 35 m ground stations (Malargüe, New Norcia, and Cebreros) are baselined to support the operational needs of the EnVision mission using existing capability in the ground segment. No ground station upgrades are currently needed to support the EnVision mission. The upgraded cryogenic capability has been assumed to be available in all ground stations supporting EnVision in both X and Ka band feeds. This cryogenic capability improves the antenna gain assumed to be available at the different ground stations and has been used in the spacecraft communications subsystem link budget calculations. For the Radio Science Experiment at least one of the three 35m is assumed to be equipped with a Water Vapour Radiometer facility or GPS techniques to correct for tropospheric effects.

The smaller ESTRACK stations, i.e. Kourou (15m) and NewNorica2 (NNO-2), are considered in addition to the 35 m antennas for support during the LEOP and initial transfer orbit phases. NNO-2 is envisaged to be used for first acquisition (assuming launcher Direct Ascent). Alternatively Maspalomas antenna could be used for early mission phase LEOP support.

The science data downlink will be dumped daily from the on-board mass memory to ESTRACK 35 m stations for a daily duration between 4 and 7 hours depending on the occultation duration and science operation profile being implemented (see §5.4.2). Ground station passes will nominally be scheduled in two slots every day, split across two of the 35 m ground stations. In the case of a missed ground pass, the spacecraft mass memory is sized to store the science data until the next opportunity. Solar conjunctions will interrupt the ground station contact periods with EnVision. The operations will be suspended when Sun-Earth-Venus angle is within ± 5 degrees during superior solar conjunctions (Venus passes behind the Sun) and ± 1 degree during inferior solar conjunctions (Venus passes in front of the Sun).

Access to the NASA DSN ground stations as support antennas during emergency phases is achieved by ensuring compatibility of EnVision with both ESTRACK and DSN networks. In case of unforeseen unavailability of the ESTRACK 35 m antennas during the science phase, or to support a critical phase or emergency recovery of the mission, NASA's 34 m DSN or 70 m equivalent antennas may be used.

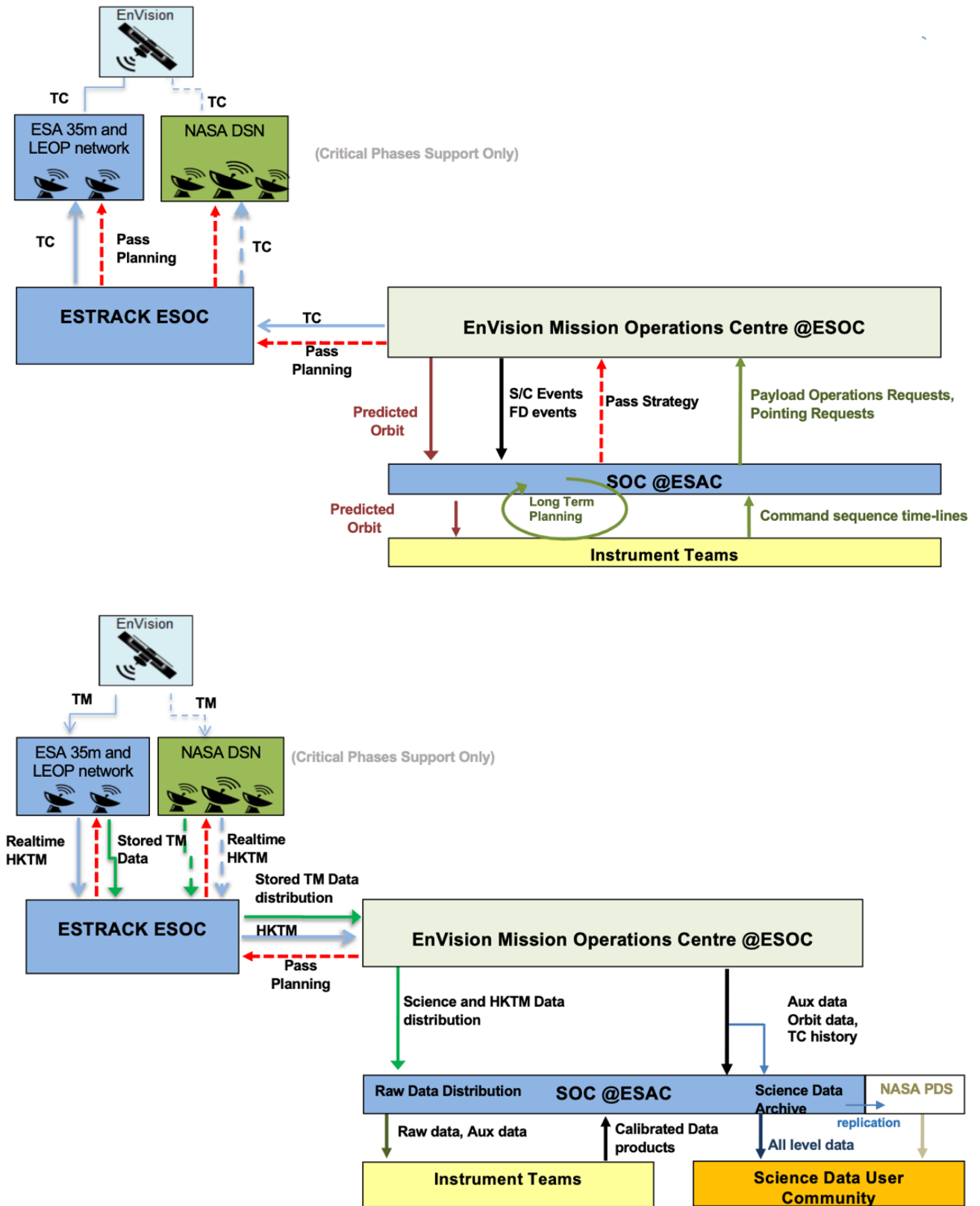


Figure 6.1 – EnVision Ground Segment and operational interfaces for uplink (top) and downlink (bottom).

6.2.2 Mission Operations Centre (MOC)

The EnVision mission will be operated from a single ESA MOC located at ESOC, Darmstadt. The ESOC OGS includes all facilities, hardware, software, documentation, flight control teams and support engineers needed to conduct the mission operations.

The MOC is responsible for the monitoring and control of EnVision ensuring the spacecraft safety and health. The MOC executes mission platform and payload operations preparation, planning (using planning inputs from SOC) and execution. Spacecraft monitoring and performance analysis is routinely performed together with payload health and status monitoring. Flight Dynamics service is provided including determination and control of the satellite's orbit and attitude.

The MOC performs all communications with the satellite through the ground stations for the upload of the platform and payload telecommands and reception of the downloaded telemetry data. MOC is also responsible for downloading the science data and its distribution to the SOC, along with the required raw telemetry, housekeeping and auxiliary data. The spacecraft will be primarily controlled via execution of timed activities from an onboard mission timeline. It is foreseen for the majority of the routine ground station pass activities to be automated. Due to the One Way Light time and subsequent delay in command and visible response, real time commanding activities are minimised. Any on board anomalies will normally also be detected with a slight delay. The mission control system monitoring and alert functions support anomaly detection and the Flight Control Team and on call engineers will respond and intervene to the anomalies as defined in the agreed procedures.

The different mission phases from the launch and LEOP, commissioning, interplanetary and orbit transfer, through to the science phases follow the same basic concept with adaptation of response times, team coverage, planning cycles and ground station coverage dependent on the criticality of the operations being executed. Detailed operational plans are prepared for all mission phases. All plans for critical phases are verified and validated using simulators. The Flight Control Teams are fully trained to execute both critical and routine operations via simulations training program.

The science phase mission planning consists of two cycles (§ 6.3.3) with science inputs provided by the SOC and Instrument teams. The planning interface between SOC and MOC will be designed to avoid iteration loops with respect to resources. Event timelines and reference orbit will be provided by MOC flight dynamics to the SOC allowing independent planning of the science activities.

The mission planning needs to take into account specific mission constraints such as the periods of HGA coverage/outage and periodic radio occultations of EnVision behind Venus. These two constraints define the periods when Space-to-Ground links can be established. These periods are considered together with the allocated ground station availability to establish uplink and downlink communication slots. The mission planning adopts a success oriented approach assuming that the ground station is operational at the requested scheduled time. The start of TC uplink, reception of real time housekeeping telemetry and onboard telemetry dumps slots are shifted to account for Earth-to-Venus light time delay. Tuning of these margins is nominally executed early in flight phase to maximise ground station return/usage.

Orbit control manoeuvres for pericentre control are planned to be executed at most once per Venus cycle (243 days). Reaction wheel momentum management is planned from ground and scheduled to execute avoiding wheel offloading during science windows. Spacecraft slew manoeuvres to the observable targets are performed based on the SOC science plan targets and executed from the uploaded mission timeline. Orbit event updates are envisaged to be needed up to three times per week based on updated tracking information. This requires a shift of the onboard mission timeline for payload operations avoiding changes to platform activities. This functionality can be met using standard mission timeline control services and slew timing margins. The nominal science phase operations assume a weekly commanding pattern, a cycle which is typically followed for ESA planetary missions.

6.3 Science Ground Segment

6.3.1 Overview

EnVision Science Ground Segment (SGS) will be similar to that of the current Solar System missions performed by ESA, comprising the Science Operations Centre (SOC) in ESAC (Madrid), instrument teams

and operational interfaces. The SGS concept will be based on maximum sharing and reuse of manpower, expertise, facilities and tools from the other ESA missions. The SOC benefits from common and/or re-usable tools and cross-mission support in the Science and Operations Department of ESA's Science Directorate. The Department also provides the data archives for all ESA scientific missions, and a dedicated team ensures the same level of quality and tailoring to the mission needs for the archives together with added value tools for the science community.

The SOC supports the development and operational phase by providing manpower, expertise, tools and systems in order to support the instrument teams in observations planning, coordinate and implement science operations, ensure the implementation of the data handling and archiving. As part of the SGS, the SOC and instrument teams will work together under guidance of the Project Scientist on planning of science operations and coordination of the scientific input.

6.3.2 Science Operations Centre Responsibilities

The SOC is responsible for:

- development and maintenance of the SGS system;
- supporting the Science Working Team (SWT) in development of the Science Activity Plan (SAP);
- simulation and validation of the Mission Operations Plan (MOP);
- coordination, preparation and validation of science operations and submission of planning inputs to the MOC;
- interfacing with MOC for reception of science and auxiliary data;
- operation and maintenance of the raw data processing and archiving pipeline.

The SOC is the single interface to the MOC during the science operations phase for commanding.

The SWT and the instrument teams are responsible for the SAP development, providing inputs for science and calibration operations, and developing and running data processing pipelines. The analysis of instruments health and performance and the delivery of science data products is under the responsibility of the instrument teams.

6.3.3 Science Operations Planning

The science objectives of the mission lead to requirements on coverage, swath overlap, frequency and repetition of observations. The mission, spacecraft and instrument design impose constraints on when and how often observations can take place. All science operations will be conducted using an offline planning process coordinated by the SOC. The planning process is split into several phases.

Mission level planning (MLP) aims at developing a plan covering the whole mission and which demonstrates the achievability of the science requirements. This is documented in the SAP. The plan incorporates scientific inputs from the SWT and considers data volumes, power and operational constraints. The mission level plan is updated when needed, e.g. following an update to a boundary condition which invalidates the plan. The resulting plan is used as an input into the long-term planning.

Long term planning (LTP) covers 6 months of operations and ensures that operations are compatible with the predicted resources (e.g., data and power), the spacecraft and the ground station schedule. A reference trajectory is provided by ESOC Flight Dynamics for this period. The SOC consolidates and validates the payload activities using inputs from the Instrument teams and mission constraints. The spacecraft pointings are frozen at this stage. Requests for calibration activities should also be submitted during this step. Inputs regarding preferred times for communication passes and wheel-off loadings are to be provided to the MOC before the start of the long-term planning, in order to avoid conflicts with the preferred times for science observations. The science strategy is frozen at the end of this planning phase. The LTP plan will remain unchanged until the Short Term Planning (STP) cycle when LTP plan will be refined using the latest orbit information if appropriate. This simplification is possible due to selection of surface Regions of Interest well in advance and the need to cover them with a certain observation pattern and coverage that requires end-to-end planning of the entire nominal mission.

Short Term Planning (STP) is performed on a weekly basis and includes Flight Dynamics update of the orbit using latest tracking data, corrections for deviations from reference trajectory, refines the timeline of payload operations. At this stage, changes to timing of observations may still be accommodated, as long as they continue to meet spacecraft resource and thermal constraints; for example, this may be used

to change the latitude of targeted high-resolution VenSAR imaging. The Instrument teams' requests for payload science operations at command sequence level will be collected by the SOC, validated and checked before being merged into payload operation requests to be submitted to the MOC. The MOC will be in charge of including the requests in the overall mission operations timeline which will be uplinked periodically to the spacecraft. No real time science operations are envisaged.

6.3.4 Data Handling and Archiving

The following science data types are defined:

- *Telemetry packets* that are decommutated, decompressed and provided in a well-documented format;
- *Uncalibrated/raw data* expressed in engineering units (counts) that may contain extra engineering metadata from other sources;
- *Calibrated data* ready for scientific analysis;
- *High-level data* products possibly derived from analysis of several instruments/observations.

Calibration data are used typically to derive calibrated products from the raw data.

Ancillary data are any data products derived from spacecraft or payload housekeeping telemetry that are useful for scientific analysis, i.e. instrument status for all payload, SPICE kernels for orbit and spacecraft attitude, time conversion files, etc.

The MOC receives science and housekeeping telemetry from the spacecraft and distributes it to the SOC. The SOC will develop, maintain and run the data processing pipeline from telemetry to raw data and make this data available to the instrument teams in an agreed standard. The Planetary Data System (PDS4) format will be used for EnVision data.

Generation of the calibrated data is to be performed by the instrument teams. Raw and calibrated data will be made publicly available as soon as they are properly processed, validated and calibrated. Actual time for this phase may vary from instrument to instrument and it is expected to be no longer than six months. High-level data products will require advanced science analyses and longer periods to be produced. These higher level data products will, where possible, be made also publicly available. The strategy for the archiving of the EnVision science data will be outlined in the archive plan. An archive scientist will support the project scientist and participate in data archiving working groups. The archive will provide easy access to EnVision science data and tools.

The SOC will ensure the long-term archiving and storage of the calibrated and un-calibrated data products. This activity would include verification and ingesting of the data products into the dedicated ESA PSA, sharing of data as needed with the Planetary Data System Archive (NASA) and assisting the science community in using the data. Table 6.1 shows a list of notional data products EnVision plans to provide to the science community.

Table 6.1 – List of science data products provided by EnVision Mission.

| Product | Description |
|---------------------------|---|
| Downlinked Raw Radar Data | This is the raw radar data that would be downlinked from the spacecraft for all modes (SAR, Altimeter and Radiometer) |
| SAR 30 m Imagery | Strip and mosaicked calibrated backscatter imagery, range/Doppler and incidence angles for each pixel for both HH and HV data, includes SLCs and ground projected data |
| SAR 10 m Imagery | Strip and mosaicked calibrated backscatter imagery, range/Doppler and incidence angles for each pixel for both HH and HV data, includes SLCs and ground projected data |
| SAR Stereo | Match data, strip stereo elevation data, gridded DEM mosaics, height precision layers & point cloud data |
| Altimeter Data | Planned products include echo profiles for each pulse, Doppler sharpened echo profile data, and elevation products based on leading edge detection and centroid algorithms. |
| Radiometer Data | Surface brightness temperature and derived estimated microwave emissivity from nadir, near-nadir and off-nadir geometries |
| VenSpec-M | Pole-to-pole radiance maps in six spectral bands; 6 wavelength surface emissivity maps; cloud optical depth and water vapour maps |
| VenSpec-H | Spectra spectrally calibrated, expressed in radiance factors and in radiance units; maps of tropospheric trace gas abundances; maps of mesospheric trace gas abundances |
| VenSpec-U | Spectra in radiance units; Spectral radiance factors; cloud top altitude; mesospheric trace gas column densities; UV absorber relative abundance |
| SRS | Line profile backscatter data; geolocated cross sections |
| Radio Science | Calibrated Doppler residuals; precise orbit reconstruction; gravity map; profiles of T, p, H ₂ SO ₄ vapour and liquid |

7 Management

7.1 Project Management

EnVision project management will follow the current practices of ESA science missions. Should EnVision be selected as the M5 mission, ESA will invite the two parallel industrial contractors to perform the Definition Phase (B1), for a typical duration of 24 months. This phase will build upon the results of the Assessment Phase (O/A) at platform, ground segment and payload levels. Phase B1 will be concluded by the Mission Adoption Review (MAR), after which EnVision will go through the process of mission adoption and SPC approval. By the time of the MAR, all science requirements should be frozen, the subsystem level requirements documents (for both the Payload and the Platform) should be available and the overall technical and programmatic feasibility of the mission should be confirmed with a design supported by detailed analyses. In parallel, all Technology Development Activities (TDAs) required will have been issued and completed, so that all platform and payload units reach a TRL \geq 5-6 before mission adoption.

Until MAR (included), the EnVision project will remain under the responsibility of the Study Manager within ESA's Future Mission Department of the Science Directorate (SCI-F). The Study Manager will continue to be supported by the Study Scientist for science-related aspects of the mission. Following mission adoption, EnVision will move into the Implementation Phase (B2/C/D/E1). A Prime industrial contractor will be selected following an Invitation to Tender phase. The final industrial organisation will be completed in Phase B2, mostly through a process of competitive selection and by taking into account geographical distribution requirements in place at the time. At the start of this phase, a project team will be established in the Project Department of the Science Directorate (SCI-P). This team will be led by the Project Manager (PM), who will have overall responsibility to ESA for implementing the EnVision mission. The PM will be supported by the Project Scientist who will have responsibility for science-related aspects of the mission.

Over the course of the implementation phase, the project team will conduct a Preliminary Design Review (PDR), a Critical Design Review (CDR) and finally a Flight Acceptance Review (FAR).

Responsibility for the EnVision mission will transfer from the PM to the Mission Manager, located at ESAC, following the successful commissioning of the satellite and scientific payload. The task of the PS will continue throughout the operations and post-operations phases.

7.2 Operations Management

ESA will be responsible for the launch, checkout and operation of the EnVision spacecraft. ESA will establish a mission operations centre (MOC), to be located at ESOC, and a science operations centre (SOC) that will be located at ESAC.

Definition of the MOC will commence at the beginning of the definition phase, under the responsibility of a Ground Segment Manager located at ESOC who will report to the Project Manager. The responsibility for the MOC will transfer from the Ground Segment Manager to the EnVision Spacecraft Operations Manager (SOM, located at ESOC), following the successful commissioning of the satellite and scientific payload.

Definition of the SOC will commence at the same point in time, and will be under the responsibility of a SOC Development Manager in the Operations Development Division at ESAC. The SOC Development Manager will work closely with the PS, but will formally report to the Project Manager.

Management of the Science Ground Segment will be transferred from the Operations Development Division to the Operations Division following successful commissioning of the satellite and scientific payload. As described in Chapter 6 the mission operations will be under the overall control of the EnVision SOC at ESAC in close collaboration with the IOSDC provided by the instruments.

7.3 Share of responsibilities

EnVision is an ESA mission in collaboration with NASA, and contributions from individual ESA Member States for the provision of payload elements.

- ESA will have the overall EnVision mission responsibility including spacecraft manufacturing, launch and operations, as well as the data archiving and distribution;

- NASA will provide the VenSAR instrument and its associated ground data processing, as well as DSN support;
- ESA’s Member States participating in EnVision will be responsible for the nationally-funded payload elements as illustrated in Table 7.1.

A provisional product tree highlighting the share of responsibilities between these three entities is given in Figure 7.1.

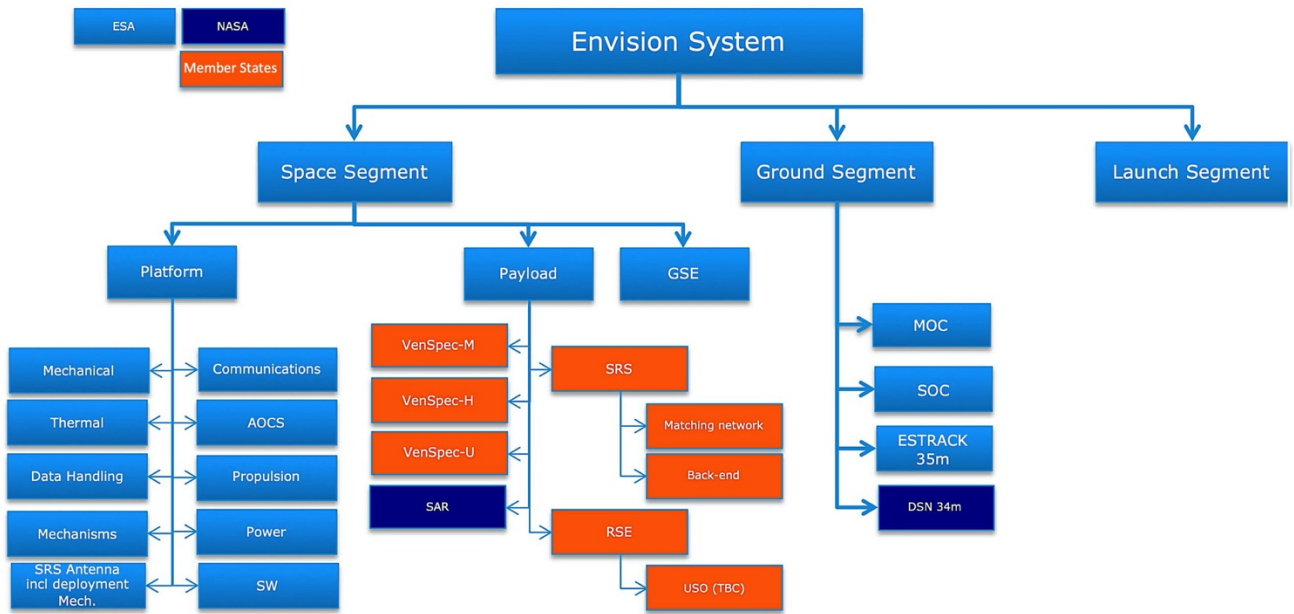


Figure 7.1 – EnVision high level product tree.

Table 7.1 – Instruments responsibilities

| Instrument | Investigation | Instrument Lead | Instrument responsibility |
|---------------|--|--|---------------------------|
| VenSAR | SAR Standard Imaging 30 m @ 3.15 GHz, 30 m SAR Stereo Imaging, 10 m SAR High Resolution Imaging, SAR Nadir Altimetry, Dual-Polarimetry 30 m SAR, Radiometric brightness, Off-nadir Microwave Radiometry both H and V polarizations. Repeated 30 m/pix SAR Standard Imaging. | Scott Hensley Jet Propulsion Laboratory, Pasadena, USA | |
| SRS | Subsurface radar Sounder. Central frequency 9 MHz with 5 MHz bandwidth. Subsurface penetration of up to 1000 m, vertical resolution of 20 m. Low density, High Density, SRS Nadir Altimetry. | Lorenzo Bruzzone Università di Trento, Italy | |
| VenSpec-M | Near-IR spectral / thermal emission from Venus’ surface using six narrow bands ranging from 0.86 to 1.18 μm, and three bands to study cloud microphysics and dynamics. | Jörn Helbert DLR Institute of Planetary Research, Berlin, Germany | |
| VenSpec-H | High-Res. composition and distribution of minor species in the lower atmosphere on the night side and above the cloud on the day side. Four spectral bands: 1.165 - 1.180 μm (B#1), 2.34 - 2.48 μm (B#2), 1.72 - 1.75 μm (B#3) and 1.37 - 1.39 μm (B#4). | Ann Carine Vandaele Royal Belgian Institute for Space Aeronomy (BIRA- IASB), Brussels, Belgium | |
| VenSpec-U | Distribution and spatial and temporal variations of sulfur bearing gases (SO, SO ₂) and unknown particulate absorber at the cloud tops. Dual channel UV spectral imager HR channel 205-235 nm at 0.2 nm spectral resolution; LR channel 190-380 nm at 2 nm spectral resolution. | Emmanuel Marcq LATMOS, IPSL, Université Versailles Saint-Quentin, Guyancourt, France | |
| Radio Science | Tracking using a 2-way coherent carrier Doppler link, X (up) / X-Ka (down); gravity field with a spatial resolution better than 200 km, k ₂ Love number accuracy < 1%; USO + 1-way X-Ka coherent downlinks during radio-occultations; H ₂ SO ₄ vapor (at 1 ppm) and liquid (at 1 mg/m ³) content, T and P profiles of the neutral atmosphere. | Caroline Dumoulin Pascal Rosenblatt LPG, Université de Nantes, France | |

7.4 Development plan

7.4.1 S/C model philosophy

The spacecraft development plan is based a Proto Flight Model (PFM) development approach. A satellite Structural Model (SM) will be developed, aiming at mechanical qualification of the structure and will be refurbished into protoflight model (PFM). A functional Avionics Model is foreseen for the functional validation of EnVision, interfacing with the engineering models of the main electronic units at platform and payload levels. All payload teams will deliver instrument models of adequate detail to fully support the system tests with each model. The satellite level thermal and EMC qualification will both be achieved on the satellite PFM in line with ESA standards for protoflight element level testing. Spares would be manufactured depending on criticality and will range from sub-unit to spare kit level.

EnVision relies on fully flight validated thermal hardware in high temperature environments, and all space segment equipments will be fully thermally qualified prior to their integration on the PFM. The spacecraft will therefore proceed through a PFM thermal campaign composed of thermal balance tests and thermal vacuum, with an acceptable level of risk.

7.4.2 Schedule

The key dates for EnVision schedule are given in table below

Table 7.2 – EnVision project development schedule: key milestones.

| Milestone | Schedule |
|---------------------------------------|-------------|
| Mission Adoption Review (MAR) | Q2 2024 |
| Phase B2/C/D Kickoff (KO) | Q1 2025 |
| Industrial B2/C/D KO (Prime selected) | Q3 2025 |
| Systems Requirements Review (SRR) | Q1 2026 |
| Preliminary Design Review (PDR) | Q4 2026 |
| Critical Design Review (CDR) | Q1 2029 |
| Flight Acceptance review (FAR) | Q3 2031 |
| Launch | 29 May 2032 |

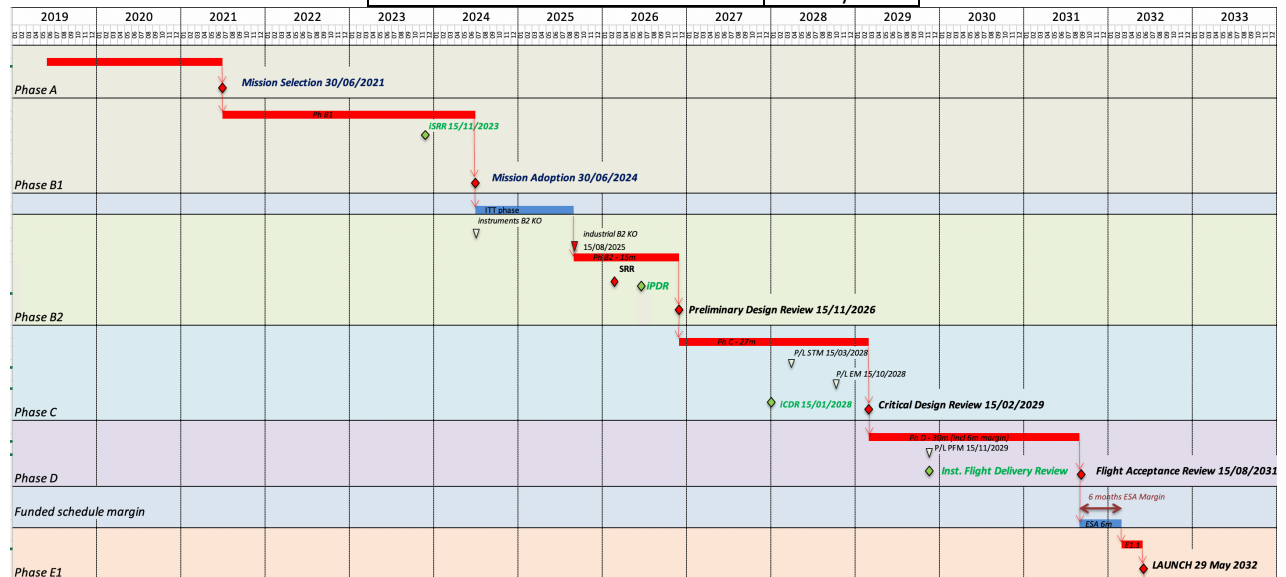


Figure 7.2 – EnVision Master development schedule.

The critical path contains the manufacturing, testing and assembly of the instruments, followed by the Proto-Flight Model (PFM) with Assembly, Integration, Verification and Tests (AIV/T) of the complete spacecraft, and finally the launch campaign. The instruments PFM will be delivered to the spacecraft in a staged approach in Q2/Q3 2029.

7.4.3 Critical elements and risks mitigation

The main risk for EnVision is linked to the uncertainty on the Ariane 62 performance in direct escape, the launcher maiden flight being planned only in 2021. This risk can be fully mitigated by using the aerobraking duration as a buffer (a longer aerobraking allows to decrease the propellant mass) and by using a lighter launch vehicle adapter. A 10% extra mass margin has also been considered on the wet mass of the spacecraft to provide an additional mitigation.

The mission needs to return a high data volume to fulfil its science objectives. To achieve that, the mission relies on a regular, daily use of the ESTRACK 35 m ground stations, and on a stable operations planning (months before the observations). Any short term perturbation to the plan (e.g. non availability of ground station at the planned slot, delayed ground station acquisition, or complete loss of contact due to ground station failure, for example) pose a risk on the science data return. This risk is mitigated at various levels by (1) oversizing the on-board solid state mass memory to cope with a worst case for such contingency occurring at the period of highest data rate (when Earth is the closest to Venus) (2) by considering a 30% system margin on the instruments data rates, which result in a de facto margin on the SSMM sizing (3) by the introduction of regular SSMM offload sessions based on offline arraying of two of the ESA's Deep Space Antennas. This technique allows to double the data rate without modifying the observation plan for specific spots and is explained in more details in chapter 5.5. and (4) by nominally targeting a significantly higher data return than actually required (e.g. the achieved stereo performance is 28.3% for a requirement of 20%).

Aerobraking technique is well mastered by ESA, it has been tested experimentally on ESA's Venus Express in 2014, and successfully implemented on the recent ESA's ExoMars Trace Gas Orbiter mission. The knowhow acquired in those missions will directly benefit to EnVision mission and to the reduction of the operational risk. Early aerobraking risk reduction will also be achieved during phase B1 by specific characterisation and testing of the foreseen surface materials (e.g. MLI) and their thermal performance with the planned aerobraking profile in terms of thermal loads and atmospheric conditions (e.g. atomic oxygen).

The mission cost is capped by the ESA M5 allocated budget. Maintaining the cost of the mission under control is a critical requirement and is achieved in particular by relying on mature technologies at ground and space segment levels with significant heritage from the most recent ESA science missions e.g. BepiColombo, EUCLID and Solar Orbiter. As a consequence, the mission development plan is compatible with reaching TRL 6 by mission adoption in 2024 for all its elements. The only technology pre-development activity identified is in the domain of high data rate deep space communications at ground segment level, and will modify the architecture for the on-ground Turbo decoder to sustain operationally data rates of up to 80 Mbs. This activity is considered low risk, has started mid 2020 and will reach TRL 6 by end of 2021.

The EnVision mission present several levels of intrinsic flexibility (at payload, ground segment and space segment levels) that could be considered in case of cost overrun.

7.5 Science Management

This section outlines the current assumptions about science management of the EnVision mission. A "Science Management Plan" (SMP) will be written in the next stage of the study and will be a subject for approval by the ESA Science Programme Committee (SPC) in view of mission adoption.

A proper representation in the EnVision science teams and for all scientific positions will be granted to US scientists, based on ESA-NASA agreements.

A Science Working Team (SWT) is planned to be appointed by ESA after the mission adoption. Main tasks of the SWT are to provide scientific oversight of the mission, monitor its implementation, advise ESA on aspects affecting its scientific performance, and act as a focus for the interest of the science community. The SWT comprises the Instrument Leads and IDSs, and is chaired by the ESA-appointed Project Scientist (PS). The PS acts as interface between ESA and external participants on science matters.

To enhance participation of the scientific community to the mission, the plan is that after mission adoption ESA will issue competitive calls for the selection of Interdisciplinary Scientists (IDS) and Guest Investigators (GI). IDSs are experts in specific overarching science themes connected to the mission objectives who take advantage of synergistic use of the data delivered by several experiments. GIs are scientists participating in the data collection and analysis of one or more instruments and/or performing laboratory studies, theoretical or numerical investigations essential for the mission success.

EnVision data will be of great interest to the planetary community at large as well as to other communities, such as exoplanetary scientists. The intention is to provide high quality data products in a timely manner and to have continuous and inclusive involvement of the wider science community.

The plan for EnVision is to follow an open data policy, with no proprietary period for data exploitation by the Instrument Lead teams, including spacecraft and navigation data relevant for data analysis. Level 1 and 2 data will be made publicly available as soon as they are properly processed, validated and calibrated. Actual time for this phase may vary from instrument to instrument and it is expected to be no longer than six months from data delivery to the teams. Higher level data products (image mosaics, DEMs, thermal and mineralogical maps, etc.) will require advanced science analyses and longer periods to be produced. These higher-level data products will also be made publicly available.

All the data will be available on the ESA Planetary Science Archive (PSA). The data will be also made available through the NASA's Planetary Data System (PDS), based on ESA-NASA agreements. Details of the data processing and archiving will be elaborated in the EnVision SMP. The Instrument Lead teams will be responsible for calibration and science analysis of the data from their instrument and timely publication of the results in scientific and technical journals and presentations at conferences.

8 Communications and Outreach

EnVision will be an exciting mission and provides an exceptional opportunity to engage and educate the general public as well as inspire students of all ages in the excitement of scientific discovery and planetary exploration. Venus already has great name recognition among the public and is an easy planet to “recognise”, as Earth’s nearest neighbour and the brightest object in the sky after the Sun and Moon. The story of how Earth and Venus diverged in their evolution, and discussions of what may or may not trigger a runaway greenhouse effect, are similarly engaging in an era where our own changing climate is of increasing public interest. At the same time, these science questions offer an opportunity to highlight the wider work which ESA and NASA are doing in Earth and Space Science domains. These themes are further detailed below in §8.1, then the methods and mechanisms of outreach and communication are further elaborated in §8.2.

8.1 EnVision public outreach and education themes

The three top-level science questions of EnVision lend themselves well to public outreach.

History: How does Venus’ surface (and subsurface) record its tumultuous past? Here, the star of the show will be the radar imagery and digital elevation models, similar to those produced from the Magellan but with much better image quality and resolution, which will reveal the wealth of both familiar and utterly unfamiliar geophysical features. Subsurface layering and compositional clues offer more in-depth stories to tell about geological evolution. Comparisons with ESA’s and NASA’s geomorphological investigations at Mars can be made here.

Activity: Is our neighbouring planet geologically alive or dead? Searching for volcanic activity through thermal, gaseous signatures, as well as image change and surface movement, is an easily understandable investigation, yet an opportunity to explain much about geology. This offers excellent opportunities to link in with ESA Sentinel EO spacecraft conducting similar observations at Earth, and JUICE observations of volcanism at Io and crustal deformation at Europa and many other NASA missions.

Climate: Why and when did Venus develop such a hostile climate? What determines the climate of an Earthlike planet? Venus’ massive greenhouse effect and hellish surface temperatures provide a clear example to emphasise that greenhouse warming (and climate change) are real. The habitability of Venus through time will also be used to inform the debate on exoplanet habitability, tying in with both exoplanet missions such as PLATO & ARIEL, as well as EO missions like the Copernicus Programme, the Sentinel satellites and many other NASA & ESA planetary missions: Cassini-Huygens, Venus Express, Mars Express, Mars Reconnaissance Orbiter, Messenger, BepiColombo, Juno, Juice, Dragonfly..

8.2 EnVision communication and public outreach resources

As with other Space Science missions, EnVision communications will be co-ordinated by the ESA communications office, working closely with counterparts at NASA, national agencies and scientific institutions participating in the science dissemination. The details of an outreach programme will be developed by ESA in consultation with the EnVision science team and NASA, but potential elements are described below.

8.2.1 Website

A dedicated mission website at ESA is maintained, coordinated with linked websites at NASA, Instrument payload institutes and national agencies, regularly updated for the public to follow mission progress/discoveries, with animations and interactive activities, and links to the wealth of resources developed across Europe.

8.2.2 Image and video library

A selection of the most striking images and animations produced by the mission, along with explanatory captions for press and writers to use, and a series of film clips explaining aspects of the mission will be made

available. Europe's Venus science community are already experienced in this field, following the commissioning of films for the EuroVenus FP7-funded consortium, including a research documentary, Venus Express legacy films, and a 360° "Journey to Venus" film; these films can be viewed online (https://www.youtube.com/channel/UCFkIS39wzTQN9jQO5z0h_pg/playlists).

8.2.3 Public access to datasets

NASA's VenSAR, which will be the source of much of the most striking high-res surface imagery, will adopt an open data policy, where the data are publicly accessible as soon as they been validated, with no proprietary period of exclusive Instrument team access. Special data products from the EnVision payload (i.e. VenSAR, VenSPEC, SRS, etc) will be made available for public consumption. This will greatly assist in engaging enthusiastic amateurs to use the datasets. The science team will work with organisations such as OpenPlanetary to develop tools to facilitate access to the data by generic Geographic Information Systems (or GIS) tools to increase use of the products by specialists, as well as web-based tools to facilitate access by non-specialists and the general public.

8.2.4 Teacher resources for formal education

The EnVision science team will work with European Space Education Resource Offices (ESEROs) in individual nations, and similar American institutions (i.e. National Science Teacher Associations, etc), in order to create Science, Technology, Engineering and Math, STEM resources tailor-made for the different languages and curriculum needs of each nation. The ESEROs will also maintain contact lists of scientists, and material via websites (i.e. generic EnVision presentations, EnVision Ambassador Program, etc.) to engage educators who will be able to talk about the EnVision mission (or Venus science in general) in schools and at events, engaging educational actions at all levels with appropriate materials from elementary to high school to universities.

8.3 Implementation

ESA will have overall responsibility for co-ordinating the Communications and Public Outreach activities related to the EnVision mission, in coordination with the EnVision science team, and NASA who will be carrying out many of the activities particularly at the member state level of activities. For this purpose, the EnVision team will work with the ESA and NASA communications and outreach teams to initiate and identify opportunities for maximizing public awareness and educational impact. Materials suitable for release to the public will be provided by the Science Working Team during the development, operational and post-operational phases of the mission. Public outreach will take advantage of existing pan-European infrastructures, including the ESEROs, Europlanet, the ESA education and communications departments, and their equivalents at NASA. The communication/outreach plan will be developed further in Phases B-D.

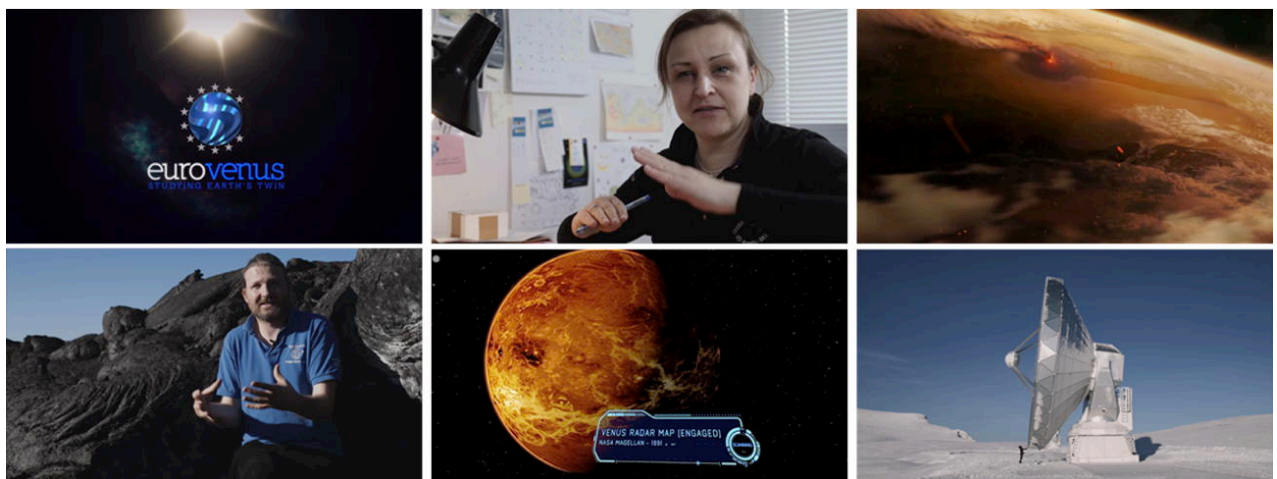


Figure 8.1 – Screenshots from films produced for the EuroVenus project. EnVision public outreach will build on this experience.

9 References

- Airey, M. et al., *Planet. and Space Sci.* Vol. 113, p. 33-48 (2015) doi:10.1016/j.pss.2015.01.009
- Antonita, M., Isro's Venus Orbiter Mission. Presentation to the Venus Panel on Decadal Survey on Planetary Science and Astrobiology, 10 Nov 2020, via spacenews.com (2020)
- Armann, M., and P. J. Tackley, *J. Geophys. Res.*, 117, E12003 (2012) doi:10.1029/2012JE004231
- Arney, G. et al., *J. Geophys. Res. Planets*, Volume 119, Issue 8, pp. 1860-1891 (2014) doi:10.1002/2014JE004662
- Arvidson et al., *Icarus* 112, 171-186 (1994)
- Arvidson, R.E., Greely, R., Malin, M.C., et al., *J. Geophys. Res.*, vol. 97, no. E8, pp. 13 303-13 318 (1992)
- Anderson, Geological Society of America Special Paper 388 (2005)
- Aveline et al., *LPSC*, 2165 (2011)
- Barstow, J.K., C.C.C. Tsang, C.F. Wilson, P.G.J. Irwin, F.W. Taylor, K. McGouldrick, P. Drossart, G. Piccioni, S. Tellmann, *Icarus*, Vol.217, Issue 2, 542-560 (2012) doi:10.1016/j.icarus.2011.05.018
- Basilevsky et al., *GSAB*, 96, 1,137 (1985)
- Bertaux, J.L., et al., *Planet. and Space Sci.* 55, 1673-1700 (2007)
- Bertaux, J.L., Widemann, T., Hauchecorne, A., Moroz, V.I., Ekonomov, A.P., *J. Geophys. Res.*, Vol. 101, N°E5, pp. 12709-12745 (1996).
- Bézar, B., C. C. C. Tsang, R. W. Carlson, G. Piccioni, E. Marcq, and P. Drossart, *J. Geophys. Res.*, 114, E00B39 (2009) doi:10.1029/2008JE003251
- Bézar, B., Fedorova, A., Bertaux, J.-L., et al., *Icarus* 216, 173–183 (2011)
- Bjornnes, E., V. Hansen, B. James, J. Swenson, *Icarus* 217(2), 451–461 (2012) doi: 10.1016/j.icarus.2011.03.033
- Bondarenko, N.V. et al., *Geophys. Res. Letters*, Vol. 37, Issue 23, CiteID L23202 (2010) doi:10.1029/2010GL045233
- Bondarenko, N. & Kreslavsky, M., *Icarus*, Volume 309, p. 162-176 (2018) doi:10.1016/j.icarus.2018.03.013
- Brackett, R. A., Fegley, B., and Arvidson, R. E., *J. Geophys. Res.*, Vol. 100, Issue E1, pp.1553–1563 (1995) doi:10.1029/94JE02708
- Breuer, D. und Moore, B, in: *Physics of Terrestrial Planets and Moons Treatise on Geophysics* (2nd edition), Elsevier, pp. 255-305. ISBN 978-0-444-53803-1 (2015)
- Bridges, N. T., et al., *Nature* 485, 339 (2012)
- Brown, C.D., and Grimm, R.E., *Icarus* Vol. 139, Issue 1, pp. 40-48 (1999)
- Bruzzone L. et al., *IEEE/IGARSS International Geoscience and Remote Sensing Symposium* (2020)
- Bruzzone, L. et al., *IEEE/IGARSS International Geoscience and Remote Sensing Symposium* (2015)
- Bullock, M.A., and Grinspoon, D.H. *Icarus* 150, 19-37 (2001)
- Byrne, P.K., Ghail, R.C., Gilmore, M.S., Celâl Şengör, A.M., Klimczak, C., Senske, D.A., Whitten, J.L., Khawja, S., Ernst, R.E., and Solomon, S.C., *Geology* 49 (1):81–85 (2021) doi:10.1130/G47940.1
- Campbell, L.H., and S.R. Taylor, *Geophys. Res. Lett.* 10 (11), 1061–1064 (1983)
- Campbell, B.A., G.A. Morgan, J.L. Whitten, L.M. Carter, D.B. Campbell, and L.S. Glaze, *J. Geophys. Res.*, 122, 1580-1596 (2017) doi:10.1002/2017JE005299
- Campbell, B.A., Putzig, N.E., Carter, L.M. and Phillips, R.J., *IEEE Geoscience and Remote Sensing Letters*, 8(5), pp.939-942 (2011)
- Campbell, B.A., and P.G. Rogers, *J. Geophys. Res.*, 99, 21,153-21,171 (1994)
- Campbell, B.A., *Icarus*, 112, 187-203 (1994)
- Campbell, B.A., and D.B. Campbell, *J. Geophys. Res.*, 97, 16293-16314 (1992)
- Carpy et al., *EnVision Paris Conference* (2020)
- Carrer, LK., F. Zancanella, L. Bruzzone, *IEEE Trans. on Geosci. and Remote Sensing*, Vol. 59 (2021) doi:10.1109/TGRS.2020.3006586
- Carrer, L., L. Bruzzone, *Nature Communications*, Vol. 8, Article number 2248, 21 Dec. 2017 (2017) doi:10.1038/s41467-017-02334-1
- Carter, L. M., Campbell, B. A., Holt, J. W., Phillips, R. J., Putzig, N. E., Mattei, S., Seu, R., Okubo, C. H., and Egan, A. F., *Geophys. Res. Lett.*, 36, L23204 (2009) doi:10.1029/2009GL041234.
- Chamberlain, S., et al., *Icarus*. 346, 113819 (2020)
- Claudin, P. and B. Andreotti, *Earth and Planetary Science Letters* 252, 30–44 (2006)
- Cottreau, L.; Rambaux, N.; Lebonnois, S. and Souchay, J., *Astron. Astrophys.*, vol. 531, pp.A45 (2011) doi:10.1051/0004-6361/201116606
- Cottini, V. et al., *Plan. Sp. Sci.* 113-114, 219-225 (2015) doi:10.1016/j.pss.2015.03.012
- Coustenis, A., Taylor, F., & Plainaki, C. in T. Beer, J. Li, & K. Alverson (Eds.), *Global Change and Future Earth: The Geoscience Perspective*, pp. 40-54. Cambridge University Press (2018) doi:10.1017/9781316761489.006
- D'Amore, M., et al., in *Infrared Remote Sensing and Instrumentation XXVII* (2019)
- Davaille, A., S.E. Smrekar et S. Tomlinson, *Nature Geosciences*, 10, 349-355 (2017) doi.org/10.1038/ngeo2928
- D'Incecco, P. et al. *Plan. Sp. Sci.*, Vol.136, p. 25-33 (2017) doi:10.1016/j.pss.2016.12.002
- D'Incecco, P. et al. *Earth and Plan. Sci. Let.*, Vol. 546, article id. 116410 (2020) doi:10.1016/j.epsl.2020.116410
- Diniega, S. et al., *Aeolian Research*, Vol. 26, p. 5-27 (2017) doi:10.1016/j.aeolia.2016.10.001
- Donahue., T.M., Hoffman, J.H., Hodges Jr., R.R., Watson A.J., *Science* 07 May 1982, Vol. 216, Issue 4546, pp. 630-633 (1982) doi:10.1126/science.216.4546.630
- Dumoulin, C., G. Tobie, O. Verhoeven, P. Rosenblatt, and N. Rambaux, *J. Geophys. Res.: Planets*, 122, 1338–1352 (2017) doi:10.1002/2016JE005249
- Duran, Winent et al., *NatGeo*, 12, 345 (2019)
- Dyar, M. D., Helbert, J., Maturilli, A., Müller, N. T., & Kappel, D., *Geophys. Res. Lett.*, 47,

- e2020GL090497 (2020)
doi.org/10.1029/2020GL090497
- Encrenaz, T., Greathouse, T.K., Marcq, E., Sagawa, H., Widemann, T., Bézard, B., Fouchet, T., Lefèvre, F., Lebonnois, S., Atreya, S.K., Lee, Y. J., Giles, R., Watanabe, S., Shao, W., Zhang, X., and Bierson, C.J. *Astron. Astrophys.*, Vol.639, A69 (2020)
doi:10.1051/0004-6361/202037741
- Encrenaz, T., Greathouse, T.K., Marcq, E., Sagawa, H., Widemann, T., Bézard, B., Fouchet, T., Lefèvre, F., Lebonnois, S., Atreya, S.K., Lee, Y. J., Giles, R. and Watanabe, S., *Astron. Astrophys.*, Vol. 623, id. A70, 11 pp. (2019)
- Encrenaz, T., Greathouse, T.K., Richter, M.J., DeWitt, C., Widemann, T., Bézard, B., Fouchet, T., Atreya, S.K., and Sagawa, H., *Astronomy & Astrophysics*, Vol. 595, id.A74, 15 pp. (2016)
- Encrenaz, T., Greathouse, T. K., Roe, H., Richter, M., Lacy, J., Bézard, B., Fouchet, T., Widemann, T., HDO and SO₂ thermal mapping on Venus: Evidence for strong SO₂ variability, *Astron. Astrophys.* 543, A153 (2012)
- ESA BR-247, Cosmic Vision, Space Science for Europe 2015-2025, ESA Publications Division, ESTEC, PO Box 299, 2200 AG Noordwijk, The Netherlands (2005).
- Esposito, L., *Science*, 223, 1072 (1984)
doi:10.1126/science.223.4640.1072
- Esposito, L. et al., *J. Geophys. Res.* 93 (D5), 5267-5276 (1988) doi:10.1029/JD093iD05p05267
- Fedorova, A. et al., *Icarus*, 275, 143-162 (2016)
doi:10.1016/j.icarus.2016.04.010
- Fegley, B., Jr; in *Planets, Asteroids, Comets and The Solar System*, Vol. 2 of *Treatise on Geochemistry (Second Edition)*. Edited by Andrew M. Davis. Elsevier, p.127-148 (2014)
- Fegley, B., Klingelhofer, G., Lodders, K. Widemann, T. in *Venus II: Geology, Geophysics, Atmosphere, and Solar Wind Environment*. University of Arizona Press p.591 (1997)
- Ferraria et al., *EPSL*, 534, 116089 (2020)
- Ferro, A. Pascal, L. Bruzzone, *IEEE Transactions on Geoscience and Remote Sensing*, Vol. 51, pp. 3037-3055 (2013)
- Filiberto, J., Trang, D., Treiman, A. H. and Gilmore, M. *S. Sci. Adv.*, Vol. 6, Issue 1, p. eaax7445 (2020)
doi:10.1126/sciadv.aax7445
- Ford, P. et al., *Journ. Geophys. Res.* Vol. 97, Issue E8, p. 13103-13114 (1992) doi:10.1029/92JE01085
- Gaillard and Scaillet, *Earth and Pl. Sci. Let.* 403:307-316 (2014)
- Ganesh, I.L. M, et al., *JVGR*, 390, 106748 (2020)
- Genova, A., Goossens, S., Lemoine F.G., Mazarico, E., Neumann G.A., Smith, D.E., et al., *Icarus*, 272, 228-245 (2016) doi:10.1016/j.icarus.2016.02.050
- Gerekos, G., A. Tamponi, L. Carrer, D. Castelletti, M. Santoni, L. Bruzzone, *IEEE Transactions on Geoscience and Remote Sensing*, Vol. 56, No. 12, pp. 7388-7404 (2018)
- Gerya, T., Stern, R., Baes, M. et al., *Nature* 527, 221–225 (2015) doi:10.1038/nature15752
- Ghail, R., abstract #2132 LPSC (2019)
- Ghail, R.C. & Wilson, L. Geological Society, London, Special Publications, vol. 401, issue 1, pp. 97-106 (2015) doi:10.1144/SP401.1
- Gillmann, C., Golabek, G.J., Raymond, S.N., Schönbachler, M., Tackley, P., Dehant, V., Debaille, V., *Nat. Geosci.* 13, 265–269 (2020)
doi.org/10.1038/s41561-020-0561-x
- Gillmann, C., and P. Tackley, *J. Geophys. Res. Planets*, 119, 1189–1217 (2014) doi:10.1002/2013JE004505
- Gillmann, C., Chassefière, E., and Lognonné, P., *Earth and Plant. Sci. Lett.*, Vol. 286, Issues 3–4, pp. 503–513 (2009)
- Gilmore et al., *Icarus*, 254, 350 (2015)
- Gilmore, M.S., N. Mueller, and J. Helbert, *Icarus*, 254: p. 350-361 (2015)
- Greeley, R., K. Bender, P.E. Thomas, G. Schubert, D. Limonadi, C. Weitz, *Icarus* 115, 399 (1995)
- Greeley, R. et al., *J. Geophys. Res.* 97, 13319–13345 (1992)
- Greeley, R., Marshall, J.R., Leach, R.N., *Icarus* 60, 152–160 (1984)
- Grieger, B., et al., IPPW meeting, Lisbon (2003)
- Gülcher, A. J. P, Gerya, T.V., Montési, L. G. J., & Munch, J., *Nature Geoscience* 13, 547-554 (2020)
doi.org/10.1038/s41561-020-0606-1
- Hamano, K., Abe, Y. & Genda, H., *Nature* 497, 607–610 (2013) doi:10.1038/nature12163
- Hansen, V.L., & Willis, J.J., *Icarus*, 123, 296-312 (1996)
- Hashimoto, G. & Abe., Y., *Planet. Space Sci.* Vol. 53, Issue 8, p. 839-848 (2005)
doi:10.1016/j.pss.2005.01.005
- Helbert, J., et al., *Infrared Remote Sensing and Instrumentation XXVI*, 10765 (2018)
doi:10.1117/12.2320112.
- Helbert, J., et al., *Infrared Remote Sensing and Instrumentation XXVII* (2019)
- Helbert, J., et al., in *Infrared Remote Sensing and Instrumentation XXV* (2017)
- Herrick, R. and Rumpf, M.E., *J. Geophys. Res. Planets* 116 (2011) doi:10.1029/2010JE003722
- Herrick, R. & Sharpton, V., *J. Geophys. Res.*, Vol. 105, Issue E8, p. 20245-20262 (2000)
doi:10.1029/1999JE001225
- Herrnstein, A., and T.E. Dowling, *J. Geophys. Res.* Vol. 112, E04S08 (2007) doi:10.1029/2006JE002804
- Hensley, S. et al., *IEEE Radarcon* (2020)
- Ignatiev, N., Moroz, V.I., Zasova, L., Khatuntsev, I., *Adv. Space Sci.* 23 (9), 1549–1558 (1999)
- Ignatiev, N. et al., *Plan.Space Sci.*, Vol. 45, Issue 4, p. 427-438 (1997) doi:10.1016/S0032-0633(96)00143-2
- Imamura, T. & Hashimoto, G., *Adv. Space Res.* Vol. 29, No. 2, pp. 249-254 (2002) doi:10.1016/S0273-1177(01) 00575-0
- Imamura, T. & Hashimoto, G., *J. Geophys. Res.* 103 (E13) (1998) doi:10.1029/1998JE900010
- Ivanov, M. A., and J. W. Head III, *Planet. Space Sci.*, 113-114, 10-32 (2015) doi:10.1016/j.pss.2015.03.016
- Ivanov, M. A., and J. W. Head III, *Planet. Space Sci.*, 59, 1559-1600 (2011) doi:10.1016/j.pss.2011.07.008
- Izenberg et al., *Geophys. Res. Lett.* 21, 289-292 (1994)
- James, E.P. et al., *Icarus* 129, 147–171 (1997)
doi:10.1006/icar.1997.5763

- Jessup, K.L., Marcq, E., Mills, F., Mahieux, A., Limaye, S., Wilson, C., Allen, M., Bertaux, J.-L., Markiewicz, W., Roman, T., Vandaele, A.C., Wilquet, V., Yung, Y., *Icarus*, Vol. 258, 309-336 (2015) doi:10.1016/j.icarus.2015.05.027.
- Kappel, D. et al., *Icarus*, Vol. 265, p. 42-62 (2016) doi:10.1016/j.icarus.2015.10.014
- Kane, S., G. Arney, D. Crisp, S. Domagal-Goldman, L. Glaze, C. Goldblatt, D. Grinspoon, J. Head, A. Lenardic, C. Unterborn, M. Way, and K. Zahnle, *J. Geophys. Res. Planets*, 124, p.2015-2028 (2019)
- Kasting, J.F. (1988), *Icarus* 74, 472-494.
- Khawja, S., Ernst, R.E., Samson, C., Byrne, P.K., Ghail, R.C., MacLellan, L.M., *Nat. Commun.* 11, 5789 (2020) doi:10.1038/s41467-020-19336-1
- Kiefer, W., & Swafford, L.C., *Journ. of Structural Geology*, Vol. 28, issue 12, pp. 2144-2155 (2006)
- Kitahara, T. et al., *J. Geophys. Res.*, 124 (5), 1266-1281 (2019) doi:10.1029/2018JE005842
- Kleine, T., Münker, C., Mezger, K., Palme, H, *Nature*. 2002 Aug 29; 418(6901):952-5 (2002) doi:10.1038/nature00982.
- Klose et al., *J. Geophys. Res. Planets* 97, 16353-16370 (1992)
- Kobayashi, T., Lee, S. R., Kumamoto, A., & Ono, T., In L. Pajewski, C. Craeye, A. Giannopoulos, F. Andre, S. Lambot, & E. Slob (Eds.), *Proc. of the 15th International Conference on Ground Penetrating Radar GPR 2014*, pp. 1037-1041 (2014)
- Konopliv, A.S. and Yoder, C.F., *Geophys. Res. Lett.* 23, 1857-1860 (1996) doi:10.1029/96GL0158
- Korablev, O., et al., *Planet. Space Sci.*, 65(1): p. 38-57 (2012)
- Kreslavsky, M., and Bondarenko, N.V., *Aeolian Res.* 26, 29 (2017) doi: 10.1016/j.aeolia.2016.06.001
- Lammer, H., Zerkle, A.L., Gebauer, S. et al., *Astron Astrophys Rev* 26, 2 (2018) doi:10.1007/s00159-018-0108-y
- Lebonnois, S., *J. Geophys. Res.* 115, E6 (2010) doi:10.1029/2009JE003458
- Lee, C. et al., *J. Geophys. Res.*, 112, E04S11 (2007) doi:10.1029/2006JE002874
- Lefèvre, M., Spiga, A., Lebonnois, S., *Icarus* 335, 113376 (2020)
- Lorenz, R.D., *Planet. Space Sci.* (2015) doi:10.1016/j.pss.2015.07.009i
- Lorenz, R.D., Le Gall, A., Janssen, M. A., *Icarus*, 270, 30-36 (2016)
- Lorenz, R.D., *Icarus*, 264, 311 (2016)
- Lorenz, R. D., *Progress in Earth and Planetary Science* 5, 34 (2018) doi:10.1186/s40645-018-0181-x
- Lucas, A., O. Aharonson, C-A. Deledalle, A. Hayes, R. Kirk, E. Howington-Kraus and the CRST, *J. Geophys. Res.*, Vol. 119, Issue 10, pp. 2149-2166 (2014) doi:10.1002/2013JE004584
- Määttänen, A. et al., *J. Geophys. Res.*, Vol. 123, Issue 2, pp. 1269-1296 (2018) doi:10.1002/2017JD027429
- Malin, M. C., *J. Geophys. Res.: Planets* 97, 16337-16352 (1992) doi:10.1029/92je01343
- Marcq, E., Jessup, K.L., Baggio, L., Encrenaz, T., Lee, Y.J., Montmessin, F., Belyaev, D., Oleg Korablev, O., Bertaux, J.-L., *Icarus*, Vol. 335, 113368 (2020) doi.org/10.1016/j.icarus.2019.07.002
- Marcq, E., Bertaux, J.L., Montmessin, F. et al., *Nature Geosci* 6, 25-28 (2013) doi:10.1038/ngeo1650
- Marcq, E. et al., *J. Geophys. Res.*, Volume 113, CiteID E00B07 (2008) doi:10.1029/2008JE003074
- Margot, J.L., Hauck II, S.A., Mazarico, E., Padovan, S. and Peale, S.J., arXiv preprint arXiv:1806.02024 (2018)
- Markiewicz, M. et al., *Nature* 450, 29 Nov. 2007, 633-636 (2007) doi:10.1038/nature06320
- Marov, M. Y., and D. H. Grinspoon, *The planet Venus*, Yale University Press (1998)
- Marshall, J.R. and Greeley, J. *Geophys. Res.* 97, 1007-1016 (1992)
- Marshall, J.R., Fogleman, G., Greeley, R., Hixon, R., Tucker, D., *J. Geophys. Res.*, 96, B2, 1931 (1991)
- Marty, J.C., Balmino, G., Duron, J., Rosenblatt, P., Le Maistre, S., Rivoldini, A., et al., *Planet. Space Sci.*, 57(3), 350-363 (2009) doi:10.1016/j.pss.2009.01.004
- Massol, H., K. Hamano, F. Tian, M. Ikoma, Y. Abe, E. Chassefière, A. Davaille, H. Genda, M. Gudel, Y. Hori, F. Leblanc, E. Marcq, P. Sarda, V.I. Shematovich, A. Stökl, H. Lammer, *Space Sci. Rev.* 205, 153-211 (2016) doi:10.1007/s11214-016-0280-1.
- McGouldrick, T. & Toon, O.B., *Planet. Space Sci.*, Vol. 56, Issue 8, p. 1112-1131 (2008a) doi:10.1016/j.pss.2008.02.010
- McGouldrick, T. & Toon, O.B., *Icarus*, Vol. 196, Issue 1, p. 35-48 (2008b) doi:10.1016/j.icarus.2008.02.020
- McGouldrick, T. & Toon, O.B., *Icarus*, Vol.191, Issue 1, p. 1-24 (2007) doi:10.1016/j.icarus.2007.04.007
- McKinnon, W.B., K.J. Zahnle, B.A. Ivanov and H.J. Melosh, in *Venus II: Geology, Geophysics, Atmosphere, and Solar Wind Environment*. Edited by Stephen W. Bougher, D.M. Hunten, and R.J. Philips. Tucson, AZ: University of Arizona Press, p.969 (1997)
- Meadows, V.S. and D. Crisp, *J. Geophys. Res.*, Vol. 101, Issue E2, p. 4595-4622 (1996)
- Moruzzi S.A. and W. S. Kiefer, *Lunar Planet. Sci. Conf.* 51, abstract 1430 (2020).
- Mueller, N., et al., *J. Geophys. Res.*, 113(2008-12):E00B17 (2008) doi:10.1029/2008JE003118
- Mueller, N. T., S. Smrekar, J. Helbert, E. Stofan, G. Piccioni, and P. Drossart, *Journal of Geophysical Research-Planets*, 122(5): p.1021-1045 (2017) doi:10.1002/2016JE005211
- Mueller, N.T., S.E. Smrekar, and C.C.C. Tsang, *Icarus*, 335, 113400 (2020) doi: 10.1016/j.icarus.2019.113400
- Namiki, N, and S.C. Solomon, *J. Geophys. Res.: Planets*, 103, pp. 3655-3677 (1998)
- Neakrase et al., *AR*, 26, 47 (2017)
- Nealley et al., *LPSC XLVIII*, Abstract #2498 (2017)
- Neefs, E., A.C. Vandaele, R. Drummond, I.R. Thomas, S. Berkenbosch, R. Clairquin, S. Delanoye, B. Ristic, J. Maes, S. Bonnewijn, G. Pieck, E. Equeter, C. Depiesse, F. Daerden, E. Van Ransbeeck, D. Nevejans, J. Rodriguez, J.-J. Lopez-Moreno, R. Sanz, R. Morales, G.P. Candini, C. Pastor, B. Aparicio del Moral, J.M. Jeronimo, J. Gomez, I. Perez, F. Navarro, J. Cubas, G. Alonso, A. Gomez, T. Thibert, M.R. Patel, G. Belucci, L. De Vos, S. Lesschaeve, N. Van Vooren, W. Moelans, L. Aballea, S. Glorieux, A. Baeke, D. Kendall, J. De Neef, A. Soenen, P.Y.

- Puech, J. Ward, J.F. Jamoye, D. Diez, A. Vicario, and M. Jankowski, *Applied Optics*, 54(28): p. 8494-8520 (2015)
- Noack, L., Breuer, D. & Spohn, T., *Icarus* Vol. 217, Issue 2, pp. 484-498 (2012)
- O'Neill, C., A.M. Jellinek, A. Lenardic, *Earth and Planetary Science Letters*, Vol. 261, Issues 1–2, pp. 20-32. doi.org/10.1016/j.epsl.2007.05.038 (2007)
- Ono, T. et al., *Science* 13 Feb 2009: Vol. 323, Issue 5916, pp. 849 (2009) doi:10.1126/science.323.5916.849d
- O'Rourke, J.G., J. Korenaga, *Icarus* 260, 128–140 (2014)
- Oschlisniok, J., Häuser, B., Pätzold, M., Tyler, G.L., Bird, M.K., Tellmann, S., Remus, S., Andert, T., *Icarus* 221, Issue 2, p. 940-948 (2012)
- Oschlisniok, J., Häuser, B., Pätzold, M., Tellmann, S., Bird, M., 14th Europlanet Science Congress Sept. 2020, EPSC2020-139 (2020)
- Parmentier, E.M. and Hess, P.C., *Geophys. Res. Lett.* Vol. 19, Issue 20, pp. 2015-2018 (1992) doi:10.1029/92GL01862
- Peter, G., et al., *Proceedings Volume 8867, Infrared Remote Sensing and Instrumentation XXI*; 886707 (2013) doi:10.1117/12.2024375
- Pettengill, G.H., Ford, P.G., Simpson, R.A., *Science* 272:1628–1631 (1996)
- Pettengill, G.H., Ford, P.G., Wilt, R.J., *J. Geophys. Res.* 97(E8):13067–13090 (1992)
- Pettengill, G.H. P. G. Ford, W. T. K. Johnson, R. K. Raney and L. A. Soderblom, *Science, New Series*, Vol. 252, No. 5003, Apr. 12, 1991, pp. 260-265 (1991)
- Phillips, R.J., R.F. Raubertas, R.E. Arvidson, I.C. Sarkar, R.R. Herrick, N. Izenberg, R.E. Grimm, *J. Geophys. Res.* 97, 15,923–15,948 (1992)
- Picardi, G. et al., *Science* 310.5756:1925-1928 (2005)
- Piccialli, A. et al., 2015, *Planet. Space. Sci.* 113(144), 321-335 (2015) doi:10.1016/j.pss.2014.12.009
- Plesa et al., *Geophys. Res. Lett.* 45, 12198-12209 (2018)
- Pollack, J.B., et al., *Icarus*, 103(1): p. 1-42 (1993)
- Port, S.T., et al., *LPSC*, 2083 (2018)
- Port, S.T., et al., *LPSC*, 2132 (2019)
- Port, S.T., Chevrier, V.F., Kohler, E., *Icarus* 336, 113432 (2020).
- Pruppacher, H. R. and Klett, J. D., *Atmospheric and Oceanographic Sciences Library*, Kluwer Academic Publishers, Dordrecht, The Netherlands (1997)
- Quémerais, E., Chaufray, JY., Koutroumpa, D. et al., *Space Sci. Rev.* 216, 67 (2020) doi: 10.1007/s11214-020-00695-6
- Restano, M., Seu, R. and Picardi, G., *IEEE Geoscience and Remote Sensing Letters*, 13(6), pp.806-810 (2016)
- Rivoldini et al., *Icarus* 213, 451-472 (2011)
- Robert, S., A.C. Vandaele, E. Neefs, L. Jacobs, S. Berkenbosch, I.R. Thomas, J.T. Erwin, V. Wilquet, W. Moelans, S. Lesschaeve, A. Algoedt, L. De Vos, B. Bézard, E. Marcq, and C. Wilson, *Planet. Space Sci.*, under review, (2021)
- Salvador, A., H. Massol, A. Davaille, E. Marcq, P. Sarda, and E. Chassefière, *J. Geophys. Res. Planets*, 122, 1458–1486 (2017) doi:10.1002/2017JE005286
- Seiff, A. et al., *Adv. in Space Res.*, Vol. 5, Issue 11, p. 3-58 (1985) doi:10.1016/0273-1177(85)90197-8
- Seu, R. et al., *J. Geophys. Res. Planets* 112.E5 (2007) doi:10.1029/2006JE002745
- Shalygin, E. V., W. J. Markiewicz, A. T. Basilevsky, D. V. Titov, N. I. Ignatiev, and J. W. Head, *Geophys. Res. Lett.* Vol. 42, Issue 12, pp.4762-4769 (2015) doi:10.1002/2015GL064088
- Shao, W. D., Zhang, X., Bierson, C. J., & Encrenaz, T., *J. Geophys. Res.: Planets*, 125, e2019JE006195 (2020) doi:10.1029/2019JE006195
- Shepard, M.K., Arvidson, R.E., Brackett, R.A., and Fegley Jr., B., *Geophys. Res. Lett.* Vol 21, Issue 6, pp. 469-472 (1994) doi:10.1029/94GL00392
- Shields, A.L., Ballard, S., and Johnson, J.A., *Physics Reports*, Vol. 663, 5 Dec 2016, pp.1-38 (2016) doi: 10.1016/j.physrep.2016.10.003.
- Smrekar, S.E., Davaille, A. & Sotin, C., *Space Sci. Rev.* 214, 88 (2018a) doi:10.1007/s11214-018-0518-1
- Smrekar, S.E. et al., 2018 *IEEE Aerospace Conference*, pp. 1-19 (2018) doi: 10.1109/AERO.2018.8396625.
- Smrekar, S.E., et al., *Science*, 328(5978): p.605-8 (2010) doi:10.1126/science.1186785
- Smrekar, S.E., *Icarus* 112, 2-26 (1994)
- Smrekar, S., and Phillips, R.J., *Earth and Planetary Science Letters*, Vol. 107, Issues 3–4, 582-597 (1991) doi:10.1016/0012-821X(91)90103-O
- Solomon et al., *J. Geophys. Res. Planets* 97, 13199-13255 (1992)
- Spohn, T., *Icarus*, Vol. 90, Issue 2, p. 222-236 (1991) doi:10.1016/0019-1035(91)90103-Z
- Steinberger et al., *Icarus* 207, 564-577 (2010)
- Stevenson, D.J., *Earth Planet. Sci. Lett.* 208, 1-11 (2003)
- Stoddard, P.R., & Jurdy, D.M., *Icarus*, Vo. 217, pp. 524-533 (2012) doi:10.1016/j.icarus.2011.09.003
- Stofan, E.R., Smrekar, S.E., Mueller, N., Helbert, J., *Icarus*, Vol. 271, p. 375-386 (2016) doi:10.1016/j.icarus.2016.01.034
- Strom, R.G., Schaber, G.G., & Dawson, D.D., *J. Geophys. Res.*, Vol. 99, Issue E5 (1994) doi.org/10.1029/94JE00388.
- Tellmann S., Pätzold M., Häusler B., Bird M. K., Tyler G.L., *J. Geophys. Res. Planets*, Vol. 114, Issue E9 (2009) doi:10.1029/2008JE003204
- Titov, D.V. et al., *Icarus*, Vol. 217, Issue 2, p. 682-701 (2012) doi:10.1016/j.icarus.2011.06.020
- Thakur, S., L. Bruzzone, *IEEE Transactions on Geoscience and Remote Sensing*, Vol. 57, No.8, pp. 5266-5284 (2019)
- Treiman, A., Harrington, E., & Sharpton, V., *Icarus*, Vol. 280, pp.172-182 (2016)
- Treiman, A.H., et Schwenzer, S.P., *Venus Geochemistry, Progress, Prospects, and New Missions*, Abstract #2011 (2009)
- Treiman, A.H., *Exploring Venus as a Terrestrial Planet*, Vol. 176, AGU Monograph Series, L.W. Esposito, E.R. Stofan, T.E. Cravens Eds, pp. 7-22 (2007) doi.org/10.1029/176GM03
- Tsang, C.C.C., Wilson, C.F., Barstow, J.K., Irwin, P.G.J., Taylor, F.W., McGouldrick, K., Piccioni, G., Drossart, P., Svedhem, H., *Geophys. Res. Lett.* 37, 2202 (2010) doi:10.1029/2009GL041770.
- Turcotte, D.L., *J. Geophys. Res. Planets* Vol 100, issue E8, pp. 16931-16940 (1995) doi:10.1029/95JE01621

- Turcotte, D.L., *J. Geophys. Res. Planets* Vol.98, Issue E9, p.17061-17068 (1993) doi.org/10.1029/93JE01775
- Turcotte, D.L., *J. Geophys. Res.*, Vol. 94, p. 2779-2785 (1989) doi:10.1029/JB094iB03p02779
- Vandaele, A.C., J.-J. Lopez-Moreno, M. R. Patel, G. Bellucci, F. Daerden, B. Ristic, S. Robert, I.R. Thomas, V. Wilquet, M. Allen, G. Alonso-Rodrigo, F. Altieri, S. Aoki, D. Bolsée, T. Clancy, E. Cloutis, C. Depiesse, R. Drummond, A. Fedorova, V. Formisano, B. Funke, F. González-Galindo, A. Geminale, J.-C. Gérard, M. Giuranna, L. Hetey, N. Ignatiev, J. Kaminski, O. Karatekin, Y. Kasaba, M. Leese, F. Lefèvre, S.R. Lewis, M. López-Puertas, M. López-Valverde, A. Mahieux, J. Mason, J. McConnell, M. Mumma, L. Neary, E. Neefs, E. Renotte, J. Rodriguez-Gomez, G. Sindoni, M. Smith, A. Stiepen, A. Trokhimovsky, J.V. Auwera, G. Villanueva, S. Viscardy, J. Whiteway, Y. Willame, and M. Wolff, *Space Sci. Rev.*, 214:article number:80 (2018) doi.org/10.1007/s11214-018-0517-2
- Vandaele, A.C., Korablev, O., Belyaev, D., Chamberlain, S., Evdokimova, D., Encrenaz, T., Esposito, L., Jessup, K.L., Lefèvre, F., Limaye, S., Mahieux, A., Marcq, E., Mills, F.P., Montmessin, F., Parkinson, C.D., Robert, S., Roman, T., Sandor, B., Stolzenbach, A., Wilson, C., & Wilquet, V., *Icarus*, 295, 1-15 (2017a) doi.org/10.1016/j.icarus.2017.05.001
- Vandaele, A.C., Korablev, O., Belyaev, D., Chamberlain, S., Evdokimova, D., Encrenaz, T., Esposito, L., Jessup, K.L., Lefèvre, F., Limaye, S., Mahieux, A., Marcq, E., Mills, F.P., Montmessin, F., Parkinson, C.D., Robert, S., Roman, T., Sandor, B., Stolzenbach, A., Wilson, C., & Wilquet, V., *Icarus*, 295, 16-33 (2017b) doi.org/10.1016/j.icarus.2017.05.003
- Vandaele, A.C., Mahieux, A., Chamberlain, S., Ristic, B., Robert, S., Thomas, I.R., Trompet, L., Wilquet, V., & Bertaux, J.L., *Icarus*, 272, 48-59 (2016) doi.org/10.1016/j.icarus.2016.02.025
- Vandaele, A.C., Mahieux, A., Robert, S., Drummond, R., Wilquet, V., & Bertaux, J.L., *Planet. Space Sci.*, 113-114, 237-255 (2015) doi.org/10.1016/j.pss.2014.12.012
- Venera-D Joint Science Definition Team, Venera-D: 174 p. (2019) URL: https://www.lpi.usra.edu/vexag/reports/VeneraD_2019Wkshp_techRp_cover_21July20_v12Final.pdf
- Waltham et al., *J. Geophys. Res.*, 113, EO2012 (2008)
- Watters, T.R. et al., *Nature*, 444, 905 (2006)
- Way, M.J., A.D. Del Genio, N.Y. Kiang, L.E. Sohl, D.H. Grinspoon, I. Aleinov, M. Kelley, and T. Clune, *Geophys. Res. Lett.*, 43, no. 16, 8376-8383 (2016) doi:10.1002/2016GL069790
- Way, M.J. & A.D. Del Genio, *J. Geophys. Res. Planets*, 125, no. 5, e2019JE006276 (2020) doi:10.1029/2019JE006276.
- Weitz, C.M., et al., *Icarus* 112, 282–285 (1994)
- Weller, M. B., and Lenardic, A., *Geoscience Frontiers* 9, 91-102 (2018)
- Weller, M.B. and Kiefer, W.S., *J. Geophys. Res. Planets*, 10.1029/2019JE005960, 125, 1 (2020)
- Wendlandt, R. F., Baldrige, W. S. and Neumann, E.-R., *Geophys. Res. Lett.* 18, 9, 1759-1762 (1991) doi.org/10.1029/91GL01881
- Williams, J.G., Konopliv, A.S., Boggs, D.H., Park, R.S., Yuan, D.N., Lemoine, F.G., Goossens, S., Mazarico, E., Nimmo, F., Weber, R.C. and Asmar, S.W., *J. Geophys. Res. Planets* 119(7), pp.1546-1578 (2014)
- Wilson, C. & Lefèvre, F., *EnVision Science Conference*, Feb. 2020, CNES, Paris (2020).
- Yoder et al., *Science* 300, 299-303 (2003)
- Young, E.F. et al., *13th Europlanet Science Congress* Sept. 2019, EPSC (2019).

10 List of Acronyms

| | | | |
|---------|---|-----------|--|
| ADEV | Allan Deviation | TWTA | Travel Waveguide Tube Amplifier |
| AIT/V | Assembly, Integration and Test/Verification | UCS | Unconfined Compressive Stress measurements |
| AKE | Absolute Knowledge Error | UHF | Ultra-High Frequency |
| AOCS | Attitude & Orbit Control Systems | USO | Ultra-Stable Oscillator |
| APE | Absolute Pointing Error | UV | Ultraviolet |
| CCSDS | Consultative Committee for Space Data Systems | VHF | Very-High Frequency |
| CCU | Central Control Unit | | |
| CFDP | CCSDS File Delivery Protocol | RSE | Radio Science Experiment |
| CFRP | Carbon Fibre Reinforced Polymer | SRS | Subsurface Radar Sounder |
| CMA | Cost Model Accuracy | VenSAR | Venus Synthetic Aperture Radar |
| CP | Chemical Propulsion | VenSpec | Venus Spectroscopy (suite) |
| DES | Digital Electronics Subsystem | VenSpec-H | Venus Spectroscopy High Resolution |
| DMM | Design Maturity Margin | VenSpec-M | Venus Spectroscopy Mapper |
| DoF | Degree of Freedom | VenSpec-U | Venus Spectroscopy Ultraviolet |
| DSP | Digital Signal Processing | | |
| DST | Deep Space Transponder | | |
| EOL | End of Life | | |
| FoV | Field of View | | |
| GNC | Guidance, Navigation and Control | | |
| GS | Ground Segment | | |
| GSE | Ground Support Equipment | | |
| HF | High Frequency | | |
| HGA | High Gain Antenna | | |
| HKTM | House-Keeping TeleMetry | | |
| IMU | Inertial Measurement Unit | | |
| IR, nIR | Infrared, Near-Infrared | | |
| ITP | Interplanetary Transfer Phase | | |
| LEOP | Launch and Early Operations Phase | | |
| LT | Local Time | | |
| LTP | (Operations) Long Term Plan | | |
| MAR | Mission Adoption Review | | |
| MOC | Mission Operations Centre | | |
| NISAR | NASA/ISRO Synthetic Aperture Radar | | |
| OCC | Operations Control Centre | | |
| OSR | Optical Surface Reflectors | | |
| OWLT | One-Way Light time | | |
| RF | Radio Frequency | | |
| RoI | Region of Interest | | |
| RPE | Relative Pointing Error | | |
| SADM | Solar Array Drive Mechanism | | |
| SAR | Synthetic Aperture Radar | | |
| SMM | Shared Memory Model | | |
| SNR | Signal to Noise Ratio | | |
| SOC | Science Operations Centre | | |
| SORS | Science Operations Reference Scenario | | |
| SSMM | Solid-State Mass Memory | | |
| SSPA | Solid State Power Amplifier | | |
| STP | (Operations) Short Term Plan | | |
| SWOT | NASA Surface Water and Ocean Topography | | |
| SZA | Solar Zenith Angle | | |
| TRP | Thermal Reference Point | | |
| TT&C | Telemetry, Track and Command | | |

Units:

| | |
|-----|--------------------------------|
| ppb | parts per billion |
| ppm | parts per million |
| gal | 1 Gal = 0.01 m s ⁻² |

Abbreviations:

| | |
|-------|-----------|
| Lat. | Latitude |
| Long. | Longitude |

Molecular species:

| | |
|--------------------------------|-------------------|
| CO | Carbon monoxide |
| CO ₂ | Carbon dioxide |
| COS | Carbonyl sulphide |
| H ₂ O | Water vapour |
| H ₂ SO ₄ | Sulphuric acid |
| HCl | Hydrogen chloride |
| HDO | Deuterated water |
| HF | Hydrogen fluoride |
| SO | Sulphur monoxide |
| SO ₂ | Sulphur dioxide |

11 Glossary

Absorber: atmospheric constituent (in a gaseous or condensed phase) which significantly absorbs some incident radiation (e.g. solar, thermal infrared).

Allan Deviation (ADEV): Measurement of stability of the Ultra-Stable-Oscillator frequency for a given count time (square root of the two-sample variance of the signal frequency). After David W. Allan (b. 1936).

Altimetry: a technique for measuring height (here derived from the time taken by a radar pulse to travel from the s/c antenna to the surface and back to the s/c).

Apocentre: the point in a keplerian orbit furthest from the centre of mass, i.e. from the planet.

Basalt: a fine-grained dark basic volcanic rock consisting of plagioclase feldspar, a pyroxene, and olivine.

Cloud layer: atmospheric layer where condensed particulate matter (aerosols) are present, and contribute significantly to the opacity. On Venus, there are three main cloud layers, located between 48 and 70 km in altitude, straddling the troposphere/mesosphere boundary (tropopause).

Corona/coronae: oval-shaped features interpreted on Venus as the result of upwellings of warm material below the surface forming volcanoes and tectonic structures at the surface.

Eccentricity: parameter describing how elliptical an orbit is. Ellipticity of zero denotes a circular orbit.

Emissivity: the ability of a surface to emit radiant energy compared to that of a black body at the same temperature and with the same area.

Fault: a fracture or discontinuity in a volume of rock across which there has been displacement.

Felsic: adjective relating to a rock containing more light-coloured minerals than other rocks, including feldspar, feldspathoids, quartz, and muscovite.

Fold: a continuous bent or curved rock resulting of crustal/lithospheric stress.

Granite: a light-coloured coarse-grained acid plutonic igneous rock consisting of quartz, feldspars, and such ferromagnesian minerals as biotite or hornblende.

Hadean Period: Geologic eon extending -4.6 to -4 Ga preceding earliest known minerals on Earth.

High Frequency (HF): Range of radio frequencies extending from 3 MHz to 30 MHz i.e from 10 to 100 m in wavelength.

Highland(s): elevated areas higher than 2 km above the mean radius (5091 km) of the planet. On Venus two large highlands: Ishtar Terra with the highest area (Maxwell Montes with an elevation >10km) near the North pole, and Aphrodite Terra forming a ~15,000 km long equatorial relief belt.

Incidence angle: refers to the angle at which the sun's rays or radar waves strike the surface of the planet with respect to the normal to the surface.

Infrared window: spectral interval where gaseous absorption is small enough so that most of the thermal radiation originates from comparatively deeper atmospheric layers (or even from the surface).

k₂ Love number: gravitational potential modification due to the tidal deformation of the planet. After Augustus E. H. Love (1863-1840).

Ka-band: a nominal frequency range, from 26 to 40 GHz (0.8-1.1 cm in wavelength) within the microwave portion of the electromagnetic spectrum.

Local (solar) time (LT): Hour angle of the Sun as observed from a given point on Venus.

Lowland(s): flat areas at altitude < 0 km beneath the mean radius (5091 km) of the planet, covering ~20% of the planet surface.

Mafic: adjective relative to a rock containing more dark-coloured mineral and iron than other rocks, including olivine, pyroxene.

Magma: molten material beneath or within the planetary crust/lithosphere, from which igneous rock is formed.

Magmatic: adjective related rocks derived from molten material beneath or within the planetary crust/lithosphere.

Meridian: any great circle joining the North and South poles of a planet.

Mesosphere: atmospheric layer at local thermodynamic equilibrium and where vertical energy transport is performed through thermal radiation only. On Venus, it corresponds to the 60-100 km altitude range.

Microwave: domain of the electromagnetic spectrum extending from 0.3 to 300 GHz i.e. from 1 mm to 1 m in wavelength.

Mineral: a class of naturally solid inorganic substances with a characteristic crystalline form and a homogeneous chemical composition. Their association forms a rock.

(volume) Mixing ratio: amount of an atmospheric constituent (in moles) divided by the total (in moles) of all other atmospheric constituents. For minor species, it is usually expressed in parts per million (ppm) or parts per billion (ppb).

Nadir: the direction pointing directly below a particular location. The radar nadir refers to the downward-facing viewing geometry of an orbiting radar.

Oxidation: chemical processes by which atoms lose electron, combining a chemical substance with oxygen, resulting in an oxide.

Pericentre: the point in a keplerian orbit nearest to the centre of mass, i.e. nearest to the planet

Plutonic: adjective related to rocks derived from magma that has cooled and solidified below the surface of the Earth, consisting of well crystallised minerals.

Polarimetry: a radar ability to measure different polarization signatures of every resolution element.

Polarization: orientation of the electric field vector in an electromagnetic wave, frequently "horizontal" (H) or "vertical" (V) in conventional imaging radar systems. Polarization is established by the antenna, which may be adjusted to be different on transmit and on receive. Reflectivity of microwaves from an object depends on the relationship between the polarization state and the geometric structure of the object.

Radiometry: a set of techniques to measure electromagnetic radiation. In its passive mode, VenSAR will perform microwave radiometry to record the thermal emission emanating from Venus's surface at 9.5 cm-wavelength.

S-band: a nominal frequency range, from 2 to 4 GHz (7.5-15 cm in wavelength) within the microwave portion of the electromagnetic spectrum.

Sigma nought (σ_0): Scattering coefficient, the conventional measure of the strength of radar signals reflected by a distributed scatterer, usually expressed in dB. It is a normalized dimensionless number, comparing the strength observed to that expected from an area of one square metre. Sigma nought is defined with respect to the nominally horizontal plane, and in general has a significant variation with incidence angle, wavelength, and polarization, as well as with properties of the scattering surface itself.

Silicate: mineral consisting of SiO_2 or SiO_4 groupings and one or more metallic ions, with some forms containing hydrogen. Silicates constitute well over 90 percent of the rock-forming minerals of the earth's crust.

Spatial resolution: minimum distance interval required to detect spatial variations with a given imaging instrument.

Spatial sampling: distance interval between consecutive elements of an image (*pixels*) with a given imaging instrument. Should be at least twice smaller than the spatial resolution to avoid *undersampling*.

Spectral resolution: minimum frequency/wavelength/wavenumber interval required to detect spectral variations with a given spectroscopic instrument.

Spectral sampling: frequency/wavelength/wavenumber interval between consecutive elements of a spectrum (*spectels*) with a given spectroscopic instrument. Should be at least twice smaller than the spectral resolution to avoid *undersampling*.

SPICAV-UV: the UV channel of the SPICAV spectrometer aboard Venus Express.

Stereogrammetry: calculation of 3-D positions by using two or more imaging views obtained using different viewing angles. In the context of EnVision, this is used to calculate a digital elevation model of topography with VenSAR.

Stratigraphy: scientific discipline concerned with the description of rock successions and their interpretation in terms of a general time scale

Tectonic: adjective qualifying a structure resulting of deformation of planetary crust and lithosphere subduction.

Tessera/tesserae: Venusian landforms characterised by high topography and highly deformed terrains.

Topography: relief or three-dimensional quality of the planet surface enabling the identification of specific landforms.

Trace gas: on Venus, any other atmospheric gaseous species than CO_2 (~96.5 %) and N_2 (~3.5%).

Troposphere: atmospheric layer at local thermodynamic equilibrium and where vertical energy transport is performed through thermal radiation and fluid convection. On Venus, it corresponds to the 0-60 km altitude range.

VIRTIS-H: the high spectral resolution channel of the Venus Express VIRTIS IR spectrometer aboard Venus Express

Volume scattering: multiple scattering events occurring inside a medium, generally neither dense nor having a large loss tangent.

X-band: a nominal frequency range, from 8 to 12 GHz (2.5-3.8 cm in wavelength) within the microwave portion of the electromagnetic spectrum.